Comparative study of toxicological effect of iron oxide nanoparticles in human nerve cells

Natalia Fernández-Bertólez

Doctoral Thesis

UDC / 2018

Thesis supervisors:

Blanca Laffon Lage

Vanessa Valdiglesias García

Cellular and Molecular Biology

UNIVERSIDADE DA CORUÑA

UNIVERSIDADE DA CORUÑA

Comparative study of toxicological effect of iron oxide nanoparticles in human nerve cells

Doctoral Thesis

UDC / 2018

PhD student	Thesis supervisor	Thesis supervisor
		
Signed.	Signed.	Signed.
Natalia Fernández Bertólez	Blanca Laffon Lage	Vanessa Valdiglesias García

Funding

The experimental work presented in this thesis was performed at the:

- Toxicology laboratory, University of A Coruña, Spain.
- Genetics laboratory, University of A Coruña, Spain.
- EPIUnit Institute of Public Health, University of Porto, Porto, Portugal.
- Department of Environmental Health, Portuguese National Institute of Health, Porto, Portugal.

This work was supported by Xunta de Galicia (ED431B 2016/013), INDITEX-UDC 2017 stay abroad grants, and the COST Action CA15132 (hCOMET).

Scientific production derived from this Thesis

Scientific papers:

1. Valdiglesias, V., Kiliç, G., Costa, C., **Fernández-Bertólez, N.,** Pásaro, E., Teixeira, J.P., Laffon, B., 2014. Effects of iron oxide nanoparticles: Cytotoxicity, genotoxicity, developmental toxicity, and neurotoxicity. Environ. Mol. Mutagen. 56, 125–148.
2. Kiliç, G., Costa, C., **Fernández-Bertólez, N.,** Pásaro, E., Teixeira, J.P., Laffon, B., and Valdiglesias, V., 2015. In vitro toxicity evaluation of silica-coated iron oxide nanoparticles in human SHSY5Y neuronal cells. Toxicol. Res., 5 (1), 235–247.
3. Costa, C., Brandão, F., Bessa, M.J., Costa, S., Valdiglesias, V., Kiliç, G., **Fernández-Bertólez, N.,** Quaresma, P., Pereira, E., Pásaro, E., Laffon, B., and Teixeira, J.P., 2016. In vitro cytotoxicity of superparamagnetic iron oxide nanoparticles on neuronal and glial cells. Evaluation of nanoparticle interference with viability tests. Journal of Applied Toxicology, 36 (3), 361–372.
4. Valdiglesias, V., **Fernández-Bertólez, N.,** Kiliç, G., Costa, C., Costa, S., Fraga, S., Bessa, M.J., Pásaro, E., Teixeira, J.P., and Laffon, B., 2016. Are iron oxide nanoparticles safe? Current knowledge and future perspectives. Journal of Trace Elements in Medicine and Biology, 38, 53–63.
5. Laffon, B., **Fernández-Bertólez, N.,** Costa, C., Pásaro, E., and Valdiglesias, V., 2017. Comparative study of human neuronal and glial cell sensitivity for in vitro neurogenotoxicity testing. Food and Chemical Toxicology, 102, 120–128.
6. **Fernández-Bertólez, N.,** Costa, C., Brandão, F., Kiliç, G., Duarte, J.A., Teixeira, J.P., Pásaro, E., Valdiglesias, V., and Laffon, B., 2018. Toxicological assessment of silica-coated iron oxide nanoparticles in human astrocytes. Food and Chemical Toxicology, 118, 13–23.

7. **Fernández-Bertólez, N.,** Costa, C., Brandão, F., Kiliç, G., Teixeira, J.P., Pásaro, E., Laffon, B., and Valdiglesias, V., 2018. Neurotoxicity assessment of oleic acid-coated iron oxide nanoparticles in SH-SY5Y cells. Toxicology, 406–407 (May), 81–91.
8. **Fernández-Bertólez, N.,** Costa, C., Bessa, M.J., Park, M., Carriere, M., Dussert, F., Teixeira, J.P., Pasaro, E., Laffon, B., Valdiglesias, V., 2018. Assessment of oxidative damage induced by iron oxide nanoparticles on different nervous system cells. Mutation Research - Genetic Toxicology and Environmental Mutagenesis. En revisión.
9. **Fernández-Bertólez, N.,** Costa, C., Brandão, F., Duarte, J.A., Teixeira, J.P., Pásaro, E., Valdiglesias, V., Laffon, B., 2018. Evaluation of cytotoxicity and genotoxicity induced by oleic acid-coated iron oxide nanoparticles in human astrocytes. International Journal of Pharmaceutics. En revisión.

Book chapters:

1. Kiliç, G., **Fernández-Bertólez, N.,** Costa, C., Brandão, F., Teixeira, J.P., Pásaro, E., Laffon, B., Valdiglesias, V., 2017. The Application, Neurotoxicity, and Related Mechanism of Iron Oxide Nanoparticles, In Neurotoxicity of Nanomaterials and Nanomedicine. Elsevier, pp. 127–150.
2. Laffon, B., **Fernández-Bertólez, N.,** Costa, C., Brandão, F., Teixeira, J.P., Pásaro, E., Valdiglesias, V., 2018. Cellular and molecular toxicity of iron oxide nanoparticles, In Advances in Experimental Medicine and Biology. pp. 199–213.

Conference proceedings:

1. Sánchez-Flores, M.; Kiliç, G.; Costa, C.; **Fernández-Bertólez, N.;** Costa, S.; Teixeira, J.P.; Pasaro, E.; Valdiglesias, V.; Laffon, B., 2015. Silica-coated iron oxide nanoparticles do not induce DNA double strand breaks or aneugenicity in SHSY5Y neuronal cells. Toxicol. Lett. 238S, S197
2. Costa, C.; Brandao, F.; Bessa, M.J.; Costa, S.; Valdiglesias, V.; Kiliç, G.; **Fernández-Bertólez, N.;** Pásaro, E.; Laffon, B.; Teixeira, J.P. 2015. In vitro toxicity screening of silica-coated superparamagnetic iron oxide nanoparticles in glial cells. Toxicol. Lett. 238S, S265.
3. Kiliç, G.; Costa, C.; **Fernández-Bertólez, N.;** Costa, S.; Teixeira, J.P.; Laffon, B.; Vdz Park, M.; Valdiglesias, V. 2015. Oxidative stress induced by silica coated iron oxide nanoparticles in SHSY5Y neuronal cells. Toxicol. Lett. 238S, S200.
4. Teixeira J.P., Laffon B, Kiliç G., **Fernández-Bertólez N.,** Costa C., Costa S., Passaro E. and Valdiglesias V. 2015. Comet assay assessment of oleic acid-coated magnetite nanoparticles on human SHSY5Y neuronal cells. Front. Genet. DOI: 10.3389/conf.fgene.2015.01.00026.

5. **Fernández Bertólez, N.,** Costa, C., Brandao, F., Fraga, S., Teixeira, J.P., Pásaro Méndez, E., Laffon Lage, B., Valdiglesias García, V. 2018. Toxicity assessment of iron oxide nanoparticles for biomedical applications. 2nd International Conference DiMoPEx working groups meeting: Pollution in living and working environments and health. pp. S71 - S72.

Congress communications:

1. Laffon, B., Kiliç, G., **Fernández-Bertólez, N.,** Costa, C., Costa, S., Teixeira, J.P., Pásaro, E., Valdiglesias, V. (2015, septiembre). Neuronal DNA damage induced by silica-coated iron oxide nanoparticles. Póster presentado al 11th International Comet Assay Workshop (ICAW), Antwerp, Belgium.
2. Laffon, B., Kiliç, G., **Fernández-Bertólez, N.,** Costa, C., Costa, S., Teixeira, J.P., Pásaro, E., Valdiglesias, V. (2015, septiembre). Comet assay assessment of oleic acid-coated magnetite nanoparticles on human SHSY5Y neuronal cells. Póster presentado al 11th International Comet Assay Workshop (ICAW), Antwerp, Belgium.
3. Kiliç, G., Costa, C., **Fernández-Bertólez, N.,** Costa, S., Teixeira, J.P., Pásaro, E., Laffon, B., Park, M., Valdiglesias, V. (2015, septiembre). Oxidative stress induced by silica coated iron oxide nanoparticles in SHSY5Y neuronal cells. Póster presentado al 51st Congress of the European Societies of Toxicology (EUROTOX), Porto, Portugal.
4. Sánchez-Flores, M., Kiliç, G., Costa, C., **Fernández-Bertólez, N.,** Costa, S., Teixeira, J.P., Pásaro, E., Valdiglesias, V. Laffon, B. (2015, septiembre). Silica-coated iron oxide nanoparticles do not induce DNA double strand breaks or aneugenicity in SHSY5Y neuronal cells. Póster presentado al 51st Congress of the European Societies of Toxicology (EUROTOX), Porto, Portugal.
5. Costa, C., Brandao, F., Bessa, M.J., Costa, S., Valdiglesias, V., Kiliç, G., **Fernández-Bertólez, N.,** Pasaro, E., Laffon, B., Teixeira, J.P. (2015, septiembre). In vitro toxicity screening of silica-coated superparamagnetic iron oxide nanoparticles in glial cells. Póster presentado al 51st Congress of the European Societies of Toxicology (EUROTOX), Porto, Portugal.
6. Kiliç, G., **Fernández-Bertólez, N.**, Costa, C., Costa, S., Teixeira, J.P., Pásaro, E., Laffon, B., Valdiglesias, V. (2015, octubre). Toxic effects of silica coated iron oxide nanoparticles on human neuronal cells. Comunicación oral presentada en la Conference of the International Society for Trace Element Research in Humans (ISTERH), Dubrovnik, Croatia.
7. Laffon, B., **Fernández-Bertólez, N.,** Méndez, J., Pásaro, E., Valdiglesias, V. (2016, junio). Considering cell type for in vitro neurogenotoxicity testing: neuronal vs. glial cell sensitivity. Póster presentado al 3rd International Conference on Occupational & Environmental

Toxicology (ICOETOX) y 3rd Ibero-American Meeting on Toxicology and Environmental Health (IBAMTox), Oporto, Portugal.

8. **Fernández-Bertólez, N.,** Laffon, B., Kiliç, G., Costa, C., Costa, S., Teixeira, J.P., Pásaro, E., Valdiglesias, V. (2016, junio). Evaluación de la genotoxicidad de nanopartículas de óxido de hierro en células gliales humanas. Comunicación oral en el XXII Congreso de la Sociedad Española de Mutagénesis Ambiental (SEMA), Barcelona, España.

9. Laffon, B., Kiliç, G., **Fernández-Bertólez, N.**, Costa, C., Costa, S., Teixeira, J.P., Pásaro, E., Valdiglesias, V. (2016, junio). Analysis of cellular damage induced by silica-coated iron oxide nanoparticles on neuronal cells. Ponencia invitada en la 3rd International Conference on Occupational & Environmental Toxicology (ICOETOX) y 3rd IberoAmerican Meeting on Toxicology and Environmental Health (IBAMTox), Porto, Portugal.

10. Brandao, F.; Costa, C.; Valdiglesias, V.; **Fernández-Bertólez, N.;** Pásaro, E.; Laffon, B.; Teixeira, J.P. (2017, marzo). Genotoxicity evaluation of nanomaterials: What is the most suitable option of in vitro cytokinesis-block micronucleus cytome assay?. Póster presentado al 56th Society of Toxicology anual meeting and ToxExpo, Maryland (Baltimore), USA.

11. **Fernández Bertólez, N.,** Costa, C., Brandão, F., Fraga, S., Teixeira, J.P., Pásaro, E., Laffon, B., Valdiglesias, V. (2017, junio). Human astrocytes DNA repair competence: influence of iron oxide nanoparticle surface coating. Comunicación oral en el XXIII Congreso de la Sociedad Española de Mutagénesis Ambiental (SEMA), Oviedo, España.

12. **Fernández Bertólez, N.**, Costa, C., Brandao, F., Teixeira, J.P., Pásaro, E., Valdiglesias, V., Laffon, B. (2017, septiembre). Effects of two types of iron oxide nanoparticles on DNA repair competence in human astrocytes. Ponencia invitada en la 12th International Comet Assay Workshop (ICAW), Pamplona, España.

13. **Fernández-Bertólez, N.,** Costa, C., Brandao, F., Fraga, S., Teixeira, J.P., Pásaro, E., Laffon, B., Valdiglesias, V. (2017, octubre). Toxicity assessment of iron oxide nanoparticles for biomedical applications. Póster presentado en la 2nd International Conference DiMoPEx working groups meeting: Pollution in living and working environments and health. Bentivoglio, Italia.

14. **Fernández-Bertólez, N.,** Costa, C., Brandao, F., Fraga, S., Pásaro, E., Laffon, B., Valdiglesias, V., Teixeira J.P. (2018, marzo). Genotoxicity Assessment of Iron Oxide Nanoparticles on Human Astrocytes. Póster presentado en la 57th Annual Meeting and ToxExpo (SOT). San Antonio, Texas, Estados Unidos de América.

15. Valdiglesias, V., **Fernández-Bertólez, N.,** Costa, C., Brandão, F., Fraga, S., Teixeira, J.P., Pásaro, E., Laffon, B. (2018, octubre). Cytotoxicity of silica-coated iron oxide nanoparticles in human astrocytes. Póster presentado en el 4th International Congress on Occupational & Environmental Toxicology (ICOETOX), Matosinhos, Portugal.

Agradecimientos

En primer lugar, me gustaría agradecer a mis codirectoras, la Dra. Blanca Laffon Lage y la Dra. Vanessa Valdiglesias García, no sólo por brindarme la oportunidad de realizar este apasionante trabajo en su grupo de investigación, sino sobre todo y para mí más importante, por su enorme calidad humana. Con su apoyo, comprensión, inestimables consejos y su constante guía me han hecho mejor persona. Muchas gracias de corazón por haberme ayudado a conseguir este sueño.

También me gustaría agradecer a mis compañeros de laboratorio y también de aventuras, María y Diego. Por estar siempre ahí en los buenos, y no tan buenos momentos, ayudándome, escuchándome y compartiendo ésta difícil, aunque también gratificante experiencia. Sin vosotros habría sido todo mucho más complicado, y sé que más que amigos, os habéis convertido en parte de mi familia. A Gözde, Aida y a todos aquellos que compartieron su tiempo conmigo durante esta etapa. De todos ellos he aprendido algo y espero haber dejado en ellos un buen recuerdo. Gracias también al Dr. Eduardo Pásaro Méndez por darme la oportunidad de trabajar en su equipo y llevar a cabo este trabajo.

Quisiera agradecer de forma especial a los miembros del Laboratorio de Epidemiología Ambiental del Instituto de Salud Pública de la Universidad de Porto (ISPUP), Portugal, especialmente al Dr. João Paulo Teixeira por acogerme en su laboratorio durante mi estancia internacional, por darme la oportunidad de completar mi formación y por todas sus enseñanzas; y a la Dra. Carla Costa por su inestimable colaboración en este trabajo, y también por su ayuda y apoyo en esta investigación.

También me gustaría dar las gracias a los miembros del Laboratorio de Genética de la Universidade da Coruña, en especial a la Dra. Josefina Méndez Felpeto, por abrirme una puerta en un momento difícil de mi vida, de corazón, muchas gracias; y también a su grupo de investigación, Ana, Verónica y Jennifer, por su compañía y su ayuda en días interminables de trabajo.

Finalmente, dar las gracias a mi familia. A mi madre y mi tía porque todo lo que soy se lo debo a ellas, gracias a todos sus sacrificios he llegado hasta aquí, espero que estéis orgullosas de lo que he conseguido. A Daniel, mi marido, por su cariño, comprensión, apoyo y confianza en mí, por cubrirme las espaldas en tantas ausencias familiares y porque siempre me anima y empuja a conseguir la mejor versión de mí misma, desde luego el mejor compañero de vida. Y a mis hijos, porque sin saberlo también han hecho sacrificios. Espero serviros de ejemplo y que os sintáis orgullosos. Todo esto también es por y para vosotros, para que entendáis que nunca es tarde si realmente se desea, y que con trabajo y esfuerzo los sueños imposibles sólo tardan un poco más en conseguirse. Os quiero con toda mi alma.

«I know what I want, I have a goal, an opinion, I have a religion and love. Let me be myself and then I am satisfied. I know that I am a woman, a woman with inward strength and plenty of courage».

The Diary of Anne Frank

by Anne Frank

Abstract

Due to their unique physicochemical properties, iron oxide nanoparticles (ION) have great potential for several biomedical applications, particularly those focused on nervous system. ION surface can be coated to improve their properties and biocompatibility. Still, coating may affect toxicity, making it imperative knowing the potential risk associated to nervous system exposure. The aim of this Thesis was to assess the potential cytotoxicity and genotoxicity induced by differently coated ION on human neurons (SH-SY5Y) and astrocytes (A172), under a range of doses, two treatment times and presence/absence of serum in the cell culture media. Cellular uptake of ION and iron ion release from the ION surface were also determined. In general, silica-coated ION (S-ION) showed less cytotoxicity and slightly lower genotoxic effects than oleic acid-coated ION (O-ION), not related to double strand breaks (DSB) or chromosome alterations. Furthermore, A172 astrocytes proved to be more sensitive than SH-SY5Y neurons to the toxic effect of both ION. In addition, primary DNA damage observed in both cell types only included DSB in astrocytes. This work increases the knowledge on the impact of ION on human health in general, and specifically on nervous system cells.

Resumen

Debido a sus propiedades fisicoquímicas únicas, las nanopartículas de óxido de hierro (ION) tienen un gran potencial para varias aplicaciones biomédicas, particularmente aquellas enfocadas en el sistema nervioso. La superficie de ION se puede revestir para mejorar sus propiedades y biocompatibilidad. Aun así, el recubrimiento puede afectar a su toxicidad, por lo que es imperativo conocer el riesgo potencial asociado a la exposición del sistema nervioso. El objetivo de esta Tesis fue evaluar la posible citotoxicidad y genotoxicidad inducida por ION con diferentes recubrimientos en neuronas humanas (SH-SY5Y) y astrocitos (A172), en un rango de dosis, dos tiempos de tratamiento y presencia/ausencia de suero en los medios de cultivo celular. También se determinó la captación celular de las ION y la liberación de iones de hierro desde su superficie. En general, las ION recubiertas de sílice (S-ION) mostraron menos citotoxicidad y efectos genotóxicos ligeramente menores que las ION recubierto con ácido oleico (O-ION), no relacionado con roturas de cadena doble (DSB) o alteraciones cromosómicas. Además, los astrocitos A172 demostraron ser más sensibles que las neuronas SH-SY5Y al efecto tóxico de ambas ION. Además, el daño primario del ADN observado en ambos tipos de células solo incluía DSB en los astrocitos. Este trabajo aumenta el conocimiento sobre el impacto de ION en la salud humana en general, y específicamente en las células del sistema nervioso.

Resumo

Debido ás súas propiedades físicoquímicas únicas, as nanopartículas de óxido de ferro (ION) teñen gran potencial para diversas aplicacións biomédicas, en particular as que se centran no sistema nervioso. A superficie das ION pode revestirse para mellorar as súas propiedades e a súa biocompatibilidade. Aínda así, o revestimento pode afectar a toxicidade, por iso, é imperativo coñecer os riscos potenciais asociados coa exposición do sistema nervioso. O obxectivo desta Tese foi o de avaliar a posible citotoxicidade e genotoxicidade inducida polas ION con diferentes revestimentos en neuronas humanas (SH-SY5Y) e astrocitos (A172), nun intervalo de doses, dous tempos de tratamento e en presenza/ausencia de soro nos medios de cultura celular. A captación celular das ION e a liberación de ións de ferro a partir da súa superficie, tamén foron determinadas. En xeral, as ION revestidas de sílice (S-ION) amosaron menos citotoxicidade e efectos genotóxicos lixeiramente máis baixos que as ION revestidas con ácido oleico (O-ION), sen relación con roturas de cadea dobre (DSB) ou alteracións cromosómicas. Ademáis, os astrocitos A172 amosaron ser máis sensibles que as neuronas SH-SY5Y ó efecto tóxico de ambas ION. Ademáis, o dano primario no ADN observado en ambos tipos celulares só incluía DSB nos astrocitos. Este traballo aumenta o coñecemento sobre o impacto das ION na saúde humana en xeral, e específicamente nas células do sistema nervioso.

Extended summary in Spanish - Resumen amplio

La nanotecnología puede definirse como la investigación, diseño y manipulación de la materia en dimensiones de aproximadamente 1 a 100nm. En esta pequeña escala surgen nuevas propiedades físicas, químicas y biológicas diferentes a las de los materiales de mayor tamaño con la misma composición química, como consecuencia de la elevada proporción superficie/volumen.

La nanotecnología es un área en rápida expansión con perspectivas muy prometedoras; actualmente son 3037 los productos de consumo inventariados que contienen nanomateriales. Con el aumento de las aplicaciones de los nanomateriales, especialmente con fines biomédicos, también han aumentado las inquietudes con respecto a la aparición de efectos sobre la salud asociados a la exposición. Esto ha dado lugar a un creciente debate público sobre la toxicidad y el impacto ambiental de los nanomateriales, ya que sus nuevas propiedades pueden ocasionar cambios en la interacción con los componentes celulares y aparición de efectos adversos inesperados.

Entre todos los nanomateriales, las nanopartículas de óxido de hierro (ION de *iron oxide nanoparticles*) despiertan un interés particular principalmente en el campo biomédico, debido a sus características fisicoquímicas especiales, su aparente biocompatibilidad, y porque exhiben una forma única de magnetismo llamada superparamagnetismo. Las aplicaciones más prometedoras de las ION son como agente de contraste en imágenes de resonancia magnética, la administración dirigida de fármacos, terapia génica y reparación de tejidos, y el tratamiento de tumores por hipertermia. En concreto, las ION han demostrado en la última década ser muy útiles para una serie de aplicaciones relacionadas principalmente con el diagnóstico y tratamiento de enfermedades del sistema nervioso central (SNC), tales como el Parkinson, el Alzheimer, la esclerosis múltiple, neoplasias del sistema nervioso o enfermedades neurodegenerativas visuales.

Las ION generalmente están compuestas por un núcleo cristalino que puede presentar múltiples estructuras cristalográficas, entre las cuales la magnetita, la maghemita y la hematita son las más comúnmente utilizadas debido a su polimorfismo. Específicamente, la magnetita es la ION más frecuente en biomedicina, ya que su magnetización es más alta. Un problema común asociado con las ION es su inestabilidad intrínseca durante largos períodos de tiempo, ya que tienden a formar aglomerados, son altamente reactivas químicamente y se oxidan con facilidad, lo que generalmente produce pérdida de magnetismo y capacidad de dispersión. Para minimizar estos efectos, la superficie de las ION puede modificarse recubriéndolas con diferentes materiales, para estabilizarlas en medios fisiológicos, aumentar su biocompatibilidad, modificar la eficiencia de captación celular, y potenciar sus propiedades en aplicaciones biomédicas, aunque también puede alterar su toxicidad. Por otro lado, el gran potencial de las ION se debe principalmente a

sus propiedades físicas y químicas únicas, que muestran una dependencia compleja de varios factores como su forma, tamaño, estructura, composición y reactividad superficial, ausencia/presencia de recubrimiento y estabilidad química (*e.g.*, solubilidad y aglomeración/agregación). La carga superficial de las nanopartículas tiene también gran importancia en la producción de efectos biológicos, ya que es un factor principal en la determinación de las características de dispersión y también influye en la adsorción de iones y biomoléculas, en especial proteínas (corona biomolecular), que pueden cambiar la manera en la que las células interaccionan con las nanopartículas.

Se ha demostrado que las ION tienen capacidad para atravesar la barrera hematoencefálica (BHE), pudiendo así acceder al SNC. Aunque la translocación de las ION al cerebro ha sido estudiada bajo diferentes condiciones experimentales, aún no está claro si son generalmente seguras o deben usarse con prudencia. La falta de evaluaciones toxicológicas completas y estandarizadas hace difícil la interpretación de los resultados obtenidos hasta el momento, sobre todo en el caso de la neurotoxicidad. Esto se debe, al menos en parte, a que los resultados disponibles sobre los posibles efectos tóxicos de las ION en el SNC son escasos y contradictorios, y no siempre son comparables ya que están influenciados por diversos factores, como el tipo de ION y sus características fisicoquímicas, el tipo de célula analizada o las condiciones experimentales evaluadas. Se hace necesaria, por tanto, la evaluación de los efectos tóxicos que las ION puedan ocasionar en las células del sistema nervioso humano.

Para garantizar la seguridad del uso diagnóstico o terapéutico de las ION, éstas no deben ser tóxicas para las células en concentraciones adecuadas para la orientación magnética u otras aplicaciones biomédicas. Sin embargo, se ha demostrado en varios estudios *in vitro* e *in vivo* que las ION, desnudas o recubiertas con diferentes sustancias, pueden inducir efectos adversos, incluso a dosis bajas, como la disminución de la viabilidad celular, alteraciones del citoesqueleto, liberación de iones de hierro, inducción de estrés oxidativo o disfunción mitocondrial, entre otros. Además, sus posibles efectos sobre otras funciones celulares diferentes, sobre el material genético o sobre la capacidad de reparación del ADN no pueden tampoco ser descartados ya que apenas han sido abordados hasta la fecha en células nerviosas humanas.

Sobre esta base, el objetivo principal de este trabajo fue evaluar la posible citotoxicidad y genotoxicidad inducida en células neuronales y gliales (astrocitos) por exposición a ION con diferentes recubrimientos. En concreto, se analizó la citotoxicidad asociada con la exposición a las ION, en términos de alteraciones en la integridad de la membrana (mediante el ensayo de liberación de lactato deshidrogenasa [LDH]) o en el ciclo celular, y la inducción de la muerte celular (apoptosis y necrosis); se examinaron además los efectos genotóxicos relacionados con el tratamiento con las ION, analizando la inducción de daño primario en el ADN (por el ensayo del

cometa), de roturas de cadena doble (ensayo γH2AX) y de alteraciones cromosómicas (test de micronúcleos [MN]); y, por último, se evaluaron las modificaciones en los procesos de reparación del ADN causados por las ION (por el ensayo de competencia de reparación).

Cada uno de estos ensayos se realizó en células neuronales SH-SY5Y y células gliales A172 (astrocitos), testando dos tipos de ION – recubiertas con sílice (S-ION) y con ácido oleico (O-ION), cuyas características físico-químicas habían sido determinadas con anterioridad – en un rango de condiciones experimentales que incluyeron dosis de 10 a 200µg/ml para neuronas, y de 5 a 100µg/ml para astrocitos, dos tiempos de tratamiento (3 y 24h), y presencia o ausencia de suero en los medios de cultivo celular. Las concentraciones y tiempos de exposición se eligieron en base a resultados de viabilidad celular obtenidos previamente en nuestro laboratorio. Las condiciones experimentales seleccionadas para el estudio fueron aquellas que inducían una disminución máxima en la viabilidad de ambos tipos celulares del 30%, evitando así la posible influencia de la disminución excesiva de la viabilidad en los resultados de los diferentes parámetros evaluados.

Antes de analizar los posibles efectos tóxicos de las nanopartículas, se verificó la efectiva internalización de las ION en las células nerviosas a través de citometría de flujo y microscopía electrónica de transmisión. Además, se evaluó por espectroscopia de absorción atómica de llama la concentración de iones de hierro liberados en los medios de cultivo celular empleados.

En las secciones de Resultados y Discusión de la presente memoria se analizan y comparan los resultados experimentales obtenidos subdividiéndolos en función del tipo celular y la ION testada.

Células SH-SY5Y tratadas con S-ION

En el análisis de la liberación de iones de hierro a partir de las suspensiones de S-ION en medio de cultivo SH-SY5Y se detectaron bajas concentraciones de hierro en medio libre de suero, mientras que la liberación de iones fue notable en presencia de suero (medio completo), aumentando en general con el tiempo y la concentración de las S-ION. Por otra parte, los datos obtenidos confirmaron que las células SH-SY5Y captaron las S-ION de forma efectiva, siendo mayor la captación en ausencia de suero.

A pesar de que la evaluación de la integridad de la membrana celular, mediante el ensayo de liberación de LDH, mostró resultados negativos en todas las condiciones ensayadas, los resultados de la evaluación de los efectos citotóxicos mostraron un aumento de células en la fase S del ciclo celular, y/o disminución de células en la fase G_2/M, para tratamientos de 24h en ambos medios de cultivo a la dosis más alta probada. Además, el único aumento significativo observado

en la tasa de apoptosis fue para las concentraciones más elevadas de S-ION tras los tratamientos de 24h en ambos medios analizados. Por otra parte, el análisis de la muerte celular por necrosis (y/o apoptosis tardía), y el análisis de la integridad de membrana no mostraron alteraciones en las células SH-SY5Y expuestas a S-ION en ninguna de las condiciones ensayadas.

Respecto a los ensayos de genotoxicidad, no se observaron aumentos significativos en los niveles de γH2AX, ni de formación de MN en las células SH-SY5Y expuestas a las S-ION. Sin embargo, los resultados del ensayo del cometa mostraron un incremento en el daño primario en el ADN dependiente de la dosis y del tiempo en medio completo, paralela a las cantidades importantes de iones de hierro liberados de las nanopartículas en ese medio. Los iones de hierro son capaces de interactuar con el ADN entre las bases, y causar roturas de cadena sencilla (SSB) y modificación oxidativa de las bases. Analizando conjuntamente todos los resultados de genotoxicidad, el tipo de daño en el ADN inducido por las S-ION en células neuronales probablemente no esté relacionado con roturas de cadena doble (DSB), sino principalmente con lesiones fácilmente reparables (sitios sensibles al álcali y SSB).

En resumen, a pesar de ser efectivamente internalizadas por las células neuronales, las S-ION presentaron una citotoxicidad en general baja, obteniéndose resultados positivos únicamente en algunos ensayos a las concentraciones más altas y/o al tiempo de exposición más prolongado. Las evaluaciones de genotoxicidad en medio sin suero fueron negativas para todas las condiciones analizadas, mientras que en medio con suero se observó un aumento dependiente de la dosis y del tiempo en el daño en el ADN, no relacionado con la producción de DSB o la pérdida cromosómica (de acuerdo con los resultados del ensayo γH2AX y el test de MN). Las diferencias observadas en los tres ensayos de genotoxicidad aplicados, con respecto a su sensibilidad para detectar diferentes tipos de daño genético, confirman la necesidad de usarlos en combinación, ya que se complementan entre sí. La internalización de las nanopartículas por las células, la citotoxicidad y los efectos sobre la reparación del ADN fueron más pronunciados en ausencia de suero. Por el contrario, la liberación de iones de hierro y el daño primario del ADN sólo se observaron en el medio completo. La formación de una corona de proteínas en presencia de suero probablemente juegue un papel importante en estas diferencias.

Células SH-SY5Y tratadas con O-ION

La liberación de iones de hierro desde la superficie de las O-ION en medio completo se mostró dependiente de la dosis, mientras que las O-ION suspendidas en medio sin suero fueron muy estables en todas las condiciones evaluadas. Los resultados de captación celular obtenidos muestran que las células SH-SY5Y pueden internalizar de manera eficiente estas nanopartículas

en todas las condiciones experimentales probadas, independientemente de la composición del medio.

En cuanto a la citotoxicidad, los datos obtenidos sugirieron que las proteínas del suero interaccionan con el recubrimiento de ácido oleico ejerciendo un cierto efecto protector y disminuyendo ligeramente la inducción de citotoxicidad. La ausencia de liberación significativa de LDH por las células neuronales sugiere que las O-ION, en general, no alteran la integridad de la membrana celular a concentraciones bajas y medias. Por otra parte, las O-ION alteran la progresión normal del ciclo celular de SH-SY5Y, de forma particularmente notable después de 24h de tratamiento en medio sin suero, induciendo un aumento significativo dependiente de la dosis en la fase G_0/G_1 junto con una clara disminución en la región G_2/M, sugiriendo la detención del ciclo celular previo a la mitosis. Además, los resultados del análisis de muerte celular mostraron incrementos significativos en las tasas de apoptosis en ambos medios. Sin embargo, las O-ION no produjeron necrosis en ninguna de las condiciones evaluadas, lo que sugiere que inducen la muerte celular principalmente a través de la vía apoptótica.

En general, la presencia de suero tuvo una influencia ligera sobre la genotoxicidad inducida por las O-ION y los efectos sobre la capacidad de reparación. Los resultados del ensayo del cometa mostraron que las O-ION indujeron daño primario del ADN en las células expuestas, no relacionado con la inducción de DSB en ninguna condición probada. Además, sólo se detectaron aumentos significativos en la frecuencia de MN en células SH-SY5Y después de 24h de exposición a las dosis más altas de O-ION en medio sin suero, sugiriendo que el daño primario del ADN detectado en el ensayo del cometa sólo se fijó como alteraciones cromosómicas en estas condiciones. El ensayo de competencia de reparación del ADN mostró un efecto similar de las O-ION en ambos medios testados, consistente en alteraciones en la capacidad de reparación cuando las células se trataron antes o durante la incubación con H_2O_2, pero no cuando el tratamiento se realizó durante el periodo de reparación.

En conclusión, los resultados obtenidos en células neuronales mostraron que las O-ION presentan una citotoxicidad moderada a altas concentraciones, relacionada con el deterioro de la membrana celular, la disrupción del ciclo celular y la inducción de muerte celular, especialmente marcada en el medio sin suero. Por el contrario, la liberación de iones de hierro sólo se observó en medio completo, lo que indica que la citotoxicidad observada no está relacionada con la presencia de estos iones en el medio. Sin embargo, los efectos genotóxicos de las O-ION se limitaron a la inducción de daño primario en el ADN, no relacionado con DSB y fácilmente reparable, y además este daño no se fijó en las células en la mayoría de las condiciones.

Células A172 tratadas con S-ION

Mientras que las S-ION suspendidas en medio sin suero fueron muy estables en todas las condiciones probadas, las suspensiones de estas nanopartículas en medio completo mostraron un aumento en la liberación de iones de hierro dependiente de la concentración, particularmente notable en el tiempo de exposición más prolongado. Los datos de la captación celular de nanopartículas revelaron la presencia de las S-ION internalizadas en astrocitos A172 en todas las condiciones probadas, independientemente de la composición del medio o del tiempo de exposición. Además, se observó que las S-ION se acumulaban en vesículas intracelulares, lo que sugiere una entrada por endocitosis de las mismas.

Las S-ION no alteraron la integridad de la membrana plasmática en las condiciones evaluadas en este estudio, como lo demuestran los resultados negativos revelados en la evaluación de liberación de LDH. Los resultados obtenidos del análisis del ciclo celular mostraron importantes alteraciones inducidas por las S-ION dependientes de la dosis, particularmente marcadas en los tratamientos de 24h, en los que el ciclo celular de las células A172 resultó significativamente alterado en todas las condiciones probadas. Estos efectos incluyeron principalmente alteraciones en las fases G_0/G_1 y S, reflejando una posible parada mitótica. Los resultados de muerte celular mostraron la inducción de apoptosis y necrosis limitadas a las dosis más altas de S-ION y al tiempo de exposición más prolongado en medio completo. Sin embargo, en medio libre de suero se observaron aumentos significativos de las tasas de apoptosis dependientes de la dosis en ambos tiempos de exposición, al igual que aumentos significativos dependientes de la dosis de células necróticas únicamente en el tratamiento de 3h.

Por otra parte, las S-ION no indujeron incrementos significativos de γH2AX en los astrocitos A172, excepto en las concentraciones más altas después de 24h de tratamiento. Teniendo en cuenta los resultados obtenidos en la liberación de iones de hierro de las nanopartículas, el aumento detectado parece ser más probablemente debido al efecto indirecto de los iones de hierro, que a las propiedades genotóxicas de las S-ION. Los resultados del ensayo del cometa mostraron que las S-ION inducen daño primario en el ADN sólo a las concentraciones más altas después de un corto período de exposición, pero a partir de dosis más bajas, de una manera dependiente de la dosis, después de 24h de tratamiento. No se observó inducción de MN en ninguna de las condiciones probadas, lo que indica, por un lado, que las S-ION no inducen efectos aneugénicos en los astrocitos, y por otro, que estas células fueron capaces de reparar el daño primario del ADN producido inicialmente por la exposición (revelado por la respuesta positiva del ensayo del cometa), evitando así su fijación como alteraciones cromosómicas (MN). Por último, las S-ION no interfirieron en la capacidad de reparación de los astrocitos A172, en ninguna condición probada, indicativo de una reparación eficiente en presencia de S-ION.

En resumen, los resultados mostraron que la ausencia de suero en el medio tiene cierta influencia sobre la citotoxicidad de las S-ION en células A172, lo que resulta en efectos celulares más pronunciados (ciclo celular, apoptosis y necrosis). Sin embargo, en general no se encontraron diferencias notables debidas a la composición del medio en la inducción de genotoxicidad o alteraciones en la reparación del ADN, que se limitó a la producción de daño primario fácilmente reparable.

Células A172 tratadas con O-ION

Los resultados de la cuantificación de los iones de hierro liberados de la superficie de O-ION mostraron liberación de iones dependiente de la dosis y el tiempo en medio completo, mientras que en medio libre de suero resultaron muy estables. Los resultados de captación de nanopartículas demostraron la internalización efectiva de las O-ION por las células A172, independientemente de la dosis, la composición del medio o el tiempo de exposición.

Los resultados mostraron que las O-ION exhiben una citotoxicidad moderada en astrocitos. Mientras que la exposición a las O-ION no comprometió la integridad de la membrana de las células A172, el análisis de la distribución del ciclo celular mostró una parada significativa del mismo, dependiente de la dosis, en la fase S en todas las condiciones probadas, lo que indica que las O-ION alteran claramente la progresión normal de su ciclo celular. Asimismo, se observaron aumentos significativos en las tasas de apoptosis tras la exposición a O-ION, junto con un aumento ligero pero significativo en las tasas de necrosis cuando los tratamientos se realizaron en medio completo, pero no en medio sin suero.

Las pruebas de genotoxicidad demostraron la inducción de daño primario en el ADN de astrocitos dependiente de la dosis de O-ION, particularmente en presencia de suero en el medio. Además, se detectaron ligeros incrementos significativos en los niveles de γH2AX. No obstante, no se observó inducción de MN por exposición a las O-ION.

En resumen, los resultados obtenidos mostraron que las O-ION presentan citotoxicidad moderada en astrocitos, relacionada con la detención de la proliferación y la muerte celular (principalmente por vía apoptótica), y causan efectos genotóxicos, principalmente daño primario del ADN que no se fija como alteraciones cromosómicas. Estos efectos no estuvieron influidos por la presencia de suero en el medio. Por el contrario, la notable liberación de iones de hierro únicamente el medio completo indica que la citotoxicidad y genotoxicidad detectadas no fueron causadas por la disrupción de la homeostasis del hierro. Por último, no se obtuvieron alteraciones en los procesos de reparación del ADN en presencia de las O-ION.

A la luz de todos los resultados obtenidos en el presente trabajo, el recubrimiento de sílice parece ser menos tóxico y más biocompatible que el de ácido oleico para las líneas celulares nerviosas empleadas. En general, las S-ION mostraron menos citotoxicidad que las O-ION. Además, las S-ION exhibieron efectos genotóxicos de intensidad ligeramente inferior que las O-ION en ambas líneas celulares, no relacionados con la inducción de DSB y no fijados en las células SH-SY5Y o A172 después de la división celular. Una posible explicación puede ser que ocurra una transferencia más rápida de las O-ION internalizadas al compartimiento lisosómico y que se produzca una mayor tasa de disolución del recubrimiento de ácido oleico al pH ácido del lisosoma, lo que podrían generar mayores cantidades de iones de hierro disponibles, y causar mayor daño celular. Además, las O-ION presentan alta tendencia a formar aglomerados de pequeño tamaño, especialmente en medio sin suero, probablemente debido a la ausencia de interacciones superficiales con las proteínas séricas del medio biológico (corona de proteína), lo que modifica su tamaño hidrodinámico y estabilidad. Este hecho podría influir en gran medida en la interacción biológica de las O-ION con sus dianas celulares y en su mayor efecto tóxico respecto al recubrimiento de sílice.

Por otra parte, en cuanto a la comparación entre las células utilizadas, los astrocitos A172 demostraron ser más vulnerables que las neuronas al efecto tóxico de S-ION y O-ION. Aunque en ambos tipos celulares se han observado efectos citotóxicos después de la exposición a ambas ION, estos efectos fueron en general mayores en los astrocitos que en las neuronas. Además, los dos tipos celulares presentaron daño primario en el ADN tras la exposición a las ION, pero únicamente en el caso de las células A172 se relacionó con la producción de DSB, un tipo más grave de daño genético. No obstante, en ambos casos este daño parece que fue reparado, ya que no condujo a su fijación en forma de alteraciones cromosómicas en la mayoría de condiciones. La fase del ciclo celular en la que se encuentran ambos tipos celulares en el momento del tratamiento puede provocar la expresión de diferentes biomoléculas e influir en la respuesta a estímulos exógenos, tales como la exposición a las ION. Además, las diferentes características de los tipos de células involucradas en la fisiología del sistema nervioso pueden determinar una respuesta diversa ante los xenobióticos.

En suma, los resultados obtenidos en esta Tesis contribuyen a aumentar el conocimiento sobre el impacto de las ION en la salud en general, y específicamente en las células del sistema nervioso humano. Dado que las ION tienen un gran potencial en el diagnóstico y tratamiento de diversos trastornos del SNC en un futuro próximo, un conocimiento profundo sobre su potencial citotóxico y genotóxico resulta crucial para asegurar su uso con una adecuada relación beneficio/coste.

INDEX

List of abbreviations

8-oxoG	8-oxoguanine
%tDNA	percentage of DNA in the comet tail
α-Fe_2O_3	hematite
γ-Fe_2O_3	maghemite
µm	micrometre
µM	micromolar
µl	microliter
APTMS	(3-aminopropyl)trimethoxysilane
ATP	adenosine triphosphate
BBB	blood-brain barrier
BET	Brunauer-Emmett-Teller
BLM	bleomycin
Campt	camptothecin
CNS	central nervous system
DAPI	4,6-diamidino-2-fenilindol
DLS	dynamic light scattering
DMSA	dimercaptosuccinic acid
DMSO	dimethylsulfoxide
DNA	deoxyribonucleic acid
DSB	DNA double strand breaks
EC	European Commission
EDX	energy-dispersive X-ray spectroscopy
EPA	Environmental Protection Agency
FAAS	flame atomic absorption spectroscopy
FBS	foetal bovine serum
FCM	flow cytometry
FDA	United States Food and Drug Administration
Fe^{2+}	ferrous ion
Fe^{3+}	ferric ion
Fe_3O_4	magnetite
FeO	wüstite
FSC	forward scatter
h	hours
ION	iron oxide nanoparticles
ISO	International Standards Organization
LDH	lactate dehydrogenase
LMA	low-melting-point agarose
M3-PALS	mixed mode measurement phase analysis light scattering
mA	milliampere
MMC	mitomycin C
MN	micronucleus
MRI	magnetic resonance imaging
MTT	3-(4,5-dimethylthiazol-2-yl)-2,5-diphenyltetrazolium bromide
mV	millivolt
NIOSH	National Institute for Occupational Safety and Health
nm	nanometre
NMA	normal melting point agarose

NP	nanoparticles
NRU	neutral red uptake
O-ION	oleic acid-coated ION
OECD	Organization for Economic Co-operation and Development
OH•	hydroxyl radicals
PBS	phosphate buffer solution
PI	propidium iodide
RNA	ribonucleic acid
ROS	reactive oxygen species
SiO_2	silica
S-ION	silica-coated ION
siRNA	small interfering RNA
SSB	DNA single strand breaks
SSC	side scatter
TEM	transmission electron microscope
TEOS	tetraethyl-orthosilicate
UV	ultraviolet
W	watt
WHO	World Health Organization
XPS	photoelectron spectroscopy

List of figures

Figure I.10. Summary of possible mechanisms used by nanoparticles to enter cells and cellular compartments. From left to right, nanoparticles may actively be taken up by cells by passive diffusion, clathrin-mediated endocytosis, caveolae-mediated endocytosis, via phagocytosis, or macropinocytosis (from Cores *et al.,* 2015).

Figure I.11. Flow cytometry analysis of nanoparticle uptake in cells: a) light scattering by a cell that is not associated with any nanoparticle; b) nanoparticles adhere to the cell surface, leading to an increase in forward scatter (FSC) and side scatter (SSC); c) nanoparticle internalization by the cell, leading to an increase in SSC only; d) FSC/SSC dot plot from FCM analysis with cells no exposed to ION; e) FSC/SSC dot plot from FCM analysis showing a high proportion of cells with internalized nanoparticles (R2).

Figure I.12. In normal cells, phosphatidylserines (purple membrane phospholipids) are held on the inner layer of the cell membrane, so annexin V does not attach to the cells. During early apoptosis, the phosphatidilserines are exposed on the outer layer, where they attach to the FITC-labeled Annexin V and stain the cell surface green. During late apoptosis, propidium iodide (PI) enters the cell and stains the contents red (from https://www.nacalai.co.jp/global/download/pdf/AnnexinV-FITC.pdf).

Figure I.13. Fluorescence microscopy image of cell nucleoids after comet assay: A) not damaged nucleoid, B) mildly damaged nucleoid, C) highly damaged nucleoid.

Figure I.14. Representation of H2AX phosphorylation as a response to double strand breaks (DSB). ATM, ataxia telangiectasia mutated (modified from Hoeller and Dikic, 2009).

Figure I.15. Representation of MN formation in cells undergoing nuclear division (from Fenech *et al.,* 2011).

Figure IV.1: Analysis of iron ions released from S-ION in (A) complete cell culture medium and (B) serum-free cell culture medium. Bars represent the mean ± standard error.

Figure IV.2: Neuronal cell uptake of S-ION prepared in complete and serum-free medium. Bars represent the mean ± standard error. $^{**}P<0.01$, significant difference with regard to the corresponding negative control.

Figure IV.3: Results of membrane integrity assessment in SH-SY5Y cells exposed to S-ION in complete and serum-free medium. Bars represent the mean ± standard error. PC: positive control (1% Triton X-100). $^{**}P<0.01$, significant difference regarding the corresponding negative control.

Figure IV.4: Analysis of SH-SY5Y cell cycle after 3 and 24h of treatment with S-ION prepared in complete and serum-free medium. Bars represent the mean ± standard error. PC: positive control (1.5µM MMC). $^{**}P<0.01$, significant difference with regard to the corresponding negative control.

Figure IV.5: Apoptosis (% of cells in the subG$_1$ region of cell cycle distribution) in neuronal cells treated with S-ION prepared in complete and serum-free medium. Bars represent the mean ± standard error. PC: positive control (1.5µM MMC). $^{*}P<0.05$, significant difference with regard to the corresponding negative control.

Figure IV.17: Late apoptosis (cells in the subG$_1$ region of cell cycle distribution) assessment in neural cells treated with O-ION in complete and serum-free medium. Bars represent mean ± standard error. *P<0.05, **P<0.01, significant differences compared to the corresponding negative control.

Figure IV.18: Apoptosis induction by exposure of SH-SY5Y cells to O-ION in complete and serum-free medium. Bars represent the mean ± standard error. PC: positive control (10µM Campt). *P<0.05, **P<0.01, significant difference with regard to the corresponding negative control.

Figure IV.19: Necrosis induction after exposure of SH-SY5Y neurons to O-ION in complete and serum-free medium. Bars represent mean ± standard error. PC: positive control (10µM Campt). **P<0.01, significant difference with regard to the corresponding negative control

Figure IV.20: H2AX histone phosphorylation after treatment of neuronal cells with O-ION in complete and serum-free medium. Bars represent mean ± standard error. PC: positive control (1µg/ml BLM). **P<0.01, significantly different from the corresponding negative control.

Figure IV.21: Micronuclei rates in SH-SY5Y neurons exposed to O-ION in complete and serum-free medium. Bars represent mean ± standard error. PC: positive control (1.5µM MMC). *P<0.05, **P<0.01, significant differences with respect to the corresponding negative control.

Figure IV.22: Results of interference testing between O-ION (10-200µg/ml) and comet assay methodology in complete and serum-free cell culture medium. Bars represent mean ± standard error. *P<0.05, significant difference with regard to the corresponding control.

Figure IV.23: Primary DNA damage in SH-SY5Y cells treated with O-ION in complete and serum-free medium. Data corresponding to treatment with 200µg/ml in serum-free medium are not shown due to interference of the nanoparticles with the comet methodology. Bars represent mean ± standard error. PC: positive control (100µM H_2O_2). *P<0.05, **P<0.01, significant differences with regard to the corresponding negative control.

Figure IV.24: Effects of O-ION on repair of H_2O_2-induced DNA damage in neurons in complete and serum-free medium. Incubation with 50µg/ml O-ION was conducted independently prior to exposure to 100µM H_2O_2 (for 3 or 24 h, phase A), simultaneously with H_2O_2 (phase B), or during the repair period (phase C). Bars represent mean ± standard error. *P<0.05, **P<0.01, significant differences with regard to the same treatment before repair. $^{\#\#}P$<0.01, significant differences with regard to the negative control.

Figure IV.25: Analysis of iron ion release from S-ION in complete and serum-free cell culture medium. Bars represent mean ± standard error.

Figure IV.26: Transmission electron micrographs of A172 cells incubated with 100µg/ml of S-ION for 3h in complete (a) and serum-free (b) medium and after 24h of exposure in complete (c) medium showing nanoparticle internalization (arrows indicate S-ION agglomerates) in opposition to control cells (d). All bars (down left side) are 0.5µm long.

Figure IV.27: Results of membrane integrity assessment (LDH assay) in A172 cells exposed to S-ION in complete and serum-free medium. Bars represent mean ± standard error. PC: positive

Figure IV.39: Results of membrane integrity assessment (LDH assay) in A172 cells exposed to O-ION in complete and serum-free medium. Bars represent mean ± standard error. PC: positive control (1% Triton X-100). **P*<0.05, significant differences compared to the corresponding negative control.

Figure IV.40: Analysis of A172 cell cycle after treatment with O-ION for 3h in complete (upper left) and serum-free medium (upper right), or for 24h in complete (lower left) and serum-free medium (lower right). Bars represent mean ± standard error. PC: positive control (1.5µM MMC). **P*<0.05, ***P*<0.01, significant differences with regard to the corresponding negative control.

Figure IV.41: Late apoptosis (cells in the $subG_1$ region of cell cycle distribution) assessment in A172 cells treated with O-ION in complete and serum-free medium. Bars represent mean ± standard error. ***P*<0.01, significant differences compared to the corresponding negative control.

Figure IV.42: Apoptosis induction by exposure of A172 cells to O-ION in complete and serum-free medium. Bars represent the mean ± standard error. PC: positive control (10µM Campt). **P*<0.05, ***P*<0.01, significant difference with regard to the corresponding negative control.

Figure IV.43: Necrosis induction after exposure of A172 astrocytes to O-ION in complete and serum-free medium. Bars represent mean ± standard error. PC: positive control (10µM Campt). **P*<0.05, ***P*<0.01, significant difference with regard to the corresponding negative control.

Figure IV.44: H2AX histone phosphorylation after treatment of A172 cells with O-ION in complete and serum-free medium. Bars represent mean ± standard error. PC: positive control (1µg/ml BLM). **P*<0.05, ***P*<0.01, significantly different from the corresponding negative control.

Figure IV.45: Micronuclei rates in A172 cells exposed to O-ION in complete and serum-free medium. Bars represent mean ± standard error. PC: positive control (15µM MMC). ***P*<0.01, significant differences with respect to the corresponding negative control.

Figure IV.46: Results of interference testing between O-ION (100µg/ml) and comet assay methodology in complete and serum-free cell culture medium. Bars represent mean ± standard error.

Figure IV.47: Primary DNA damage in A172 cells treated with O-ION in complete and serum-free medium. Bars represent mean ± standard error. PC: positive control (100µM H_2O_2). **P*<0.05, ***P*<0.01, significant differences with regard to the corresponding negative control.

Figure IV.48: Effects of O-ION on repair of H_2O_2-induced DNA damage in A172 cells in complete and serum-free medium. Incubation with 50µg/ml O-ION was conducted independently prior to exposure to 200µM H_2O_2 (for 3 or 24h, phase A), simultaneously with H_2O_2 (phase B), or during the repair period (phase C). Bars represent mean ± standard error. **P*<0.05, ***P*<0.01, significant differences with regard to the same treatment before repair.

List of tables

I. INTRODUCTION

I. INTRODUCTION

1. NANOTECHNOLOGY AND NANOMATERIALS

Nanotechnology is the understanding and control of matter at dimensions of roughly 1-100nm, where unique phenomena enable novel applications. A nanometer is 10^{-9} of a meter; a sheet of paper is about 100,000nm thick. Encompassing nanoscale science, engineering and technology, nanotechnology involves imaging, measuring, modelling, and manipulating matter at this length scale. At this level, the physical, chemical and biological properties of materials differ in fundamental and valuable ways from both the properties of individual atoms and molecules or bulk matter. Nanotechnology is directed toward understanding and creating improved materials, devices and systems that exploit these new properties. An engineered nanomaterial may then be defined as any intentionally produced material that has a characteristic size from 1 to 100nm in at least one dimension. Because of this very small size and the resultant high surface to volume ratio, nanomaterials exhibit properties that are different from larger-sized materials of the same chemical composition (Landsiedel *et al.,* 2012). The unique properties of nanotechnology originate from:

- **Small dimensions**, enabling high speed and high functional density (nanoelectronics, lab-on-chip), small and lightweight devices and sensors (smart dust), high sensitivity (sensors, nanowires) and special surface effects.
- Very **large surface area**, providing reinforcement and catalytic effects; quantum effects, such as highly efficient optical fluorescent quantum dots.
- **New molecular structures**, with new material properties: high strength nanotubes, nanofibers and nanocomposites.

Nanotechnology is a rapidly expanding area which has highly promising prospects for turning fundamental research into successful innovations, currently reaching 3037 inventoried consumer products containing nanomaterials (http://nanodb.dk/, consulted on September 4th, 2018). Not only to boost the competitiveness of our industry but also to create new products that make positive changes in the lives of our citizens, be it in medicine, environment, electronics or any other field, nanosciences and nanotechnologies open up new avenues of research and lead to new, useful, and sometimes unexpected applications (Simonis and Schilthuizen, 2006). Nanotechnology has taken advantage of most of the new properties and so has expanded into various domains from industrial applications (*e.g.*, which may lead to stronger and lighter building materials) and biomedical uses (*e.g.*, as new tools for the diagnosis and treatment of diseases) to commercially available consumer products including transparent sunscreens, stain resistant

clothing, self-cleaning glass, paints, sport equipment, etc. (Figure I.1) (Buzea *et al.,* 2007; Card *et al.,* 2008; Amstad *et al.,* 2011; Vance *et al.,* 2015; Long *et al.,* 2015; Bobo *et al.,* 2016).

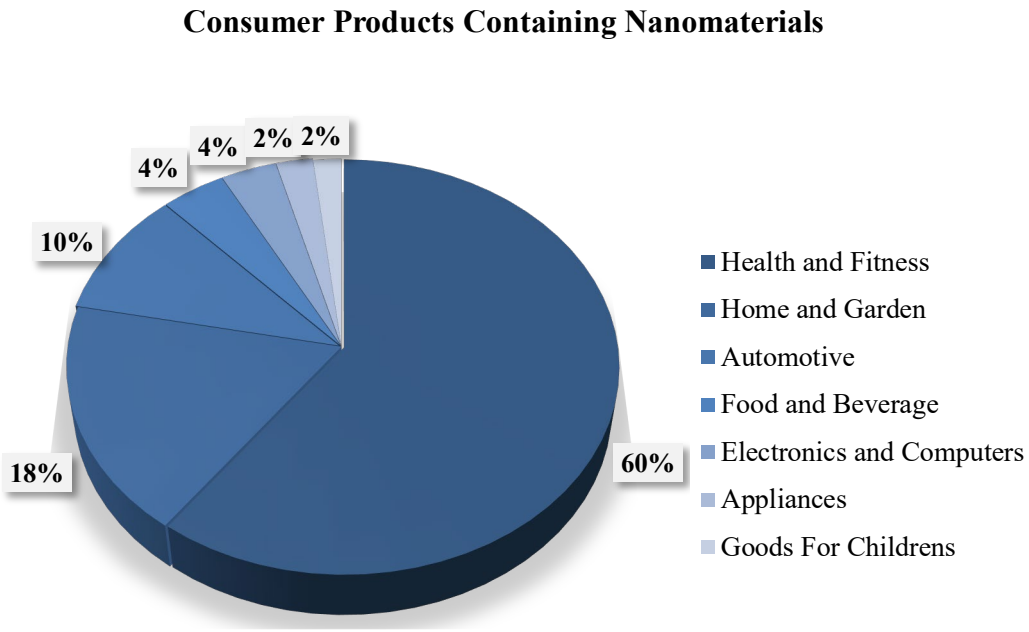

Figure I.1. Distribution of nanotechnology products into the major categories of the commercial marketplace (data source from www.nanodb.dk/; August 2018).

The development of nanotechnology has resulted in a growing public debate on the toxicity and environmental impact of nanomaterials. The reduction in size provides greater bioavailability as compared to the bulk material, leading to enhanced absorption of nanoparticles in biological systems (Das *et al.,* 2009). Living organisms are made of cells that usually range 10 to 100nm. However, cellular parts are much smaller, and proteins are even smaller with a typical range of just 5 to 50nm (Figure I.2). These size differences enable the potential use of nanoparticles as very small probes to directly observe cellular machinery without too much interference (Taton, 2002; Salata, 2004); however, nanomaterials can also interact with cellular components and induce toxic effects. Indeed, particle toxicology suggests that, for toxic particles in general, more particle surface equals more toxicity (Borm *et al.,* 2006).

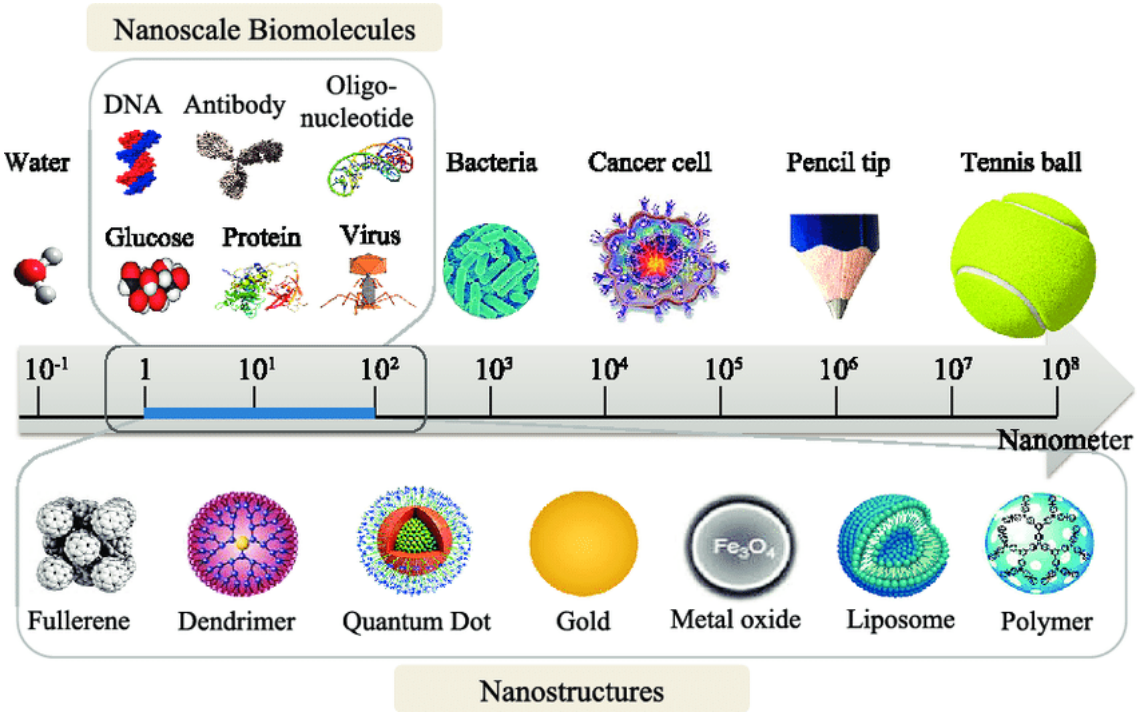

Figure I.2. Nanoscale integration of nanoparticles and biomolecules (from Saallah and Lenggoro, 2018). Schematic representation of a scale bar to visualize the range of nanomaterials and nanosystems as compared with biological components.

With the increased applications of nanotechnology products, especially for biomedical purposes, concerns regarding the onset of unexpected adverse health effects following exposure have been also raised. Understanding of toxicological profiles of engineered nanomaterials is necessary in order to ensure that these materials are safe for use and are developed responsibly, with optimization of benefits and minimization of risks. Nevertheless, development and production of engineered nanomaterials are increasing faster than generation of toxicological information (Figure I.3). This lack of information on possible adverse effects of nanomaterials has been taken into consideration by many organizations worldwide such as the US Environmental Protection Agency (EPA), the World Health Organization (WHO), the US National Institute for Occupational Safety and Health (NIOSH), the European Commission (EC) and the Organization for Economic Co-operation and Development (OECD). Official documents have been prepared by these organizations addressing the need of dedicated research on appropriate methodological assays for assessing engineered nanomaterial toxicity (Colognato *et al.,* 2012).

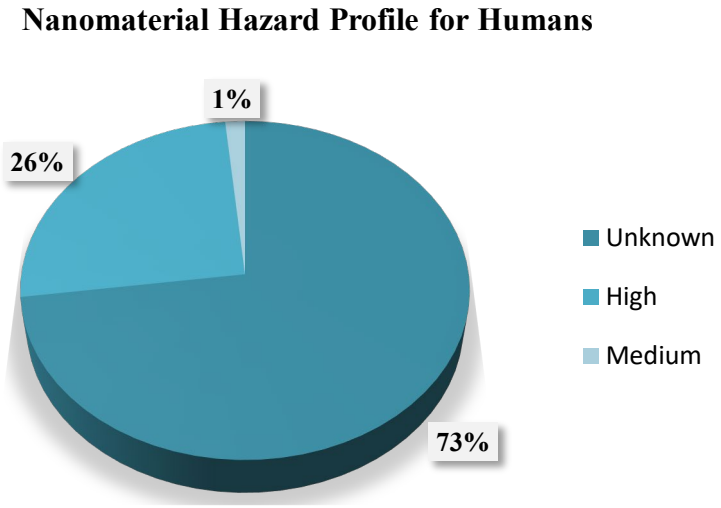

Figure I.3. Toxicological and hazard profile for humans of consumer products containing engineered nanomaterials present in marketplace (data source from www.nanodb.dk/; August 2018).

Consequently, starting in the early 2000s, concerns about the potential human and environmental health effects of nanomaterials were being expressed by many scientists, regulators, and non-governmental agencies. Indeed, as a proof of the growing interest on this topic, the number of scientific articles published on 'nanotoxicity' or 'nanotoxicology' increased progressively in the last decade (around 2550 until August 2018, according to PubMed database); before 2008 it was almost negligible (Figure I.4).

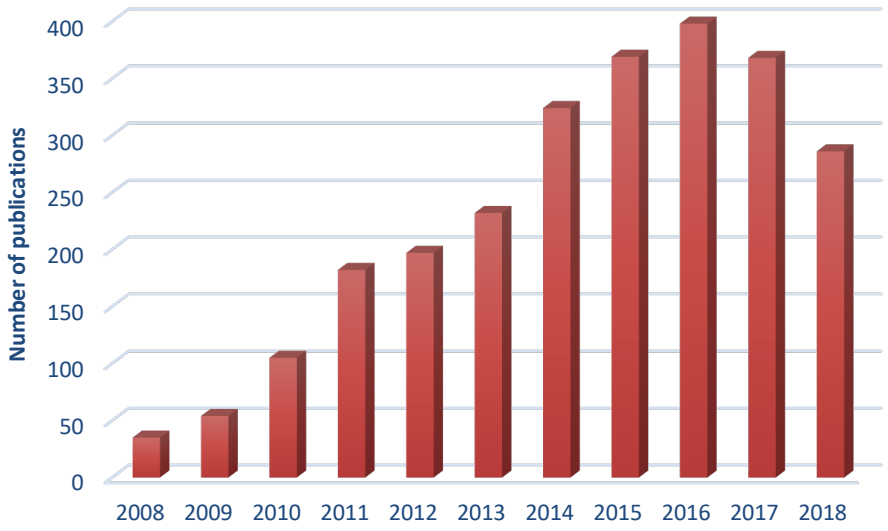

Figure I.4. Number of publications from PubMed database on 'nanotoxicity' or 'nanotoxicology' topics. Data for year 2018 is up to August 10th.

2. IRON OXIDE NANOPARTICLES

Among all engineered nanomaterials, magnetic nanoparticles – made of iron, cobalt, or nickel oxides – arouse a particular interest in biomedical field mainly due to their special physicochemical features, including their proven biocompatibility and their magnetic properties that allow them to be manipulated by an external magnetic field gradient (Gupta and Gupta, 2005). Particularly, nanoparticles made of a ferro or ferromagnetic material, *i.e.*, iron oxide nanoparticles (ION), can exhibit a unique form of magnetism called superparamagnetism, which appears when the ION size is below a critical value – depending on the material, but typically around 10-20nm – and when the temperature is above the so-called blocking temperature (Lu *et al.,* 2010). This feature, together with their high colloidal stability, and their unique biochemical and catalytic properties makes them very attractive for a broad range of technical and biomedical uses (Shah *et al.,* 2013; Wu *et al.,* 2015; Gkagkanasiou *et al.,* 2016; Blanco-Andujar *et al.,* 2016).

From an industrial perspective, ION are frequently used in building materials, as pigments – which are low cost, colorfast, nontoxic and capable of imparting different colors – and as a food additive, which fortifies foods without altering their color or taste (Dissanayake *et al.,* 2015). However, the most promising uses of ION are in the biomedicine field. Among others, they have applications in magnetic resonance imaging, targeted drug delivery, tumor location and treatment, gene therapy, and tissue repair (reviewed in Revia and Zhang, 2016). These biomedical uses, which require that nanoparticles are directly introduced in the human body, give rise to concerns regarding the potential toxic effects that may be associated with ION exposure. Indeed, clinical use of several ION as contrast agents for imaging were already approved by the US Food and Drug Administration since 1996 (US FDA) (Reimer and Balzer, 2003; Lu *et al.,* 2007a; Maier-Hauff *et al.,* 2011; Sharma *et al.,* 2014). Therefore, due to the current and promising biomedical uses of ION involving the direct contact with different tissues and organs, studies addressing their potential toxicity are especially relevant. Specifically, in the last decade, ION have shown highly useful for a number of applications mainly related to diagnosis, drug delivery, and imaging of the central nervous system (CNS) for neurovascular, neurooncological or neuroinflammatory processes and diseases (Huber, 2005; Kanwar *et al.,* 2012; Ittrich *et al.,* 2013).

ION are usually made of a crystalline core and a surface coating. Even though technically speaking particles larger than 50nm (size of core/shell) ION are classified as superparamagnetic iron oxides (SPIO), and particles smaller than 50nm are ultra-small superparamagnetic iron oxides (USPIO) (Estelrich *et al.,* 2015), the term ION is usually employed in the literature to designate both of them. Likewise, in this memory ION will be used to refer to both types of magnetic nanoparticles. ION may present multiple crystallographic structures that include: magnetite (Fe_3O_4), maghemite (γ-Fe_2O_3), hematite (α-Fe_2O_3), wüstite (FeO), ε-Fe_2O_3, and β-

Fe_2O_3, among which magnetite, maghemite and hematite are the most commonly used due to their polymorphism involving temperature-induced phase transition (Dissanayake *et al.,* 2015). The crystalline core of ION, made of ferri- (Fe^{3+}) or ferro- (Fe^{2+}) magnetic material, is generally synthesized through protocols with controlled precipitation of iron oxides in organic solution (Wu *et al.,* 2013a), or in aqueous solution by adding a base (Mohapatra and Anand, 2010). And, specifically, ION manufactured for biomedical purposes, both diagnostics and therapeutics, are typically formed by a core of magnetite or maghemite. This crystalline core is usually surface modified. Surface modification prevents particle agglomeration, provides biocompatibility, and modifies cellular uptake efficiency of ION (Mahmoudi *et al.,* 2009b; Zhu *et al.,* 2012; Mahdavi *et al.,* 2013; Wu *et al.,* 2015).

2.1. Surface modification of iron oxide nanoparticles

A common problem associated with nanoparticles is their intrinsic instability over long periods of time, since they tend to form agglomerates to reduce the energy associated with the high surface area to volume ratio. Moreover, naked nanoparticles introduced into the body can be easily trapped by the immune system as foreign materials, which means that they cannot reach their desired target (Santhosh and Ulrih, 2013). Furthermore, naked metallic nanoparticles are highly chemically active, and are easily oxidized in air, generally resulting in loss of magnetism and dispensability (Lu *et al.,* 2007b). In order to minimize these effects, the surface of commercially available nanoparticles may be modified by coating with different materials including: natural (gelatine, dextran, chitosan, pullulan, etc.) or synthetic (polyethylene glycol [PEG], polyacrylic acid, polyvinyl alcohol, etc.) polymeric coatings, inorganic molecules (silica, gold, silver, platinum, palladium, iron, carbon, etc.) and numerous biological molecules (polypeptides, proteins, antibodies, biotin, etc.) (reviewed in Gupta and Gupta, 2005 and Santhosh and Ulrih, 2013). Surface modification often serves multiple purposes (Kim *et al.,* 2012). On one hand, it stabilizes nanoparticles in an environment of slightly alkaline pH or high salt concentrations. For example, ION coated with silica, which achieves the isoelectric point at pH of 2 to 3, are negatively charged at blood pH, helping to avoid aggregate formation in body fluids (McBain *et al.,* 2008). On the other hand, surface modification allows biomolecule binding favoring surface attachments between ION and antibodies, peptides, hormones or drugs (Sadeghiani *et al.,* 2005). The polymer coating significantly increases their overall size, which may also be used to modify the toxicokinetic behavior of the particles, since it may limit their absorption, tissue distribution, and excretion (Wang *et al.,* 2001; Bjørnerud and Johansson, 2004). Moreover, the use of coatings by forming monolayers on the nanoparticle surface, such as stable gold or silica shell structures, allows for the application of core materials that would be toxic otherwise.

Therefore, the iron oxide core is usually covered with a biocompatible coating. While the iron oxide core is responsible for the magnetic properties of ION, the ligand coat is essential to stabilize ION in physiological media. The choice of coating is mainly determined by the desired application concerning functionalization, stability or size, since every material has advantages and drawbacks (Petters *et al.,* 2014b). Some of the most commonly used coatings for ION are silica, largely used for bioimaging and biosensing purposes (Alwi *et al.,* 2012); oleic acid, suitable for lipid-soluble and non-ionic coatings required for applications directed to the brain (Dilnawaz and Sahoo, 2015), polyethylene glycol, with good compatibility, favorable chemical properties, and solubility (Yu *et al.,* 2012); carboxydextran, used for cell labelling since it provides stability and increases intravascular retention time of nanoparticles (Tong *et al.,* 2011); and polyethylene imine, used as gene/drug delivery vehicle due to its high cellular uptake (Xia *et al.,* 2009b; Duan *et al.,* 2014). Together with this primary coating, targeting efficiency of ION can be further improved by employing conjugation biomarkers on their surface such as peptides, antibodies or small molecules (Figuerola *et al.,* 2010; Jin *et al.,* 2014). Thus, ION coating has frequently been modified with fluorescent dyes for imaging, targeting molecules (Agemy *et al.,* 2011; Kumar *et al.,* 2012), drugs or nucleic acids (Krötz *et al.,* 2003; Kumar *et al.,* 2010; Choi *et al.,* 2015).

The potential of the surface coatings that enable special probing and/or monitoring of local physical mechanistic changes at a length scale may greatly assist in improving disease detection, monitoring, and treatment (Sun *et al.,* 2008). For this purpose, ION are required to be magnetically targeted to a tissue/organ in order to benefit a therapeutic or diagnostic application. Moreover, in a study using a number of cell lines it was demonstrated that cellular uptake efficiency of ION is dependent on surface coating of the nanoparticles, irrespective of the cell line used (Zhu *et al.,* 2012). Hence, a strategy to adjust the cellular uptake efficiency and precision of ION is to modify their surface coating.

Nevertheless, besides providing generally increased biocompatibility and enhancing ION properties to be used in biomedical applications, surface coating may also alter ION toxicity (reviewed in Singh *et al.,* 2010). Therefore, it is important to carefully monitor the influence of surface modifications (chemical nature of coating, presence of functional groups, and net size) on ION toxicity, since this great variety of coatings leads to many diverse types of ION with different potential action mechanisms and toxic patterns. The use of ION in biomedical research is progressively gaining importance, leading to the rapid development of novel ION types. Therefore, consequently, a growing number of toxicological studies have now been carried out with a great variety of ION, cell types, incubation conditions, etc. However, it is still unclear whether ION are generally safe or should be used prudently.

2.2. Physicochemical characteristics of ION

Nanoparticle toxicity can be attributed to nonspecific interactions with biological structures due to their physical properties (*e.g.*, size and shape) and biopersistence, or to specific interactions with biomolecules through their surface properties (*e.g.*, surface chemistry and reactivity) (Nel *et al.,* 2009). As mentioned before, the reason for ION to have a great potential for industrial and biomedical applications is mainly because of their unique physical and chemical properties (Nel, 2006), displaying a complex dependence upon several factors such as their shape, size, surface structure, absence/presence of surface coating, and chemical stability (*e.g.*, solubility and aggregation) (Sakulkhu *et al.,* 2014; Sutariya *et al.,* 2016). These potential uses of ION have raised concerns regarding their impact on biological response in living organisms and the environment at large (Pettitt and Lead, 2013). Therefore, it is highly difficult to correlate the biological response observed (overall potential toxicity) with their intricate physicochemical characteristics. Hence, carrying out an exhaustive physicochemical characterization for a proper interpretation of the potential ION toxic effects is crucial (Podila and Brown, 2013).

The nanometric size is one of the main physicochemical features that make nanoparticles different from same bulk material. Decreases in size open the potential for crossing the various biological barriers within the body [*e.g.*, blood-brain barrier], since the mobility, potential transport across cellular membranes, and availability of the nanoparticles in the biological environment increase (De Jong and Borm, 2008). Also, as a direct consequence, while the size of a nanoparticle decreases, its surface area increases (Figure I.5), which determines the potential number of reactive groups on the particle surface and therefore it is strongly possible that biological activity might increase. This may be one of the reasons why ION are generally considered more toxic than larger particles of the same material (Fröhlich *et al.,* 2012). Furthermore, as particle size decreases concomitant changes in other physicochemical parameters such as crystalline form or oxidation state may be responsible for altered toxicity. Also, for soluble nanoparticles, where the ions themselves could be toxic (*e.g.* Fe^{2+}/Fe^{3+}), increased toxicity may result from an increase in particle dissolution with decreasing size and increasing specific surface area (Pettitt and Lead, 2013). Therefore, size seems to be an important indicator of potential ION toxicity, as different particle sizes have fundamentally different modes-of-action which alter their toxicity, persistence and bioavailability, or are responsible for size-dependent changes in other physicochemical characteristics. Theoretically, particle size is likely to contribute to cytotoxicity, since smaller nanoparticles have a larger specific surface area and thus more available surface area to interact with cellular components such as nucleic acids, proteins, fatty acids, and carbohydrates (Pettitt and Lead, 2013). The smaller size also likely enhances their ability to cross membranes, enter the cell, and causing cellular damage (Huang *et al.,* 2017).

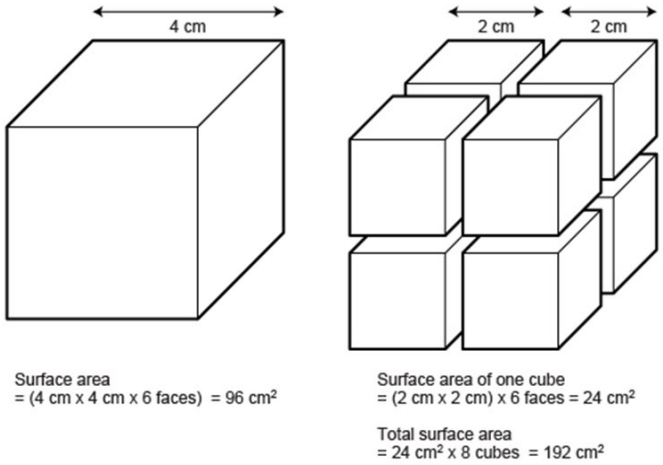

Figure I.5. The decrease in particle size means a high increase in surface area for the same quantity of material, (from www.bbc.co.uk/staticarchive/1ba786c30a635037b6a1fc3d8a992d477c68bbc9.jpg)

Nano-scale materials are known to have various shapes and structures such as spherical, oval, cubic, prism, helical, needle-like, tubes, platelets, etc. (Colognato *et al.,* 2012). The shape of nanomaterials may have effects on the kinetics of deposition and cellular uptake mechanisms (Lai, 2015). Particularly, ION usually present spherical shapes, which was reported to be taken up by cells 500% more efficiently than rod-shaped particles of similar size (Verma and Stellacci, 2010). As in the case of size, particles may also have a 'shape distribution', depending on the state of dispersion of the nanoparticle system, and interactions with the different moieties of the surrounding medium that may contribute to the behavior and biological responses of ION. This important factor derived from surface properties of nanoparticles and refers to the relative number of single particles in a suspending medium in comparison to agglomerates/aggregates (Powers *et al.,* 2006). These agglomerates/aggregates may be formed directly from attractive interparticle forces (*e.g.*, Van der Waals and hydrophobic interactions) or through the binding of molecules in the surroundings (*e.g.*, polymers, proteins, polysaccharides) (Powers *et al.,* 2007). The smaller the nanoparticle, the stronger the interparticle forces that attract them. Thus, they might agglomerate/aggregate into vastly different shapes and sizes, which may also profoundly change the dynamics and properties of the resultant potential hazards (Maynard *et al.,* 2011; Shin *et al.,* 2015).

There is a wide variety of methods for determining nanoparticle size, size distributions, and hydrodynamic size, including dynamic light scattering (DLS), differential mobility analysis, time of flight mass spectroscopy, transmission electron microscopy (TEM), and surface area measurements, among many others. Microscopy is one of the most powerful techniques and is

often relied on exclusively to provide valuable information regarding size, shape, and morphology (Powers *et al.,* 2007).

Surface characteristics affect how nanoparticles react with other biological entities in solution through attractive and repulsive electrochemical forces. In particular, hydrophobicity, surface charge, and charge distribution have been demonstrated to influence nanoparticle fate and behavior in an organism (Teske and Detweiler, 2015). Most nanoparticles are poorly soluble and persistent to interaction with biological systems. However, dissolution of some nanoparticles occurs in culture medium or biological fluids, and cellular uptake, subcellular localization, and toxic effects can be affected by their solubility (Lai, 2015). For instance, dissolved and non-dissolved nanoparticles have been shown to have different cellular uptake pathways and cytotoxicity due to their differing ability in releasing the toxic ions (Xia *et al.,* 2009a). Under aqueous conditions, ION nanoparticles dissolution can induce higher cytotoxicity and apoptosis in mammalian cells than non-dissolved ION due to the release of ions and the production of reactive oxygen species (ROS) and oxidative stress (Jeng and Swanson, 2006; Xia *et al.,* 2009a). Also, the surface properties of nanoparticles are as fundamental as the other key characteristics that dictate internalization. For some biomedical applications of ION, high circulation time in the body is required for the nanoparticles to recognize their specific target of interest. Biomolecules adsorbing to the surface of hydrophobic ION decrease circulation time by initiating the immune response cascade which allows phagocytosis of the nanoparticles following recognition as foreign objects (Saptarshi *et al.,* 2013). Thus, hydrophobicity may instigate redundant interaction with plasma proteins, phagocytic internalization, immune cell stimulation and nanoparticle clearance (Park *et al.,* 2014; Easo and Mohanan, 2015). Therefore, minimizing the recognition of nanoparticles by the reticuloendothelial system and subsequently by the immune system will enhance the probability of uptake by the target cells. Hence, recent research is focused on modifying conventional hydrophobic nanoparticle surfaces with a hydrophilic protective layer to cause steric repulsive forces against plasma proteins and increase the blood circulation half-life of targeted nanocarriers (Loh *et al.,* 2012).

Surface chemistry consists of a wide variety of properties that conduct the way in which ION interact with biomolecules and biological systems through their chemical composition. In case of presence of surface modification, results on surface chemical composition reflect the effectiveness of coating to avoid nanoparticle core dissolution. Electron spectroscopy for chemical analysis, x-ray photoelectron spectroscopy (XPS) and secondary ion mass spectroscopy have been extensively used for characterizing the surface chemistry of nanoparticles as well as correlating biomaterial surface properties with physiological endpoints (Ratner, 1996). In the same way, surface charge of nanoparticles has great importance in the induction of biological effects, as it is a major factor in determining the particle dispersion characteristics and also

influences the adsorption of ions and biomolecules (biomolecular corona), which may change how cells react to the nanoparticles (Powers *et al.,* 2006; Baber *et al.,* 2011).

The surface charges of particulate systems are approximated through zeta potential measurements. Zeta potential (measured by DLS) refers to the function of the surface charge of the particle and the nature and composition of the surrounding medium in which the particle is dispersed. It is a measure of the total electric potential of all ions and nanoparticles in solution, and therefore is affected by changing pH, or ionic strength. Zeta-potential measurements range from 0 to ±60mV. High readings (>±30mV) suggest increased stability due to increased electrostatic repulsion. Lower readings (<±30mV) indicate a tendency to coagulate (aggregate and precipitate) (Teske and Detweiler, 2015).

Differences in physicochemical properties between nanoparticles and larger particles determine their behavior and biodistribution in the body following translocation from the portal of entry, their cellular interactions, and their effects (Oberdörster, 2010). Thus, the importance of the physicochemical properties of the ION (particle size and size distribution, state of agglomeration/aggregation, shape, crystalline structure, chemical composition, surface area, surface chemistry and surface charge) is highlighted to understanding the toxic effects on cells (Yang *et al.,* 2010).

2.3. Iron ion release

Due to iron capacity to switch between ferric (Fe^{3+}) and ferrous (Fe^{2+}) ionic forms by easily accepting and donating electrons (reduction-oxidation reactions), it plays a critical role in important organic metabolic pathways such as cytochrome P450 function, mitochondrial oxidative phosphorylation, oxygen transport, DNA synthesis, and energy production (Shander *et al.,* 2009). Once surface coatings degrade, the iron oxide core can be metabolized easily and free iron released from ION, which can be transported by proteins like ferritin, transferrin, and hemosiderin (Santhosh and Ulrih, 2013) from the endocytic compartment (Soenen and De Cuyper, 2010) and incorporated into the body iron pool (Almeida *et al.,* 2011; Lin *et al.,* 2015). Nevertheless, as excess of this metal can be very toxic, iron levels in the organism are strictly controlled. Thus, ION exposure caused elevated intracellular iron concentrations in a variety of cells, dependent on the dose (Geppert *et al.,* 2009, 2011; Rosenberg *et al.,* 2012; Paolini *et al.,* 2016). Therefore, the normal body capacity to manage iron should be taken into account when considering administration of high or frequently repeated doses of ION (Kunzmann *et al.,* 2011).

Apart from nanoparticle exposure characteristics, also cell features can influence ION effects since, depending on cell type, iron ions released from ION can be harmless for cells (Geppert *et al.,* 2009, 2011; Rosenberg *et al.,* 2012), induce cytotoxicity (Singh *et al.,* 2010), or even be used by cells for their own metabolism, as it was observed for oligodendroglial OLN-93

cells (Hohnholt *et al.,* 2010a, 2011). A possible explanation is that, under normal conditions, iron released from ION can be accumulated in cells where it is stored as an iron-ferritin complex to annul the high toxicity associated with free iron (Singh *et al.,* 2010; Hohnholt and Dringen, 2013). Hence, this storage likely contributes to high cell resistance to iron toxicity and is especially relevant in the nervous tissue, since even the prolonged presence of large amounts of accumulated ION does not harm these cells. On this regard, a review on ION uptake and metabolism in brain astrocytes suggests that the efficient uptake of extracellular iron (released slowly from ION) by astrocytes, as well as their strong up-regulation of the synthesis of ferritin contribute to the high resistance of these cells to iron toxicity (Hohnholt and Dringen, 2013). So, astrocytes deal well with an excess of iron and protect the brain against iron-mediated toxicity. These results are supported by recent findings showing that astrocytes, and also neurons, are more resistant against acute ION toxicity, likely due to a slow transfer of internalized nanoparticles into the lysosomal compartment, required for iron ion release from ION (Petters *et al.,* 2016). However, under pathological conditions (such as cancer, atherosclerosis, hypertension or arthritis) iron may effectively be released from ferritin leading to increased oxidative damage and causing cellular toxicity (Reif, 1992*;* Valko *et al.,* 2007).

2.4. Exposure and kinetics

Growing commercialization of nanomaterials in last years, and particularly ION successfully translated to the clinic, substantially increase the potential human exposure to these materials. As their toxicity is generally related to their abundance and persistence, the effective dose, and the duration of the exposure, a systematic and comprehensive analysis is essential (Yoshioka *et al.,* 2014).

Accidental or intentional exposure routes to nanomaterials may include inhalation (Kwon *et al.,* 2014), ingestion (Wang *et al.,* 2010), or dermal uptake (Lorenz *et al.,* 2011). In addition, for medical purposes parenteral, systemic or local administration must be considered (Kim *et al.,* 2006) (Figure I.6). Examples for unintentional exposures to ION include emissions from anthropogenic sources into air (power plants, incineration, internal combustion engines, occupational settings), water and soil (households, effluents from manufacturing sites) or consumer goods (textiles, cosmetics); intentional exposures occur also from biomedical applications, food additives, etc. (Oberdörster, 2010). End-product users, occupationally exposed subjects, medical patients and the general public may be at risk of adverse effects due to the direct contact with the organism (Buzea *et al.,* 2007; Martirosyan and Schneider, 2014; Huang *et al.,* 2017). Because drugs, cosmetics, and various skin care products contain ION, their contact with the skin occurs intentionally as well as accidentally. Furthermore, as the use of nanoparticles in food as food additive and in pharmaceuticals is increasing, people in developed countries ingest an estimated 10^{12}-10^{14} manufactured particles per person every day (Mahler *et al.,* 2012).

Systemic administration by intravenous injection is the most commonly used approach for administration of ION, especially for biomedical uses as magnetic resonance imaging contrast agents (Arami *et al.,* 2015). The blood half-life of different types of ION ranges from several minutes to several days in rodents, and from 1 hour to 24 hours in humans. Further, blood half-life values are highly dependent on dose levels of the injected ION (Arami *et al.,* 2015).

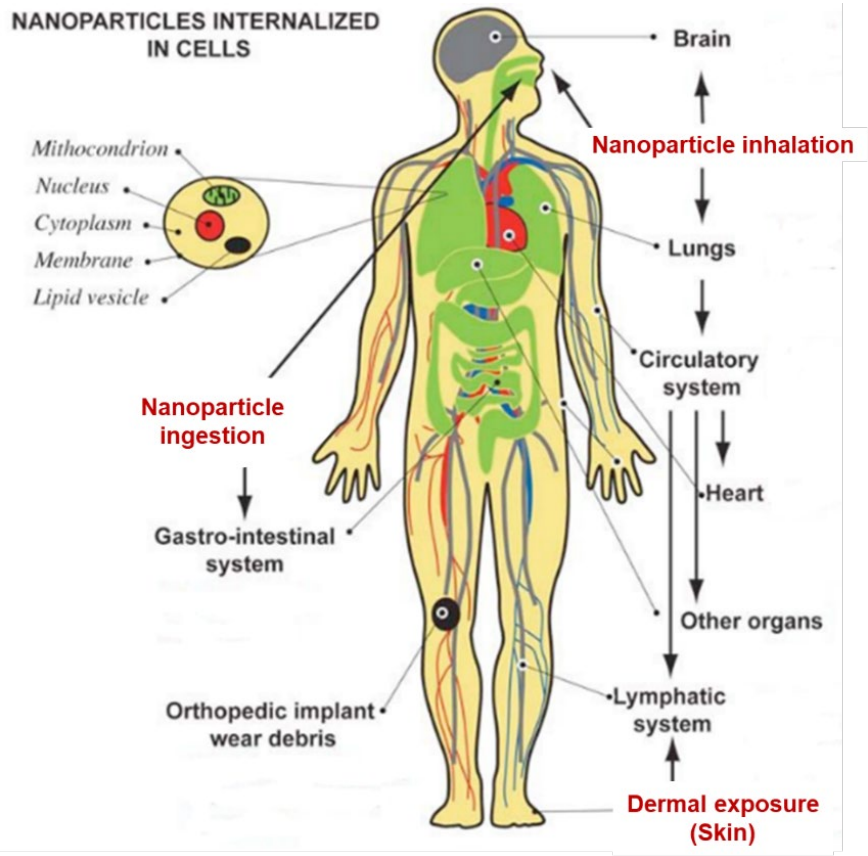

Figure I.6. Schematics of human body showing routes of exposure to nanoparticles, and potential target organs (modified from Buzea *et al.,* 2007).

One of the most important absorption pathways is the respiratory tract. Inhalation is probably the major route for nanoparticles in atmospheric pollutants, combustion-derived nanoparticles, and freely dispersible mineral or metal nanoparticles resulting from bulk manufacture and handing (Wang *et al.,* 2009). Inhaled nanoparticles are deposited in all regions of the respiratory tract; however, larger particles may be filtered out in the upper airways, whereas smaller particles reach distal airways (Forbe *et al.,* 2011). After absorption across the lung epithelium, they enter the blood and lymph to reach cells in the bone marrow, lymph nodes, spleen, heart, brain or any other organ (Basinas *et al.,* 2018). ION can even reach the central nervous system and ganglia following translocation via olfactory bulb or sensory nerves existing in the nasopharyngeal and tracheobronchial regions of the respiratory tract (Oberdörster *et al.,*

2009). Immediately after their administration *in vivo*, several immunological mechanisms start to recognize and collect these foreign particles and direct them to the major elimination pathways of the body. Therefore, there is always a competition between the desired distributions of the ION in specific target organs and their highly active clearance mechanisms (Arami *et al.,* 2015). Knowing the biodistribution and kinetic patterns of administered ION is crucial to enhance they the expected functionality in any selected region or organ of the body and to minimize their toxicological side effects due to any undesirable kinetic behavior (Veiseh *et al.,* 2010).

Regardless the absorption pathway, distribution of the nanoparticles in the body is strongly dependent on their surface characteristics (Hoet *et al.,* 2004), and varies depending on their material, size, presence of coating, and charge. ION are small enough to penetrate very small capillaries throughout the body and to translocate across cell barriers. Therefore, they might enter cells by various mechanisms and associate with subcellular structures and secondary organs (Kettiger *et al.,* 2013). Thus, effects such as inflammation, oxidative stress and molecular cell activation are likely to occur not only in the primary organ of entry, but also in secondary target organs (Oberdörster *et al.,* 2009).

2.4.1. Blood-brain barrier

Although translocation of nanoparticles to the brain is possible and well-studied in the literature under different experimental conditions (Cheng *et al.,* 2010; Shim *et al.,* 2014; Pedram *et al.,* 2014; Yemisci *et al.,* 2015; Mc Carthy *et al.,* 2015), the relevance for real-life situations is far from clear. Therefore, the evaluation of the potential toxic effects of ION on cells from neural origin is required, as specific mechanisms and pathways through which nanoparticles may exert their toxic effects remain largely unknown. The brain is probably the best protected organ in the human body. Besides the protection against mechanical damage, it is also shielded from possibly damaging compounds (circulating pathogens, toxins, and also endogenous signaling substances) in the blood by means of structural barriers (Burkhart *et al.,* 2014; Thomsen *et al.,* 2015). The blood-brain barrier (BBB) is a structural separation between circulating blood and cerebrospinal fluid (CSF) maintained by the choroid plexus in the CNS, which results from the selectivity of the tight junctions between endothelial cells in CNS vessels that restrict the passage of solutes (Stamatovic *et al.,* 2011). At the interface between blood and brain, endothelial cells and associated astrocytes are stitched together by tight junctions (Figure I.7). Endothelial cells restrict the diffusion of microscopic objects and large or hydrophilic molecules into the CSF, while allowing the diffusion of small hydrophobic molecules (*e.g.* O_2, hormones, CO_2). Cells associated with the BBB actively transport metabolic products such as glucose across the barrier with specific proteins (Yang *et al.,* 2010). Due to their special physicochemical properties, such as size or large surface area, ION could cross the BBB and accumulate within the brain, and may cause neurotoxicity after reaching the nervous system (Masserini, 2013).

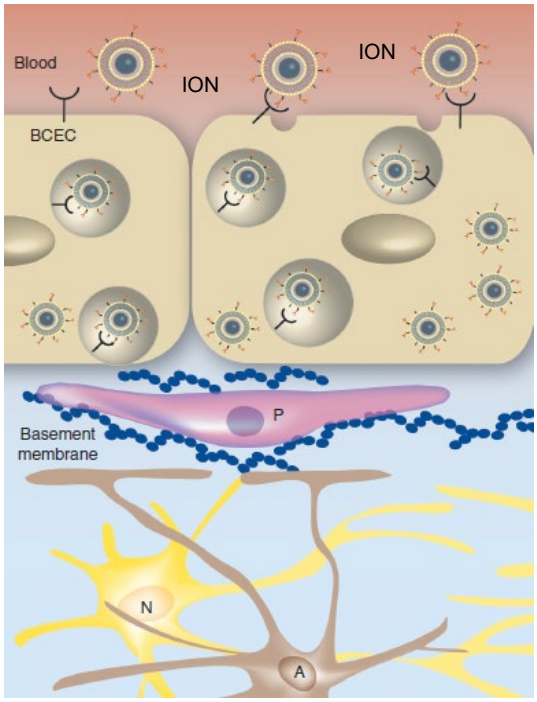

Figure I.7. Illustration showing the transport of ION though the blood–brain barrier and beyond. Step 1: Blood-to-brain endothelium transport: ION are targeted to the transferrin receptor on brain capillary endothelial cells. Step 2: Endothelium-to-brain transport: Once accumulated inside the brain endothelium, magnetic force is applied externally on the cranial surface, which leads to subsequent dragging of the ION through the brain endothelial cells, and the basal membrane. This leads to the occurrence of the ION inside the brain from where they can meet target neuronal or glial cells. BCEC: Brain capillary endothelial cells; N: Neuron; A: Astrocyte; BM: Basement membrane; P: Pericyte (modified from Thomsen *et al.,* 2015).

2.5. Toxic effects of iron oxide nanoparticles

ION have attracted much attention not only because of their superparamagnetic properties, which make them suitable for interesting biomedical applications, but also because they are thought to have low toxicity to the human body (Jeng and Swanson, 2006; Laurent and Mahmoudi, 2011). Thus, in general, ION are classified as biocompatible, mostly due to negative results obtained in cytotoxicity studies (Kunzmann *et al.,* 2011). However, absence of cytotoxicity does not guarantee that ION pose no risk for use in specific applications, as recent studies report different harmful cellular effects including DNA damage, oxidative stress, mitochondrial membrane dysfunction, and changes in gene expression as a result of ION exposure in the absence of cytotoxicity (reviewed in Singh *et al.,*, 2010). Hence, criteria to define the toxicity of nanoparticles must be clearly defined (Huang *et al.,* 2012), and it has been suggested that terms such as "biocompatibility" should be re-evaluated (Singh *et al.,* 2010). Nevertheless, reviews on application of magnetic nanoparticles for drug delivery suggested that the possible toxicity of

these nanoparticles does not mean that they cannot be applied biomedically, but optimal benefits and potential risks need to be identified (Thomsen *et al.,* 2015; Elzoghby *et al.,* 2016).

2.5.1. Cytotoxicity

Most studies analyzing ION toxicity are focused on cytotoxic effects of these nanoparticles on cell cultures. A number of different cell lines and testing conditions have been assessed reporting ION cellular effects at different levels, mainly decrease in viability [by the MTT (3-[4,5-dimethylthiazol-2-yl]-2,5 diphenyl tetrazolium bromide) assay (viability based on mitochondrial functionality), and the LDH (lactate dehydrogenase) assay (explained in section 3.2.1.)], ROS production, and iron ion release, but also apoptosis induction, cell cycle alterations, cell membrane disruptions, cytoskeleton modifications, etc. (Figure I.8).

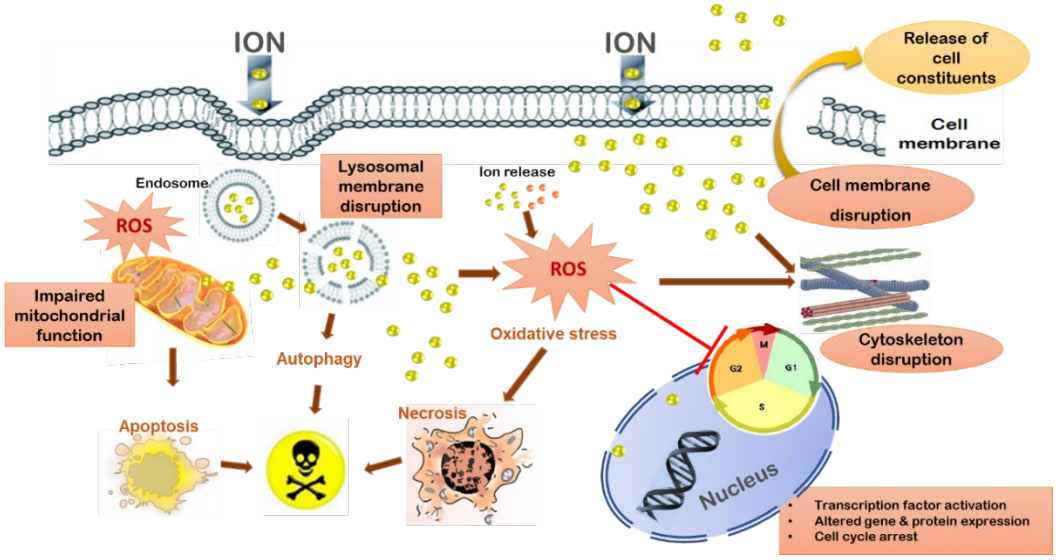

Figure I.8. Reported cellular toxicity induced by ION. ION exposure may lead to different cellular toxic effects including impaired mitochondrial function (and, consequently, apoptosis), lysosomal damage/dysfunction, cell membrane disruption, cytoskeleton disruption, DNA damage and cell cycle alterations. Besides, accumulation of high amounts of ION and iron in the cytoplasm leads (in fewer cases) to cell death by autophagy. All these effects may be produced by ION not only directly, but also indirectly through generation of reactive oxygen species (ROS) and iron ion release. Increased ROS levels would lead to enzyme depletion/inactivation, protein denaturation, genetic alterations or impacts on cell cycle or on cytoskeleton, among others; whereas ion release would cause genomic damage, iron imbalance and might eventually result in cell death. ION: iron oxide nanoparticles; ROS: reactive oxygen species.

Magnetite/maghemite combinations have already been approved for clinical use as magnetic resonance imaging contrast agents (Gould 2006; Li *et al.,* 2013; Al Faraj *et al.,* 2015). Nevertheless, there are some inconsistencies in the literature about the cytotoxicological

assessment in different cells and the interpretation of these results. It appears that dose, exposure time and cell type are factors affecting the results obtained. For example, iron (II,III) oxide nanoparticles induced moderate time- and concentration-dependent cytotoxicity in Vero cells after 24h exposure (Szalay *et al.,* 2012), and mild cytotoxicity for either Fe_3O_4 at mesoporous silica composites (Huang *et al.,* 2012) or various ION coated with polyvinyl alcohol on L-929 fibroblast cells (Mahmoudi *et al.,* 2009a) using the MTT assay. A slight degree of cytotoxicity, evaluated by trypan blue exclusion, in human alveolar epithelial A549 cells was also reported for Fe_2O_3 nanoparticles, but not for Fe_3O_4 nanoparticles (Karlsson *et al.,* 2009). Although in another study using L-929 fibroblasts ION modified with different functional groups induced a dose-dependent reduction in viability (water-soluble tetrazolium salt proliferation assay, WST-8), suggesting that ION concentration is more critical for cytotoxicity than any other factor including surface modification or size (Han *et al.,* 2011). Nevertheless, ION cytotoxicity was also reported to be mainly dependent on nanoparticle size and surface coating (Ying and Hwang, 2010; Rivet *et al.,* 2012). Thus, uncoated Fe_3O_4 nanoparticles were not cytotoxic (trypan blue exclusion assay), while oleate-coated Fe_3O_4 nanoparticles were cytotoxic in a dose-dependent manner, and intrinsic properties of sodium oleate were excluded as a cause of the toxic effect (Magdolenova *et al.,* 2013). Furthermore, a comparative cytotoxicity study (measuring intracellular enzymatic activity with calcein-AM and membrane disruption with ethidium homodimer-1) in a human cervical cancer cell line (HeLa) and an immortalized normal human retinal pigment epithelial cell line (RPE) indicated that, although uncoated magnetite nanoparticles at a high concentration (0.40mg/ml) were toxic to both HeLa and RPE cells, their cytotoxicity at low concentrations was cell-type specific (Li *et al.,* 2012).

Investigations aimed at using ION-labeled stem cells in regenerative therapies did not report cytotoxic effects for these nanoparticles (Au *et al.,* 2009). In addition, no significant cytotoxicity in stem cells incubated with ferucarbotran (Resovist, clinically approved carboxydextran-coated ION, used as a negative magnetic resonance imaging contrast agent) was found (Yang *et al.,* 2011; Bigini *et al.,* 2012). However, several reports have stated that these particles can in fact exert large effects on cell wellbeing (reviewed in Soenen and De Cuyper, 2009). Numerous studies showing cytotoxicity following ION exposure (L-glutamic acid-coated ION [Fe_2O_3], nanomagnetite, palladium-coated magnetite, etc.) relate this effect to mitochondrial impairment (membrane depolarization), dose- and time-dependent ROS generation, glutathione depletion and inactivation of several antioxidant enzymes and oxidative stress (Auffan *et al.,* 2008; Buyukhatipoglu and Clyne, 2011; Khan *et al.,* 2012; Zhang *et al.,* 2012; Ahamed *et al.,* 2013; Malvindi *et al.,* 2014; Dwivedi *et al.,* 2014; Patil *et al.,* 2015; Wang *et al.,* 2017). Other authors suggested that modification of the surface coating could mediate the cytotoxicity of ION (Hildebrand *et al.,* 2010; Naqvi *et al.,* 2010; Könczöl *et al.,* 2011). Other forms of cytotoxicity

reported after ION exposure include cell cycle alterations (Wu and Sun, 2011; Lai *et al.,* 2015; Augustin *et al.,* 2016; Periasamy *et al.,* 2016), cytoskeleton alterations (Wu *et al.,* 2008, 2010; Cromer Berman *et al.,* 2013), disruption of mitochondrial membrane potential (Dwivedi *et al.,* 2014; Shukla *et al.,* 2015; Sanganeria *et al.,* 2015; Kermanizadeh *et al.,* 2015), plasmatic membrane impairment (Watanabe *et al.,* 2013; Rajiv *et al.,* 2015), apoptosis/necrosis (Berry *et al.,* 2004; Kim *et al.,* 2015; Ahamed *et al.,* 2016), autophagy (Schütz *et al.,* 2014; Shi *et al.,* 2015; Du *et al.,* 2017), and decreases in cell integrity or viability (Astanina *et al.,* 2014; Costa *et al.,* 2016).

Studies regarding the potential cytotoxic effects of ION on CNS are scarce and conflicting so far (reviewed in Valdiglesias *et al.,* 2014), and their potential risk on human brain cells have raised concern (Braeuer *et al.,* 2015). This is, at least in part, due to the great variety of ION, bare or with different coatings, tested. Furthermore, results of toxicity assays available are not always comparable since they are influenced by several factors such as the cell type tested (Ding *et al.,* 2010; Kunzmann *et al.,* 2011), experimental conditions assessed (Pisanic *et al.,* 2007), and physicochemical properties of ION (Thorek and Tsourkas, 2008). Indeed, general knowledge about ION toxic effects indicates that they mainly depend on nanoparticle size and surface coating (Rivet *et al.,* 2012).

2.5.2. Genotoxicity

A number of *in vitro* studies have evaluated the effects of ION exposure on the genetic material (reviewed in Dissanayake *et al.,* 2015). Different kinds of DNA damage, including strand breaks (Hildebrand *et al.,* 2010; Bhattacharya *et al.,* 2011; Han *et al.,* 2011) and micronucleus (MN) formation (Singh *et al.,* 2012), induced in cell systems after treatment with ION were reported (Figure I.9). Rajiv *et al.,* (2015) observed DNA breaks and chromosome aberrations in human lymphocytes exposed to ION (Fe_2O_3). And Pongrac *et al.,* (2016) observed that ION (γFe_2O_3), uncoated or coated with d-mannose or poly-L-lysine, induced DNA damage (also evaluated by comet assay) in murine neural stem cells irrespective of the surface coating. In this case, lower doses of any ION induced heavier DNA damage, and the lack of genotoxic effects at higher doses was explained by the aggregation behavior of ION at such concentrations. In agreement with these studies, Cicha *et al.,* (2015) evaluated the levels of H2AX phosphorylated (γH2AX), as indicative of DNA double strand breaks, in human primary tubular epithelial cells exposed to lauric acid-coated ION functionalized with mitoxantrone. They observed a significant increase in γH2AX foci upon treatment. Other studies describe positive genotoxic effects as well: in the comet assay and MN test in A549 alveolar cells treated with bare nanomagnetite (Könczöl *et al.,* 2011); in DNA damage in murine L-929 fibroblast cells treated with ION coated with (3-aminopropyl) trimethoxysilane (APTMS), tetraethyl orthosilicate (TEOS)-APTMS, or citrate

(Han *et al.,* 2011); in primary and oxidative DNA damage in human lymphoblastoid TK6 cells and primary human leukocytes exposed to oleate-coated nanomagnetite (Magdolenova *et al.,* 2013); in the comet assay in human IMR-90 lung fibroblasts and human BEAS-2B bronchial epithelial cells exposed to hematite (Bhattacharya *et al.,* 2009); and also in DNA damage in both skin epithelial A431 and lung epithelial A549 cells treated with smooth nanomagnetite (Ahamed *et al.,* 2013). MN induction was also observed in human MCL5 lymphoblastoid cells treated with dextran-coated γFe_2O_3 nanoparticles (Singh *et al.,* 2012).

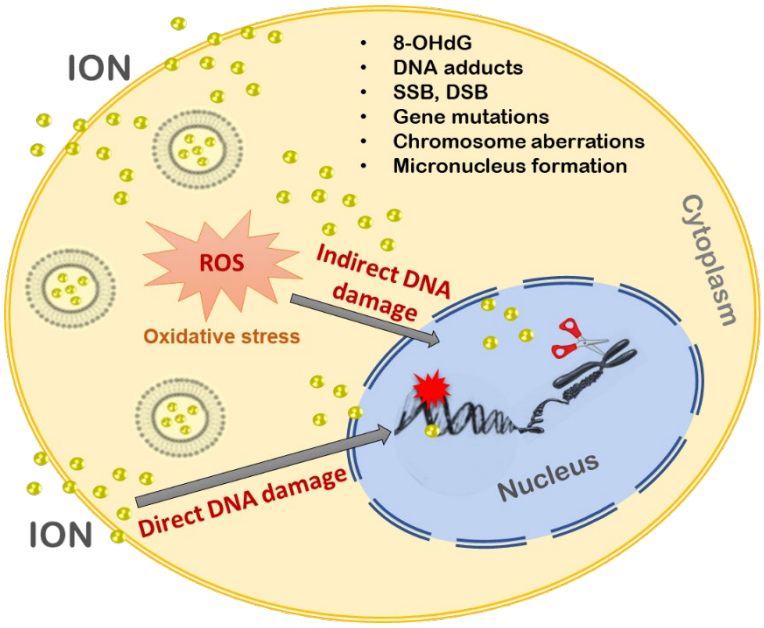

Figure I.9. Reported ION-induced genotoxic effects. ION may cause DNA damage through direct interaction with the DNA structure or result in the generation of oxidative radicals that in turn have the potential to indirectly cause DNA damage, mainly through base oxidation (mostly 8-OHdG). Consequently, ION exposure may induce genotoxic clastogenic or aneugenic effects. 8-OHdG: 8 hydroxydeoxyguanosine; ION: iron oxide nanoparticles; ROS: reactive oxygen species; DSB: double strand breaks; SSB: single strand breaks.

Opposite to these findings, studies showing negative results for ION genotoxicity are more frequent. Couto *et al.,* (2015) demonstrated absence of ION effects on the genetic material of human T-lymphocytes, reporting no chromosome aberrations in cells treated with polyacrylic acid-coated and uncoated nanomagnetite. Similar absence of genotoxicity was described by Magdolenova *et al.,* (2013) in human lymphoblastoid TK6 cells treated with uncoated nanomagnetite, and Paolini *et al.,* (2016) reported no genotoxicity or carcinogenicity for rhamnose-coated ION (magnetite) on mouse fibroblast Balb/c-3T3 cells. Some other works showed negative genotoxicity results (*i.e.* no induction of primary DNA damage and no increase in MN frequency) in many cell types exposed to different ION (Auffan *et al.,* 2006; Karlsson *et al.,* 2008, 2009; Guichard *et al.,* 2012; Singh *et al.,* 2012; Zhang *et al.,* 2012). Two independent

studies also evaluated the mutagenic potential of ION [AMI-25 ION (Weissleder *et al.,* 1989), and ferumoxtran-10 (Bourrinet *et al.,* 2006)] by means of the Ames test with negative results as well.

Short term *in vitro* genotoxicity tests may be prone to overestimating the *in vivo* genotoxicity of ION. Although *in vivo* genotoxicity studies are time-consuming, expensive and involve ethical issues and complex procedures (*e.g.,* toxicokinetic processes), they have an obvious advantage over *in vitro* tests. Although there are insufficient *in vivo* studies in literature on genotoxic effects of ION, the available ones provide important insight into potential *in vivo* genotoxicity. In particular, (Yang *et al.,* 2012) exposed Kunming mice to Fe_3O_4 nanoparticles via intraperitoneal injection in order to determine the potential safe dose range for medical use. The results indicated that ION are easily able to pass across the intestinal barrier and although they mainly accumulated in the liver, spleen, kidney, heart and bone marrow, the exposure did not induce genotoxicity in leukocytes (evaluated by the comet assay), chromosome aberrations in bone marrow cells, or MN in either of these cell types. Contradictory results were also observed among studies evaluating MN frequency in bone marrow cells of mice exposed *in vivo* to ION: positive results were obtained by Freitas *et al.,* (2002) and Sadeghiani *et al.,* (2005), while negative results were shown by Bourrinet *et al.,* (2006), Estevanato *et al.,* (2011) and Wu *et al.,* (2010).

Hence, given the general lack of consistence in the available results from *in vitro* and *in vivo* studies of ION genotoxicity, even at similar doses, further investigations are required to determine the specific mechanisms underlying the effects on the genetic material induced by these nanoparticles.

2.5.3. Neurotoxicity

ION have been shown to display the ability to cross the BBB after oral (Wang *et al.,* 2010), inhalatory (Kwon *et al.,* 2014), and intraperitoneal (Kim *et al.,* 2006) administration, and to directly reach the brain through the olfactory nerve after intranasal installation (Wang *et al.,* 2011). This ability makes them especially eligible for medical purposes on nervous system, such as drug delivery and imaging diagnostics, but also potentially harmful for this system. Hence, a special attention must be payed to the nervous tissue physiology and behavioral outcomes in animal studies. Most studies reported so far on the consequences of *in vitro* exposure of nervous system cells to different uncoated and coated ION have been performed in nervous system cells from different origin, particularly PC12 rat cells (Wu and Sun, 2011; Wu *et al.,* 2013b; Deng *et al.,* 2014), SH-SY5Y human cells (Imam *et al.,* 2015), mouse c17.2 neural progenitor cells (Soenen *et al.,* 2012), chick cortical neurons (Rivet *et al.,* 2012), culture brain microglial cells

(Luther *et al.,* 2013; Petters *et al.,* 2016), oligodendroglial OLN-93 cells (Petters *et al.,* 2014a), primary rat cerebellar granule neurons (Petters and Dringen, 2015), and endothelial cells (Kenzaoui *et al.,* 2012a, b), but scarcely in human neurons or glial cells.

Nevertheless, unlike the considerable amount of studies addressing *in vitro* effects of ION on nervous system cells, the number of *in vivo* studies on potential neurotoxicity of these nanoparticles is quite restricted. For example, the conjugation of the drug daunorubicin with ION (oleic acid-capped Fe_3O_4) nanocomposites for delivery can reduce the neurotoxicity caused by this anticancer drug on rat brains *in vivo*, suggesting a possible application of these nanoparticles to lessen the side effects of cancer therapies (Xu *et al.,* 2012). Most of the *in vivo* studies on ION neurotoxicity employed rats as experimental model. Hence, Kumari *et al.,* (2012) observed dullness and irritation in Wistar rats after 28 days of oral daily exposure to ION (Fe_2O_3). Moreover, a significant dose-dependent inhibition of total, Na^+-K^+, Mg^{2+} and Ca^{2+}-ATPases in brain, as well as acetylcholinesterase in brain and red blood cells, were found in exposed animals, suggesting that ION exposure may affect synaptic transmission and nerve conduction. Similarly, Bourrinet *et al.,* (2006) observed different physiological responses, including signs of polypnea, exophthalmos and mydriasis in Sprague-Dawley rats after intravenous treatment of ION (ferumoxtran-10), although no neurobehavioral, neurovegetative, or psychotropic effects were detected. More recently, Kim *et al.,* (2013) treated Sprague-Dawley rats with different ION [dimercaptosuccinic acid (DMSA)-coated maghemite, and DMSA-, PEG- and PEG-Au-coated magnetite] by intraneural injection (sciatic nerve); ION caused immune cell infiltration, neural inflammation and apoptosis, and induced neural antioxidant response. Wu *et al.,* (2010) detected a regional distribution of ION (magnetite) in brain of rats intranasally instilled for seven days. ION induced oxidative damage in striatum but not in hippocampus, despite the presence of nanoparticles in both regions resulted particularly high.

Agreeing with these studies in rats, neurotoxicity of ION has been also reported in mice and fish. In mice, intranasal administration of Fe_2O_3 nanoparticles induced pathological alterations in olfactory bulb, hippocampus and striatum; microglial proliferation, activation and recruitment were also observed in these areas, especially in the olfactory bulb (Wang *et al.,* 2011). In addition, mice treated with magnetite nanoparticles by intragastric administration showed less activity and a slight loss of appetite (Wang *et al.,* 2010). In fish, dextran-coated Fe_3O_4 nanoparticles intraperitoneally administered to adult zebrafish were found to accumulate in brain inducing apoptosis and inhibition of acetylcholinesterase in this tissue. Moreover, although no alterations in the expression of genes associated with inflammation were observed, increased levels of ferric iron and enhanced mRNA levels of caspase 8, caspase 9 and transcriptional factor AP-1 in brain of treated animals were also detected (de Oliveira *et al.,* 2014).

3. CELLULAR INTERACTION WITH NANOPARTICLES

3.1. Cellular uptake

The actual entry of nanoparticles into the cells should be verified prior to toxicity evaluation. As it can be seen in Figure I.10, ION may be actively incorporated by cells mainly via passive diffusion, clathrin-mediated endocytosis, caveolae-mediated endocytosis, phagocytosis, or macropinocytosis (Sahay *et al.,* 2010; Cores *et al.,* 2015). Particles internalized via active uptake are commonly transported in vesicular structures that then fuse to result in phagolysosomes or endosomes (Kuhn *et al.,* 2014). Sometimes, they might be endocytosed upon pinocytosis. Alternatively, they may also be carried to the cytosol, or transported via caveosomes to the endoplasmic reticulum, or cross the cell as part of transcytotic processes. Besides active transport, smaller nanoparticles may also enter the cell passively via diffusion through the plasma membrane (Sahu, 2009). From the cytoplasm they may then gain access to subcellular compartments such as the nucleus and mitochondria (Hart and West, 2009). The speed of these processes seems to be strongly dependent on the surface properties of the ION and on their *in vivo* surface modifications (*e.g.*, by endogenous proteins or lipids found in surfactant or plasma) (Oberdörster *et al.,* 2005). These observations led to the formulation of the "corona" theory, which states that, in a biological environment (*e.g.*, surfactant, blood, mucus), the particle surface is covered by biological macromolecules (*e.g.*, proteins, lipids) (Jud *et al.,* 2013). This makes ION uniquely suitable for therapeutic and diagnostic uses, but it also may leave target organs, such as the CNS, vulnerable to potential adverse effects.

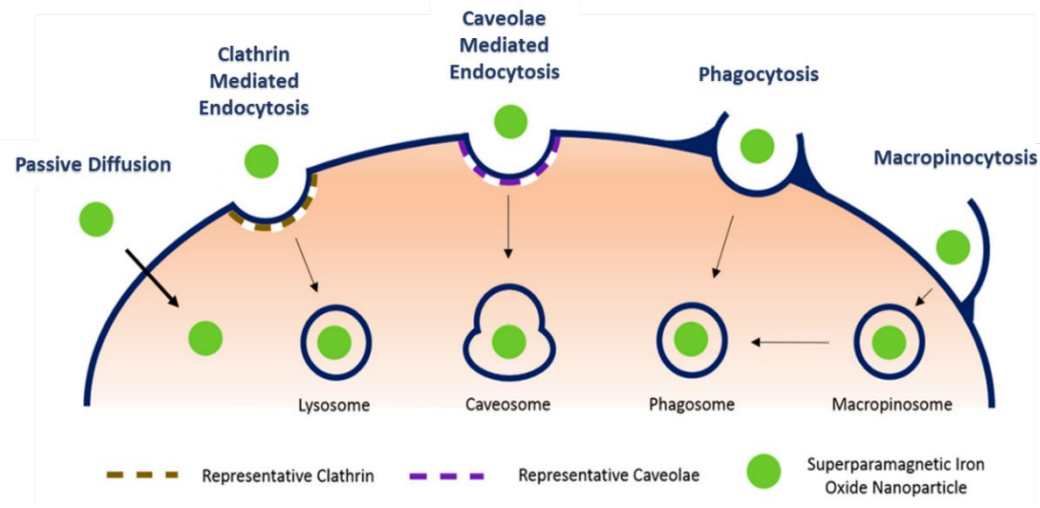

Figure I.10. Summary of possible mechanisms used by nanoparticles to enter cells and cellular compartments. From left to right, nanoparticles may actively be taken up by cells by passive diffusion, clathrin-mediated endocytosis, caveolae-mediated endocytosis, via phagocytosis, or macropinocytosis (from Cores *et al.,* 2015).

The method of choice determining ION uptake mainly depends on the research question, the available analytical devices as well as on the type of ION of interest. Therefore, it is not possible to recommend one specific technique for all cases. As well-known from the convincing evidence from the literature, physicochemical properties of nanoparticles, such as size, shape, composition of the core and surface coating and/or functionalization, have a key role on nanoparticle cellular interaction including uptake, intracellular fate and induction of cell response, issues that also may require very different analytical methods (Drasler *et al.,* 2017).

One sensitive and rapid method to determine cellular uptake is flow cytometry (FCM). In FCM, single cells pass in a steady stream in front of a laser detection unit that collects the signals from a single cell on appropriate detectors. Forward scattering (FSC) light is useful to determine the size or volume of the cell, while side-scattering (SSC) is a measure of cellular complexity (Shapiro, 1995). The integrated signal from individual cells as measured by FSC and SSC is interpreted as either nanoparticle-containing cell or nanoparticle-free cell (Suzuki *et al.,* 2007) (Figure I.11). The signal integration increases the sensitivity compared with fluorescence imaging methods, but it is not possible to establish the relative location of the nanoparticle in the cell.

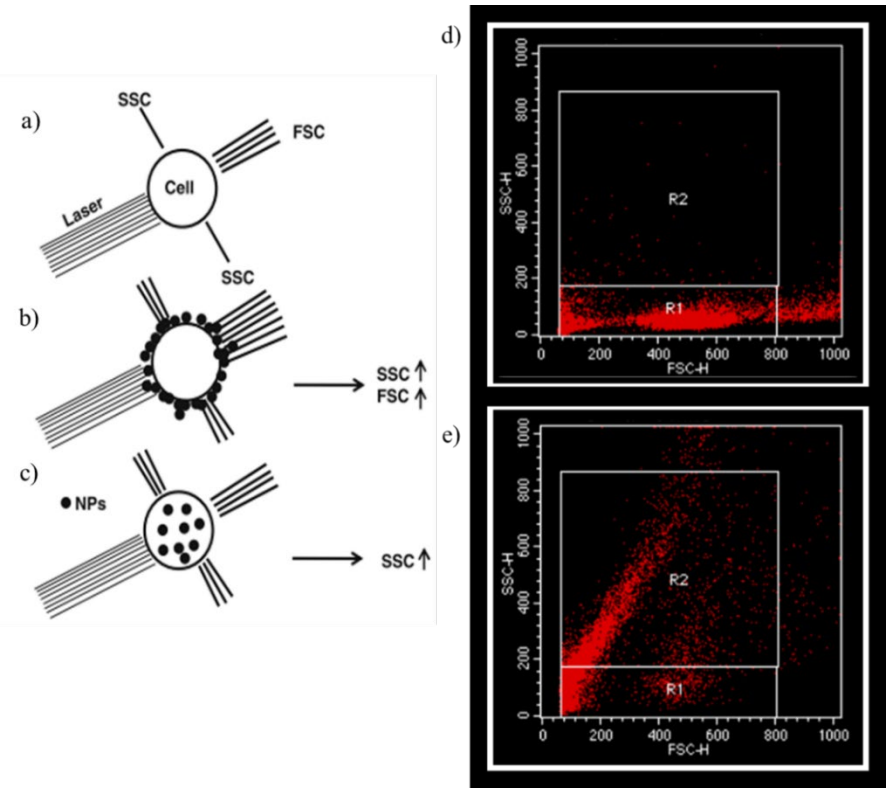

Figure I.11. Flow cytometry analysis of nanoparticle uptake in cells: a) light scattering by a cell that is not associated with any nanoparticle; b) nanoparticles adhere to the cell surface, leading to an increase in forward scatter (FSC) and side scatter (SSC); c) nanoparticle internalization by the cell, leading to an increase in SSC only; d) FSC/SSC dot plot from FCM analysis with cells no exposed to ION; e) FSC/SSC dot plot from FCM analysis showing a high proportion of cells with internalized nanoparticles (R2).

Electron microscopy (EM) techniques (*e.g.*, scanning EM [SEM], focused ion beam [FIB]-SEM, transmission EM [TEM]), are among the analytical methods widely used for nanoparticle uptake assessment, which can provide an adequate resolution for the quantification of absolute nanoparticle number into the cell. An EM micrograph provides the signal of electron dense nanoparticles and the biological context which requires interpretation prior to quantification. Therefore, computer-assisted counting is often not an option. With increased human intervention in the interpretation, observer expectancy effects may affect the accuracy.

3.2. Cytotoxicity

3.2.1. Membrane integrity

In a cellular context, the membranes, which are bilayers of phospholipids, divide different intracellular compartments, each of which has specific functions, and whose integrity determine the viability of the cell. They also encapsulate the whole cell. In order to facilitate exchanges between compartments and/or cells, membranes have to be permeable. The outer cell membrane is the cell interface to its external environment and allows selective transport of ions, molecules and also nanoparticles (Vasir and Labhasetwar, 2008). It is the ability of membranes to control intracellular homeostasis, through selective permeability and transport mechanisms, which makes them a vulnerable target for possible damaging effects of nanoparticles.

Lactate dehydrogenase (LDH) assay, based on determination of LDH release from the cytoplasm, is commonly used to determine membrane integrity. It is a widely recommended nonradioactive, rapid, very sensitive and safety assay for cytotoxicity testing of cultured cells as well as viability testing. LDH is a ubiquitous enzyme present in cytosol of a wide variety of organisms. Since LDH is a fairly stable enzyme, it has been widely used to evaluate the presence of damage and toxicity of tissue and cells. LDH is released through the altered cell membrane following cell death process. After cell membrane damage, LDH is released and thus dead cells can be detected.

3.2.2. Cell cycle

The cell cycle is the process by which eukaryotic cells duplicate and divide. The cell cycle consists of three specific and distinct phases: G_1 (Gap 1) during which the cell grows and accumulates the energy necessary for duplication; phase S (synthesis) in which cellular DNA replicates; and G_2 (Gap 2) where cell prepares to divide. Mitosis (M) phase is divided into two differentiated stages: mitosis and cytokinesis. During mitosis a parent cell chromosomes are divided between two sister cells. In cytokinesis, division of the cytoplasm occurs, leading to the formation of two distinct daughter cells. Each phase of the cell cycle is tightly regulated, and

checkpoints exist to detect potential DNA damage and allow it to be repaired before a cell divides. If the damage cannot be repaired, a cell becomes targeted for apoptosis. Cells can also reversibly stop dividing and temporarily enter a quiescent or senescent state, G_0. The first checkpoint is at the end of G_1, making the decision if a cell should enter S phase and divide, delay division, or enter G_0. The second checkpoint, at the end of G_2, triggers mitosis if a cell has all the necessary components (Crosby, 2007).

The most common method for assessing the cell cycle is using FCM to measure cellular DNA content. During this process, a fluorescent dye that binds to DNA is incubated with a single cell suspension of permeabilized or fixed cells. Since the dye binds to DNA stoichiometrically, the amount of fluorescent signal is directly proportional to the amount of DNA. Because of the alterations that occur during the cell cycle, analysis of DNA content allows discrimination between G_1 (2n), S (2n~4n), G_2 (4n) and M phases. Briefly, cells are fixed and permeabilized to allow the dye(s) enter the cell and to prevent them of being exported out. Staining with the DNA binding dye is carried out after cells have been treated with RNase to ensure only DNA is being measured. Several data sets, including forward scatter vs side scatter, pulse area vs pulse width, and cell count *vs.* fluorescence, are collected to ensure only single cells are measured (Darzynkiewicz *et al.,* 1980; Nunez, 2001). There are a number of important considerations when carrying out analysis of cell cycle with FCM data: (1) the forward scatter/side scatter plots are an integral part of the analysis and should not be overlooked, since this is how single cells are identified; (2) if doublets (when the DNA content of two cells in G_1 are recorded as a single G_2/M event) are allowed in to the analysis, it can lead to over-representation of G_2/M; and (3) cellular aggregates and flow rates below 1000 cells/second should also be avoided to allow a low sample pressure differential to be used, which leads to an optimal coefficient of variance (Cobb, 2013).

3.2.3. Cellular death

Apoptosis is a genetically programmed and well-orchestrated mode of cell death that is characterized by a series of morphological and biochemical alterations to the cell architecture that package a cell up for removal by phagocytic cells, *i.e.* activation of initiator and effector caspases, cellular shrinkage, chromatin condensation, membrane blebbing, loss of mitochondrial integrity and DNA fragmentation (Elmore, 2007). Crucially, apoptotic cells are recognized by phagocytes and are engulfed before they leak their contents. Thus, apoptosis ensures that when a cell needs to be removed from a tissue, this occurs in an orderly manner that minimizes disruption to neighboring cells. The major consideration during apoptosis is that intracellular contents do not leak into the extracellular space because this could damage surrounding cells, and trigger inflammation through release of molecules with immune-activating activity (Favaloro *et al.,* 2012; Elmore *et al.,* 2016). Most of the biochemical and morphological changes that typify

apoptosis are the consequence of activation of a subset of the caspase family of proteases (caspases 3, 6, 7, 8 and 9). The caspases operate similar to a controlled demolition squad, coordinating the packaging and disposal of cells in a manner that minimizes damage to neighbors and the initiation of inflammation (Galluzzi *et al.,* 2015). There are two different proximal pathways leading to caspase activation: (1) the extrinsic pathway initiated by binding of a specific subset of ligands, such as Fas ligand, to their corresponding receptors at the cell plasma membrane surface, via activated cytokine ‘‘death’’ receptors that process initiator caspase 8; and (2) the intrinsic pathway initiated through the death receptor after cytosolic release of mitochondrial derived cytochrome c (mediated by members of the B-cell lymphoma-2 (Bcl-2) protein family), in which initiator caspase 9 is activated. Both pathways terminate with activation of the effector caspase, caspase 3, that lead finally to the cell death (Dorn, 2013). The initiation phase is largely dependent on cell type and apoptotic stimulus (*e.g.*, oxidative stress, DNA damage, ion fluctuations, and cytokines) (Solier and Pommier, 2009).

Necrosis, as opposed to apoptosis, is a rather passive, unorganized and generally uncontrolled process that is caused by a plethora of external stress factors, including extremely high concentrations of xenobiotics, and involves the sudden loss of membrane integrity, release of extracellular contents, leading to activation of the immune system and extensive inflammation. It usually starts with the loss of ion homeostasis, which eventually evokes cell swelling, loss of cell plasma membrane integrity, and cell lysis (Maes *et al.,* 2015). Necrosis of cells is irreversible and most often results from acute cellular injury that lead to a metabolic breakdown of the cell that coincides with rapid depletion of ATP. In contrast to apoptosis, necrosis has not historically been considered to be a genetically controlled process that requires energy (Elmore *et al.,* 2016). Necrosis is typically not associated with caspase activation, although the exception to this is when cell death follows aggressive activation of the inflammatory subset of caspases (caspases 1, 4 and 5), a mode of cell death termed pyroptosis. Necrotic cell death bears none of the striking features that characterize apoptotic cells, such as extensive membrane blebbing and hypercondensation and fragmentation of the nucleus. Instead, necrotic cells undergo extensive organelle and cell swelling, leading to decondensation of nuclei. Thus, this mode of cell death is relatively easy to distinguish from apoptosis on the basis of morphological criteria (Davidovich *et al.,* 2014).

Methods for measuring apoptosis typically rely on the detection of caspase-dependent events, such as exposure of plasma membrane phosphatidylserine, that precede uptake of vital dyes such as trypan blue or propidium iodide (PI). Alternatively, the striking morphological features of apoptotic cells (such as compaction and fragmentation of the cell nucleus), which are also effected through caspase activation, are still highly relevant for methods detecting this mode of cell death (Martin and Henry, 2013). Flow cytometry-based methods for assessing apoptosis

based upon DNA fragmentation, caspase activation and phosphatidylserine externalization are very well-established methods in the field (Henry *et al.,* 2013). Analysis of annexin V/PI double staining by flow cytometry is based on the estimation of cell membrane changes during apoptosis and ability of the protein annexin V to bind to phosphatidylserine exposed on the outer membrane leaflet in apoptotic cells. In viable cells, phosphatidylserine is located in the inner membrane leaflet, but upon induction of apoptosis, it is translocated to the outer membrane leaflet and becomes available for annexin V binding. However, phosphatidylserine is also appearing on the necrotic cell surface. Using a simultaneous combination of annexin V and PI discriminating apoptotic from necrotic cells is feasible (Figure I.12) (Jurisic and Bumbasirevic, 2008).

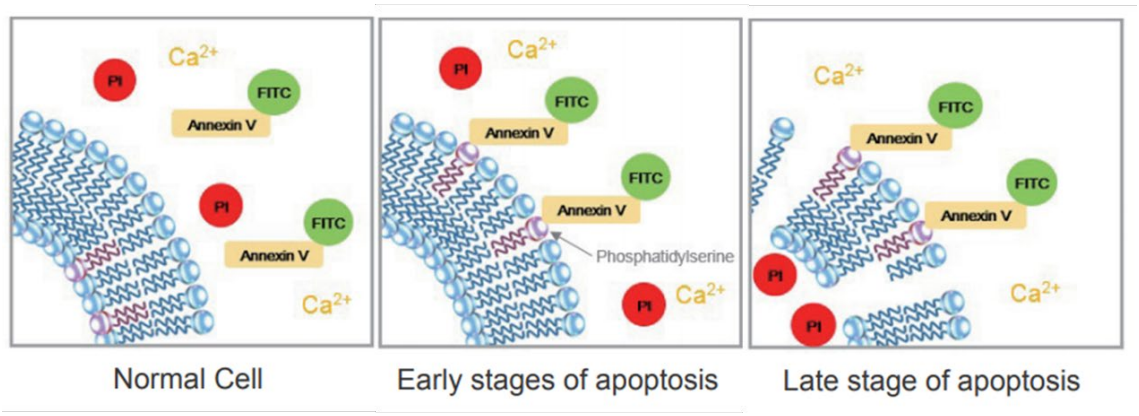

Figure I.12. In normal cells, phosphatidylserines (purple membrane phospholipids) are held on the inner layer of the cell membrane, so annexin V does not attach to the cells. During early apoptosis, the phosphatidilserines are exposed on the outer layer, where they attach to the FITC-labeled Annexin V and stain the cell surface green. During late apoptosis, propidium iodide (PI) enters the cell and stains the contents red (from https://www.nacalai.co.jp/global/download/pdf/AnnexinV-FITC.pdf).

3.3. Genotoxicity

3.3.1. Comet assay

The single cell gel electrophoresis assay, commonly known as comet assay, is a simple, reliable, sensitive and widely used technique to assess DNA damage in single cells (Singh *et al.,* 1988). The comet assay protocol was originally proposed by Ostling and Johanson (1984) and later modified by Singh *et al.,* (1988).

Depending on the pH employed, the comet assay allows detection of several types of DNA damage, such as single and double strand breaks, incomplete excision repair sites, crosslinks, and alkali-labile sites (Collins, 2015). The alkaline version of the comet assay is the most commonly used. In brief, after embedding in agarose on a microscope slide, cells are lysed employing a solution containing a detergent, to remove the membranes, and high salt

concentrations, to eliminate the nuclear proteins, leaving nucleoids (residual DNA structures). Afterwards, the nucleoids are incubated in an alkaline solution to facilitate DNA unwinding and then electrophoresed in alkali. During the electrophoresis, the DNA loops containing breaks relax and move away from the nucleoid to the anode due to their negative charge, forming a comet shape which is observed by fluorescence microscopy using a suitable fluorescent stain (Figure I.13). The more damaged the DNA, the farther migration to the anode. Length and intensity of the comet tail is proportional to the number of breaks in the DNA. Not damaged cells will not show a tail (Singh *et al.,* 1988).

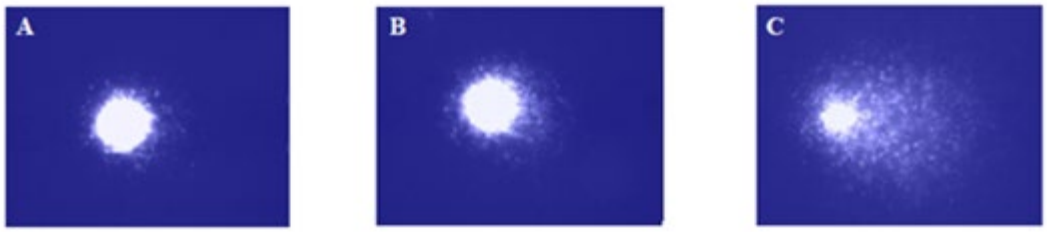

Figure I.13. Fluorescence microscopy image of cell nucleoids after comet assay: A) not damaged nucleoid, B) mildly damaged nucleoid, C) highly damaged nucleoid.

The comet assay is widely employed to evaluate primary DNA damage. It is used in (i) both *in vivo* and *in vitro* genotoxicity testing, to screen novel drugs, cosmetics, or chemicals for potential carcinogenic properties, (ii) in human biomonitoring, to evaluate the effects of toxic agents at DNA level, and its involvement in diseases or individual variations, for instance in DNA repair capacity, (iii) in environmental monitoring, as a marker of genetic damage by pollutants, and (iv) in basic research into mechanisms of DNA damage and repair (Azqueta and Collins, 2013; Azqueta *et al.,* 2014). Moreover, some of the most recent applications of the comet assay are in the assessment of genotoxic effects of nanomaterials (Collins, 2015).

Since nanoparticles exhibit unique physicochemical properties, evaluation of their potential genotoxic effect is crucial. Genotoxic activities of nanoparticles may be due to direct interaction with the DNA, or by secondary damage induced through ROS production (Bowman *et al.,* 2012). In the past few years, the comet assay has been extensively used to study genotoxic effects of nanoparticles; automated image analysis softwares are commercially available, making the use of comet assay simple and effective (Tice *et al.,* 2000).

3.3.2. γH2AX assay

Genotoxic insults such as ultraviolet light (UV) exposure, drugs, chemicals, and endogenous DNA processes can lead to double strand breaks (DSB) (Mah *et al.,* 2010). When a

DSB is produced, a very early cell response occurs. The H2AX variant histones flanking the DSB sites are rapidly phosphorylated at the serine 139 residue, leading to the formation of the so-called γ-H2AX (Ivashkevich *et al.,* 2012) (Figure I.14). γ-H2AX serves as a platform for the recruitment of other DNA repair proteins but also increases DNA accessibility, recruits cohesins that maintain the proximity between DNA strands during the repair process, and modulates the checkpoint response (Rogakou *et al.,* 1998; Dickey *et al.,* 2009; Carriere *et al.,* 2017). Under normal conditions, γH2AX appear within few minutes after the lesion, reach maximum levels after about 30min and then decline and disappear after approximately 24h (Rogakou and Sekeri-Pataryas, 1999; Bourton *et al.,* 2012). Therefore, H2AX phosphorylation represents an early event in the DNA damage response against DSB and plays a central role in sensing and repairing these lesions (Matsuzaki *et al.,* 2010; Scarpato *et al.,* 2013). Due to the severity of this kind of DNA damage, cells respond rapidly and massively to nascent breaks in order to locate them in the chromatin and repair the damage as quickly and accurately as possible, since erroneously repaired breaks can lead to cancer and cell death.

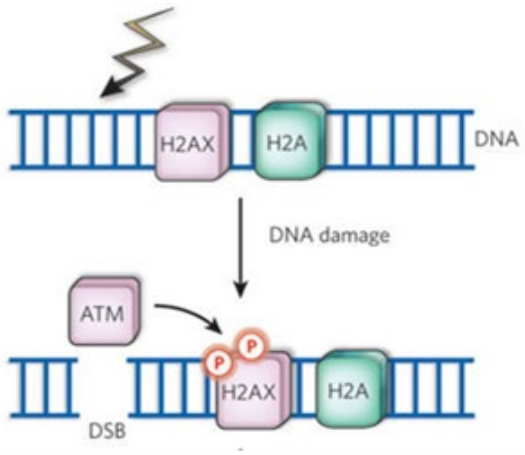

Figure I.14. Representation of H2AX phosphorylation as a response to double strand breaks (DSB). ATM, ataxia telangiectasia mutated (modified from Hoeller and Dikic, 2009).

Although the use of γH2AX as a genotoxic marker is a good way to identify the genotoxic potential of nanoparticles, its use in this field is extremely novel and scarce. The alteration in the expression profile of γH2AX induced by nanoparticles may be detected by different techniques such as immunohistochemistry, flow cytometry, and western blot. Analysis of immunofluorescence γ-H2AX staining by FCM provides an automated high-throughput platform that is fast, practical, reliable way to analyze the DSB formation (Toduka *et al.,* 2012), and the correlated potential genotoxicity due to nanoparticle exposure (Kumar and Dhawan, 2013;

Dissanayake *et al.,* 2015). Besides, FCM evaluation provide tools to take into consideration variations due to cell-cycle effects (Watters *et al.,* 2009), and increases considerably the number of cells evaluated, diminishing the variability and enhancing the statistical power of the results (Sánchez-Flores *et al.,* 2015).

3.3.3. Micronucleus test

The study of DNA damage at the chromosome level is an essential part of genetic toxicology because chromosomal mutation is an important event in carcinogenesis (Fenech, 2008). It is known that chromosome aberrations are a direct consequence and manifestation of DNA damage, *e.g.*, chromosome breaks due to unrepaired DSB and/or chromosome rearrangements from misrepair of strand breaks in DNA (Fenech, 2000). Micronuclei (MN) result from acentric chromatids or chromosome fragments, *i.e.* those lacking a centromere (clastogenic events), or whole lagging chromosomes (aneugenic events) that are unable to migrate to the mitotic spindle poles and subsequently are not incorporated into either of the daughter nuclei (Figure I.15). Therefore, MN can only arise in cells that have undergone cell division (Avlasevich *et al.,* 2011; Lukamowicz *et al.,* 2011). MN are nuclear entities independent of the main nucleus, numbering anywhere between 1 and 6 per cell, with diameter between 1/3 and 1/16 of the diameter of the main nucleus (Botta and Benameur, 2011).

Figure I.15. Representation of MN formation in cells undergoing nuclear division (from Fenech *et al.,* 2011).

MN test have emerged as a widespread method for assessing chromosome damage because it enables both chromosome loss and chromosome breakage to be measured reliably, and hence is a well-established assay for detecting clastogenic and aneugenic compounds (Lukamowicz *et al.,* 2011). As an alternative to the traditional MN scoring by microscopy (subjective, tedious and time consuming), a first automatic measurement of MN by flow cytometry was developed by Nüsse and Kramer (1984) and Nüsse *et al.,* (1994). However, the same two technical problems were consistently encountered: (i) the need to remove background ‘‘noise’’, and (ii) the fact that some subcellular particles were mistakenly scored as MN. Since

Nüsse and Kramer (1984) developed a two-step method to improve the separation of small MN from the main nuclei, a number of groups attempted to improve the staining or analysis techniques, where the exclusion of necrotic and late apoptotic DNA is possible (Avlasevich *et al.,* 2006; Bryce *et al.,* 2007). Thus, FCM method is also used in genetic toxicology testing, as it adds the benefits of automated scoring and low time-consuming measurements (Laingam *et al.,* 2008).

For nanoparticles as a whole, as well as ION in particular, MN test appear to be one of the most popular genotoxicity tests based on the numbers of corresponding reports (Magdolenova *et al.,* 2014; Golbamaki *et al.,* 2015). Although the number of studies on ION genotoxicity is increasing, some results for the same core chemical composition are inconsistent. They need to be confirmed by additional experiments, determining whether they reflect genuine differences due to differences in nanoparticle characteristics, such as size, coating, functionalization, etc. Another consideration about the *in vitro* MN assay when applied to nanomaterial hazard assessment is that it is highly advisable to use fluorescent DNA dyes for staining the cells, in order to avoid falsely identifying nanoparticle agglomerates as MN (Magdolenova *et al.,* 2014).

3.3.4. DNA repair competence assay

DNA repair mechanisms are the cell defense system to protect and maintain the genome integrity. DNA repair involves three main mechanisms: (i) direct reversal of the damage, (ii) excision repair – which according to the type of DNA damage induced could involve three pathways: base excision repair, nucleotide excision repair and mismatch repair – and (iii) DSB repair, which may be conducted by two routes, depending on the cell cycle phase: homologous recombination and non-homologous end joining. Deficiencies in these systems can often promote genome instability and directly lead to various human diseases, particularly cancer, neurological abnormalities, immunodeficiency and premature aging (Iyama and Wilson, 2013).

The DNA repair competence assay, or challenge assay, is a cytogenetic method to evaluate the effects on the cellular ability to repair the DNA damage induced by different physical or chemical agents. Exposure to mutagenic agents can lead to potential genotoxic effects, important DNA alterations, as well as cause impairment or interference with the cellular repair machinery, increasing the risk of certain diseases such as cancer (Au *et al.,* 2010). Consequently, these alterations could reduce the capacity of cells to repair damaged DNA and trigger pathological processes. The basis of this *in vitro* test is that exposure of cells to a certain challenging agent can deteriorate their DNA repair machinery, thus decreasing the repair capacity of damage induced. Cells are treated *in vitro* with a known mutagen (*e.g.* X-rays, bleomycin, H_2O_2) and a subsequent time for repair of the damage induced is allowed. The genetic damage induced can be then analyzed through several common genotoxicity tests, such as chromosomal

aberrations test, MN test, comet assay, etc. The difference between the damage evaluated before and after that incubation time will show the repair capacity of the study cells (Au *et al.,* 2010).

The use of comet assay to measure DNA damage in the DNA repair competence assay provides a powerful tool to detect repair ability. Besides, it offers the advantage of quantifying the repair as progress of the DNA damage levels since, in contrast with other cytogenetic techniques such as chromosome aberrations, it allows evaluating the damage in different time points (*i.e.*, after damage induction and after the incubation period in fresh medium) (Schmezer *et al.,* 2001).

While numerous studies addressed the DNA damage induced by nanoparticles, their impact on DNA repair processes has never been specifically approached. Hence, comprehensive studies describing the DNA repair processes that could be affected by NP exposure, at the level of protein function, gene induction and post-transcriptional modifications, are needed. As well, it is quite important filling this gap of knowledge and taking into account the advantages and limitations of the different experimental approaches, to finally understand the nanoparticle interactions with the genome in an integral manner (Carriere *et al.,* 2017).

On the basis of what was explained in this memory so far, ION have a number of interesting current and potential future applications, especially in the biomedical field. All these medical applications require internalization of ION for efficient diagnosis or treatment, leading to potential risks associated with exposure. Concretely, development of ION employed in the study of CNS pathologies is especially increasing nowadays; however, data on possible consequences of exposure of human nervous system cells to ION are still scarce. ION toxicity has been demonstrated to vary considerably and also to depend on cell type and physicochemical characteristics such as size, shape, presence/type of coating, and stability in biological media. The analysis of all data collected in the bibliography so far highlights the lack of consensus in establishing the toxicity mechanism associated with ION exposure, mainly due to the high variability of nanoparticles and experimental conditions tested in the different studies.

II. OBJECTIVES

II. OBJECTIVES

Due to their particular physicochemical properties, iron oxide nanoparticles (ION) have great potential for an increasing number of biomedical applications, particularly those focused on nervous system. For such applications, ION must be introduced in the human body and be in contact with cells and tissues, making the necessity of knowing the potential risk associated to nervous system exposure imperative. In this context, the main objective of this work was to assess the potential cytotoxicity and genotoxicity induced in neuronal and glial cells by exposure to differently coated ION.

This overall goal will be achieved through the following specific objectives:

1. To determine the release of iron ions from the ION surface, and to assess the ability of the ION to enter the neuronal and glial cells.
2. To analyse the cytotoxicity associated to ION exposure, in terms of alterations in membrane integrity or cell cycle, and induction of cell death.
3. To examine genotoxic effects related to treatment with ION, determining induction of primary DNA damage, double strand breaks, and chromosome aberrations.
4. To evaluate modifications in DNA repair ability caused by ION in neuronal and glial cells.

Each one of these objectives will be conducted in SH-SY5Y neuronal cells and A172 glial cells (astrocytes), testing two types of ION – coated with silica (S-ION) and with oleic acid (O-ION) – under a range of experimental conditions including doses, treatment times and presence/absence of serum in the cell culture media.

III. MATERIALS AND METHODS

III. MATERIALS AND METHODS

1. NANOPARTICLES: PREPARATION AND CHARACTERIZATION

Silica-coated magnetite nanoparticles (S-ION) were synthesized and prepared as stable water suspensions (5mg/ml) as described by Yi *et al.,* (2006). Oleic acid coated ION (O-ION) were synthesized and prepared as stable water stock suspensions (19mg/ml) as described by Maity and Agrawal (2007).

Particle size and morphology were previously studied by transmission electron microscopy, surface chemistry was analysed by photoelectron spectroscopy, while average hydrodynamic size and zeta potential of nanoparticles in suspension were determined by dynamic light scattering in deionized water, complete and serum-free SH-SY5Y and A172 culture medium (see composition below) (Costa *et al.,* 2016).

Prior to each treatment, a stock suspension (1mg/ml) of each ION was prepared in complete or serum-free SH-SY5Y and A172 culture media (see composition below) and ultrasonicated in a water bath (Branson Sonifier, USA) for 5min. Serial dilutions were carried out to obtain the different test concentrations, and ultrasonicated in water bath for an additional 5min period.

2. DISSOLVED IRON CONCENTRATIONS IN THE CELL CULTURE MEDIUM

In order to determine the iron ions released from ION, nanoparticle suspensions were prepared in complete or serum-free SH-SY5Y and A172 cell culture media and incubated for 3h and 24h at 37°C in a humidified 5% CO_2 environment. After centrifugation at 14,000rpm for 30min, the liquid medium over the ION solid phase was collected. Flame atomic absorption spectroscopy (FAAS) (Thermoelemental Solaar S4 v.10.02) was used to quantify the iron content in the supernatant. Complete or serum-free cell culture media without nanoparticles subjected to the same experimental conditions were used as negative controls.

3. CELL CULTURES AND TREATMENTS

Human neuroblastoma SH-SY5Y cell line was purchased from the European Collection of Cell Cultures. These cells were cultured in nutrient mixture EMEM/F12 (1:1) medium supplemented with 10% heat-inactivated foetal bovine serum (FBS), 1% antibiotic and antimycotic solution, with 1% non-essential amino acids. Human glioblastoma A172 cells were obtained from the European Collection of Cell Cultures and grown in a nutrient mixture composed of DMEM with 1% L-glutamine, 1% antibiotic and antimycotic solution, supplemented with 10% heat inactivated FBS. All ingredients were obtained from Invitrogen. Cells were incubated in a humidified atmosphere with 5% CO_2 and 37ºC.

To carry out the experiments, cells were seeded in 96-well plates (5–6 x10^4 cells/well) and allowed to adhere for 24h at 37°C prior to the experiments. For each experiment, these cells were incubated with ION and controls. Concentrations tested were 10, 50, 100 and 200µg/ml when treating SH-SY5Y cells, and 5, 25, 50 and 100µg/ml when treating A172 cells, and treatment times were 3 and 24h. Previous results from cell viability assays (Costa *et al.,* 2016) were used to establish these concentrations and exposure times. The decrease in viability was lower than 30% in all cases. Cell culture media were used as negative controls in all experiments. The following chemicals were employed as positive controls: camptothecin (Campt) 10µM for apoptosis; Triton X-100 1% for lactate dehydrogenase (LDH) assay; mitomycin C (MMC) 1.5µM for cell cycle analysis in both cell lines and micronucleus (MN) test in neuronal cells, and 15µM for MN test in glial cells; bleomycin (BLM) 1µg/ml for γH2AX analysis, and H_2O_2 100µM for comet assay in both cell types and DNA repair competence assay in SH-SY5Y cells, and 200µM for DNA repair competence assay in A172 cells.

4. CELLULAR UPTAKE

The potential of the ION to enter the SH-SY5Y neuronal cells was evaluated by following the protocol described by Suzuki *et al.,* (2007). Cells were seeded in 96-well cell culture plates. After 24h of seeding, the cells were exposed to ION for 3 and 24h. After exposure, the culture medium containing nanoparticles was removed and cells were harvested using 0.025% trypsin. They were then centrifuged at 250xg for 5min. The supernatant was discarded, and the pellet was re-suspended in 0.5ml phosphate buffered saline solution (PBS). The rate of cells containing nanoparticles was determined using a FACSCalibur flow cytometer (Becton Dickinson). The analysis was carried out based on the size and the intracellular complexity of the cells by measuring the forward scatter (FSC) and the side scatter (SSC), respectively. Data were acquired from a minimum of 10^4events per sample using CellQuest Pro software (Becton Dickinson).

The uptake and intracellular localization of ION in A172 cells were assessed by transmission electron microscopy (TEM) coupled with energy-dispersive X-ray spectroscopy (EDX) as previously described (Fernández-Bertólez *et al.,* 2018b). Cells were seeded in T25 flasks and exposed to 25µg/ml and 100µg/ml of ION dispersed in complete and serum-free media for 3 and 24h. Negative controls (cells with no exposure to nanoparticles) and positive controls (cells exposed to 150µg/ml of TiO_2 nanoparticles, Sigma reference 637254) were also included in this experiment. After exposure, cells were washed twice with PBS, harvested by trypsinization and centrifuged. The pellets were then fixed in 2.5% glutaraldehyde in 0.2M sodium cacodylate pH 7.2–7.4 for 2h, post-fixed with 2% osmium tetroxide, dehydrated through graded alcohol solutions and embedded in Epon. Ultrathin sections of 100nm were mounted on copper grids and contrasted with uranyl acetate and lead citrate and examined with Jeol JEM 1400 transmission

electron microscope, equipped with an energy dispersive X-ray (EDX) spectrometer (Oxford Instruments). Digital images were captured by using a CCD digital camera Orious 1100W.

5. CYTOTOXICITY

5.1. Membrane integrity

A commercial kit (Roche Diagnostics Corp) was used to measure the LDH release in cell culture media, according to the manufacturer's instructions. After exposure, cell culture medium was collected for LDH measurement. Absorption was measured at 490 nm with a reference wavelength of 655 nm using a Cambrex ELx808 microplate reader (Biotek, KC4). Positive control experiments were performed with 1% Triton X-100 and set as 100% cytotoxicity. LDH release was calculated by the following equation:

$$LDH(\%) = \frac{[A]_{sample} - [A]_{medium}}{[A]_{positivecontrol} - [A]_{medium}} \times 100$$

where [A]sample, [A]medium, [A]positive control denote the absorbance of the sample, medium negative control and Triton X-100 positive control, respectively.

5.2. Cell cycle

In order to examine the cell distribution along the different phases of the cell cycle, the relative cellular DNA content was evaluated by means of flow cytometry as previously described by Valdiglesias *et al.,* (2011). Specifically, after treatments with each ION or positive control (MMC), cells were trypsinized and suspended in PBS. Then cells were centrifuged, washed with PBS and fixed with cold (-20ºC) 70% (V/V) ethanol. Then, fixed cells were stored overnight at 4ºC. Next, for analysis, cells were centrifuged, re-suspended in PBS containing 0.1µg/ml RNase A and 40µg/ml propidium iodide (PI) and incubated at 37ºC in the dark for 30min.

Samples were kept in ice prior to analysis. The analysis was performed using a FACSCalibur flow cytometer (Becton Dickinson). A minimum of 10^4 events were acquired, and the DNA content was assessed from the PI signal detected by the FL2 detector. In order to obtain information on the percentage of cells at G_0/G_1, S and G_2/M regions, cell cycle histograms were evaluated using Cell Quest Pro software (Becton Dickinson). Complementarily, subG_1 region of the cell cycle distribution was also evaluated, as indicative of the late stages of apoptosis.

5.3. Apoptosis and necrosis

BD Pharmingen™ Annexin V-FITC apoptosis detection kit was used to measure apoptosis cell death that may be potentially induced by ION treatment, by means of flow cytometry. Additionally, late apoptosis/necrosis was determined as the percentage of annexin V+/PI+ cells.

Annexin V-fluorescein isothiocyanate (FITC)/PI double staining was carried out with BD Pharmingen™ Annexin V-FITC apoptosis detection kit I (Becton Dickinson), following the manufacturer's protocol using flow cytometry. Contents of the kit are as follows: (i) annexin V-FITC conjugate: 50µg/ml in 50mM Tris-HCl, pH 7.5, containing 100mM NaCl; (ii) PI solution: 100µg/ml in 10mM potassium phosphate buffer, pH 7.4, containing 150mM NaCl; (iii) 10X binding buffer: 100mM HEPES/NaOH, pH 7.5, containing 1.4M NaCl.

After treatments with ION or Campt as positive control, cells were harvested with 0.025% trypsin, suspended in PBS and centrifuged at 300xg for 5min at room temperature. After centrifugation, supernatant was removed, and pellet was re-suspended in 200µl of 1X binding buffer, and 5µl of annexin V-FITC and 5µl of PI were added to each sample; then the samples were incubated at room temperature in the dark for 15min. Analysis was done immediately using a FASCalibur flow cytometer (Becton Dickinson). Events for annexin V-FITC were recorded from FL1, and events for PI were taken from FL2. Data were acquired from a minimum of 10^4 events per sample using Cell Quest Pro software (Becton Dickinson). Early apoptosis was expressed as percentage of annexin V+/PI– cells.

6. GENOTOXICITY

6.1. Micronucleus test

Micronucleus (MN) frequency was evaluated by flow cytometry following the protocols reported by Nüsse *et al.,* (1994) and Roman *et al.,* (1998), with some modifications (Valdiglesias *et al.,* 2011). After the predetermined exposure of cells to each type of ION and positive control (MMC), cell culture medium was removed, and cells were cultured for an additional period of 24h for SH-SY5Y cells and 48h for A172 cells in fresh medium, time determined on the basis of cell cycle duration. Then, cells were trypsinized at 0.025% and suspended in PBS. After centrifugation, the supernatant was removed and 0.25ml cold solution (4ºC) containing NaCl (10mM), trisodium citrate (1g/l), and nonidet P40 (0.3mg/l) was added to each tube alongside 5µl of 50µg/ml PI and 1.25µl of 0.05mg/ml RNase A. After the incubation of samples in the dark at room temperature for 15 min, a second solution consisting of citric acid (1.5mg/l) and sucrose (0.25M) was added and incubated for 30min. Subsequently, a suspension of nuclei and MN was prepared by filtering through a 50µm nylon mesh. The final suspension of nuclei and MN was analysed with a FACSCalibur flow cytometer (Becton Dickinson). PI-associated fluorescence

emission was collected in the FL2 channel. The frequency of MN was calculated using Cell Quest Pro software (Becton Dickinson), based on the acquisition of at least $5x10^4$ events.

6.2. γH2AX assay

The evaluation of H2AX histone phosphorylation was performed following the general protocol proposed by Tanaka *et al.,* (2009). After the exposure to each type of ION and positive control (BLM), cells were trypsinized at 0.025% and suspended in PBS. After centrifugation and removal of supernatant, cells were incubated with 1% p-formaldehyde for 15min at 4ºC. Then, the samples were centrifuged, and the supernatant was removed. Next, samples were incubated overnight at 4ºC with 1ml of cold (-20ºC) ethanol 70% (V/V). The following day, samples were washed with PBS and 100µl anti-γH2AX antibody labelled with Alexa Fluor® 488 [1:20, 1% bovine serum albumin in PBS] was added and incubated for 15min at room temperature. Next, samples were washed in PBS, supernatant was removed, and 500µl PBS containing PI (40µg/ml) and RNase A (0.1µg/ml) were added and incubated for 30min at room temperature. Finally, a minimum of 10^4 events were acquired with a FACSCalibur flow cytometer (Becton Dickinson). Data obtained from Alexa Fluor 488 (FL1) and PI (FL2) were analysed using Cell Quest Pro software (Becton Dickinson).

6.3. Comet assay

After treatments with both ION and the positive control (H_2O_2), the alkaline comet assay was performed following the general protocol proposed by Singh *et al.,* (1988). Briefly, after collecting cells by trypsinization at 0.025%, they were suspended in 100µl of 0.7% low-melting-point agarose (LMA) in PBS (pH 7.4). Then cells were dropped as two drops onto a slide that was previously pre-coated with a 1% layer of normal melting point agarose and covered with coverslips. Slides were placed on ice for 15min and, after the second layer of agarose solidified, coverslips were removed, and slides were immersed in freshly prepared lysis solution (2.5M NaCl, 100mM Na_2EDTA, 10mM Tris-HCl, 250mM NaOH, pH 10, and 1% triton X-100 added just before use) for at least 1h at 4°C in the dark.

After the lysis step, slides were placed on a horizontal electrophoresis tank (420x300x90mm) in an ice bath. Then, the tank was filled with freshly made alkaline electrophoresis solution (1mM Na_2EDTA, 300mM NaOH, pH 13) and left in the dark for 40min to allow DNA unwinding. Later, electrophoresis was carried out for 30min at 25V and 300mA (0.83V/cm). Slides were then washed three times for 5min with neutralizing solution (0.4M Tris–HCl, pH 7.5). Following neutralization, slides were left to air-dry in the dark, and stained with 60µl of 4,6-diamidino-2-fenilindol (DAPI), The preparations were kept in a humidified sealed box to prevent drying of the gel and analysed within six days.

Image capture and analysis were performed using the comet IV software (Perceptive Instruments). In all cases, 50 cells were scored from each replicate drop (*i.e.* 100 cells in total), and percentage of DNA in the comet tail (%tDNA) was used as DNA damage parameter.

Before carrying out the comet assay experiments, possible interference between ION and the comet assay protocol was evaluated, according to the procedure described by Magdolenova *et al.,* (2012). Briefly, untreated cells were centrifuged at 200xg for 5min at 4°C. Supernatant was removed and 40µl of ION were added directly to the cells just before mixing them with 40µl of 1.4% low-melting point agarose, so that the final concentration of ION was 200µg/ml in SH-SY5Y cells and 100µg/ml in A172 cells, the highest doses to be tested for genotoxicity. Then the alkaline comet assay was carried out following the general protocol described above. Since the O-ION concentration used in SH-SY5Y cells showed significant interference with the comet assay methodology, lower doses were then tested (10, 50, and 100µg/ml).

7. DNA REPAIR COMPETENCE ASSAY

The experimental design described by Laffon *et al.,* (2010) was followed to evaluate the effects of S-ION on DNA damage repair. It consisted of three consecutive phases: (i) in phase A (pre-treatment) cells were incubated for 3 or 24h in the presence or absence of ION (50µg/ml) at 37°C; (ii) in phase B (DNA damage induction) cells were challenged with H_2O_2 (100µM for SH-SY5Y cells and 200 µM for A172 cells) for 5min at 37°C in the presence or absence of ION (50µg/ml); and (iii) in phase C (repair) cells were washed in fresh medium to remove treatment, and incubated with or without ION (50 µg/ml) for 30min at 37°C to allow DNA repair. Alkaline comet assay was carried out just after treatment with H_2O_2 (data labelled as "before repair") and after the repair period (data labelled as "after repair") as described previously in section III.6.3.

Additionally, cells were treated with ION (50µg/ml) for 30min and the comet assay was performed immediately after. This was done to test whether 30min incubation with ION (as occurs in phase C) might induce significant damage to DNA.

8. STATISTICAL ANALYSIS

Statistical analyses were performed using SPSS for Windows statistical package (version 21.0). A minimum of three independent experiments were performed for each experimental condition tested, and each condition was always run in duplicate and under blind conditions. Experimental data were expressed as mean ± standard error. Distribution of the response variables departed significantly from normality (Kolmogorov-Smirnov test) and therefore non-parametric tests were considered adequate for the statistical analysis of these data. Differences among groups were tested with Kruskal-Wallis test and Mann-Whitney *U*-test. The associations between two

variables were analysed by Spearman's correlation. A *P*-value of less than 0.05 was considered significant.

IV. RESULTS

IV. RESULTS

The physicochemical characterization of both ION employed in the present study was previously carried out by our group (Costa *et al.,* 2016) and is shown in Table IV.1. Briefly, S-ION used are spherical particles with an average diameter of 20.2 nm, including core and silica coating; less than 2% of the S-ION surface presents iron, confirming an effective silica coating. O-ION are spherical particles with a magnetite core average diameter of 10.9nm; less than 7% of the nanoparticle surface presents iron. The mean hydrodynamic sizes and zeta potential values demonstrated the colloidal dispersion stability and low tendency to agglomeration, except for O-ION dispersed in both serum-free media.

1. SH-SY5Y CELLS EXPOSED TO S-ION

1.1. Iron ion release from the nanoparticles

The release of iron ions from the S-ION was studied in serum-free and complete cell culture media. It was found to be very low in serum-free medium at the three times tested (3, 6 and 24h) (Figure IV.1). Nevertheless, important concentrations of dissolved iron were observed when S-ION were suspended in complete media, generally increasing with exposure time and nanoparticle dose.

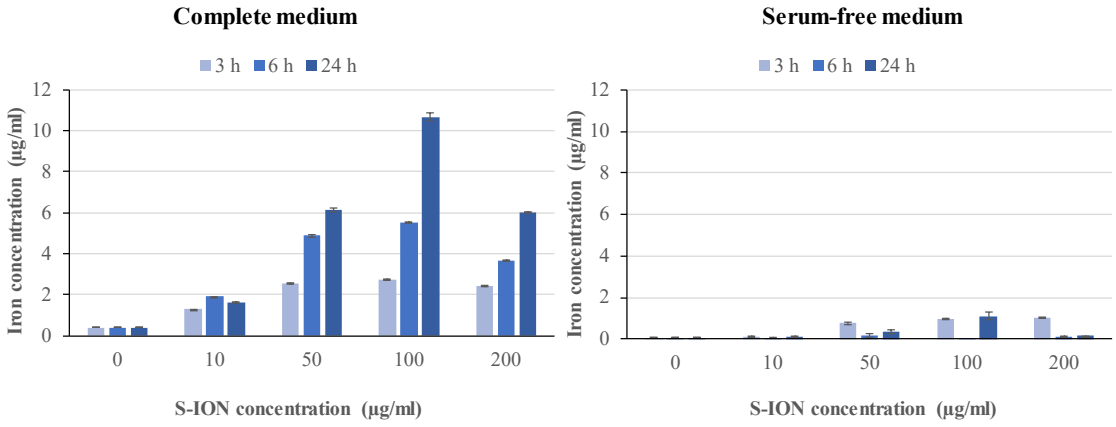

Figure IV.1: Analysis of iron ions released from S-ION in (A) complete cell culture medium and (B) serum-free cell culture medium. Bars represent the mean ± standard error.

Table IV1. Physicochemical description of silica-coated and oleic acid-coated ION (from Costa *et al.* 2015).

				Silica-coated ION	**Oleic acid-coated ION**
Primary particle size (nm)			TEM	10.0 ± 2.1 (core) 20.2 ± 2.9 (core and coating)	10.9 ± 3.4 (core)*
Particle morphology			TEM	spherical	spherical
Surface chemistry (%)			XPS	9.07 (C 1s) 0.27 (N 1s) 60.02 (O 1s) 29.22 (Si 2p) 1.41 (Fe 2p3)	67.92 (C 1s) 25.55 (O 1s) 6.54 (Fe 2p3)
Dispersed in water**		Size (nm)	DLS	93.3 ± 0.5	164.5 ± 1.1
		Zeta potential (mV)	M3-PALS	-31.8 ± 2.1 (pH=7.73)	-45.4 ± 2.0
Dispersed in SHSY5Y cell culture medium**	Incomplete medium	Size (nm)	DLS	141.6 ± 1.4	1961.3 ± 52.8
		Zeta potential (mV)	M3-PALS	-21.7 ± 1.0 (pH=8.32)	-15.9 ± 0.3
	Complete medium	Size (nm)	DLS	111.1 ± 1.1	202.7 ± 0.7
		Zeta potential (mV)	M3-PALS	-10.3 ± 1.1 (pH=8.14)	-11.6 ± 1.0
Dispersed in A172 cell culture medium**	Incomplete medium	Size (nm)	DLS	185.7 ± 11.6	2587.7 ± 382.2
		Zeta potential (mV)	M3-PALS	-20.3 ± 0.5 (pH=8.57)	-17.6 ± 0.4
	Complete medium	Size (nm)	DLS	222.6 ± 9.3	251.5 ± 4.9
		Zeta potential (mV)	M3-PALS	-10.9 ± 0.3 (pH=8.57)	-11.2 ± 0.4

1.2. Cellular uptake

Results obtained from testing the ability of S-ION to enter the human neuroblastoma cells are shown in Figure IV.2. The nanoparticles were effectively internalized by the cells at all conditions tested in a dose-dependent manner (serum-free medium: r=0.824, P<0.01 for 3h treatment and r=0.877, P<0.01 for 24h treatment; complete medium: r=0.737, P<0.01 for 3h treatment and r=0.692, P<0.01 for 24h treatment). However, uptake was slightly higher in serum-free medium than in complete medium, and for the highest dose tested it was more prominent at 3h than at 24h treatment.

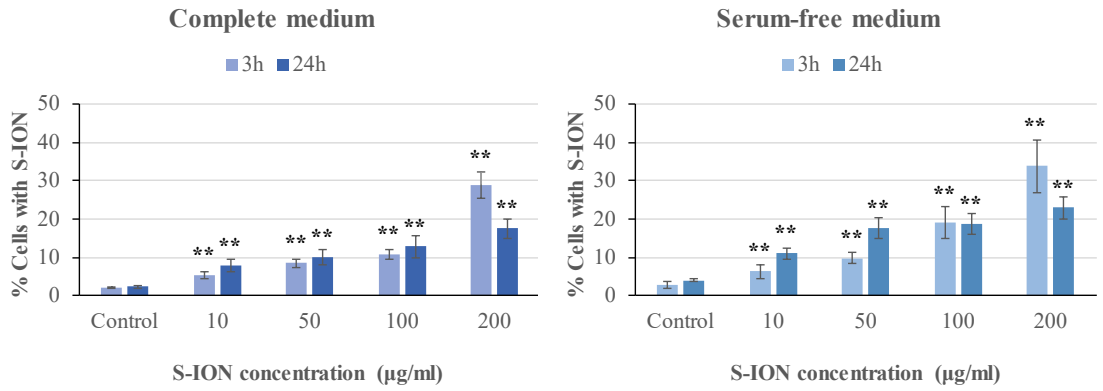

Figure IV.2: Neuronal cell uptake of S-ION prepared in complete and serum-free medium. Bars represent the mean ± standard error. **P<0.01, significant difference with regard to the corresponding negative control.

1.3. Cytotoxicity

1.3.1. Membrane integrity

The potential alterations in the neuronal cell membrane integrity caused by S-ION exposure were assessed by measuring LDH activity in extracellular medium, since LDH is released when the cell membrane is damaged. Results obtained in this test are collected in Figure IV.3. No significant alteration in the percentage of LDH activity was observed at any medium, concentration or treatment time tested.

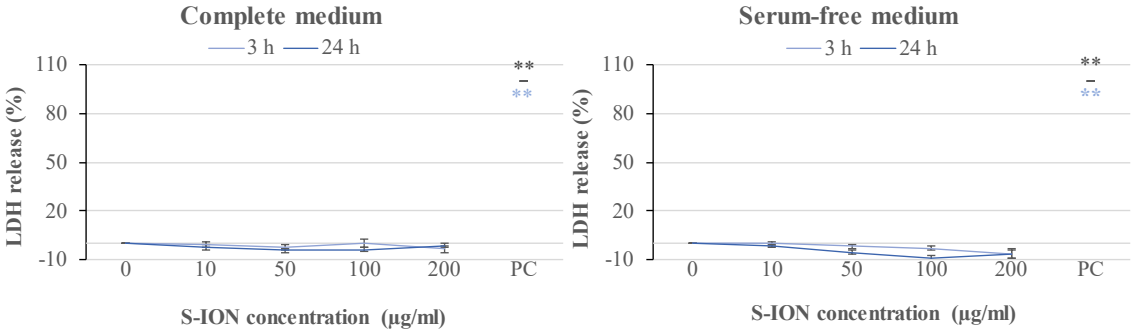

Figure IV.3: Results of membrane integrity assessment in SH-SY5Y cells exposed to S-ION in complete and serum-free medium. Bars represent the mean ± standard error. PC: positive control (1% Triton X-100). ***P*<0.01, significant difference regarding the corresponding negative control.

1.3.2. Cell cycle analysis

Figure IV.4 shows the cell distribution during the various phases of the cell cycle after exposing the neuronal cells to S-ION. The 3 h treatments, regardless of the medium employed, did not modify the cell cycle, and significant alterations at 24h treatments were only observed for the 200µg/ml concentration (decrease in G_2/M phase and notable although not significant increase in S phase for treatment in serum-free medium, and increase in S phase for treatment in complete medium).

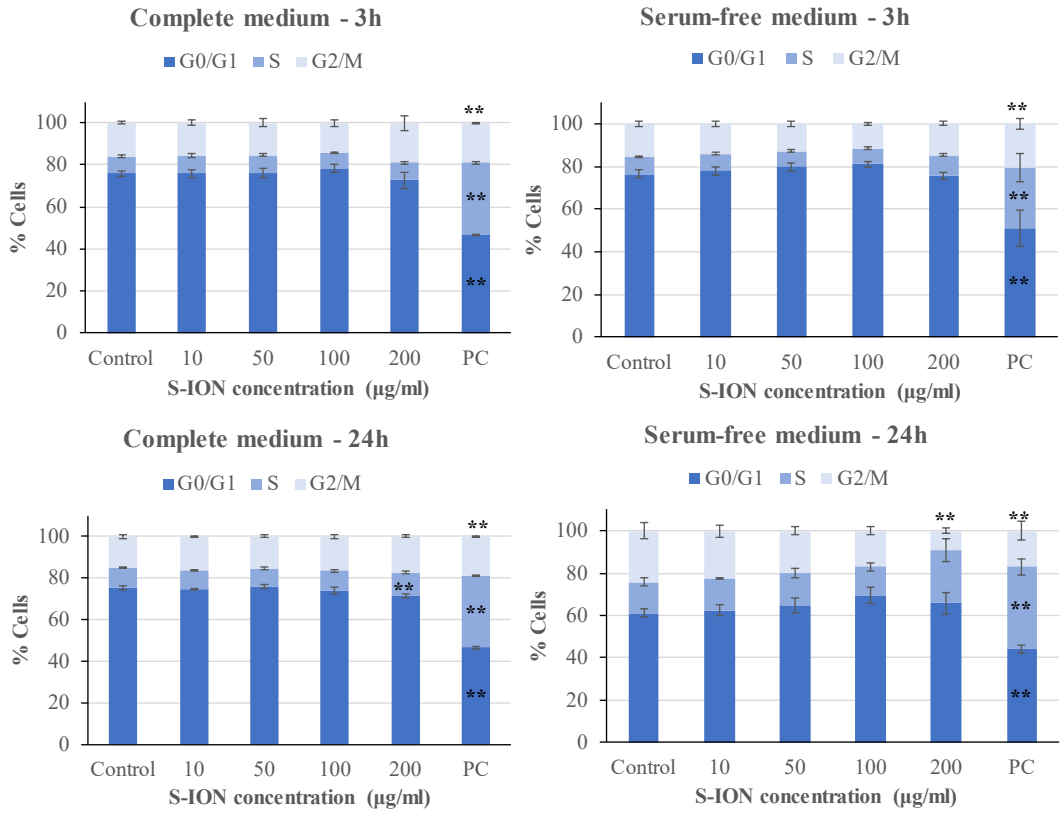

Figure IV.4: Analysis of SH-SY5Y cell cycle after 3 and 24h of treatment with S-ION prepared in complete and serum-free medium. Bars represent the mean ± standard error. PC: positive control (1.5µM MMC). ***P*<0.01, significant difference with regard to the corresponding negative control.

Besides, the subG$_1$ region of the cell cycle distribution was also evaluated, since DNA fragmentation, indicative of the late stages of apoptosis, results in the appearance of PI-stained events containing subG$_1$ levels (Fracker *et al.,* 1995); results are gathered in Figure IV.5. No significant increase in the subG$_1$ fraction was observed excepting for the cells exposed in serum-free medium to the highest S-ION dose for 24h.

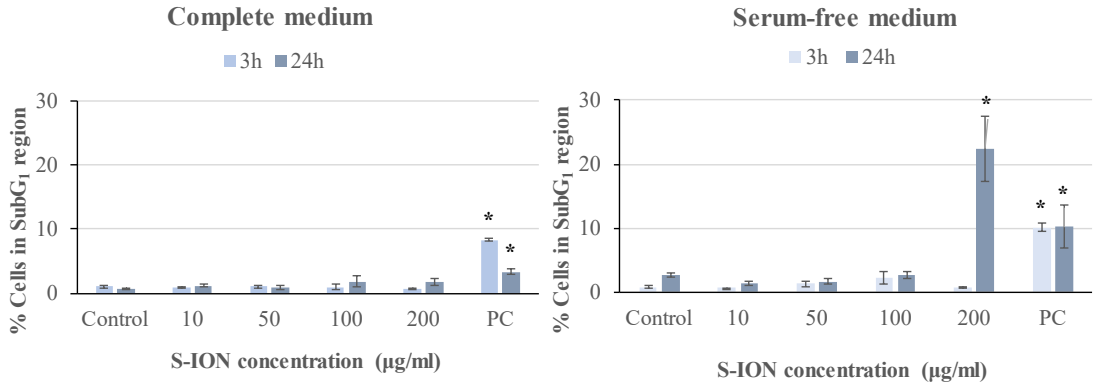

Figure IV.5: Apoptosis (% of cells in the subG$_1$ region of cell cycle distribution) in neuronal cells treated with S-ION prepared in complete and serum-free medium. Bars represent the mean ± standard error. PC: positive control (1.5µM MMC). **P*<0.05, significant difference with regard to the corresponding negative control.

1.3.3. Apoptosis and necrosis detection

To further investigate whether treatments with S-ION were able to induce cell death by apoptosis or necrosis, a double stain with annexin V and PI was carried out. Results obtained from the analyses showed that S-ION did not induce early apoptosis (events positive for annexin V but negative for PI) at any concentration after 3h of exposure regardless of the medium used (Figure IV.6). After 24h of treatment significant increases in apoptosis rate could only be observed for the highest doses assayed (200µg/ml in serum-free medium and 100 and 200µg/ml in complete medium). No significant induction of necrosis/late apoptosis (events positive for both annexin V and PI) was obtained at any experimental condition tested (Figure IV.7).

1.4. Genotoxicity

1.4.1. γH2AX assay

The genotoxic potential of the S-ION was examined using different approaches. As a rapid screening method for genotoxicity, we first analysed H2AX phosphorylation, an early cellular response to the induction of DNA double-strand breaks (DSB). As it can be clearly seen in Figure IV.8, S-ION did not induce γH2AX at either of the conditions tested.

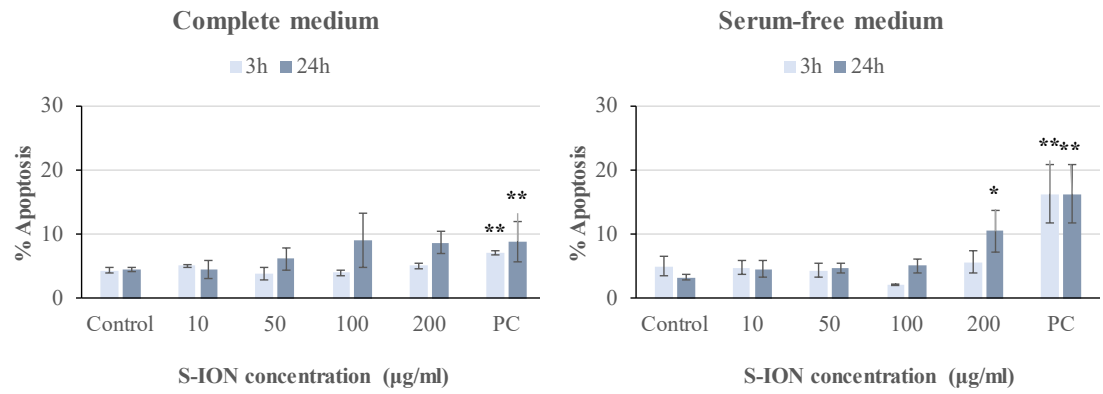

Figure IV.6: Apoptosis cell rates (%) after exposure of neuronal cells to S-ION for 3 and 24h prepared in complete and serum-free medium. Bars represent the mean ± standard error. PC: positive control (10µM Campt). **P*<0.05, ***P*<0.01, significant difference regarding the corresponding negative control.

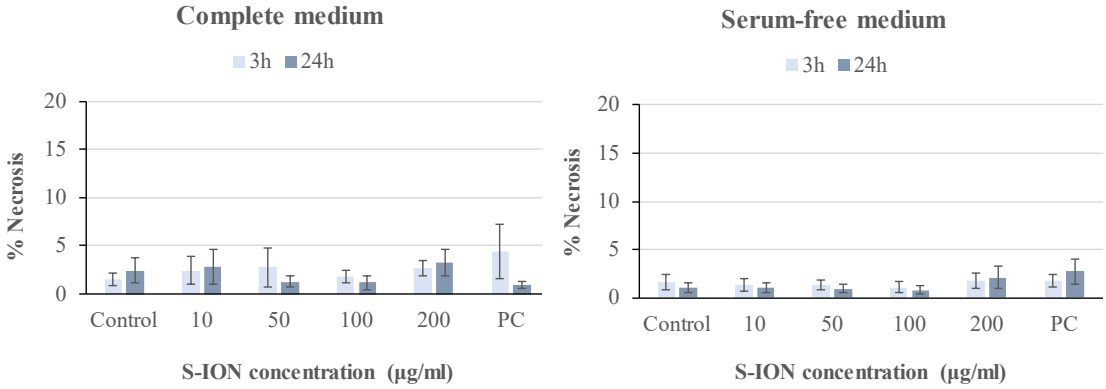

Figure IV.7: Necrosis cell rates (%) after exposure of neuronal cells to S-ION for 3 and 24h prepared in complete and serum-free medium. Bars represent the mean ± standard error. PC: positive control (10µM Campt). **P*<0.05, ***P*<0.01, significant difference regarding the corresponding negative control.

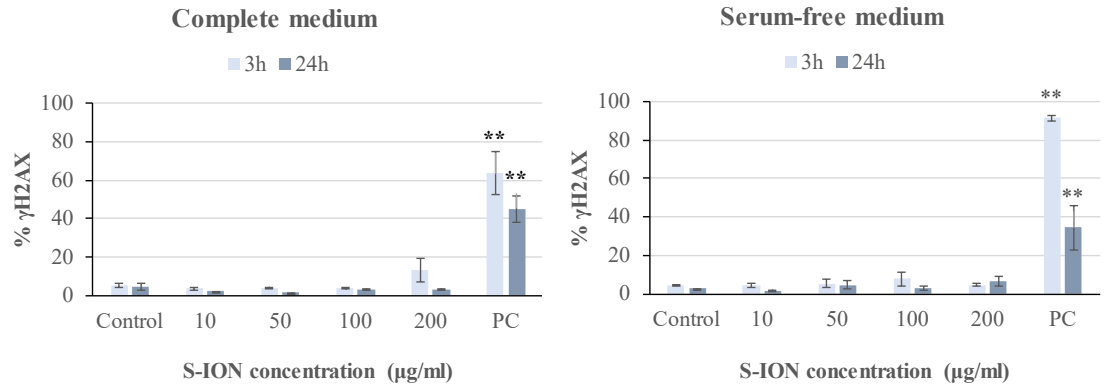

Figure IV.8: Phosphorylation of H2AX histone after treatment of neuronal cells with S-ION prepared in complete and serum-free medium. Bars represent the mean ± standard error. PC: positive control (1µg/ml BLM). ***P*<0.01, significant difference with regard to the corresponding negative control.

1.4.2. MN test

Next, we applied a relatively less specific approach, the MN test scored by flow cytometry, in order to quantify chromosome alterations. The results of MN evaluation showed that no significant changes were produced in the MN ratio after treatment of the neuronal cells with the S-ION (Figure IV.9).

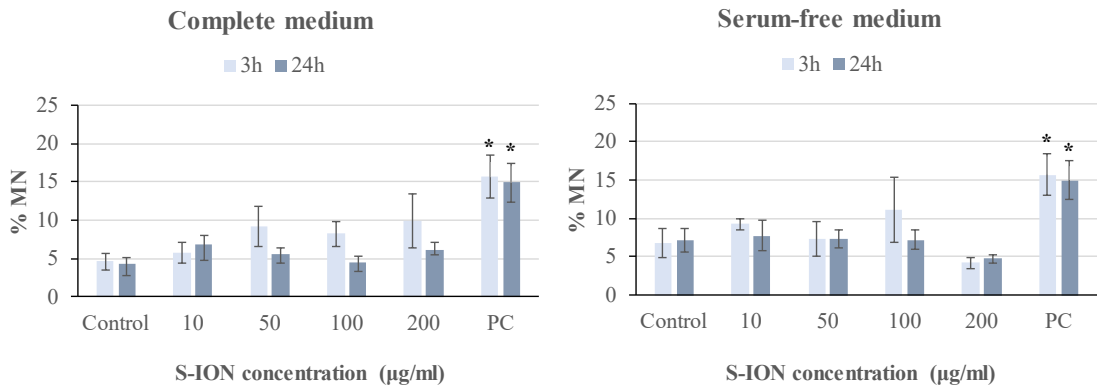

Figure IV.9: MN induction in neuronal cells after treatment with S-ION prepared in complete and serum-free medium. Bars represent the mean ± standard error. PC: positive control (1.5µM MMC). **P*<0.05, significant difference with regard to the corresponding negative control.

1.4.3. Comet assay

The comet assay was used for measuring primary DNA damage in SH-SY5Y cells caused by exposure to S-ION. Due to the especial physicochemical characteristics of nanomaterials, several possible interferences may occur with the comet assay methodology (Karlsson *et al.,* 2015). Thus, a comprehensive test for detecting these interferences was carried out before starting DNA damage evaluation, following Magdolenova *et al.,* (2012). As it can be appreciated from Figure IV.10, addition of S-ION to the cells just before the lysis step was not found to interfere with the subsequent steps of the experimental protocol, since no differences were found between the DNA damage measured in the absence and in the presence of the nanoparticles.

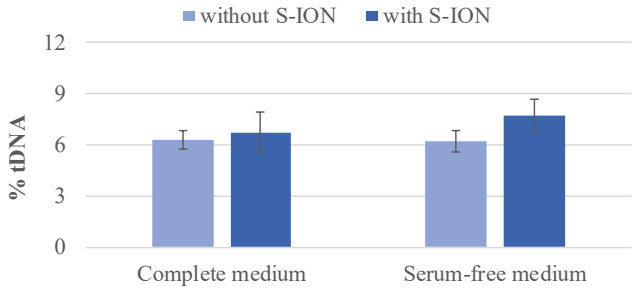

Figure IV.10: Results of interference testing between S-ION (200µg/ml) and comet assay methodology in complete and serum-free medium. Bars represent the mean standard error.

When the comet assay was applied to neuronal cells treated with S-ION in serum-free medium, no significant alteration in %tDNA was detected (Figure IV.11). Nevertheless, dose-dependent induction of DNA damage was observed in complete medium (r=0.948, $P<0.05$ for 3h treatment, and r=0.842, $P<0.05$ for 24h treatment).

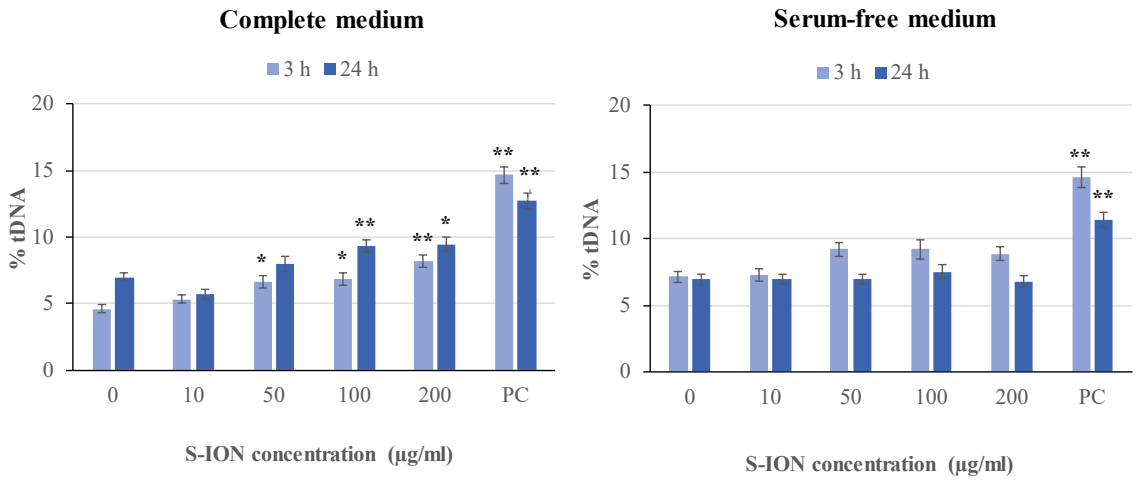

Figure IV.11: DNA damage induction in neuronal cells after treatment with S-ION prepared in complete and serum-free medium. Bars represent the mean ± standard error. PC: positive control (100µM H_2O_2). *$P<0.05$, **$P<0.01$, significant difference with regard to the corresponding negative control.

1.5. DNA repair

Results obtained in the DNA repair competence assay are shown in Figure IV.12. When cells were challenged with H_2O_2 and no exposure to S-ION was carried out, there was a significant decrease in the level of DNA damage after the 30min repair period in both media tested. When incubation with S-ION was carried out before damage induction by H_2O_2 (phase A, either 3 or 24h), no repair was observed in serum-free medium but %tDNA was significantly reduced in

complete medium, more pronounced in incubation for 24h than for 3h. Similar results were obtained when S-ION were applied only during the 30min repair period (phase C), although treatment of cells for 30min with only S-ION increased significantly the DNA damage over the control level in both cell culture media. However, the opposite occurred for experiments where treatment with H_2O_2 and S-ION were performed simultaneously (phase B), *i.e.*, significant repair observed in serum-free medium and no repair in complete medium.

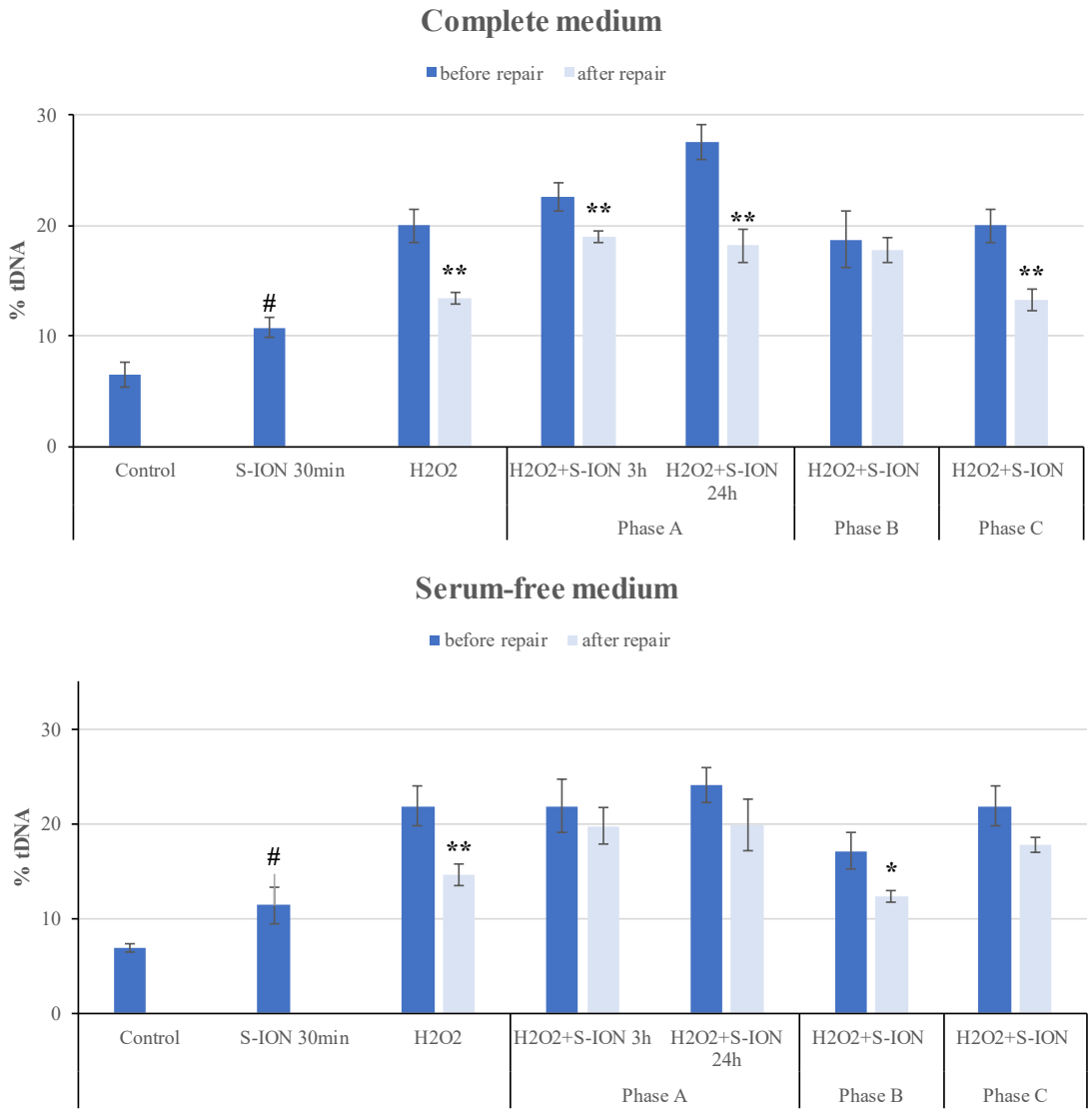

Figure IV.12: Effects of S-ION on repair of H_2O_2-induced DNA damage in neuronal cells. Incubation with S-ION (50µg/ml) was carried out either before H_2O_2 (100µg/ml) treatment (phase A), simultaneously (phase B), or during the repair period (phase C). Bars represent the mean ± standard error. *P<0.05, **P<0.01, significant difference with regard to the same treatment before repair, $^{\#}P$<0.05, significant differences with regard to the negative control.

2. SH-SY5Y CELLS EXPOSED TO O-ION

2.1. Iron ion release from the nanoparticles

Quantification of iron ion concentration in both cell culture media assessed by FAAS showed ion release from O-ION limited to the treatments in complete medium, particularly marked after 3h of exposure (Figure IV.13).

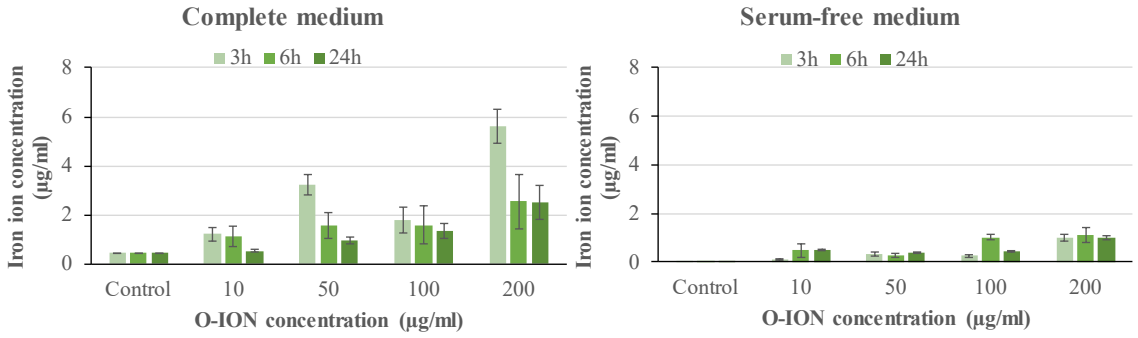

Figure IV.13: Analysis of iron ion release from O-ION in complete and serum-free cell culture medium. Bars represent mean ± standard error.

2.2. Cellular uptake

Flow cytometry analysis of O-ION internalization by SH-SY5Y cells revealed a similar dose- and time-dependent nanoparticle uptake in complete and serum-free media. Indeed, significant correlations were obtained at both exposure times in complete (r=0.929, $P<0.01$, and r=0.827, $P<0.01$, for 3 and 24h, respectively) and serum-free (r=0.964, $P<0.01$, and r=0.730, $P<0.01$, for 3 and 24h, respectively) media (Figure IV.14).

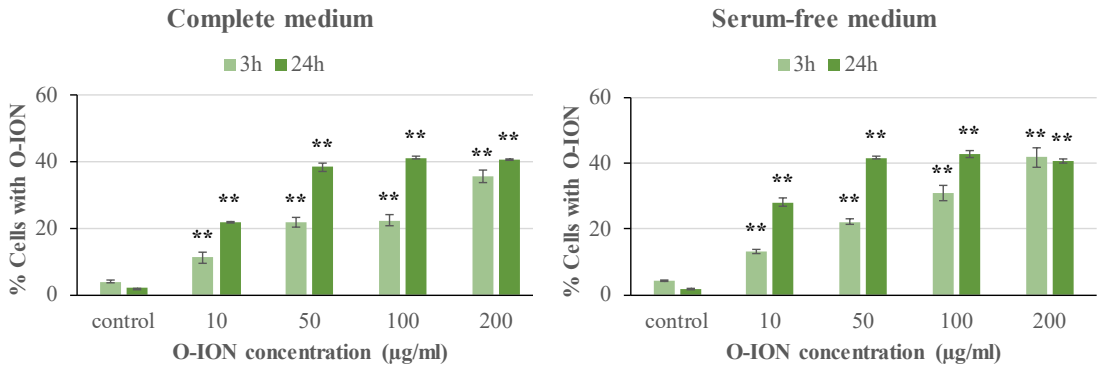

Figure IV.14: SH-SY5Y cellular uptake of O-ION in complete and serum-free medium. Bars represent mean ± standard error. $^{**}P<0.01$, significant differences with regard to the corresponding negative control.

2.3. Cytotoxicity

2.3.1. Membrane integrity

Results of cell membrane integrity evaluation are shown in Figure IV.15. A significant release of LDH was observed after treating SH-SY5Y cells with the highest O-ION concentrations in both media, but limited to 24h in the case of serum-free medium.

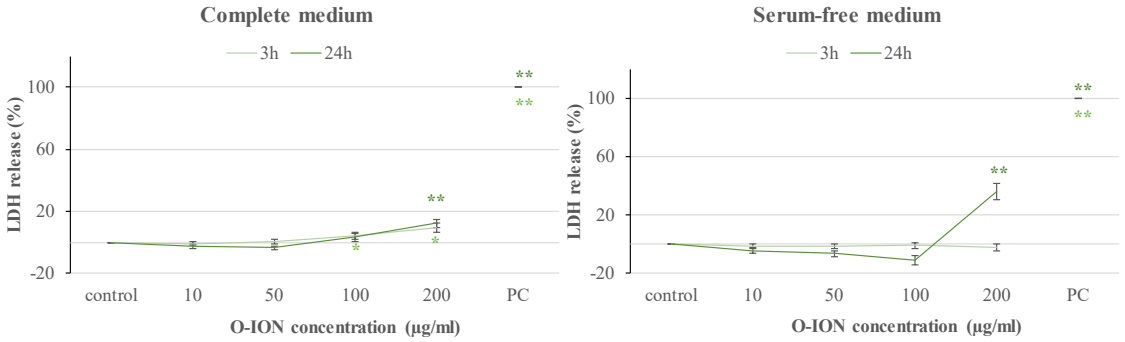

Figure IV.15: Results of membrane integrity assessment (LDH assay) in neuronal cells exposed to O-ION in complete and serum-free medium. Bars represent mean ± standard error. PC: positive control (1% Triton X-100). **P*<0.05, ***P*<0.01, significant differences compared to the corresponding negative control.

2.3.2. Cell cycle analysis

The analysis of the different phases of the cell cycle (G_0/G_1, S, G_2/M) by flow cytometry after exposure to O-ION revealed that the normal progression of SH-SY5Y cycle was generally altered (Figure IV.16). After 3h treatments these significant alterations were only observed in serum-free medium at concentrations from 50µg/ml on. More marked effects were found after 24h of treatment, with statistically significant dose-dependent increases in both media in G_0/G_1 phase (r=0.512, *P*<0.01, and r=0.531, *P*<0.01, in complete and serum-free medium, respectively), and decreases in G_2/M phase (r=-0.858, *P*<0.01, and r=-0.863, *P*<0.01, in complete and serum-free medium, respectively).

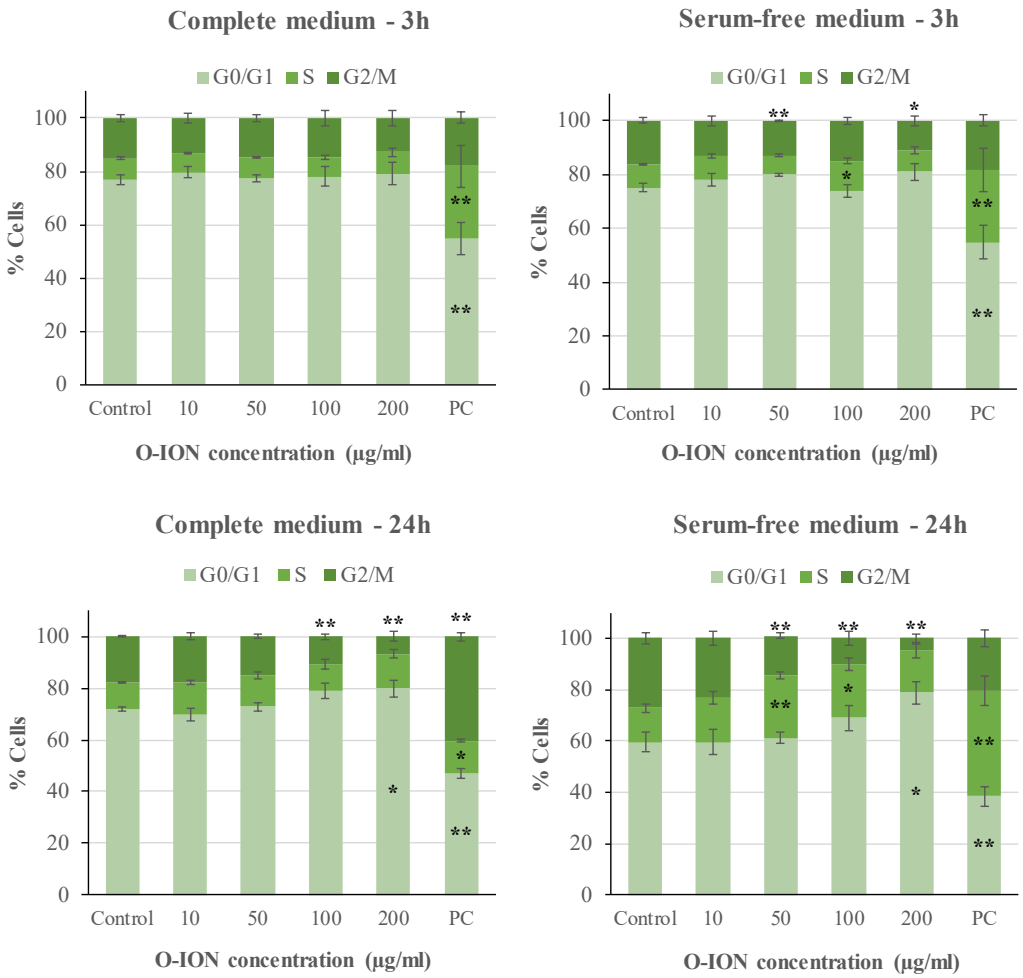

Figure IV.16: Analysis of SH-SY5Y cell cycle after treatment with O-ION for 3h in complete (upper left) and serum-free medium (upper right), or for 24h in complete (lower left) and serum-free medium (lower right). Bars represent mean ± standard error. PC: positive control (1.5µM MMC). **P*<0.05, ***P*<0.01, significant differences with regard to the corresponding negative control.

Additionally, analysis of subG$_1$ region of cell cycle histogram, as indicative of late stages of apoptosis, was carried out (Figure IV.17). O-ION exposure induced noticeable dose-dependent increases in apoptosis in both complete (3h: r=0.871, *P*<0.01; 24h: r=0.831, *P*<0.01) and serum-free (3h: r=0.710, *P*<0.01; 24h: r=0.710, *P*<0.01) media.

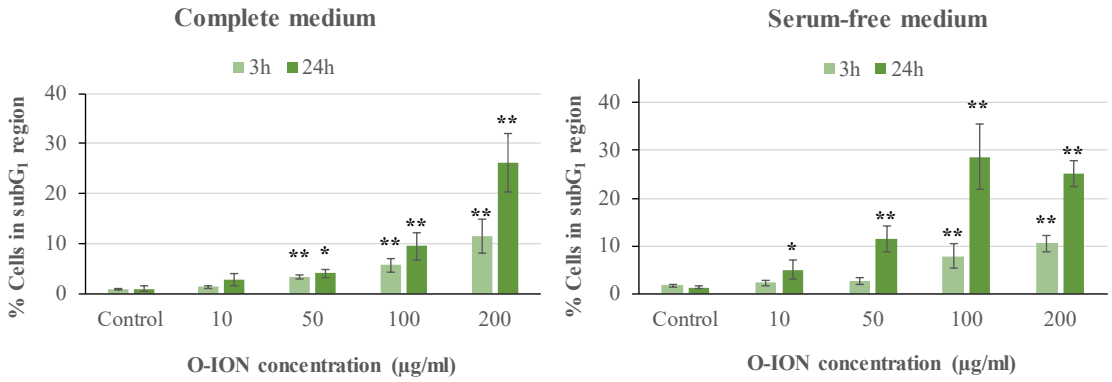

Figure IV.17: Late apoptosis (cells in the subG$_1$ region of cell cycle distribution) assessment in neural cells treated with O-ION in complete and serum-free medium. Bars represent mean ± standard error. **P*<0.05, ***P*<0.01, significant differences compared to the corresponding negative control.

2.3.3. Apoptosis and necrosis detection

Analysis of annexin V/PI double staining by flow cytometry was carried out to assess the early apoptosis and necrosis rates induced in cells by exposure to O-ION. Results obtained showed significant increases in the percentage of apoptotic cells after 24h treatments, with a slight dose-dependent effect in the serum-free medium (r=0.580, *P*<0.01) (Figure IV.18). However, necrosis rates showed no significant changes at any of the conditions tested (Figure IV19).

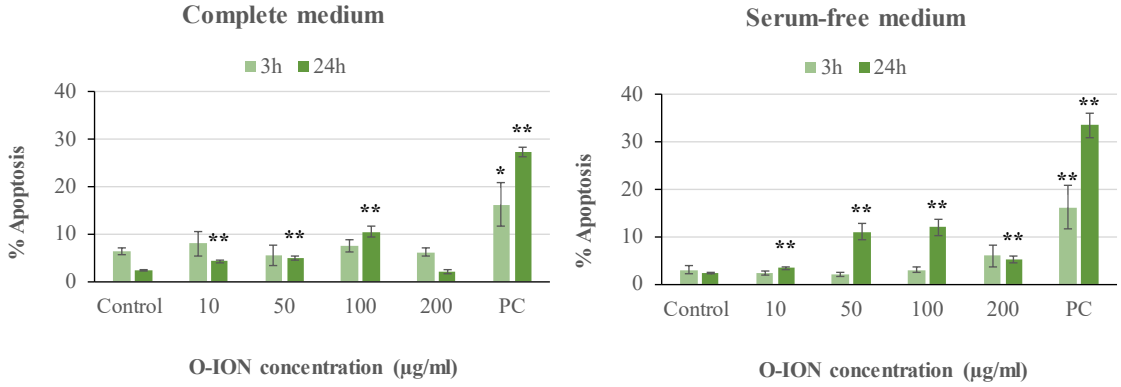

Figure IV.18: Apoptosis induction by exposure of SH-SY5Y cells to O-ION in complete and serum-free medium. Bars represent the mean ± standard error. PC: positive control (10µM Campt). **P*<0.05, ***P*<0.01, significant difference with regard to the corresponding negative control.

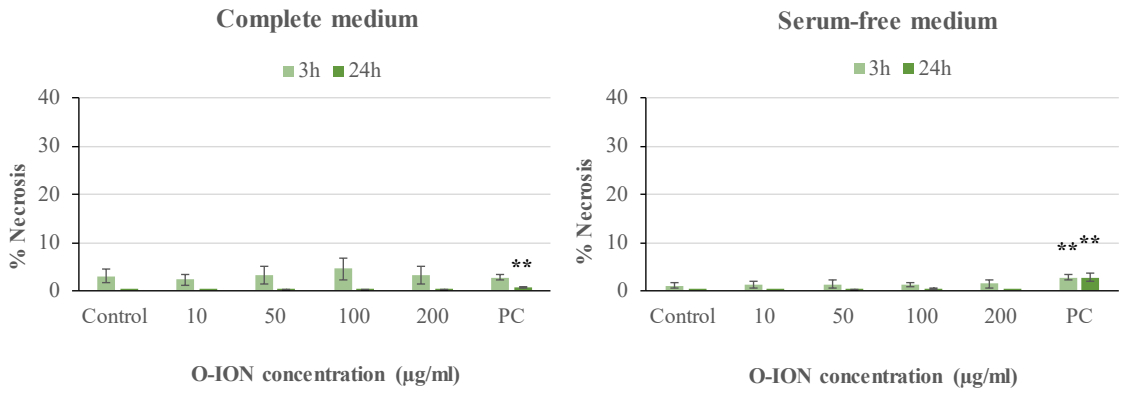

Figure IV.19: Necrosis induction after exposure of SH-SY5Y neurons to O-ION in complete and serum-free medium. Bars represent mean ± standard error. PC: positive control (10µM Campt). ***P*<0.01, significant difference with regard to the corresponding negative control.

2.4. Genotoxicity

2.4.1. γH2AX assay

Figure IV.20 shows the results obtained from analysis of H2AX phosphorylation. Exposure of SH-SY5Y cells to O-ION did not induce significant changes in %γH2AX at any time, dose or medium tested.

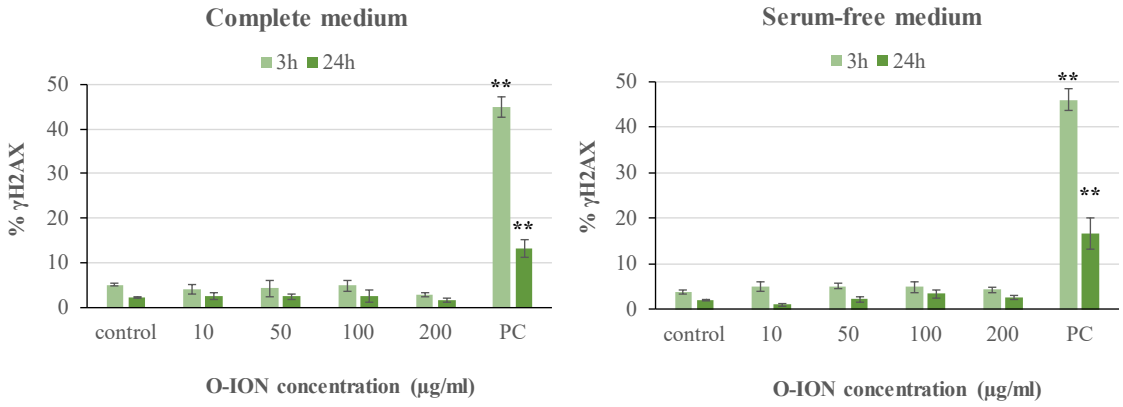

Figure IV.20: H2AX histone phosphorylation after treatment of neuronal cells with O-ION in complete and serum-free medium. Bars represent mean ± standard error. PC: positive control (1µg/ml BLM). ***P*<0.01, significantly different from the corresponding negative control.

2.4.2. MN test

According to MN test results, no MN induction was found in serum-free medium at 3h exposure or in complete medium at any time or dose tested. Significant increases in MN frequency were only observed in SH-SY5Y cells treated with the highest O-ION concentrations for 24h in serum-free medium (Figure IV.21).

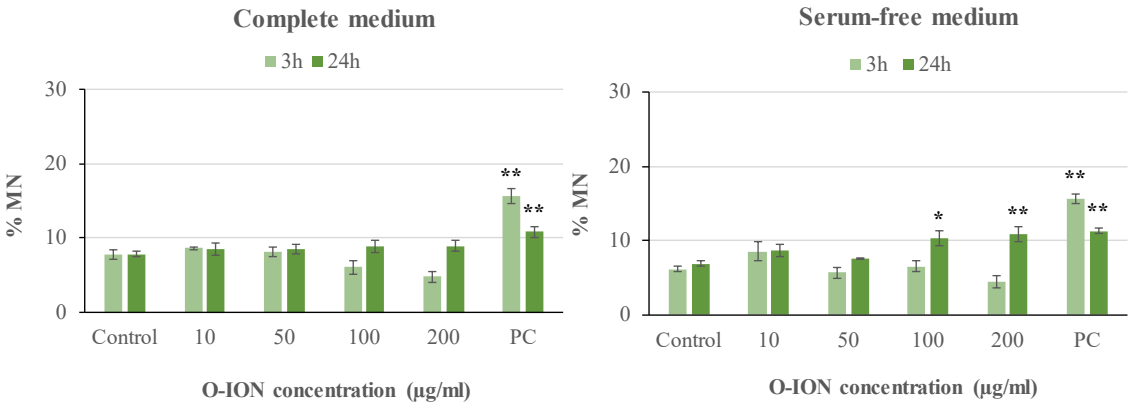

Figure IV.21: Micronuclei rates in SH-SY5Y neurons exposed to O-ION in complete and serum-free medium. Bars represent mean ± standard error. PC: positive control (1.5µM MMC). **P*<0.05, ***P*<0.01, significant differences with respect to the corresponding negative control.

2.4.3. Comet assay

Results obtained from comet assay are displayed in Figures IV.22 and IV.23. Prior to performing the experiments, the possible interference of O-ION with comet methodology was addressed (Figure IV.22). This test was initially performed with only the highest concentration to be tested for genotoxicity (200µg/ml). Since significant differences were observed between the results obtained in the presence and in the absence of O-ION in serum-free medium, indicating that nanoparticles could interfere with some step of the assay, testing was further carried out with all other concentrations in both media, but none of them showed signs of interference. Afterwards, alkaline comet assay was carried out showing general increases in primary DNA damage (%tDNA) with respect to the negative control in O-ION treated SH-SY5Y cells, regardless of serum presence in the medium (Figure IV.23). Significant dose–response relationships were only found in serum-free medium (3h: r=0.526, *P*<0.01; 24h: r=0.460, *P*<0.05).

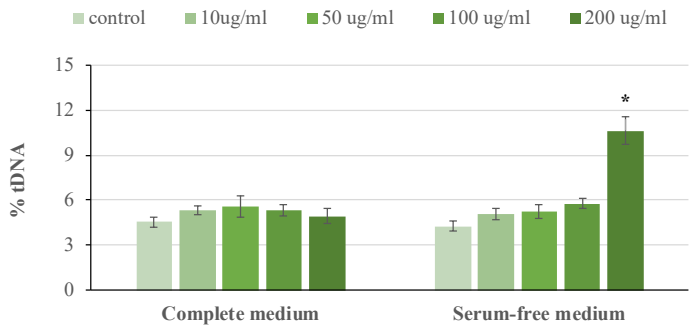

Figure IV.22: Results of interference testing between O-ION (10-200µg/ml) and comet assay methodology in complete and serum-free cell culture medium. Bars represent mean ± standard error. **P*<0.05, significant difference with regard to the corresponding control.

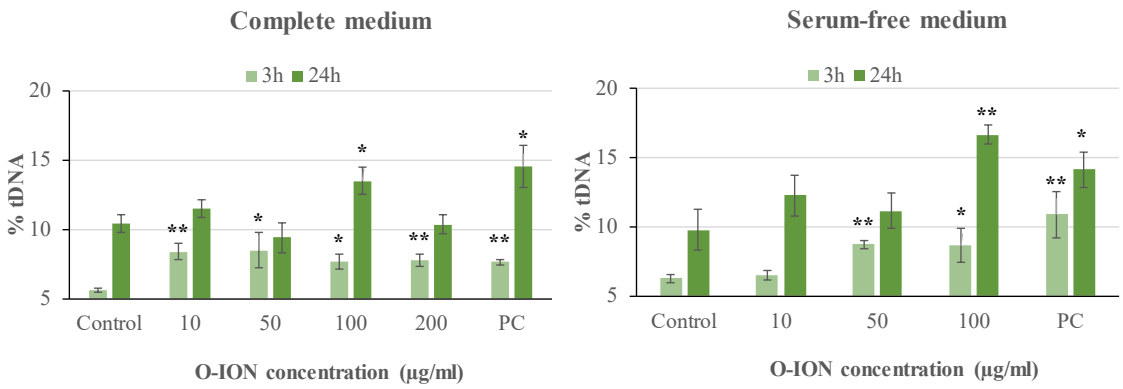

Figure IV.23: Primary DNA damage in SH-SY5Y cells treated with O-ION in complete and serum-free medium. Data corresponding to treatment with 200µg/ml in serum-free medium are not shown due to interference of the nanoparticles with the comet methodology. Bars represent mean ± standard error. PC: positive control (100µM H_2O_2). **P*<0.05, ***P*<0.01, significant differences with regard to the corresponding negative control.

2.5. DNA repair

Results obtained from the DNA repair competence assay are shown in Figure IV.24. When cells were challenged with H_2O_2 and no exposure to O-ION was carried out, a significant decrease in the level of primary DNA damage after the 30min repair period was observed in both media, confirming a proper repair ability of the cells in absence of nanoparticles. Nevertheless, ineffectiveness of cells in repairing the H_2O_2-induced DNA damage was revealed after incubation with O-ION before (phase A, both media) or during (phase B, serum-free medium) damage induction with H_2O_2. Despite significant increases in DNA damage were induced by cell treatment with the nanoparticles for only 30min in both media, no alterations in DNA repair were observed when O-ION treatments were conducted during the repair period (phase C, 30 min).

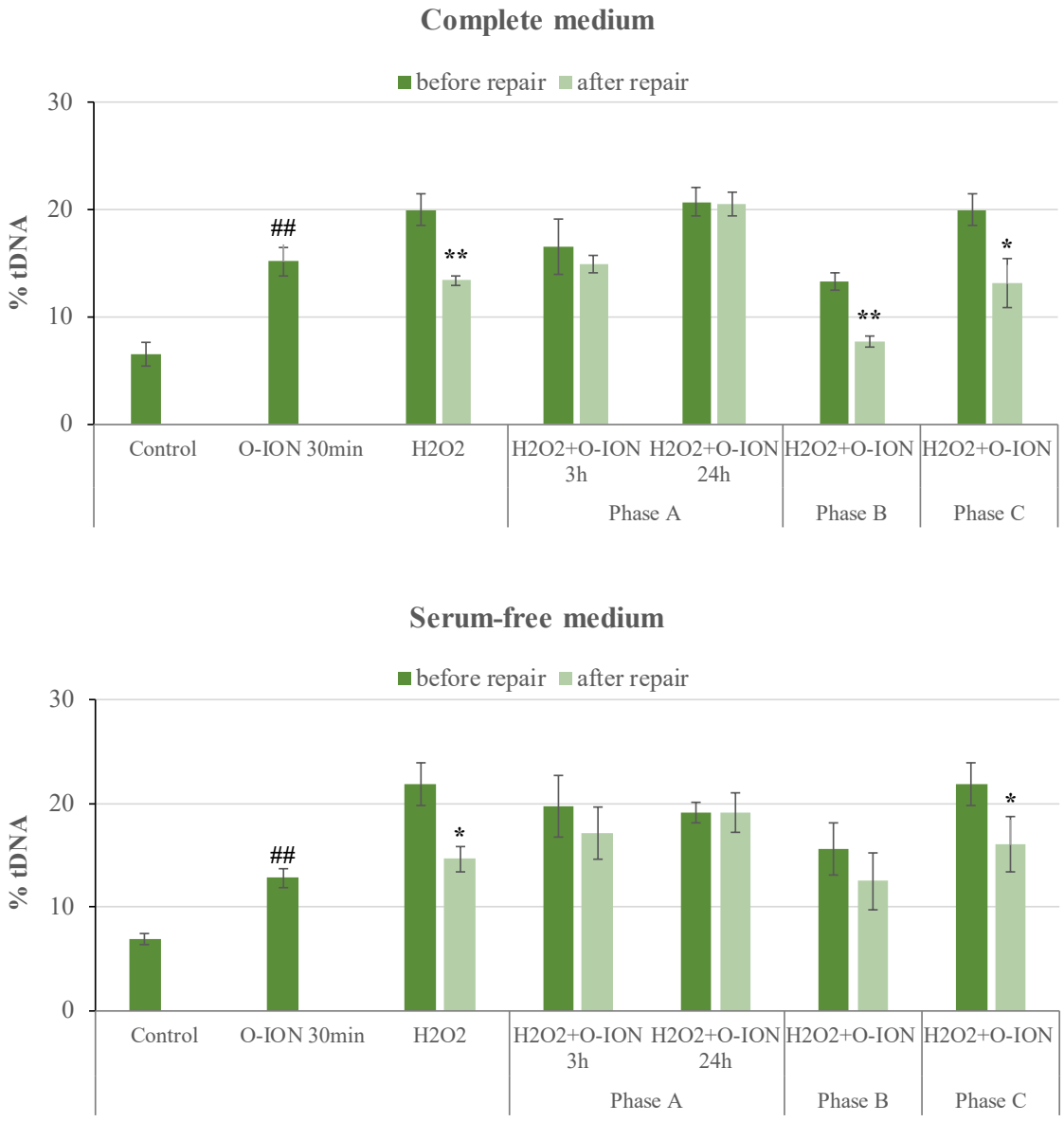

Figure IV.24: Effects of O-ION on repair of H_2O_2-induced DNA damage in neurons in complete and serum-free medium. Incubation with 50µg/ml O-ION was conducted independently prior to exposure to 100µM H_2O_2 (for 3 or 24h, phase A), simultaneously with H_2O_2 (phase B), or during the repair period (phase C). Bars represent mean ± standard error. **P*<0.05, ***P*<0.01, significant differences with regard to the same treatment before repair. $^{\#\#}P$<0.01, significant differences with regard to the negative control.

3. A172 CELLS EXPOSED TO S-ION

3.1. Iron ion release from the nanoparticles

Determination of iron ions in the culture media assessed by FAAS revealed scarce release of ions from the S-ION in serum-free medium regardless exposure time and after 3h incubation in complete medium (Figure IV.25). Nevertheless, notable time and concentration-dependent release was observed in complete medium after 6 and 24h incubations.

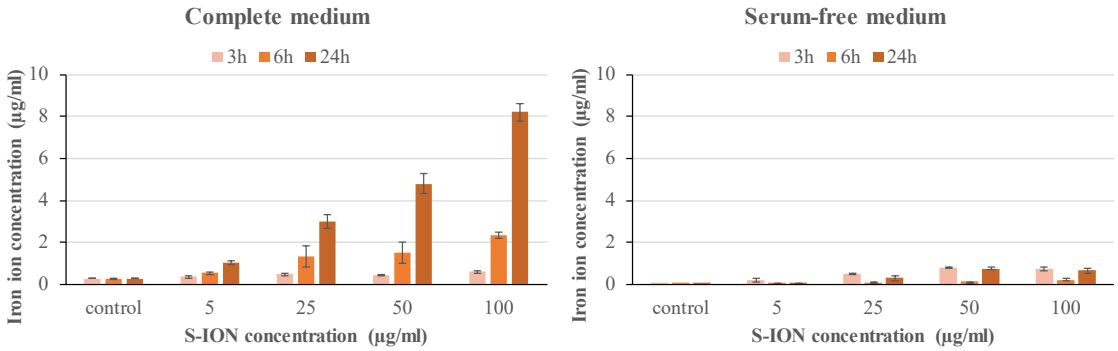

Figure IV.25: Analysis of iron ion release from S-ION in complete and serum-free cell culture medium. Bars represent mean ± standard error.

3.2. Cellular uptake

Nanoparticle internalization was analysed by TEM coupled with EDX in order to confirm nanoparticle composition. Results obtained show that glial cells are able to internalize S-ION at the conditions here tested. Electron-dense deposits were observed within endosomes after 24h of exposure to S-ION 25 and 100µg/ml and also after 3h of exposure to the highest concentration, both in complete and serum-free media (Figure IV.26). These agglomerates were also detected in the intercellular space; signs of apoptosis and necrosis were observed in cells exposed to S-ION.

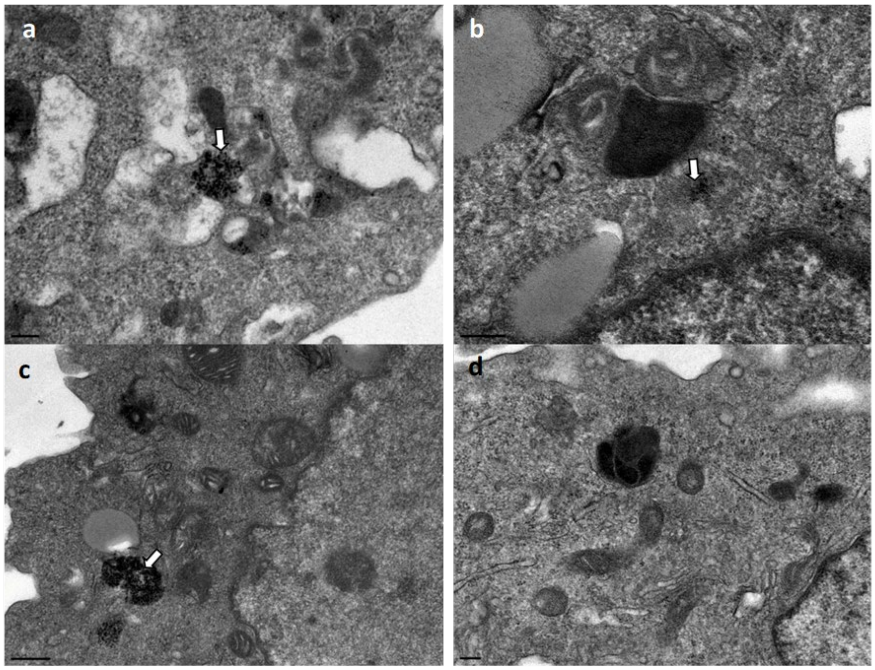

Figure IV.26: Transmission electron micrographs of A172 cells incubated with 100µg/ml of S-ION for 3h in complete (a) and serum-free (b) medium and after 24h of exposure in complete (c) medium showing nanoparticle internalization (arrows indicate S-ION agglomerates) in opposition to control cells (d). All bars (down left side) are 0.5µm long.

3.3. Cytotoxicity

3.3.1. Membrane integrity

The possible effect of S-ION on glial cell membrane integrity was analysed by measuring LDH enzyme release (Figure IV.27). It was observed that S-ION, regardless of the medium composition, did not produce significant alterations in membrane integrity, *i.e.* increases in LDH release, at any condition tested.

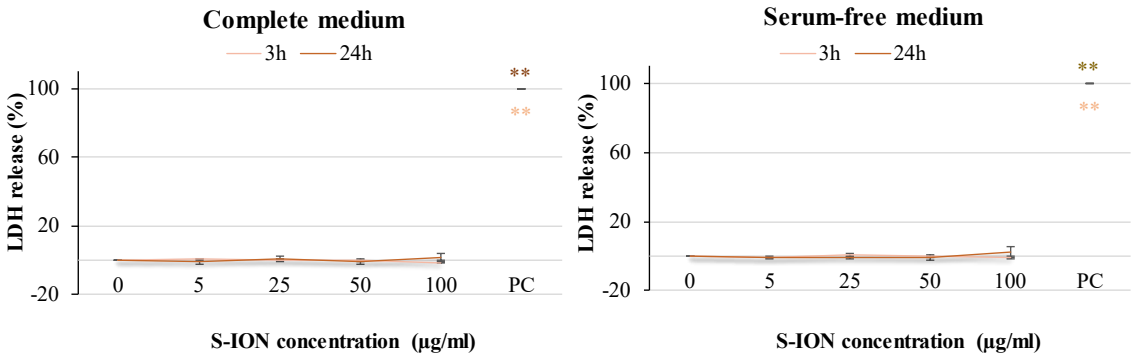

Figure IV.27: Results of membrane integrity assessment (LDH assay) in A172 cells exposed to S-ION in complete and serum-free medium. Bars represent mean ± standard error. PC: positive control (1% Triton X-100). ***P*<0.01, significant differences compared to the corresponding negative control.

3.3.2. Cell cycle analysis

Results obtained in the analysis of the different phases of the cell cycle (G_0/G_1, S, G_2/M) revealed that, in general, S-ION exposure altered the normal progression of A172 cell cycle (Figure IV.28). Although no significant differences in the cell distribution in each phase were obtained in the 3h treatments in complete medium when compared with the control, there was a statistically significant dose-dependent increase in the S-phase (r=0.406, P<0.05) with a simultaneous dose-dependent decrease in the G_0/G_1 phase (r=-0.443, P<0.05). After 3h treatments in serum-free medium, significant alterations were observed, mainly in G_0/G_1 (r=-0.594, P<0.01) and S phases (r=0.681; P<0.01). Exposure of glial cells to S-ION for 24h induced significant cell cycle alterations at all concentrations tested, regardless of the medium used. Consequently, positive dose-response relationships were obtained in all phases in complete medium (G_0/G_1: r=-0.864, P<0.01; S: r=0.900, P<0.01; G_2/M: r=0.481, P<0.05), and in G_0/G_1 and S phases in serum-free medium (G_0/G_1: r=-0.733, P<0.01; S: r=0.899, P<0.01).

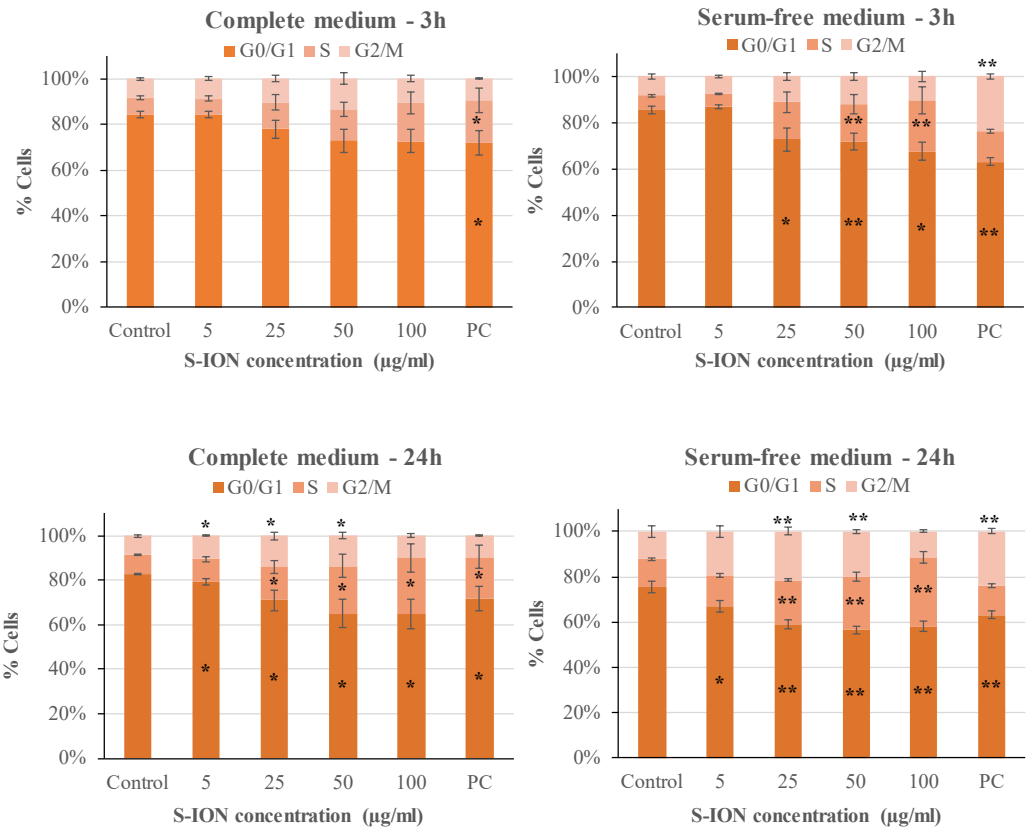

Figure IV.28: Analysis of A172 cell cycle after treatment with S-ION for 3h in complete (upper left) and serum-free medium (upper right), or for 24h in complete (lower left) and serum-free medium (lower right). Bars represent mean ± standard error. PC: positive control (1.5µM MMC). *P<0.05, **P<0.01, significant differences regarding the corresponding negative control.

In addition, analysis of subG$_1$ region of the cell cycle distribution was conducted as indicative of late stages of apoptosis (Figure IV.29). S-ION treatment in complete medium induced apoptosis only at the highest concentration and longest exposure time tested. However, a strong dose-dependent cell death generation was observed from 25µg/ml on in serum-free medium (3h: r=0.822, *P*<0.01; 24h: r= 0.880, *P*<0.01).

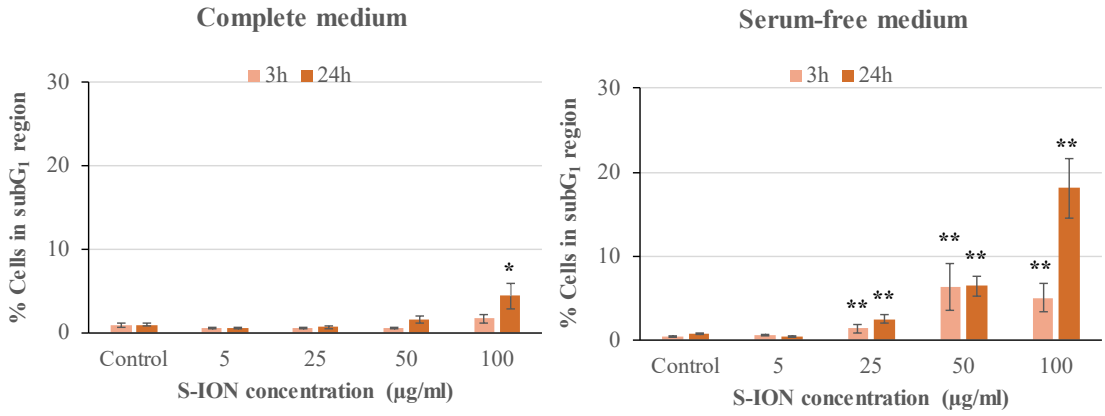

Figure IV.29: Late apoptosis (cells in the subG$_1$ region of cell cycle distribution) assessment in glial cells treated with S-ION in complete and serum-free medium. Bars represent mean ± standard error. *P<0.05, **P<0.01, significant differences compared to the negative control.

3.3.3. Apoptosis and necrosis detection

Early apoptosis was assessed by means of annexin V/PI double staining by flow cytometry. Results obtained in complete medium showed significant increases in the percentage of apoptotic cells after treatment with S-ION at the highest concentrations tested, particularly evident at 24h exposure but with significant dose-response relationships in both cases (3h: r=0.426, *P*<0.05, 24 h: r=0.673, *P*<0.01) (Figure IV.30). An even more notable apoptosis induction was observed in serum-free medium, with significant differences with regard to the negative control from 25µg/ml on and also significant dose-response relationships in both cases (r=0.860, *P*<0.01 for 3h; r=0.908, *P*<0.01 for 24h).

Furthermore, although necrosis rates obtained in the same analyses were much lower than apoptosis rates, they showed significant dose-dependent increases at the highest concentrations tested (50 and 100µg/ml) (r=0.558; *P*<0.01) only for the longest exposure time in complete medium (Figure IV.31). In contrast, in serum-free conditions, a dose-dependent relationship was observed at 3h, with statistically significant increases in the necrosis production from 25µg/ml on (r=0.832; *P*<0.01), whereas no effect at any dose was observed at 24h of exposure.

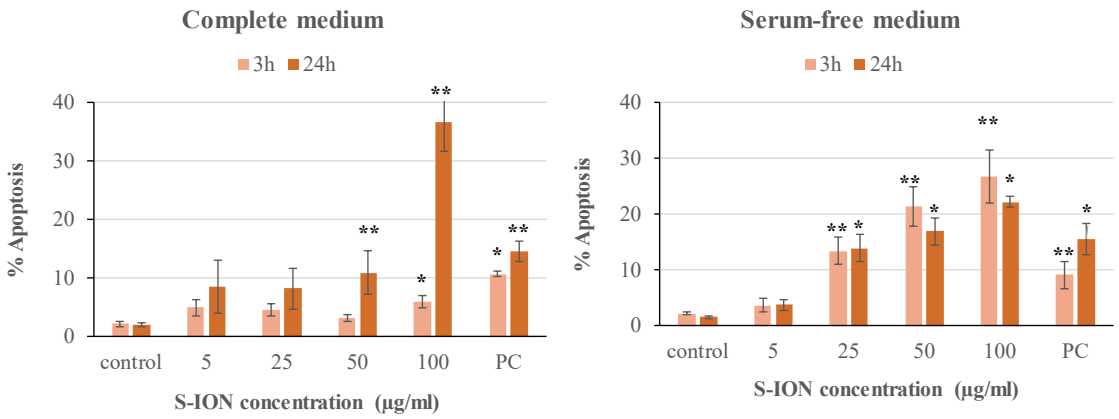

Figure IV.30: Apoptosis induction by exposure of A172 cells to S-ION for 3 and 24h in complete and serum-free medium. Bars represent the mean ± standard error. PC: positive control (10µM Campt). **P*<0.05, ***P*<0.01, significant difference with regard to the negative control.

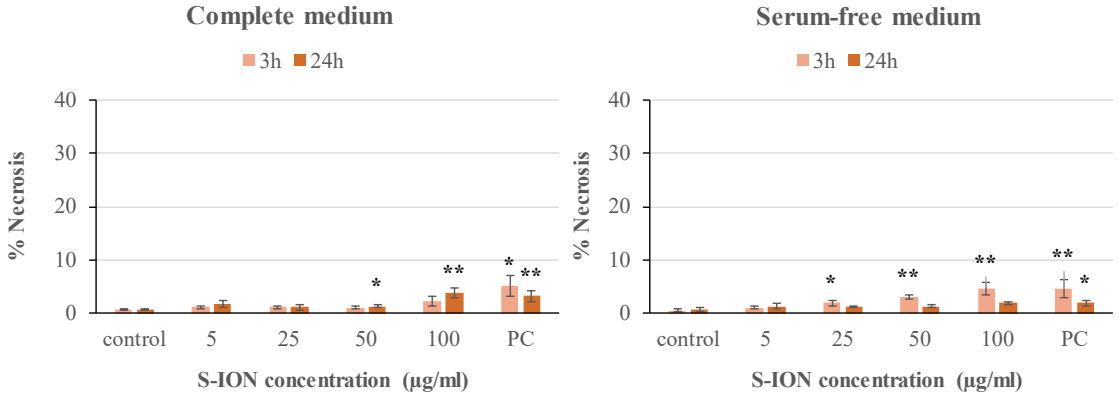

Figure IV.31: Necrosis induction after exposure of A172 astrocytes to S-ION for 3 and 24 h in complete and serum-free medium. Bars represent mean ± standard error. PC: positive control (10µM Campt). **P*<0.05, ***P*<0.01, significant difference with regard to the negative control.

3.4. Genotoxicity

3.4.1. γH2AX assay

Results obtained from analysis of H2AX phosphorylation by flow cytometry are shown in (Figure IV.32). Significant increases in %γH2AX were only observed in A172 cells treated with 50 and 100µg/ml S-ION for 24h in complete medium. No effects were observed in complete medium after 3h exposure and in serum-free medium at any time or dose tested.

3.4.2. MN test

According to MN assay results, no MN induction was observed in glial cells by S-ION treatment at any concentration or exposure time, either in complete or in serum-free medium (Figure IV.33).

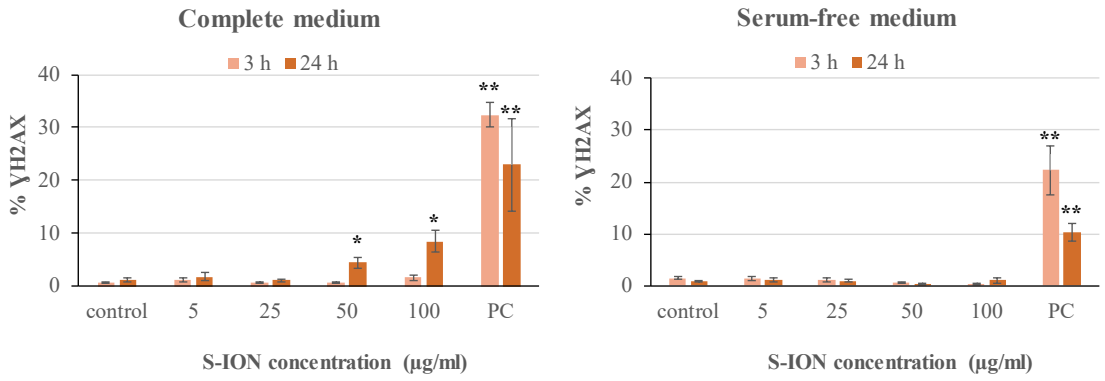

Figure IV.32: H2AX histone phosphorylation after treatment of glial cells with S-ION in complete and serum-free medium. Bars represent mean ± standard error. PC: positive control (1µg/ml BLM). **P*<0.05, ***P*<0.01, significantly different from the negative control.

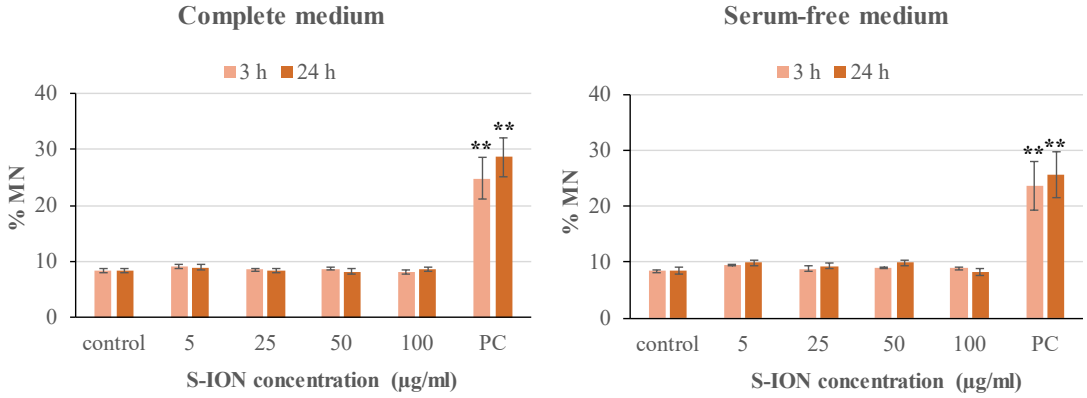

Figure IV.33: Micronuclei rates in A172 astrocytes after treatment with S-ION in complete and serum-free medium. Bars represent mean ± standard error. PC: positive control (15µM MMC). ***P*<0.01, significant differences with respect to the negative control.

3.4.3. Comet assay

When the possible interference between the nanoparticles and the comet methodology was tested, no significant differences were observed between the results obtained in the presence and

in the absence of S-ION (100µg/ml) (Figure IV.34), indicating no nanoparticle interference with any step of the assay, both in complete and serum-free media.

Subsequently, increases in primary DNA damage with respect to the controls were observed in S-ION treated cells, at the highest concentration after 3h treatment and from 25µg/ml on after 24h, regardless of serum presence in the medium (Figure IV.35). Positive dose-response relationships were also found in all cases (r=0.493, $P<0.01$ and r=0.564, $P<0.01$ for 3h, in complete and serum-free medium, respectively, and r=0.741, $P<0.01$ for 24h in both complete and serum-free medium).

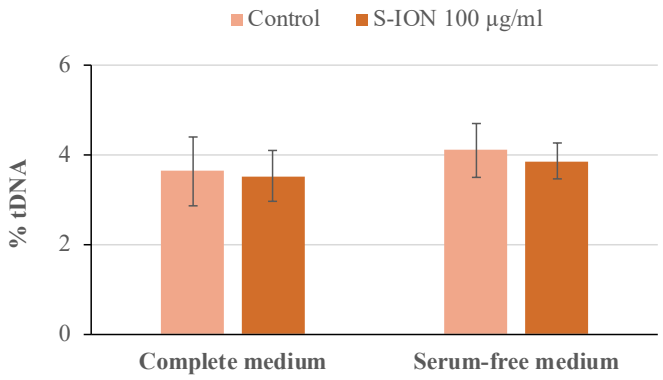

Figure IV.34: Results of interference testing between S-ION (100µg/ml) and comet assay methodology in complete and serum-free cell culture medium. Bars represent mean ± standard error.

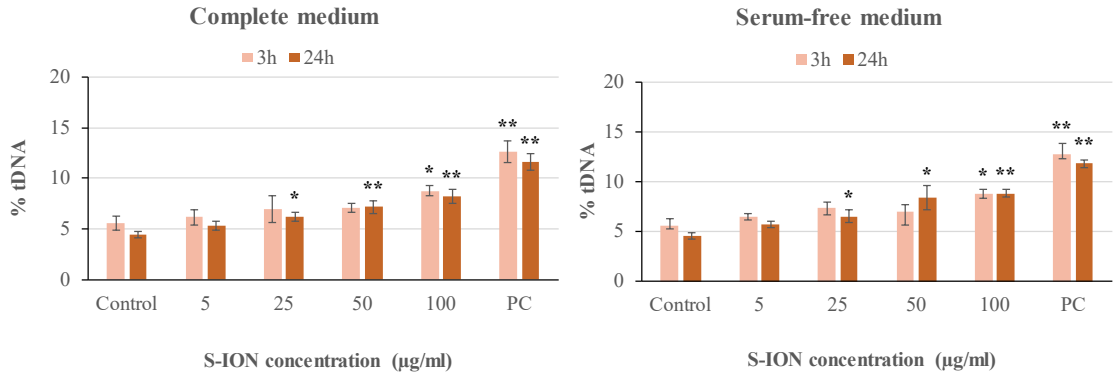

Figure IV.35: Primary DNA damage in A172 cells after treatment with S-ION in complete and serum-free medium. Bars represent mean ± standard error. PC: positive control (100µM H_2O_2). *$P<0.05$, **$P<0.01$, significant differences with regard to the corresponding negative control.

3.5. DNA repair

As shown in Figure IV.36, results obtained from the DNA repair competence assay showed a significant decrease in H_2O_2-induced damage after the repair period in all cases, independently of the assay phase in which glial cells were exposed to S-ION. In addition, the absence of damage induction by S-ION when cells were incubated for only 30min discards any additional DNA damage produced when cells were exposed during the repair phase.

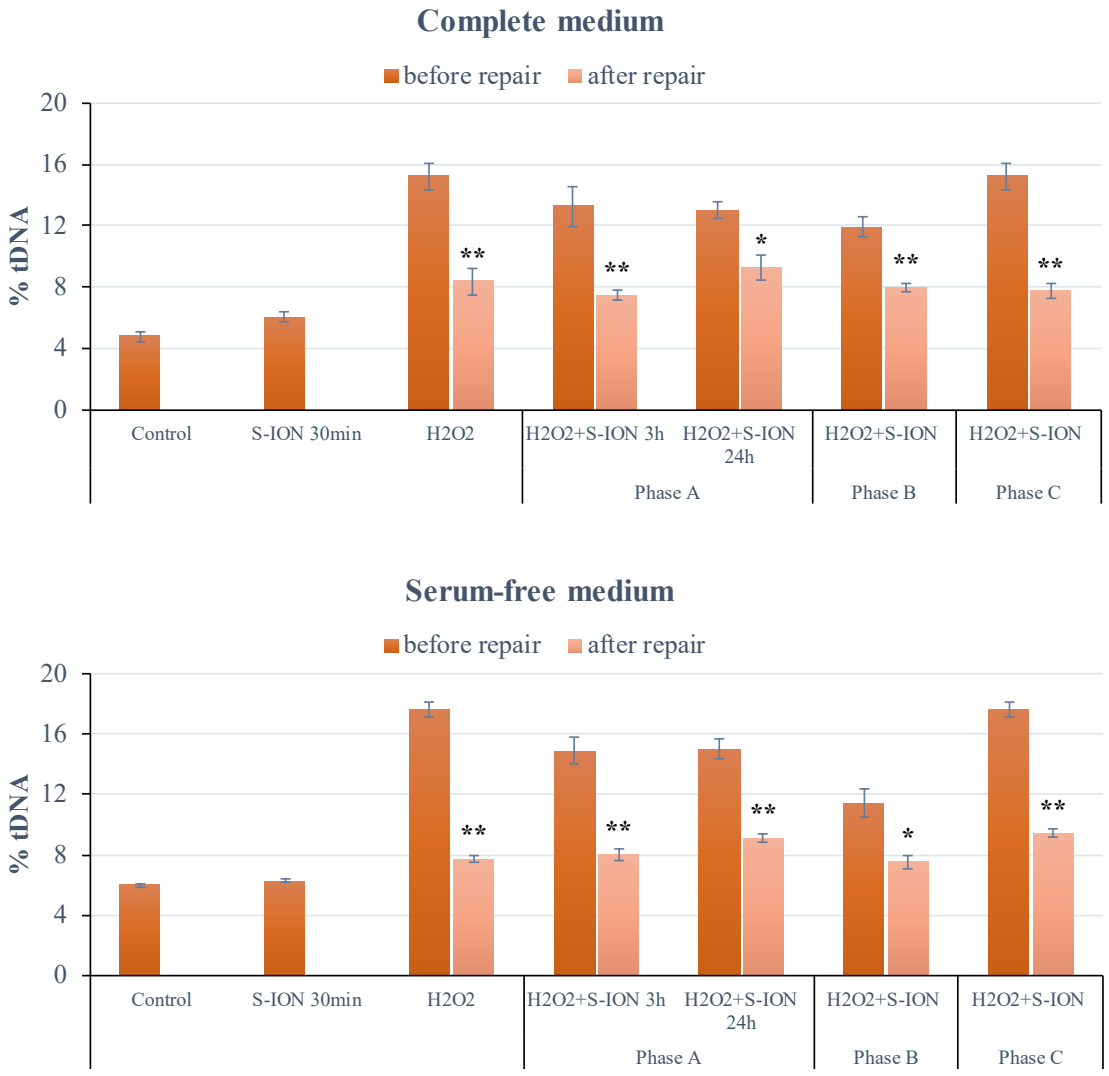

Figure IV.36: Effects of S-ION on repair of H_2O_2-induced DNA damage in astrocytes in complete and serum-free medium. Incubation with 50µg/ml S-ION was performed independently prior to exposure to 200µM H_2O_2 (phase A, for 3 or 24h), simultaneously with H_2O_2 (phase B), or during the repair period (phase C). Bars represent mean ± standard error. *P<0.05, **P<0.01, significant difference with regard to the same treatment before repair.

4. A172 CELLS EXPOSED TO O-ION

4.1. Iron ion release from the nanoparticles

Quantification of iron concentration in both cell culture media showed a dose- and time-dependent ion release from O-ION in complete medium, but only a slight increase in iron concentration at 24h treatments in serum-free medium (Figure IV.37).

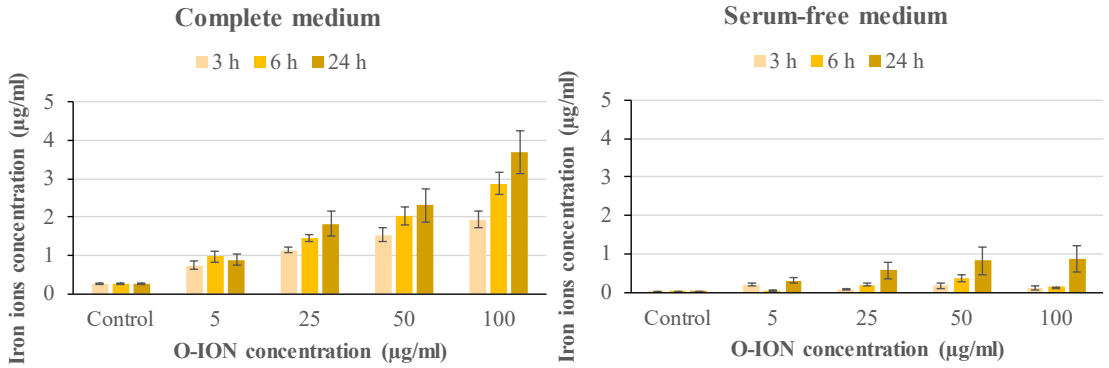

Figure IV37: Analysis of iron ion release from O-ION in complete and serum-free cell culture medium. Bars represent mean ± standard error.

4.2. Cellular uptake

The uptake and intracellular localization of O-ION in A172 cells were assessed by transmission electron microscopy (TEM) coupled with energy-dispersive X-ray spectroscopy (EDX). The presence of nanoparticles was confirmed within endosomes in all tested conditions (25 and 100µg/ml after 3 and 24h of exposure), both in complete and serum-free medium, as shown in Figure IV.38.

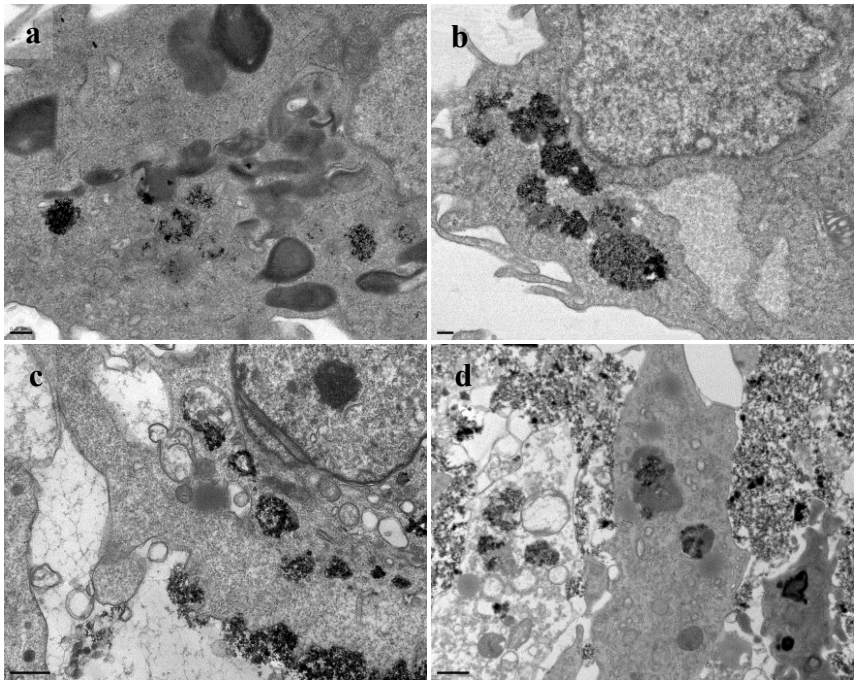

Figure IV.38: Transmission electron micrographs of A172 cells incubated with 100µg/ml of O-ION in complete medium for 3h (a) and 24h (b), and in serum-free medium for 3h (c) and 24h (d), showing nanoparticle internalization. Bar sizes are 0.2µm in (a) and (b), and 1µm in (c) and (d).

4.3. Cytotoxicity

4.3.1. Membrane integrity

Figure IV.39 shows LDH release to the cell culture media. No significant increase in enzyme leakage was detected at any condition tested.

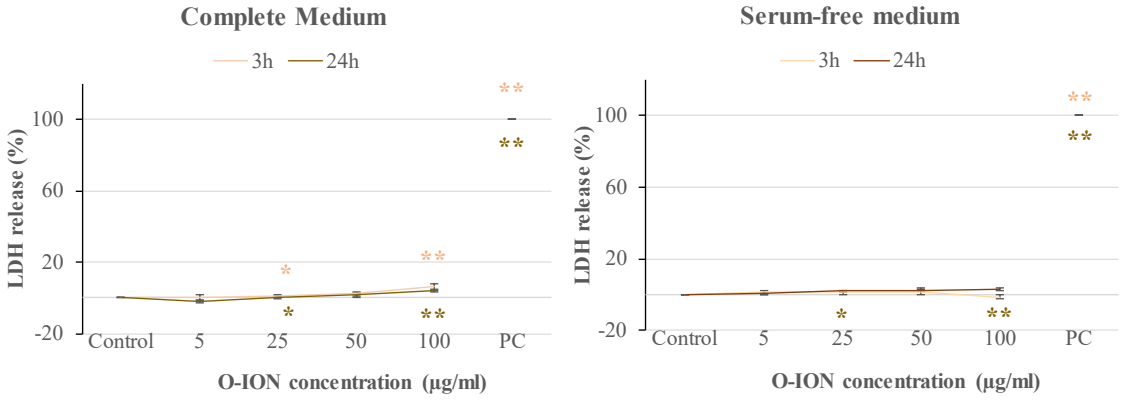

Figure IV.39: Results of membrane integrity assessment (LDH assay) in A172 cells exposed to O-ION in complete and serum-free medium. Bars represent mean ± standard error. PC: positive control (1% Triton X-100). *P<0.05, significant differences compared to the corresponding negative control.

4.3.2. Cell cycle analysis

The flow cytometry analysis of the DNA content in the different phases of the cell cycle (G_0/G_1, S, G_2/M) revealed that O-ION treatments altered significantly the normal progression of A172 cell cycle (Figure IV.40). A marked S phase arrest from 25 µg/ml on was observed at the two times tested, regardless of the presence of serum in the culture medium. Accordingly, strongly significant dose-dependent increases in S phase in complete (3 h: r=0.945, P<0.01; 24 h: r=0.931, P<0.01) and serum-free (3h: r=0.934, P<0.01; 24 h: r=0.654, P<0.01) media were observed, together with decreases in G_0/G_1 and G_2/M phases.

Additionally, evaluation of subG_1 region of the cell cycle histogram was performed as indicative of late stages of apoptosis. Results showed noticeable dose- and time-dependent increases in late apoptosis rates in astrocytes exposed to O-ION, in both complete (3h: r=0.931, P<0.01; 24h: r=0.942, P<0.01) and serum-free (3h: r=0.923, P<0.01; 24h: r=0.926, P<0.01) media (Figure IV.41).

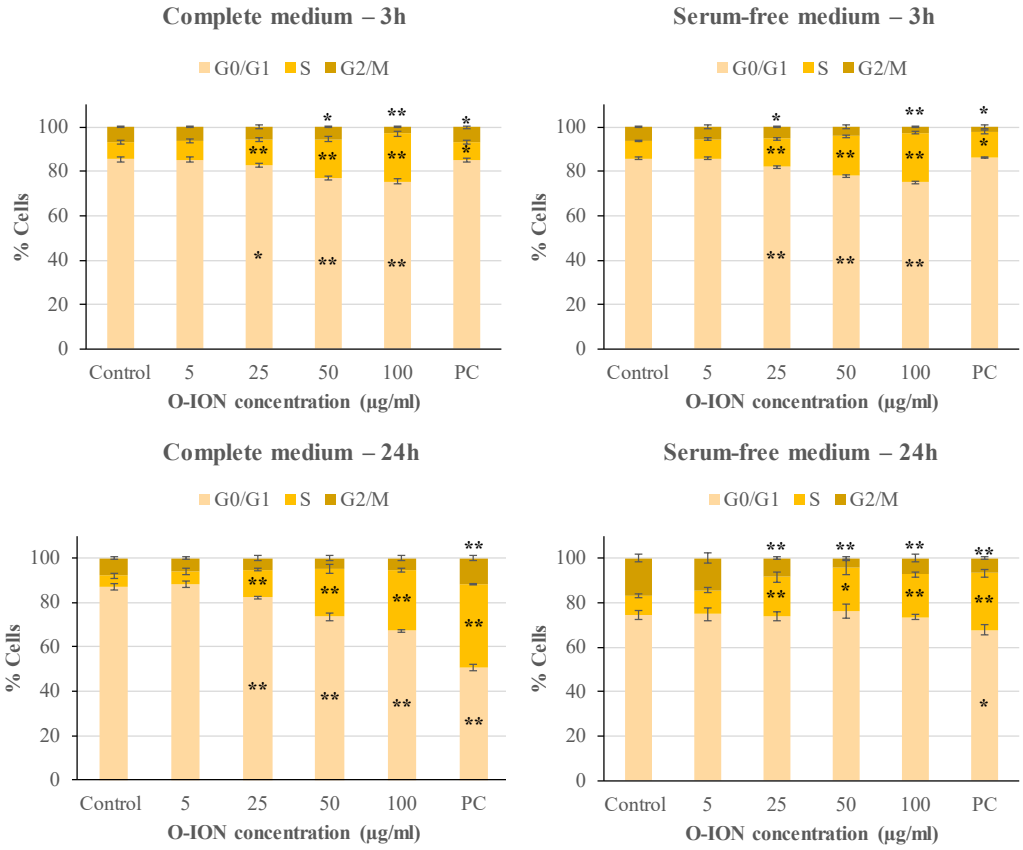

Figure IV.40: Analysis of A172 cell cycle after treatment with O-ION for 3h in complete (upper left) and serum-free medium (upper right), or for 24h in complete (lower left) and serum-free medium (lower right). Bars represent mean ± standard error. PC: positive control (1.5µM MMC). *P<0.05, **P<0.01, significant differences with regard to the corresponding negative control.

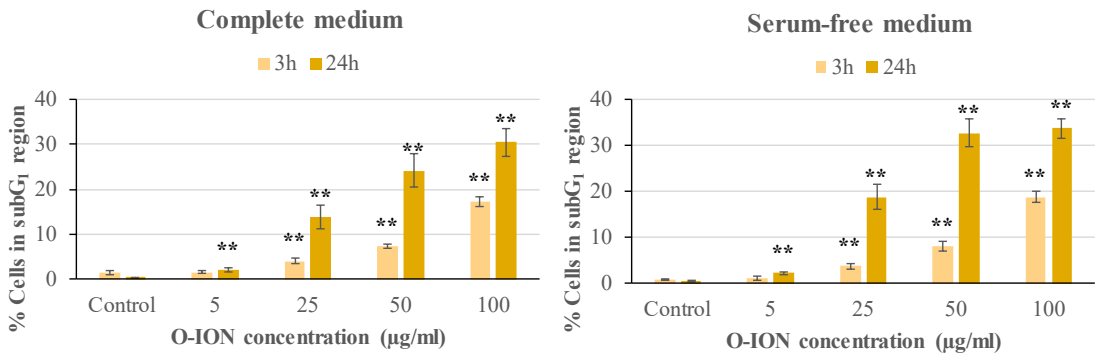

Figure IV.41: Late apoptosis (cells in the subG$_1$ region of cell cycle distribution) assessment in A172 cells treated with O-ION in complete and serum-free medium. Bars represent mean ± standard error. ***P*<0.01, significant differences compared to the corresponding negative control.

4.3.3. Apoptosis and necrosis detection

In line with subG$_1$ region analysis, evaluation of annexin V/PI double staining also exhibited significant dose-dependent increases in the percentage of apoptotic cells after O-ION treatments in complete (3h: r=0.852, *P*<0.01; 24h: r=0.931, *P*<0.01) and serum-free (3h: r=0.912, *P*<0.01; 24h: r=0.942, *P*<0.01) media (Figure IV.42). Moreover, slight increases in necrosis rates, particularly in complete medium, were observed, although rate values were always below 5% (Figure IV.43).

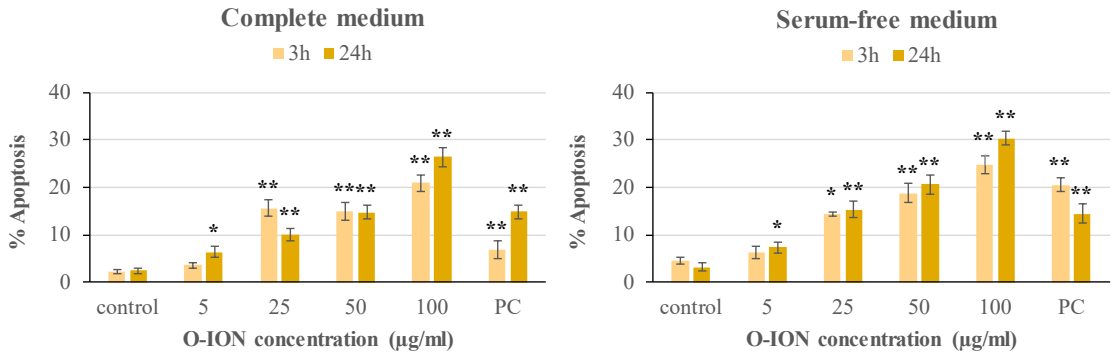

Figure IV.42: Apoptosis induction by exposure of A172 cells to O-ION in complete and serum-free medium. Bars represent the mean ± standard error. PC: positive control (10µM Campt). **P*<0.05, ***P*<0.01, significant difference with regard to the corresponding negative control.

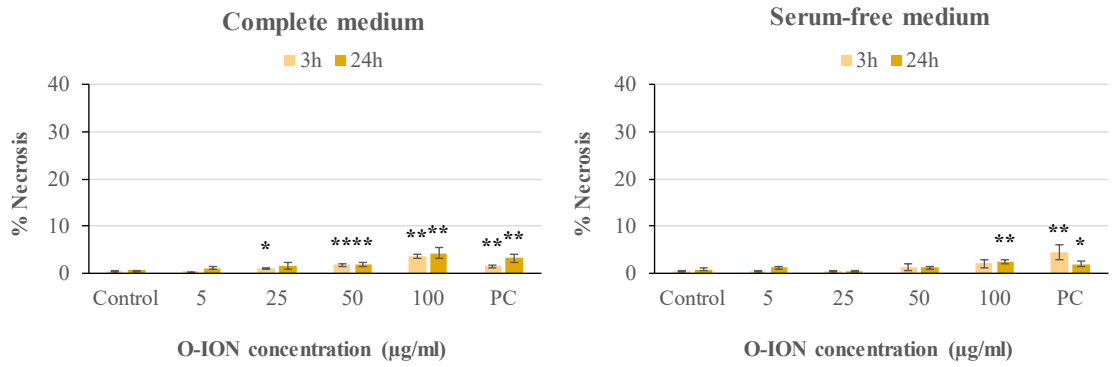

Figure IV.43: Necrosis induction after exposure of A172 astrocytes to O-ION in complete and serum-free medium. Bars represent mean ± standard error. PC: positive control (10µM Campt). **P*<0.05, ***P*<0.01, significant difference with regard to the corresponding negative control.

4.4. Genotoxicity

4.4.1. γH2AX assay

Results obtained from analysis of H2AX phosphorylation are shown in Figure IV.44. Only slight increases were observed in the percentage of γH2AX at certain experimental conditions.

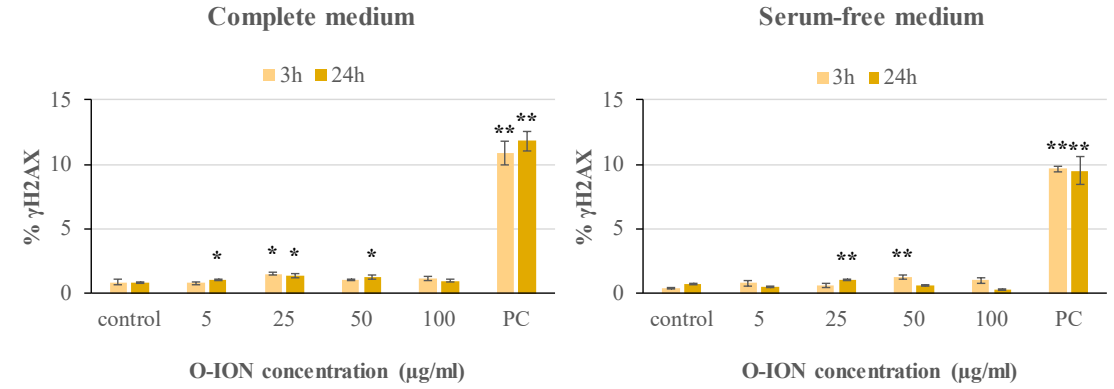

Figure IV.44: H2AX histone phosphorylation after treatment of A172 cells with O-ION in complete and serum-free medium. Bars represent mean ± standard error. PC: positive control (1µg/ml BLM). **P*<0.05, ***P*<0.01, significantly different from the corresponding negative control.

4.4.2. MN test

As it can be seen in Figure IV.45, no significant MN induction was found in A172 cells exposed to O-ION at any dose, time, or culture medium tested.

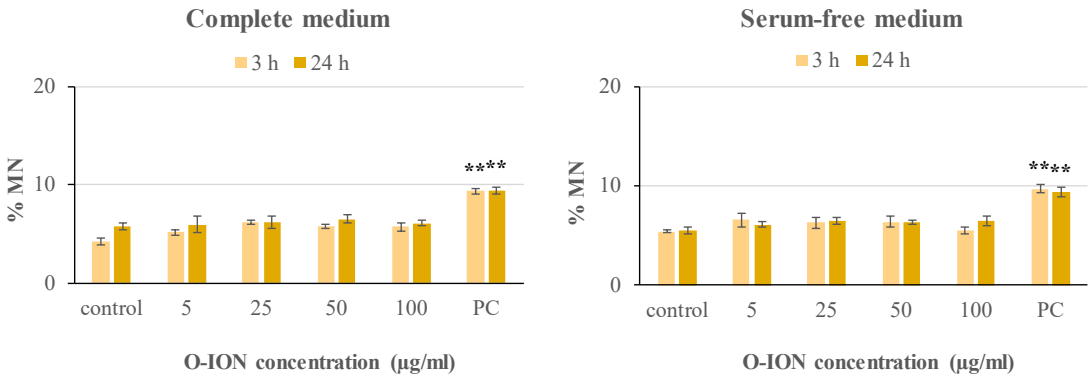

Figure IV.45: Micronuclei rates in A172 cells exposed to O-ION in complete and serum-free medium. Bars represent mean ± standard error. PC: positive control (15µM MMC). ***P*<0.01, significant differences with respect to the corresponding negative control.

4.4.3. Comet assay

Prior to conducting the comet assay experiments, the possible interference of O-ION with any step of its methodology was discarded since very similar results were obtained when performing the assay in the presence and in the absence of O-ION (Figure IV.46). Subsequently, alkaline comet assay was carried out, and results showed general increases in primary DNA damage (%tDNA) with respect to the negative control in astrocytes exposed to the highest O-ION concentrations, at both exposure times for complete medium but limited to 24h in serum-free medium (Figure IV.47). Significant dose-response relationships were found in complete (3h: r=0.689, *P*<0.01; 24h: r=0.452, *P*<0.05) and serum-free (3h: r=0.585, *P*<0.01; 24h: r=0.654, *P*<0.01) media.

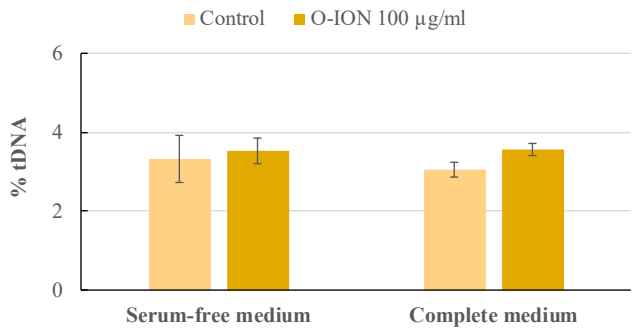

Figure IV.46: Results of interference testing between O-ION (100µg/ml) and comet assay methodology in complete and serum-free cell culture medium. Bars represent mean ± standard error.

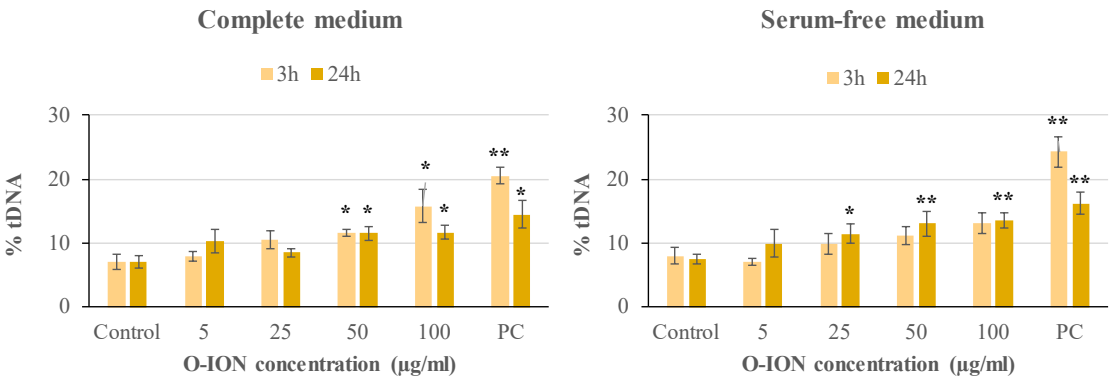

Figure IV.47: Primary DNA damage in A172 cells treated with O-ION in complete and serum-free medium. Bars represent mean ± standard error. PC: positive control (100µM H_2O_2). **P*<0.05, ***P*<0.01, significant differences with regard to the corresponding negative control.

4.5. DNA repair

Figure IV.48 shows the results from the DNA repair competence assay. No alteration in DNA repair ability caused by O-ION exposure was observed at any condition, since significant decreases in H_2O_2-induced damage were registered after the repair period, similar to those exhibited in the presence of H_2O_2 alone. Similar results were obtained for all phases tested and regardless of media composition.

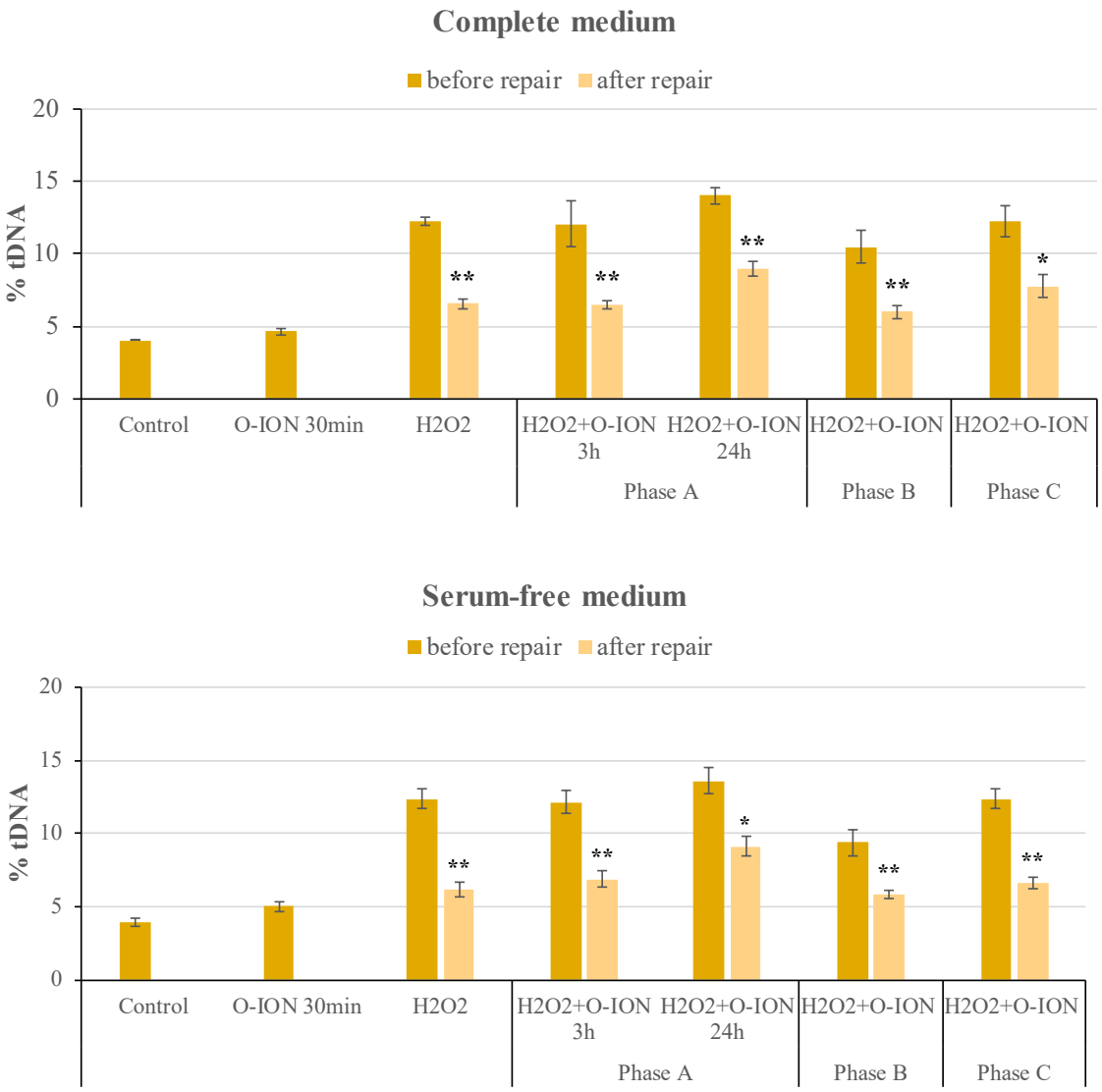

Figure IV.48: Effects of O-ION on repair of H_2O_2-induced DNA damage in A172 cells in complete and serum-free medium. Incubation with 50µg/ml O-ION was conducted independently prior to exposure to 200µM H_2O_2 (for 3 or 24h, phase A), simultaneously with H_2O_2 (phase B), or during the repair period (phase C). Bars represent mean ± standard error. **P*<0.05, ***P*<0.01, significant differences with regard to the same treatment before repair.

V. DISCUSSION

V. DISCUSSION

Magnetic nanoparticles are one of the first nanomaterials to be approved for clinical use (Gould, 2006). Among the different types of magnetic nanoparticles, iron oxide nanoparticles (ION) awaken a particular interest due to their unique properties, including superparamagnetism and high biocompatibility (Elsaesser and Howard, 2012). Iron oxide can exist in different chemical compositions, including magnetite (Fe_3O_4) or maghemite (γ-Fe_2O_3). Both oxides have very similar physical properties due to their nearly identical crystalline structure (Estelrich *et al.,* 2015), whereas magnetization is higher for magnetite than for maghemite (Turcheniuk *et al.,* 2013). This is one of the main reasons why magnetite is the most commonly ION used in biomedicine.

ION features make them very suitable for a broad variety of uses, mostly in biomedical applications, namely magnetic resonance imaging, targeted drug delivery, tumour location and magnetic hyperthermia, among others (reviewed in Revia and Zhang, 2016). In particular, over the last decade, ION are being used for diagnosis and therapy of several central nervous system (CNS) pathologies, such as Alzheimer´s, Parkinson´s, multiple sclerosis, and primary brain tumours (Kanwar *et al.,* 2012). This is mainly because the reduction in particle size gives ION the ability to cross the blood-brain barrier (BBB) and get access to brain, commonly difficult to reach (Monopoli *et al.,* 2012; Kenzaoui *et al.,* 2013; Petters *et al.,* 2014b). Besides, because of their ability to overcome the restraints of the BBB (Thomsen *et al.,* 2013), they have been used as carriers for the transport of drugs, siRNA, or DNA into the brain. ION size, combined with high surface area and reactivity, makes the nervous system extremely vulnerable to their potential toxicity. Indeed, recent investigations indicated that ION can not only reach the brain (Liu *et al.,* 2013), but also cause a certain degree of neurotoxicity (Migliore *et al.,* 2015).

However, studies regarding the potential toxic effects of ION on CNS are scarce and conflicting so far (reviewed in Valdiglesias *et al.,* 2014), and their potential risk on human brain cells have raised concern (Braeuer *et al.,* 2015). Still, the lack of robust toxicological screenings, and poor comprehension of predictive paradigms of nanoneurotoxicity are the major obstacles in translating the advancing nanoparticle designs into viable biomedical platforms system (Kim *et al.,* 2013). This is, at least in part, due to the great variety of ION, bare or with different coatings, tested. Besides, most studies were focused on addressing cytotoxic effects, *e.g.,* decrease in viability, cytoskeleton alterations, iron ion release or reactive oxygen species (ROS) generation (Suh *et al.,* 2009; Soenen and De Cuyper, 2010). However, their possible effects on other different cellular functions, on the genetic material, or on the DNA repair ability have been hardly addressed on human nervous cell types (reviewed in Valdiglesias *et al.,* 2016). Furthermore, results of toxicity assays available are not always comparable since they are influenced by several

factors such as the cell type tested (Ding *et al.,* 2010; Kunzmann *et al.,* 2011), experimental conditions assessed (Pisanic *et al.,* 2007), and physicochemical properties of ION (Thorek and Tsourkas, 2008). Indeed, general knowledge about ION toxic effects indicates that they mainly depend on nanoparticle size and surface coating (Rivet *et al.,* 2012).

On this basis, the present study was designed to elucidate the potential adverse effects of S-ION and O-ION on human neuronal and glial cells (astrocytes) by evaluating a dose range and short- and long-term exposure times (3 and 24 h, respectively), in complete and serum-free media conditions. In particular, after cellular uptake assessment of ION, the measurement of membrane integrity, cell cycle progression and apoptosis/necrosis rates were evaluated as indicators of cytotoxicity, whereas histone H2AX phosphorylation, MN frequency and primary DNA damage were determined as genotoxicity parameters. Complementarily, possible effects on DNA repair ability and iron ion release capacity were also assessed.

ION have high chemical activity and oxidation capacity, resulting in loss of magnetism and dispersibility. In order to avoid this and to improve their properties, ION surface can be coated with different natural or synthetic polymers and/or numerous biological molecules (Mahdavi *et al.,* 2013). For *in vivo* purposes, nanoparticles are required to be biocompatible, water-dispersible, stable in biological media, and uniform in size to maintain the suitable magnetic properties (Chang *et al.,* 2012; Lee *et al.,* 2015). Surface coatings are known generally to influence advantageously nanoparticle features. Nevertheless, as mentioned before, surface modifications may also alter their biocompatibility, stability, aggregation state, size, and toxicity (Mahmoudi *et al.,* 2011a,c). The type of coating employed usually depends on the functionalization needed for each particular ION application.

In this study ION with two different coatings were tested: silica and oleic acid. Silica coating has several advantages that make it very suitable for biomedical applications, including negative charge at blood pH or transparent matrix (Alwi *et al.,* 2012). Silica can increase ION biocompatibility without affecting magnetic properties, may convert hydrophobic nanoparticles into hydrophilic water-soluble particles, helps to prevent aggregation by improving the nanoparticle chemical stability, and the silanol-terminated surface groups may be modified with various coupling agents to covalently bind to specific ligands, reviewed in Andrade *et al.,* (2009). All these properties make silica one of the most commonly used agents for ION coating, particularly for bioimaging and biosensing purposes (Alwi *et al.,* 2012). Still, the possible neurotoxicity of silica-coated ION (S-ION), particularly on nervous cells different from neurons, has not been discarded yet.

ION coated with an oleic acid bilayer (O-ION) are also a good option for biomedical purposes since oleic acid coating stabilizes the nanoparticles in organic solvents (Sahoo *et al.,* 2001). This mono-unsaturated fatty acid is commonly used as high affinity surfactant agent to modify the surface of ION through the formation of strong chemical bonds between the carboxylic acid and ION, resulting in highly uniform, monodispersed and biocompatible nanoparticles (Soares *et al.,* 2016). Moreover, the lipid-soluble and non-ionic oleic acid coating improves the nanoparticle ability to cross the blood-brain barrier and reach the brain, being particularly useful in specific applications directed to this organ, as targeted drug delivery or hyperthermia (Dilnawaz and Sahoo, 2015).

In vitro studies are essential to initially evaluate the potential risk for the different CNS cells, from neurons to glial cells, associated with the use of ION (Dwane *et al.,* 2013; Migliore *et al.,* 2015). However, studies on the potential toxic effects of ION in the CNS are still scant and their possible toxic effects on human brain cells have not been ruled out (Braeuer *et al.,* 2015). The use of primary human cell culture models, although more representative, are limited, since differentiated nervous cells are difficult to obtain, have a limited proliferating capacity in culture, and present associated ethical constraints. The use of standardized stocks of cell lines have the advantage of the proliferative potential of an immortal cancer cell line and its high throughput in culture, combined with ability to be differentiated cells that can then be used in functional assays. Thus, in the present work, we have sought a balance between advantages such as performance in cell culture or toxic sensitivity of the nervous cell lines employed, with disadvantages such as the absence of some morphological and functional characteristics due to differentiation.

Among all glial cells, astrocytes are especially interesting since they are the most abundant brain cell type. The astrocytic end-feet cover the majority of the BBB which makes them the first cellular obstacle ION interact with (Yang *et al.,* 2010). Moreover, astrocytes are strategically distributed between the blood vessels and neurons (Geppert *et al.,* 2011). Besides, they seem to play a key role in the etiology of neurodegenerative disorders and, consequently, have been proposed as new targets for the treatment of important neuropathologies such as Alzheimer's disease, amyotrophic lateral sclerosis, and Parkinson's disease (Barker and Cicchetti, 2014; Phatnani and Maniatis, 2015; Finsterwald *et al.,* 2015). At the beginning of glial research, astrocytes were thought to give only structural support. However, nowadays a number of new important astrocytic functions have been known, and due to their morphological and physiological heterogeneity it is quite difficult to define what an astrocyte is (Sofroniew and Vinters, 2010; Kimelberg and Nedergaard, 2010; Verkhratsky *et al.,* 2015). They not only provide other neural cells with energy substrates and nutrients, but they also play a key role in the homeostasis of ions, pH and water, regulate the vasopressure in brain, recycle neurotransmitters,

as well as fulfill a wide range of other homeostasis maintaining functions in the brain (Sofroniew and Vinters, 2010; Pekny and Pekna, 2014). During the past two decades, astrocytes emerged also as increasingly important regulators of neuronal functions including the generation of new nerve cells and structural as well as functional synapse remodeling. Moreover, they interact with neurons and modulate their signal transmission (De Bock *et al.,* 2014; Howarth, 2014). The A172 cell line employed in this Thesis is an astrocytoma non-tumorigenic and p53 wild-type cell line derived from a human glioblastoma that has been commonly used in *in vitro* studies to elucidate basic neurobiological principles and as a glial model in neurotoxicity testing (Wolff *et al.,* 1999; Qiang *et al.,* 2009; Sato *et al.,* 2009).

Neurons are the core constituent of the brain and are crucial for the maintenance of its function. In general, neurons have the specific function to transmit electrochemical signals, and can differ regarding their morphology, location, type of neurotransmitter produced, function (motor, sensory) or effect (excitatory, inhibitory) (Zeng and Sanes, 2017). The damage of neurons, such as loss of structure or function, was considered to play a key role in the etiology of certain neurodegenerative diseases as well (Wu *et al.,* 2011). The human neuroblastoma SH-SY5Y neuronal cell line employed in this work is a dopaminergic cell line which express tyrosine hydroxylase and dopamine-beta-hydroxylase, as well as the dopamine transporter, and can be differentiated into a functionally mature neuronal phenotype in the presence of various agents. It is one of the more frequently and extensively used cell lines as an *in vitro* model in neurobiological, neurochemical, and neurotoxicological studies (Xie *et al.,* 2010; Kovalevich and Langford, 2013), due to their ability to differentiate and proliferate in culture for long periods, and they also possess many biochemical and functional features of primary neurons (Xie *et al.,* 2010).

Recent studies have demonstrated that nanoparticles exposed to biological fluids interact with a variety of biomolecules (mainly serum proteins, although lipids, sugars, etc. may adhere with), which lead to formation of a functional layer or "corona" on their surfaces (Monopoli *et al.,* 2012). The corona formation is in turn dependent on the physicochemical properties of the nanoparticles (*e.g.,* surface chemical composition and surface charges, presence/absence of coating) (Mahmoudi *et al.,* 2011a; Sakulkhu *et al.,* 2014; Arami *et al.,* 2015), the type of biomolecules and their concentration, and incubating temperature, among others (Zanganeh *et al.,* 2016). It is evident that the functionality and effectiveness of nanoparticles exposed to living organisms (*e.g.,* cells) depend more on the nature and amount of the proteins present in the corona than on their bare surface (Mahmoudi *et al.,* 2015). The protein corona plays an important biological role; it can change the way nanoparticles interact with cells, because it can modify their physicochemical characteristics, leading to structural and functional changes, such as

internalization ability, enzymatic function, and toxic effects (Nel *et al.,* 2009; Lesniak *et al.,* 2010; Mahmoudi *et al.,* 2011b, 2012; Bertrand and Leroux, 2012; Monopoli *et al.,* 2012). Hence, protein corona makes it challenging to distinguish the relationship between chemical functionality of nanoparticles and their biological effects (Zanganeh *et al.,* 2016). Investigation on the possible formation and composition of this protein corona is crucial to understanding their correspondence with the ION toxicological profile, and attempt to mimic their behavior *in vivo* (Mahmoudi *et al.,* 2012). The protein corona has been found to provide multiple protective effects to biological systems. However, interpretations of these beneficial effects can often be unclear due to the variation in conditions and reported outcomes. Conflicting reports on cytotoxicity and biological fates, even when identical nanoparticles were studied, have been reported (Mahmoudi *et al.,* 2011a; Mao *et al.,* 2013; Sakulkhu *et al.,* 2014; Behzadi *et al.,* 2014; Sharifi *et al.,* 2015). In order to assess the potential influence of this protein corona on ION effects investigated in the present study, all experiments were carried out in the presence and absence of serum in the media (complete and serum-free media, respectively).

Concentrations and exposure times employed in the present study were chosen based on previous cell viability results, obtained from 3-(4,5-dimethylthiazol-2-yl)-2,5-diphenyltetrazolium bromide (MTT), neutral red uptake (NRU), and alamar blue (AB) assays (Costa *et al.,* 2016). Experimental conditions selected to be tested were those producing a maximum decrease in SH-SY5Y or A172 cell viability of 30%, thus avoiding the possible influence of excessive decline in viability on the results of the different parameters tested. As for the physiological meaning of the ION concentrations chosen, the dose range recommended for carboxydextran coated-ION (ferucarbotran, Resovist®) to be used in clinical magnetic resonance imaging (0.2–0.8mg Fe/kg body weight) (Reimer and Balzer, 2003) is roughly equivalent to the lower doses tested in this study (2.5-10µg/ml).

1. SH-SY5Y CELLS EXPOSED TO S-ION

Analysis of iron ion release from the S-ION suspensions showed a different behaviour of the nanoparticles depending on the media composition. Low concentrations of iron were detected in serum-free medium, whereas the release of ions was notable in the presence of serum (complete medium), in general increasing with time and S-ION concentration. Release of iron ions from ION was previously described in a number of studies (Soenen and De Cuyper, 2009). However, this release can vary depending on the suspension conditions and the nanoparticle surface coating (Malvindi *et al.,* 2014). Results obtained here suggest that degradation of the studied S-ION is not dependent on particle size, since similar hydrodynamic diameters obtained in different media showed very different dissolution rates.

The chemical synthesis, as well as the presence of coating, which surrounds and isolates the magnetic material from the environment, and its physicochemical properties, may influence the degradation rate of the particles and so the release of iron ions (Lévy *et al.,* 2010; Mahon *et al.,* 2012). This would explain the differences found in our study, since ION suspended in complete medium may externally interact with serum proteins, thus favouring the silica coating degradation and causing a higher iron release from the nanoparticle core. In fact, proteins may increase the dissolution rates of iron oxides through both aqueous complexation and ligand-enhanced dissolution (Nel *et al.,* 2009).

The evaluation of cellular uptake of nanoparticles by flow cytometry using side scatter parameter (indicative of cell granularity/complexity) is suitable for initial screening of nanotoxicity (Ibuki and Toyooka, 2012). Experimental data confirmed that the S-ION were effectively taken up by neuroblastoma cells, and the uptake was higher when exposure was performed in the absence of serum. These findings agree with previous studies in other cell types showing that S-ION are quickly internalized by macrophages (Kunzmann *et al.,* 2011), and by A549 and HeLa cells (Malvindi *et al.,* 2014). Differences in nanoparticle uptake were previously reported by Krais *et al.,* (2014), who studied the role of serum proteins on ION uptake, and observed that the presence of a protein corona may indeed influence the cellular uptake of folic acid-functionalized ION. Agreeing with our results, Salvati *et al.,* (2013) speculated that excessive binding of serum proteins may prevent selective, ligand-mediated uptake of nanoparticles. Besides, our *in vitro* studies revealed a remarkable lower degree of internalization for the highest S-ION concentration at 24h when compared to the one obtained at 3h. This is likely due to the progressive nanoparticle agglomeration at this high concentration, which causes a more noticeable interference with the uptake process at the longest exposure period.

Cell cycle machinery corresponds to series of events which lead the cell to its division and duplication (Crosby, 2007). Results obtained from analysis of cell cycle showed that exposure for 3h to S-ION did not alter it at any concentration, which agrees with previous findings from some other studies using bare or differently coated ION (Mahmoudi *et al.,* 2011c). However, significant mitotic arrest (increase in the rate of cells in S phase and/or decrease in the rate of cells in G_2/M phase) was observed for 24h treatments in both culture media at the highest dose tested. Similar alterations in the cell cycle were observed by Namvar *et al.,* (2014) after exposing Jurkat cells to bare magnetite nanoparticles prepared by green biosynthesis (using a brown seaweed), but the dose used was much lower (6.4µg/ml, corresponding to the inhibitory concentration 50 [IC50], calculated by MTT assay). In the previous cell viability assays with the current S-ION (Costa *et al.,*, 2016), viabilities obtained for treatments up to 200µg/ml were always higher than or equal to 70% as calculated by MTT, neutral red uptake and alamar blue assays; therefore cytotoxicity

of these nanoparticles, at least to SH-SY5Y cells, was much lower than cytotoxicity of the ION used by Namvar *et al.,* (2014) in Jurkat cells. These observations agree with the general assumption that ION coated with silica are indeed less toxic that bare ION. Besides, in a recently published study, Couto *et al.,* (2015) were unable to find any alteration on cell cycle when testing polyacrylic acid (PAA)-coated and non-coated ION on human T lymphocytes (48h treatments).

In order to evaluate apoptosis, which is critical in many physiological and pathological processes, we used two alternative strategies: analysis of the $subG_1$ region of the cell cycle distribution, indicative of DNA fragmentation at the late stages of apoptosis, and Annexin V/PI staining for sensitive detection of early stage apoptosis. Results obtained with the two strategies were quite similar. The only significant increase in apoptosis rate observed was for the highest S-ION concentrations after 24h treatments in both media tested. The exception was the $subG_1$ region in complete medium, which did not show any significant alteration. This difference may be explained on the basis of the methodological differences between the two techniques used. Annexin V/PI staining and measurement is carried out just after the treatments, and reflects early stage apoptosis, meanwhile $subG_1$ region analysis is performed after an additional 24h incubation period following the treatments, and is indicative of late stage apoptosis. Hence, probably the cells undergoing early apoptosis detected by Annexin V/PI staining have already been mostly removed when $subG_1$ region was analysed. Similar apoptosis results were reported by Jeng and Swanson (2006), who found that ION only induce apoptosis in mouse Neuro-2A neuroblastoma cells after exposure to concentrations higher than 100µg/ml. Contrarily, Namvar *et al.,* (2014) described time-dependent (from 12 to 48h) increases in the apoptosis rates in Jurkat cells treated with bare magnetite nanoparticles (6.4µg/ml), evaluated by the two same methodologies used in the current work. Likewise, significant apoptosis induction (evaluated by means of mitochondrial membrane potential, JC-1 assay) in cervical and lung cells exposed to 2.5nM S-ION (magnetite) for 48h was reported (Malvindi *et al.,* 2014). This concentration is equivalent to approximately 30µg/ml of the current S-ION, dose which produced negative results at all conditions tested in this study.

Cell death by necrosis (and/or late apoptosis) was also determined by annexin V/PI staining, and no alterations in this rate were found in SH-SY5Y cells exposed to S-ION at any of the conditions assayed. Namvar *et al.,* (2014) obtained again contrary results: time-dependent increase in the necrosis/late apoptosis rate in Jurkat cells treated with ION but, as mentioned above, toxicity of these nanoparticles (in terms of cell viability decrease) was much higher.

Possible effects of S-ION exposure on cell membrane integrity of neurons were evaluated by LDH leakage assay. Negative results were obtained for all experimental conditions evaluated, which is essentially in agreement with most results obtained for cell cycle and apoptosis or

necrosis induction, and also with previous results from the same nanoparticles, doses and cell line using MTT and alamar blue viability assays (Costa *et al.,* 2016). Nevertheless, positive LDH leakage results were obtained by Malvindi *et al.,* (2014) after treatment of A549 and HeLa cells for 48 and 96 h with 2.5nM S-ION (as already mentioned, equivalent to 30µg/ml of the current S-ION), according to their apoptosis assessment results and confirming the lower cytotoxicity of the present silica-coated nanoparticles.

Taking all cytotoxicity results together, S-ION tested showed low cytotoxic potential; data from serum-free medium indicate a slightly larger harmful potential [viability reduction (Costa *et al.,* 2016), cell cycle alterations and apoptosis induction (present study)], agreeing with the faintly higher entrance of the nanoparticles into the cells.

For testing the potential of S-ION to induce damage on genetic material, we used a battery of genotoxicity tests, *i.e.*, γH2AX assay, MN test, and comet assay. As response to the formation of DNA double strand break (DSB), H2AX flanking the DSB sites are rapidly phosphorylated at the serine 139 residue to become γH2AX. Reliability and specificity of the γH2AX assay as a biomarker of DNA damage have already been proved (Garcia-Canton *et al.,* 2012; Nikolova *et al.,* 2014). We used the γH2AX assay evaluated by flow cytometry since it provides an automated, fast, practical, and reproducible high-throughput platform that increases considerably the number of cells evaluated, diminishing the variability and enhancing the statistical power of the results (Sánchez-Flores *et al.,* 2015). No significant increase in the γH2AX levels was observed in SH-SY5Y cells after exposure to S-ION. No other study employing γH2AX assay for testing genotoxicity caused by any type of ION could be found in the literature; however, this cell line showed significant H2AX phosphorylation activity when treated with ZnO nanoparticles (Valdiglesias *et al.,* 2013a) but not when exposed to different types of TiO_2 nanoparticles (Valdiglesias *et al.,* 2013b).

The purpose of MN test is to identify chromosome aberrations, since MN may contain lagging chromosome fragments or whole chromosomes; therefore, it detects both clastogenic and aneugenic events. After S-ION treatment no effects were observed in the neuronal cells in terms of MN formation. To our knowledge no studies have been reported on MN induction by S-ION in any type of cells so far, but passiveness of other types of ION on MN formation have been documented in cells from different origin in *in vitro* (Li *et al.,* 2011; Zhang *et al.,* 2012; Shah *et al.,* 2013) and *in vivo* studies (Wu *et al.,* 2010; Li *et al.,* 2011; Fang *et al.,* 2012).

The comet assay is one of the most frequently used methods for genotoxicity testing. It is a sensitive, user-friendly, and rapid technique to detect primary DNA damage, including single strand breaks (SSB) and DSB, abasic and alkali-labile sites, and incomplete excision repair sites.

Due to its simplicity, versatility and ability to detect different DNA lesions, it has been claimed to be the most promising assay to measure potential genotoxicity of nanomaterials (Magdolenova *et al.,* 2014). Thus, we applied the alkaline comet assay to examine primary DNA damage induced by S-ION. But before that, we confirmed that these nanoparticles do not interfere with the assay methodology, since interference of different nanomaterials had been previously reported (Stone *et al.,* 2009; Karlsson, 2010; Magdolenova *et al.,* 2012). When treatments were carried out in serum-free medium no significant induction of DNA damage was observed. However, in complete medium S-ION induced dose- and time-dependent increase in the comet parameter, in agreement with the iron ion dissolution determination, which showed important amounts of ions released from the nanoparticles in complete medium. Although the human body contains relatively high concentrations of iron, the presence of this metal at concentrations higher than physiological can lead to deleterious effects. Iron ions are able to interact with DNA in-between the bases, thereby unwinding the double-helix (Eichhorn and Shin, 1968) and causing single strand breaks (SSB) and oxidative base modification (Toyokuni and Sagripanti, 1999). This kind of damage, especially SSB, is detected by the standard alkaline comet assay but is not related to phosphorylation of H2AX or MN production. Therefore, this may help to explain the positive results obtained in the comet assay and the negative ones from γH2AX assay and MN test. According to the current results, the type of DNA damage induced by S-ION on neuronal cells is likely not related to DSB but mostly to repairable DNA lesions (alkali labile sites and SSB), indicating recent damage (Azqueta and Collins, 2013). Similar increases in comet assay parameters (tail length and tail DNA intensity) were reported by Malvindi *et al.,* (2014) in A549 and HeLa cells treated with S-ION, by Hong *et al.,* (2011) in murine L-929 fibroblast cells exposed to ION coated with (3-aminopropyl) trimethoxysilane (APTMS), tetraethyl-orthosilicate (TEOS)-APTMS, or citrate, and by Bhattacharya *et al.,* (2009) in human lung IMR-90 fibroblasts and bronchial epithelial BEAS-2B cells treated with bare hematite. Moreover, no induction of chromosome aberrations (which require DSB production) was observed in human T lymphocytes treated with PAA-coated and non-coated ION (Couto *et al.,* 2015), what further supports our results.

Possible effects of S-ION on DNA repair processes were tested by DNA repair competence assay using H_2O_2 as challenging agent. H_2O_2 causes damage to DNA by generating hydroxyl-free radicals (OH·) (Jaruga and Dizdaroglu, 1996). These radicals attack DNA at the sugar residue of the DNA backbone, leading to SSB (Benhusein *et al.,* 2010). Rejoining of SSB induced by H_2O_2 is a simple cellular process; thousands of breaks per cell can be repaired in a matter of half an hour in typical cultured mammalian cells (Azqueta and Collins, 2013). In the current study, repair of approximately one-third of the DNA damage observed after H_2O_2 treatment was obtained during a 30min period, both in serum-free and in complete media. Incubations with the

nanoparticles were carried out at three different stages of the assay: before inducing DNA damage (pre-treatment or phase A, for 3 or 24h), during DNA damage induction (phase B), or during the repair period (phase C). Results obtained were different depending on the presence of serum in the medium. In serum-free medium no significant decrease in the DNA damage during the repair phase was observed when S-ION incubation was carried out before DNA damage induction, or during the repair phase. Since incubation only with S-ION for 30min caused a significant increase in the comet parameter, maybe the negative repair result obtained for phase C is related to DNA damage induced directly by the S-ION instead of (or in addition) to actual disturbance on the repair machinery. When treatment with H_2O_2 and the nanoparticles was performed simultaneously the repair process occurred normally; a possible explaining reason is the short time for this incubation (only 5 min), insufficient to cause any alteration in the repair systems.

The results observed in complete medium suggested scarce effects on DNA repair, since significant decreases in the DNA damage were observed after the repair period at all conditions tested, excepting for phase B. As indicated before, a notable release of iron ions from the S-ION took place in complete medium. The deleterious effects of transition metal ions, such as iron, to DNA are greatly enhanced by the presence of oxygen and related species; thus, iron ions readily associate with DNA and, in the presence of hydrogen peroxide, a high ratio of DSB to SSB are generated (Lloyd and Phillips, 1999). Since the repair of DSB can take hours (Frankenberg-Schwager, 1989), the result obtained for phase B in complete medium is probably related to the type of DNA damage induced, for which a 30min repair period is not long enough, more than to alterations in the repair process. To the best of our knowledge, this is the first study addressing the potential effects of ION on cellular repair systems. Therefore, further investigations are required to go into detail about all these findings.

In conclusion, despite being effectively internalized by the neuronal cells, S-ION presented general low cytotoxicity; positive results were only obtained in some assays at the highest concentrations and/or longest exposure time tested. Genotoxicity evaluations in serum-free medium were negative for all conditions assayed; in complete medium dose and time-dependent increase in DNA damage, not related to the production of DSB or chromosome loss (according to the results of γH2AX assay and MN test), was obtained. Differences in the three genotoxicity assays applied, regarding their sensitivity to detect different types of genetic damage, confirm the need for using them in combination, since they complement one another.

Medium composition (presence or absence of serum) influenced the behaviour of S-ION, although not in a great extent. Uptake of the nanoparticles by the cells, cytotoxicity, and effects on DNA repair were more pronounced in the absence of serum. On the contrary, iron ion release and primary DNA damage were only observed in complete medium. Formation of a protein

corona in the presence of serum has probably an important role in these differences. Further studies are needed to determine the protein corona formation and to elucidate the possible role of redox imbalance in the generation of harmful effects, particularly those related to DNA damage.

2. SH-SY5Y CELLS EXPOSED TO O-ION

In the study of exposure of neuronal cells to O-ION, prior to evaluating toxicity, internalization of these nanoparticles into SH-SY5Y cells was analysed by flow cytometry. Results obtained show that SH-SY5Y cells are able to efficiently internalize these nanoparticles at all experimental conditions tested, regardless the medium composition. Accordingly, in the previous section of this work, cultured SH-SY5Y cells were also reported to efficiently uptake silica-coated ION at the same dose and time conditions.

The lack of a significant LDH release from neuroblastoma cells after O-ION treatment suggests that these nanoparticles do not generally disturb the cellular membrane integrity at low and medium concentrations, as previously shown in rat astrocytes treated with 10µg/ml of Fe_3O_4 or γ-Fe_2O_3 for 6h (Au *et al.,* 2007), or in oligodendroglial OLN-93 cells exposed to 1mM dimercaptosuccinate-coated ION for 4h (Petters *et al.,* 2014a). These results support other studies reporting membrane damage in A549 cells exposed to magnetite only at high concentration (100µg/ml) for 24h (Watanabe *et al.,* 2013), or human peripheral lymphocytes treated with maghemite (50-100µg/ml) for 24h (Rajiv *et al.,* 2015).

Cell cycle machinery is managed by a highly ordered set of events that lead to the proper division and duplication of the cell (Crosby, 2007). Results from the flow cytometry analysis of the relative DNA content of neuronal cells exposed to O-ION showed that the normal progression of SH-SY5Y cell cycle was impaired after nanoparticle exposure, and this was particularly notable after 24h treatment in serum-free medium. Cell cycle arrest was mainly observed as a significant dose-dependent increase in G_0/G_1 phase together with a clear decrease in G_2/M region, indicating a possible mitotic arrest. These results agree with the induction of mitotic arrest in S and G_2/M phases observed after 24h treatment of SH-SY5Y cells with 200µg/ml S-ION, recently discussed in this Thesis. Similar effects of ION on cell cycle of other different neuronal cells were also reported (Mahmoudi *et al.,* 2009a, 2012; Wu *et al.,* 2013a).

Results from analysis of cell death showed significant increases in the rates of early apoptosis (evaluated by annexin V/PI staining) and late apoptosis (determined as subG_1 phase of cell cycle analysis) in both complete and serum-free media. Previously reported data on apoptosis induction by ION confirm our results. Imam *et al.,* (2015) found increases in apoptosis rate in SH-SY5Y cells after exposure to 2.5-40µg/ml of 10nm, but not 30nm, uncoated ION for 24h. Wu *et al.,* (2013b) demonstrated that high doses of bare magnetite nanoparticles (>50µg/ml) increased

phosphorylation of P53 (protein involved in the G_2/M DNA damage checkpoint) and promoted apoptosis in PC12 cells after 24h of exposure.

The potential of O-ION to induce necrosis, passive and energy-independent mode of death, was also evaluated in this study. Unlike the results obtained in the Wu *et al.,* (2013b) study, in which necrosis induction was described after PC12 cells treatment with bare ION (>50 μg/ml) for 24h, O-ION did not produce necrosis in the SH-SY5Y cells at any of the conditions evaluated. Similarly, as previously described, the same cell line did not show increase in the necrosis rates after being exposed to S-ION (10 to 200μg/ml) for 3 or 24h. Taking together, results obtained in the present study from apoptosis and necrosis analyses, suggest that O-ION seem to induce cell death mainly via the apoptotic pathway.

Besides, in order to evaluate the potential genotoxic effects of O-ION three different methodological approaches were carried out, *i.e.* comet assay, γH2AX assay and MN test. Since several previous works reported interference of different nanoparticles with comet assay methodology (Stone *et al.,* 2009; Karlsson, 2010; Magdolenova *et al.,* 2012), a comprehensive test for detecting potential ION interferences with the alkaline comet assay protocol was carried out prior to DNA damage evaluation. A significant additional DNA damage at 200μg/ml O-ION concentration in serum-free conditions was found, indicating residual nanoparticle interference limited to these specific conditions. This may be due to the high tendency to aggregation of O-ION dispersed in serum-free medium (Costa *et al.,* 2016), particularly exacerbated at elevated concentrations. Results from standard alkaline comet assay showed that O-ION induced primary DNA damage in the exposed cells. Similarly, Magdolenova *et al.,* (2013) found significant genotoxic effects (by comet assay) in human TK6 cells and lymphocytes treated with oleate-coated magnetite (lowest observed adverse effect level at 0.5h treatment: 144μg/ml and 56.4μg/ml, respectively, and at 24h treatment: 2.9μg/ml and 1.13μg/ml, respectively), and Kenzaoui *et al.,* (2012b) reported DNA damage induction in human brain-derived endothelial cells treated with uncoated ION and O-ION (0.4-235μg/ml) for 24 and 48h. Results from all these studies indicate a different sensitivity to O-ION exposure depending on cell type and experimental conditions.

In the present work, treatment with O-ION did not induce H2AX phosphorylation at any condition tested. The same negative results were found in this Thesis in SH-SY5Y cells treated with S-ION under the same experimental conditions. Given its novelty, application of γH2AX assay in nanogenotoxicity evaluation is still extremely unusual. However, according to the present results, Harris *et al.,* (2015) reported no DSB detection (phosphorylated H2AX) in Balb/3T3 cells treated with uncoated and O-ION. Hence, considering together the results obtained from γH2AX analysis and comet assay, it seems that primary DNA damage detected in the comet assay was

likely due to other kind of genetic damage (*i.e.* SSB, alkali-labile sites, abasic sites), which involves consequences much less relevant for the cell.

In order to identify possible chromosome alterations in SH-SY5Y cells due to exposure to O-ION, MN test was carried out. MN analysis may reveal both clastogenic and aneugenic events (Fenech, 2008). In our study, significant increases in MN frequencies were only detected in SH-SY5Y cells after 24h of exposure to O-ION highest doses in serum-free medium, suggesting that primary DNA damage detected in the comet assay was only fixed as chromosome alterations at these high O-ION concentrations and long exposure time in the absence of serum. Nevertheless, cytotoxicity observed at these same conditions, namely high apoptosis rates and cell cycle arrest at S phase, may have also influenced MN test results by generating artefacts, for instance due to the nuclear fragmentation into smaller nuclear bodies occurring during apoptosis cell death, which can be considered as MN in the flow cytometry analysis. Significant induction of MN had been already observed in other human cell types (Könczöl *et al.,* 2011; Singh *et al.,* 2012; Rajiv *et al.,* 2015).

DNA repair systems are recognized as one of the most important cellular defence mechanisms responsible for DNA integrity. In order to evaluate whether O-ION exposure has some impact on the DNA repair capacity of SH-SY5Y cells, which would lead to increased DNA damage in response to other internal or external insults, DNA repair competence assay was carried out with O-ION treatment in different phases. Results obtained showed a similar effect of O-ION on the cell repair ability regardless of media composition, although slightly higher in serum-free medium. In particular, alterations in repair ability were observed when cells where treated before or during the challenge with H_2O_2. Still, the presence of nanoparticles during the repair period did not cause any alteration in the repair capacity at any condition tested, even though exposure to O-ION for the duration of the repair period (30 min) induced a significant increase in DNA damage. To our knowledge, the only study available in the literature addressing the potential effects of ION on cellular repair mechanisms reported that silica-coated magnetite nanoparticles significantly altered the repair ability of SH-SY5Y cells, being the effect more pronounced in the absence of serum proteins.

Results of quantification of iron ion release from the O-ION surface was markedly dependent on the medium composition. Suspensions of O-ION in complete medium displayed an increased ion release in a concentration-dependent manner, while O-ION suspended in serum-free medium were very stable at all conditions tested. Similar differences were previously found by other authors (Geppert *et al.,* 2012; Malvindi *et al.,* 2014; Hanot *et al.,* 2015). Iron ions released into the cytosol, directly from the nanoparticle surface or due to lysosomal enzymatic degradation, can participate in the Fenton reaction producing reactive oxygen species (ROS) (Valko *et al.,*

2007; Klein *et al.,* 2012), resulting in oxidative stress which would eventually lead to disruption of iron homeostasis, antioxidant defence system depletion, cytotoxic effects and DNA damage (Soenen and De Cuyper, 2009, 2010; Singh *et al.,* 2010; Malvindi *et al.,* 2014). Since the lower iron ion levels released in the absence of serum are not associated with the higher O-ION induced cytotoxicity observed in serum-free medium, further investigation is needed, *e.g.* exploring oxidative stress related pathways, to figure out the mechanism behind cytotoxicity produced by these nanoparticles.

The decrease in iron ions with incubation time in complete medium may be explained by the presence of transferrin, a major constituent of FBS (Young and Garner, 1990). This protein may bind iron ions released from the nanoparticles, with the quantity of iron bound increasing with time. If transferrin takes part in the protein corona, iron bound to this protein will not be detected in the analysis of iron ions in the supernatant medium.

When comparing complete and serum-free media results showed that, in general, the presence of serum had a slight influence on the O-ION induced genotoxicity and effects on repair capacity. As for cytotoxicity, data obtained suggested that serum proteins interact with oleic acid coating slightly preventing cytotoxicity production, *i.e.* membrane impairment, cell cycle alterations and cell death induction. These results are in line with our previous findings describing higher decreases in SH-SY5Y viability induced by O-ION in serum-free medium (Costa *et al.,* 2016). Also supporting our results, previous works reported a possible protective effect of the protein corona on ION toxicity (Nel *et al.,* 2009; Mahmoudi *et al.,* 2011a; Mahmoudi *et al.,* 2012).

In conclusion, results obtained showed that O-ION exhibit a moderate cytotoxicity related to cell membrane impairment, cell cycle disruption and cell death induction, especially marked in serum-free medium. On the contrary, iron ion release was only observed in complete medium, indicating that cytotoxicity observed was not related to the presence of iron ions in the medium. However, O-ION genotoxic effects were limited to the induction of primary DNA damage, not related to DSB and easily repairable, and this damage did not become fixed in cells in most conditions.

3. A172 CELLS EXPOSED TO S-ION

Before testing the possible harmful effects of S-ION on A172 cells, the actual entry of nanoparticles into astrocytes was verified. Results obtained from TEM revealed the presence of S-ION internalized in A172 astrocytes in all the conditions tested, regardless medium composition or exposure time, demonstrating that these cells may efficiently uptake these nanoparticles. Moreover, S-ION were found to be accumulated in intracellular vesicles, suggesting that endocytic processes are involved in S-ION uptake into astrocytes. Similarly,

cultured astrocytes were reported to efficiently accumulate ION with different types of coatings in a time-, concentration- and temperature-dependent manner (Hohnholt *et al.,* 2013).

S-ION did not impair plasmatic membrane integrity at the conditions tested in this study, as demonstrated by the negative results revealed in the assessment of LDH release. As already mentioned, no significant LDH leakage was either observed in SH-SY5Y neuronal cells treated with the same S-ION. Previous studies in other cell lines reported membrane damage only at high ION (magnetite) concentration (100µg/ml) (Watanabe *et al.,* 2013) or long exposure time (maghemite, 24h) (Rajiv *et al.,* 2015). As none of these conditions led to membrane impairment in the current study, results obtained suggest that silica coating prevents membrane damage, and/or that astrocytes are less sensitive to this effect.

The cell cycle machinery is managed by a highly ordered set of events that lead to the division and duplication of the cell (Crosby, 2007). In the presence of DNA damage or cellular stress, cell cycle checkpoint protein P53 triggers cell cycle arrest to provide time for the damage to be repaired or for self-mediated apoptosis (Alarifi *et al.,* 2013). Results obtained from the cell cycle analysis showed important dose-dependent cell cycle alterations induced by S-ION, particularly marked in the 24h treatments, in which cell cycle of A172 cells resulted altered in all conditions tested, regardless the dose or the medium composition. Still, these effects, included mainly alterations in G_0/G_1 and S phases reflecting a possible mitotic arrest, and were more pronounced in serum-free medium. These results support the previous work of Mahmoudi *et al.,* (2012) who also observed similar cell cycle effects in BE(2)-C neurons and A172 astrocytes treated with S-ION (2-32mM) for 24h. Similarly, uncoated magnetite nanoparticles induced a concentration-dependent accumulation of cells in G_2/M phase and of p53 gene expression in neuronal PC12 cells treated for 24h (100 and 200µg/ml) (Wu and Sun, 2011). And Mahmoudi *et al.,* (2009a) observed that uncoated and polyvinyl alcohol-coated ION caused cell cycle arrest in G_0/G_1 phase at 200-400mM in mouse fibroblast cell line (L929), possibly due to the irreversible DNA damage and repair of oxidative DNA lesions.

Evaluation of apoptosis induced by S-ION exposure was carried out by two approaches; on one hand the analysis of the $subG_1$ region of the cell cycle as an indicator of DNA fragmentation at the late stages of apoptosis, and on the other hand, by annexin V/PI staining flow cytometric analysis, as a sensitive measure of apoptosis early stages. Results obtained by both methodologies resulted quite similar, with apoptosis induction limited to the highest S-ION doses and longest exposure time in complete medium, but important dose-dependent increases of apoptosis rates observed at both exposure times in serum-free medium. In agreement with our results, Mahmoudi *et al.,* (2012) also observed increases in the apoptotic rate ($subG_1$ stage of cell cycle) in BE(2)-C neurons and A172 astrocytes exposed to S-ION for 24h, and Jeng and Swanson

(2006) reported a time-dependent increase of apoptotic Neuro-2A cells after 48h treatment with carboxyethylsilanetriol-coated ION (50µg/ml). In general, ION-induced apoptosis was previously described not only in nervous system cells but also in other different cell types, including human A549 lung cells (Watanabe *et al.*,, 2013), human Jurkat T lymphocytes (Namvar *et al.,* 2014), or rat lung epithelial cells (Ramesh *et al.,* 2012).

Evaluation of cell death by annexin V/PI allowed also to quantify the rate of cells undergoing necrosis together with late apoptosis. In complete medium, S-ION only induced necrosis at the highest doses and longest exposure time; whereas in serum-free medium significant dose-dependent increases were obtained only in the 3h treatment. Since results from annexin V/PI analysis and subG$_1$ region are similar, and considering that percentage of annexin V binding +/PI– cells includes not only necrotic but also late apoptotic cells, S-ION seem to induce cell death mainly via the apoptotic pathway. Accordingly, apoptosis but not necrosis induction was observed in this Thesis in SH-SY5Y neurons exposed to the same S-ION (100 and 200µg/ml) for 24h.

The potential genotoxic effects of S-ION were evaluated by means of three different genotoxicity approaches, namely γH2AX assay, comet assay and MN test. Moreover, DNA repair competence assay was applied to assess possible alterations in the astrocyte DNA repair capacity in the presence of S-ION.

As already mentioned, and given its novelty, application of γH2AX assay to ION genotoxicity studies is extremely scarce. According to the results previously described for SH-SY5Y cells, S-ION did not induce DSB, either in complete or in serum-free medium. In the present work S-ION did not induce H2AX phosphorylation in A172 astrocytes either, except at the highest concentrations after 24 h treatment. Considering the results obtained in the iron ion release from the nanoparticles, the increase detected seems to be more likely due to the indirect effect of iron ions, than to the genotoxic S-ION properties themselves. Presence of iron ions would lead to an imbalance in the Fenton reaction and, consequently, to an increase in oxidative damage, eventually causing breaks in the DNA strands (Luther *et al.,* 2013).

Comet assay was carried out in order to evaluate the possible induction of primary genetic damage by S-ION exposure. As several reports previously described the interference of different nanoparticles with the comet assay methodology (Stone *et al.,* 2009; Karlsson, 2010; Magdolenova *et al.,* 2012), the possible interference by S-ION at the highest concentration to be tested was discarded prior to performing the analysis. Subsequently, results from comet assay showed that S-ION induced DNA primary damage in astrocytes only at the highest concentrations after a short exposure period, but from 25µg/ml on, in a dose-dependent manner, after 24h treatment. This concentration-dependent increased DNA damage was previously observed in

A549 and Hela cells treated with both S-ION (Malvindi *et al.,* 2014) or ION with other different coatings (Bhattacharya *et al.,* 2009; Han *et al.,* 2011; Seo *et al.,* 2017). However, since the results obtained from γH2AX analysis in this study were mainly negative, this primary DNA damage observed in comet assay seems not be related to DSB but to other kind of DNA damage (*e.g.* SSB, abasic sites, alkali-labile sites) more easily repairable.

Micronucleus test was performed to identify possible chromosome alterations induced by exposure to S-ION, coming from clastogenic or aneugenic events. No induction of MN was found in astrocytes exposed to S-ION at any condition tested, indicating on the one hand that S-ION did not induce aneugenic effects on astrocytes. On the other hand, it seems that these cells were able to repair the primary DNA damage initially produced by S-ION exposure, revealed by positive response of comet assay, thus avoiding its fixation as chromosome alterations. A lack of MN production after nanoparticle exposure was obtained in several studies employing different cell lines and ION, as human lymphoblastoid cells treated with uncoated maghemite or with uncoated and dextran-coated magnetite (Singh *et al.,* 2012), Syrian hamster embryo cells treated with naked maghemite and magnetite nanoparticles (Guichard *et al.,* 2012), Chinese hamster lung cells exposed to glutamic acid-coated (Zhang *et al.,* 2012) and to poly ethylene imine- or poly ethylene glycol-coated ION (Liu *et al.,* 2014).

In order to evaluate whether S-ION exposure has some impact on the DNA repair ability of astrocytes, which would lead to increased DNA damage in response to internal or external insults, DNA repair competence assay was carried out with S-ION treatment in different phases. Results obtained showed that S-ION did not interfere with the repair capacity of A172 astrocytes, at any condition tested, since significant decreases in H_2O_2-induced DNA damage, indicative of efficient repair, were observed in the presence of S-ION. These decreases were consistently obtained regardless the moment the incubation with nanoparticles was conducted (before, during or after treatment with the challenging agent H_2O_2) and were also similar to the decrease detected in the absence of S-ION. Studies addressing the potential effects of ION on cellular repair mechanisms are practically inexistent. In this Thesis S-ION effects on SH-SY5Y cells repair ability was described by employing the same approach. In that case, S-ION exposure did alter the repair of H_2O_2-induced DNA damage in these cells, with considerably more pronounced effects when serum-free medium was employed. This dissimilar response to S-ION exposure of the two types of nervous system cells indicates, as previously reported, that glioma cells have a more efficient repair capability of induced DNA damage than neurons (Laffon *et al.,* 2017).

All genotoxicity results together indicate that S-ION present a low genotoxic activity, limited to easily repairable DNA damage as demonstrated by the positive results obtained in comet assay together with the negative results from γH2AX and MN assays. In any case, the DNA

damage induced by S-ION seems to be repaired, since the repair capacity resulted not altered, and, consequently, it was not fixed in the cells as proved by the lack of MN production. Besides, all these effects were not dependent on the presence/absence of serum in the medium.

Nevertheless, the quantity of iron ions released from the S-ION depended markedly on the medium composition. While S-ION suspended in serum-free medium were very stable at all conditions tested, suspensions of nanoparticles in complete medium showed a concentration-dependent increase in ion release, particularly noticeable at the longest exposure time. This iron excess may lead to an imbalance in its homeostasis and cause elevated ROS generation through the Fenton reaction, resulting in oxidative stress which would lead to cytotoxic effects and DNA-damage (Soenen and De Cuyper, 2009, 2010; Singh *et al.,* 2010; Malvindi *et al.,* 2014). Therefore, the iron ion release could help to explain the cytotoxic effects induced by S-ION when complete medium was employed. Since no ion release but cytotoxicity was observed in serum-free medium experiments, other different action mechanisms, for instance those linked to oxidative damage production, should be investigated. Differences in ion release found in our study depending on the medium composition were previously described (Geppert *et al.,* 2012; Malvindi *et al.,* 2014; Hanot *et al.,* 2015). In fact, protein presence has been associated with an increase in dissolution rates of ION through both aqueous complexation and ligand-enhanced dissolution (Nel *et al.,* 2009). Hence, it is possible that the serum proteins favour the silica coating degradation, thus causing a higher iron release from the nanoparticle core. Nevertheless, different issues such as cell type, intracellular medium pH or composition, nanoparticle composition or physical-chemical characteristics such as size, coating or aggregation capacity have been previously suggested to be other main factors influencing the iron release from ION (Geppert *et al.,* 2009, 2011; Singh *et al.,* 2012; Rosenberg *et al.,* 2012; Paolini *et al.,* 2016).

Generally speaking, current results showed that the absence of serum in the medium had some influence on cytotoxicity of S-ION, resulting in more pronounced cellular effects (cell cycle, apoptosis and necrosis). These findings are in accordance with our previous observations of higher decreases in viability induced by S-ION in both A172 and SH-SY5Y cells in serum-free medium (Costa *et al.,* 2016) and support a possible protective effect of the protein corona on the cytotoxicity induced by nanoparticles previously suggested by other authors (Nel *et al.,* 2009; Mahmoudi *et al.,* 2011a, 2012). Nevertheless, in general no notable differences in genotoxicity induction or DNA repair alterations were found between complete and serum-free medium.

In conclusion, in the present study genotoxicity and cytotoxicity associated with S-ION exposure were evaluated in glial cells by a battery of assays. Results obtained showed that S-ION exhibit certain cytotoxicity, especially in serum-free medium, related to cell cycle disruption and cell death induction. However, S-ION presented scarce genotoxic effects, not dependent on

medium composition and easily repairable. Moreover, the primary DNA damage was only related to DSB at the highest concentrations and longest time tested, probably associated with the increase in iron release in complete medium. Negative results in MN test indicate (i) no aneugenic effects and (ii) that the previously mentioned DNA strand breaks were not fixed upon cell division. No effects on the DNA repair systems were observed.

4. A172 CELLS EXPOSED TO O-ION

Before addressing the toxicological profile of O-ION, the uptake of nanoparticles by the cells was determined. Results of TEM demonstrated the presence of O-ION inside A172 cells at all conditions tested, regardless medium composition or exposure time. According with our results, significant ION uptake was previously reported in rat primary astrocytes (Geppert *et al.,* 2009, 2011, Hohnholt *et al.,* 2010b, 2013; Hohnholt and Dringen, 2013), and in human (Kiliç *et al.,* 2015; Fernández-Bertólez *et al.,* 2018a) and rat (Marcus *et al.,* 2016) neurons under different experimental conditions.

LDH release analysis indicated that exposure to O-ION do not compromise the membrane integrity of A172 cells. In line with these results, previous studies reported either no effect on rat primary astrocytes (Au *et al.,* 2007) and oligodendroglial OLN-93 cells (Petters *et al.,* 2014a) exposed to different ION, or slight membrane damage, commonly limited at high concentrations or long exposure times, in cell types not derived from CNS (Watanabe *et al.,* 2013; Rajiv *et al.,* 2015).

Results obtained in the analysis of cell-cycle distribution show significant dose-dependent arrest of the cell cycle in the S-phase at all conditions tested, indicating that O-ION clearly alter the normal cell cycle progression of these cells. Similarly, studies in other nerve cell types showed a dose-dependent S-phase arrest in human BE(2)-C (Mahmoudi *et al.,* 2012) and SH-SY5Y neuronal cells exposed silica-coated ION (Kiliç *et al.,* 2015), and in PC12 rat cells after treatment with uncoated ION (Wu *et al.,* 2013b). Cell cycle arrest induced by these nanoparticles is probably caused by alterations in the expression of regulatory genes involved in cell cycle, cell death, oxidative stress pathways, and/or DNA-damage repair (Periasamy *et al.,* 2014). Further research in this direction is required to confirm this hypothesis.

Together with significant modifications in the cell cycle progression, the proportion of A172 astrocytes in the sub-G_1 region, indicative of late apoptosis, also increased in a dose- and time-dependent manner, in both complete and serum-free media. Accordingly, results from analysis of annexin V/PI staining showed significant increases in the rates of early apoptosis after O-ION exposure as well. Previously reported data on apoptosis induction by ION confirm our results. Periasamy *et al.,* (2014) observed increased levels of early apoptosis in human

mesenchymal stem cells treated with uncoated magnetite, and Naqvi *et al.,* (2010) in murine macrophage (J774) cells exposed to Tween 80-coated ION. Besides, several studies conducted in neuronal cells also support our findings. In particular, high doses of bare magnetite nanoparticles were found to promote P53 phosphorylation and apoptosis in PC12 cells (Wu *et al.,* 2013b); exposure to uncoated ION increased apoptosis rate in SH-SY5Y cells (Imam *et al.,* 2015); Mahmoudi *et al.,* (2012) also observed raises in late apoptotic cells (subG$_1$ stage of cell cycle) in BE(2)-C neurons treated with silica-coated ION; and Jeng and Swanson (2006) reported a time-dependent increase of apoptotic Neuro-2A cells after exposure to carboxyethylsilanetriol-coated ION. Furthermore, O-ION produced a slight but significant increase in necrosis rates when treatments were performed in complete medium, but not in serum-free medium. Previous results obtained by Wu *et al.,* (2013b) exhibited induction of necrosis in PC12 cells by bare ION. Taking together all results regarding cell death assessment obtained from the present and previous studies, they suggest that ION are able to induce cell death, mainly via the apoptotic pathway.

In order to address the potential effects of O-ION on the genetic material of A172 cells, three different genotoxicity approaches were carried out, namely comet assay, γH2AX assay and MN test. A comprehensive test for detecting interferences of O-ION with the comet assay methodology was carried out prior to performing the analysis. After ruling out possible interferences, results from comet assay showed that nanoparticle treatment induced primary DNA damage in astrocytes in a dose-dependent manner, particularly in the presence of serum in the medium. Employing the same technique, Kenzaoui *et al.,* (2012b) also reported positive results in human brain-derived endothelial cells exposed to uncoated ION and O-ION, not observing differences between the two nanoparticles, and Magdolenova *et al.,* (2013) in human TK6 cells and lymphocytes treated with oleate-coated magnetite, with TK6 cells being less sensitive.

H2AX histone is quickly phosphorylated at serine 139 (γH2AX) to repair double strand breaks (DSB) produced by genetic insults or replication errors. Thus, quantification of γH2AX is widely used as a very sensitive and specific biomarker for DSB (Sánchez-Flores *et al.,* 2015). In the present study, slight significant increases in the γH2AX levels of A172 cells exposed to O-ION were detected. These results could reflect a part of the primary DNA damage observed in the comet assay (which detects not only DSB but also other types of primary DNA damage) or, most likely, be the result of the high early apoptosis rate observed after O-ION exposure, associated with the DNA fragmentation typical of this type of cell death. Indeed, Kiliç *et al.,* (2015) did not found increases in γH2AX levels, together with absence of apoptosis induction, in SH-SY5Y cells treated with silica-coated ION under the same experimental conditions. Also, no increase in DSB (γH2AX) was reported in Balb/3T3 fibroblasts treated with uncoated ION and O-ION (Harris *et al.,* 2015), in SH-SY5Y cells exposed to O-ION (Fernández-Bertólez *et al.,*

2018a), and in other non-neural cell types treated with different ION (Schütz *et al.,* 2014; Pöttler *et al.,* 2015).

The potential chromosome alterations induced by O-ION exposure in astrocytes was addressed by the MN test. The lack of MN induction observed after ION exposure was previously reported in other several studies employing different cell systems. In particular, in Syrian hamster embryo cells treated with naked maghemite and magnetite nanoparticles (Guichard *et al.,* 2012), in Chinese hamster lung cells exposed to glutamic acid-coated ION (Zhang *et al.,* 2012), in human lymphoblastoid cells treated with uncoated maghemite or with uncoated and dextran-coated magnetite (Singh *et al.,* 2012), and in human SH-SY5Y neurons exposed to silica-coated ION (Kiliç *et al.,* 2015), among others. MN are considered fixed genetic damage resulting from chromosome fragments or whole chromosomes lagged during anaphase that remain into daughter cells when the nucleus divides (Fenech, 2008). Accordingly, and considering all results obtained in this study from genotoxicity tests, O-ION exposure induced primary DNA damage, as revealed by γH2AX analysis and, particularly, comet assay, but A172 cells were able to repair this damage avoiding its fixation as chromosome alterations (MN).

DNA repair systems play a key role in cellular defence mechanisms responsible for DNA integrity. In order to evaluate whether O-ION exposure has some impact on DNA repair ability, DNA repair competence assay was performed exposing A172 cells to O-ION in three different phases. Results obtained showed that O-ION did not interfere with the DNA repair capacity at any condition tested. Studies addressing the potential effects of ION on cellular repair mechanisms are extremely scarce. Silica-coated ION effects on repair capacity of SH-SY5Y and A172 cells were previously assessed by our group by employing the same approach (Kiliç *et al.,* 2015; Fernández-Bertólez *et al.,* 2018b). In SH-SY5Y cells, the presence of nanoparticles altered the repair of H_2O_2-induced DNA damage, with considerably more pronounced effects when serum-free medium was employed (Kiliç *et al.,* 2015). However, results obtained from A172 cells were in accordance with the ones found in the present study, with no alteration in repair ability found at any condition tested (Fernández-Bertólez *et al.,* 2018b). This different response between the two types of nervous system cells are in line with the well-accepted idea that glial cells may have a more efficient repair ability in order to protect neuronal tissue from external insults (Saeed *et al.,* 2015). However, it may be also due to the less sensitivity of glial cells to this type of induced DNA damage when compared to neurons, as previously demonstrated (Laffon *et al.,* 2017).

Results of quantification of iron ions released from the O-ION surface was markedly dependent on the media composition. Suspensions of O-ION in complete medium displayed an increased ion release in a dose- and time-dependent manner, whereas O-ION suspended in serum-free medium resulted very stable. Other authors described similar differences agreeing with these

observations (Geppert *et al.,* 2012; Malvindi *et al.,* 2014; Hanot *et al.,* 2015). The higher iron release in complete medium may be related to the smaller particle size, and consequently larger surface area, since hydrodynamic size of these O-ION in complete medium was reported as 251.5 ± 4.9nm, while in serum-free medium it was 2,587.7 ± 382.2nm (Costa *et al.,* 2016). Other possible explanation may be that the interaction with the serum proteins present in the complete medium favours the oleic acid coating degradation and consequently the iron ion release. In spite of this, current cytotoxicity and genotoxicity results were quite similar in both media, suggesting that free iron ions are not responsible for the effects observed and that presence of serum proteins do not influence O-ION toxicity.

In conclusion, results obtained in the present study showed that O-ION exhibit moderate cytotoxicity, related to proliferation arrest and cell death induction (principally by apoptotic pathway), and cause genotoxic effects, mainly primary DNA damage, which is not fixed as chromosome alterations. These effects were not influenced by the presence of serum in the medium. Conversely, notable iron ion release was observed only in complete medium, indicating that cyto- and genotoxicity results were not entirely caused by iron ion homeostasis disruption. Besides, no alterations in the DNA repair processes were obtained.

5. COMPARATIVE ANALYSIS OF COATINGS AND CELL TYPES

Based on the results explained above, we can conclude that silica coating seems to be less toxic and more biocompatible than oleic acid for the nervous cell lines employed in the present study. In general, S-ION showed less cytotoxicity than O-ION. Moreover, S-ION exhibited slightly lower genotoxic effects than O-ION in both cell lines, not related to the induction of DSB and not fixed in either SH-SY5Y or A172 cells upon cell division. Previous studies stated that ION are stored in lysosomal compartment where they decompose to free iron ions (Laurent *et al.,* 2011; Laskar *et al.,* 2012). Free iron ions can affect mitochondria and/or increase free radical concentration (Fröhlich *et al.,* 2012). Given that the FCM analysis of SH-SY5Y uptake of both ION indicate similar cell internalization regardless of the coating composition, differences in cyto- and genotoxic effects may be explained by differences in the surface chemistry between O-ION and S-ION. Hence, faster transfer of internalized O-ION to the lysosomal compartment, and more intense dissolution rates of oleic acid coating at the acid lysosome pH (Malvindi *et al.,* 2014), could likely generate larger amounts of ferric iron, which may cause higher cell damage (Petters *et al.,* 2016). Indeed, the different dissolution kinetics of ION has been observed to depend on the surface coating and its physicochemical properties (Lévy *et al.,* 2010; Colombo *et al.,* 2012; Mahon *et al.,* 2012; Hanot *et al.,* 2015). Furthermore, ION with various surface modifications and different hydrodynamic size may induce slight, but possibly meaningful, changes in cell cytotoxicity and genotoxicity (Hong *et al.,* 2011; Magdolenova *et al.,* 2013). In

some conditions of this study, O-ION as micro-sized agglomerates were observed, specifically in serum-free media, probably due to the absence of interactions of oleic acid coat with serum proteins of the biological medium (protein corona), which modified their hydrodynamic size and stability. This fact could greatly influence the biological interaction with O-ION and the higher observed toxic effect regarding silica coating.

Furthermore, from the point of view of biomedical applications of ION on CNS, A172 astrocytes demonstrated to be more vulnerable than neurons to the toxic effect of S-ION and O-ION. Although cytotoxic effects have been observed in SH-SY5Y and A172 cell lines after exposure to both ION, these effects were broadly higher in astrocytes than in neurons. In addition, it was found that astrocytes and neurons exhibit primary DNA damage after ION exposure, but only in the case of A172 cells it was related to DSB, a more severe type of genetic damage. However, in both cases this damage was repaired, since it did not lead to chromosome alterations (detected by MN test). Other studies on chemical toxicity suggest that glial cells (*i.e.* astrocytes) are more sensitive than neuronal cells (Stockmann-Juvala *et al.,* 2006), as it was observed in this work. A possible bias for this comparison is the cell cycle state at the moment of treatment, since cells in diverse states of the cell cycle express different biomolecules and could have different responses to exogenous stimuli, such as xenobiotic exposures and specifically ION exposure (Bregoli *et al.,* 2013). Moreover, different features of the cell types involved in nervous system physiology may determine diverse response against toxic insults (Laffon *et al.,* 2017). Another possible explanation for this difference in sensitivity may be due to different internalization rates of ION in astrocytes and neurons, which may lead to variations in the mobilization of ION to the lysosomal compartment and, therefore, to the production of iron ions responsible for the cellular damage. However, it is not possible to contrast such a difference in the uptake of ION between the two types of cells since this parameter was analysed by different techniques (TEM and FCM).

VI. CONCLUSIONS

VI. CONCLUSIONS

From the results obtained in this study, we may draw the following conclusions:

SH-SY5Y cells treated with S-ION

1. Despite being effectively internalized by the SH-SY5Y neuronal cells, S-ION present general low cytotoxicity, only manifested at the highest concentrations and/or longest exposure time tested.

2. While S-ION do not exhibit genotoxicity in serum-free medium, they induce dose and time-dependent increase in DNA damage, not related to the production of DSB or chromosome loss, in complete medium. Exposure to S-ION influence differently the DNA repair process in complete and serum-free media, with more pronounced effects in the latter.

SH-SY5Y cells treated with O-ION

3. SH-SY5Y cells are able to take up O-ION in a dose and time-dependent manner. O-ION exhibit a restrained cytotoxicity related to cell membrane impairment, cell cycle disruption and cell death induction, especially marked in serum-free medium. Cytotoxicity is not related to the presence of iron ions in the medium.

4. O-ION genotoxic effects are limited to the induction of primary DNA damage, not related to DSB and easily repairable, and this damage do not become fixed in cells in most conditions. These nanoparticles cause alterations in DNA repair ability when cells are treated before or during the challenge with H_2O_2, regardless of the presence of serum proteins.

A172 cells treated with S-ION

5. S-ION may enter A172 glial cells, and induce a certain cytotoxicity, especially in serum-free medium, related to cell cycle disruption and cell death induction.

6. S-ION cause scarce genotoxic effects in glial cells, not dependent on medium composition and easily repairable. Primary DNA damage induced was only related to DSB at the highest concentrations and longest time tested. It is probably associated with the increase in iron release in complete medium and not fixed upon cell division. DNA repair systems are not altered by exposure to S-ION.

A172 cells treated with O-ION

7. O-ION are efficiently internalized in the A172 glial cells. They exhibit moderate cytotoxicity, related to proliferation arrest and cell death induction (principally by apoptotic pathway), and cause genotoxic effects, mainly primary DNA damage, which is not fixed as chromosome alterations. Nevertheless, they do not produce alterations in the DNA repair processes.

8. These effects are not influenced by the presence of serum in the medium and are not dependent on iron ion release from the nanoparticle surface.

Comparative analysis of coatings and cell types

9. Silica coating seems to be less toxic and more biocompatible than oleic acid for the nervous system cell lines employed in the present study.

10. A172 astrocytes demonstrated to be more sensitive than SH-SY5Y neurons to the toxic effects induced by S-ION and O-ION.

REFERENCES

REFERENCES

Agemy, L., Friedmann-Morvinski, D., Kotamraju, V.R., Roth, L., Sugahara, K.N., Girard, O.M., Mattrey, R.F., Verma, I.M., and Ruoslahti, E., 2011. Targeted nanoparticle enhanced proapoptotic peptide as potential therapy for glioblastoma. Proceedings of the National Academy of Sciences of the United States of America, 108 (42), 17450–17455.

Ahamed, M., Akhtar, M.J., Khan, M.A.M., Alhadlaq, H.A., and Alshamsan, A., 2016. Cobalt iron oxide nanoparticles induce cytotoxicity and regulate the apoptotic genes through ROS in human liver cells (HepG2). Colloids and Surfaces B: Biointerfaces, 148, 665–673.

Ahamed, M., Alhadlaq, H.A., Alam, J., Majeed Khan, M.A.A., Ali, D., and Alarafi, S., 2013. Iron Oxide Nanoparticle-induced Oxidative Stress and Genotoxicity in Human Skin Epithelial and Lung Epithelial Cell Lines. Current Pharmaceutical Design, 19 (37), 6681–6690.

Alarifi, S., Ali, D., Alkahtani, S., Verma, A., Ahamed, M., Ahmed, M., and Alhadlaq, H.A., 2013. Induction of oxidative stress, DNA damage, and apoptosis in a malignant human skin melanoma cell line after exposure to zinc oxide nanoparticles. International Journal of Nanomedicine, 8, 983–993.

Almeida, J.P.M., Chen, A.L., Foster, A., and Drezek, R., 2011. In vivo biodistribution of nanoparticles. Nanomedicine, 6 (5), 815–835.

Alwi, R., Telenkov, S., Mandelis, A., Leshuk, T., Gu, F., Oladepo, S., and Michaelian, K., 2012. Silica-coated super paramagnetic iron oxide nanoparticles (SPION) as biocompatible contrast agent in biomedical photoacoustics. Biomedical optics express, 3 (10), 2500–9.

Amstad, E., Textor, M., and Reimhult, E., 2011. Stabilization and functionalization of iron oxide nanoparticles for biomedical applications. Nanoscale, 3 (7), 2819–2843.

Andrade, A.L., Souza, D.M., Pereira, M.C., Fabris, J.D., and Domingues, R.Z., 2009. Synthesis and characterization of magnetic nanoparticles coated with silica through a sol-gel approach. Cerâmica, 55 (336), 420–424.

Arami, H., Khandhar, A., Liggitt, D., and Krishnan, K.M., 2015. In vivo delivery, pharmacokinetics, biodistribution and toxicity of iron oxide nanoparticles. Chemical Society Reviews, 44 (23), 8576–8607.

Astanina, K., Simon, Y., Cavelius, C., Petry, S., Kraegeloh, A., and Kiemer, A.K., 2014. Superparamagnetic iron oxide nanoparticles impair endothelial integrity and inhibit nitric oxide production. Acta Biomaterialia, 10 (11), 4896–4911.

Au, C., Mutkus, L., Dobson, A., Riffle, J., Lalli, J., and Aschner, M., 2007. Effects of nanoparticles on the adhesion and cell viability on astrocytes. Biological Trace Element Research, 120 (1–3), 248–256.

Au, K.-W., Liao, S.-Y., Lee, Y.-K., Lai, W.-H., Ng, K.-M., Chan, Y.-C., Yip, M.-C., Ho, C.-Y., Wu, E.X., Li, R.A., Siu, C.-W., and Tse, H.-F., 2009. Effects of iron oxide nanoparticles

on cardiac differentiation of embryonic stem cells. Biochemical and Biophysical Research Communications, 379, 898–903.

Au, W.W., Giri, A.K., and Ruchirawat, M., 2010. Challenge assay: a functional biomarker for exposure-induced DNA repair deficiency and for risk of cancer. International Journal of Hygiene and Environmental Health, 213 (1), 32–39.

Auffan, M., Achouak, W., Rose, J., Roncato, M.A., Chanéac, C., Waite, D.T., Masion, A., Woicik, J.C., Wiesner, M.R., and Bottero, J.Y., 2008. Relation between the redox state of iron-based nanoparticles and their cytotoxicity toward Escherichia coli. Environmental Science and Technology, 42 (17), 6730–6735.

Auffan, M., Decome, L., Rose, J., Orsiere, T., De Meo, M., Briois, V., Chaneac, C., Olivi, L., Berge-lefranc, J., Botta, A., Wiesner, M.R., and Bottero, J., 2006. In vitro interactions between DMSA-coated maghemite nanoparticles and human fibroblasts: a physicochemical and cyto-genotoxical study. Environmental Science & Technology, 40 (14), 4367–4373.

Augustin, E., Czubek, B., Nowicka, A.M., Kowalczyk, A., Stojek, Z., and Mazerska, Z., 2016. Improved cytotoxicity and preserved level of cell death induced in colon cancer cells by doxorubicin after its conjugation with iron-oxide magnetic nanoparticles. Toxicology in Vitro, 33, 45–53.

Avlasevich, S., Bryce, S., De Boeck, M., Elhajouji, A., Van Goethem, F., Lynch, A., Nicolette, J., Shi, J., and Dertinger, S., 2011. Flow cytometric analysis of micronuclei in mammalian cell cultures: Past, present and future. Mutagenesis, 26 (1), 147-152.

Avlasevich, S.L., Bryce, S.M., Cairns, S.E., and Dertinger, S.D., 2006. In vitro micronucleus scoring by flow cytometry: Differential staining of micronuclei versus apoptotic and necrotic chromatin enhances assay reliability. Environmental and Molecular Mutagenesis, 47 (1), 56–66.

Azqueta, A. and Collins, A.R., 2013. The essential comet assay: a comprehensive guide to measuring DNA damage and repair. Archives of Toxicology, 87 (6), 949–968.

Azqueta, A., Slyskova, J., Langie, S.A.S., O'Neill Gaivão, I., and Collins, A., 2014. Comet assay to measure DNA repair: approach and applications. Frontiers in genetics, 5 (August), 288.

Baber, O., Jang, M., Barber, D., and Powers, K., 2011. Amorphous silica coatings on magnetic nanoparticles enhance stability and reduce toxicity to in vitro BEAS-2B cells. Inhalation Toxicology, 23 (9), 532–543.

Barker, R.A. and Cicchetti, F., 2014. Neurodegenerative disorders: the glia way forward. Frontiers in Pharmacology, 5 JUL, 157.

Basinas, I., Jiménez, A.S., Galea, K.S., Tongeren, M. van, and Hurley, F., 2018. A Systematic Review of the Routes and Forms of Exposure to Engineered Nanomaterials. Annals of Work Exposures and Health, 62 (6), 639–662.

Behzadi, S., Serpooshan, V., Sakhtianchi, R., Müller, B., Landfester, K., Crespy, D., and Mahmoudi, M., 2014. Protein corona change the drug release profile of nanocarriers: the 'overlooked' factor at the nanobio interface. Colloids and Surfaces B: Biointerfaces, 123, 143–149.

Benhusein, G.M., Mutch, E., Aburawi, S., and Williams, F.M., 2010. Genotoxic effect induced by hydrogen peroxide in human hepatoma cells using comet assay. Libyan Journal of Medicine, 5 (1), 1–6.

Berry, C.C., Wells, S., Charles, S., Aitchison, G., and Curtis, A.S.G., 2004. Cell response to dextran-derivatised iron oxide nanoparticles post internalisation. Biomaterials, 25 (23), 5405–5413.

Bertrand, N. and Leroux, J.-C., 2012. The journey of a drug-carrier in the body: An anatomo-physiological perspective. Journal of controlled release: official journal of the Controlled Release Society, 161 (2), 152–63.

Bhattacharya, D., Das, M., Mishra, D., Banerjee, I., Sahu, S.K., Maiti, T.K., and Pramanik, P., 2011. Folate receptor targeted, carboxymethyl chitosan functionalized iron oxide nanoparticles: a novel ultradispersed nanoconjugates for bimodal imaging. Nanoscale, 3 (4), 1653–1662.

Bhattacharya, K., Davoren, M., Boertz, J., Schins, R.P., Hoffmann, E., and Dopp, E., 2009. Titanium dioxide nanoparticles induce oxidative stress and DNA-adduct formation but not DNA-breakage in human lung cells. Particle and fibre toxicology, 6 (6), 17.

Bigini, P., Diana, V., Barbera, S., Fumagalli, E., Micotti, E., Sitia, L., Paladini, A., Bisighini, C., de Grada, L., Coloca, L., Colombo, L., Manca, P., Bossolasco, P., Malvestiti, F., Fiordaliso, F., Forloni, G., Morbidelli, M., Salmona, M., Giardino, D., Mennini, T., Moscatelli, D., Silani, V., and Cova, L., 2012. Longitudinal tracking of human fetal cells labeled with super paramagnetic iron oxide nanoparticles in the brain of mice with motor neuron disease. PLoS ONE, 7 (2), e32326.

Bjørnerud, A. and Johansson, L., 2004. The utility of superparamagnetic contrast agents in MRI: Theoretical consideration and applications in the cardiovascular system. NMR in Biomedicine, 17 (7), 465-477.

Blanco-Andujar, C., Walter, A., Cotin, G., Bordeianu, C., Mertz, D., Felder-Flesch, D., and Begin-Colin, S., 2016. Design of iron oxide-based nanoparticles for MRI and magnetic hyperthermia. Nanomedicine, 11 (14), 1889–1910.

Bobo, D., Robinson, K.J., Islam, J., Thurecht, K.J., and Corrie, S.R., 2016. Nanoparticle-based medicines: a review of FDA-approved materials and clinical trials to date. Pharmaceutical Research, 33 (10), 2373-2387.

De Bock, M., Decrock, E., Wang, N., Bol, M., Vinken, M., Bultynck, G., and Leybaert, L., 2014. The dual face of connexin-based astroglial Ca2+ communication: a key player in brain physiology and a prime target in pathology. Biochimica et Biophysica Acta - Molecular Cell Research, 1843 (10), 2211–2232.

Borm, P.J.A., Robbins, D., Haubold, S., Kuhlbusch, T., Fissan, H., Donaldson, K., Schins, R., Stone, V., Kreyling, W., Lademann, J., Krutmann, J., Warheit, D., and Oberdorster, E., 2006. The potential risks of nanomaterials: a review carried out for ECETOC. Particle and fibre toxicology, 3 (1), 11.

Botta, A. and Benameur, L., 2011. Nanoparticle toxicity mechanisms: genotoxicity. In: P. Houdy, M. Lahmani, and F. Marano, eds. Nanoethics and Nanotoxicology. Springer Berlin Heidelberg, 111–146.

Bourrinet, P., Bengele, H.H., Bonnemain, B., Dencausse, A., Idee, J.M., Jacobs, P.M., and Lewis, J.M., 2006. Preclinical safety and pharmacokinetic profile of ferumoxtran-10, an ultrasmall superparamagnetic iron oxide magnetic resonance contrast agent. Investigative Radiology, 41 (3), 313–324.

Bourton, E.C., Plowman, P.N., Zahir, S.A., Senguloglu, G.U., Serrai, H., Bottley, G., and Parris, C.N., 2012. Multispectral imaging flow cytometry reveals distinct frequencies of γ-H2AX foci induction in DNA double strand break repair defective human cell lines. Cytometry Part A: the journal of the International Society for Analytical Cytology, 81 (2), 130-137.

Bowman, L., Castranova, V., and Ding, M., 2012. Single cell gel electrophoresis assay (Comet assay) for evaluating nanoparticles-induced DNA damage in cells. In: Nanoparticles in Biology and Medicine. Totowa, NJ: Humana Press, 415–422.

Braeuer, A.U., Neubert, J., Wagner, S., Kiwit, J., and Glumm, J., 2015. New findings about iron oxide nanoparticles and their different effects on murine primary brain cells. International Journal of Nanomedicine, 10, 2033.

Bregoli, L., Benetti, F., Venturini, M., and Sabbioni, E., 2013. ECSIN's methodological approach for hazard evaluation of engineered nanomaterials. Journal of Physics: Conference Series, 429 (1), 012017.

Bryce, S.M., Bemis, J.C., Avlasevich, S.L., and Dertinger, S.D., 2007. In vitro micronucleus assay scored by flow cytometry provides a comprehensive evaluation of cytogenetic damage and cytotoxicity. Mutation Research - Genetic Toxicology and Environmental Mutagenesis, 630 (1–2), 78–91.

Burkhart, A., Azizi, M., Thomsen, M.S., Thomsen, L.B., and Moos, T., 2014. Accessing targeted nanoparticles to the brain: the vascular route. Current medicinal chemistry, 21 (36), 4092–4099.

Buyukhatipoglu, K. and Clyne, A.M., 2011. Superparamagnetic iron oxide nanoparticles change endothelial cell morphology and mechanics via reactive oxygen species formation. Journal of Biomedical Materials Research - Part A, 96 (1), 186-195.

Buzea, C., Pacheco, I.I., and Robbie, K., 2007. Nanomaterials and nanoparticles: sources and toxicity. Biointerphases, 2 (4), MR17-MR71.

Card, J.W., Zeldin, D.C., Bonner, J.C., and Nestmann, E.R., 2008. Pulmonary applications and toxicity of engineered nanoparticles. AJP: Lung Cellular and Molecular Physiology, 295 (3), L400–L411.

Carriere, M., Sauvaigo, S., Douki, T., and Ravanat, J.-L., 2017. Impact of nanoparticles on DNA repair processes: current knowledge and working hypotheses. Mutagenesis, 32 (1), 203–213.

Chang, Y.-K., Liu, Y.-P., Ho, J.H., Hsu, S.-C., and Lee, O.K., 2012. Amine-surface-modified superparamagnetic iron oxide nanoparticles interfere with differentiation of human mesenchymal stem cells. Journal of Orthopaedic Research, 30 (9), 1499–1506.

Chen, B., Fang, L., Liu, S., and Chen, B., 2012. Synergistic effect of a combination of nanoparticulate Fe3O4 and gambogic acid on phosphatidylinositol 3-kinase/Akt/Bad pathway of LOVO cells. International Journal of Nanomedicine, 7, 4109-4118.

Cheng, Z., Zhang, J., Liu, H., Li, Y., Zhao, Y., and Yang, E., 2010. Central nervous system penetration for small molecule therapeutic agents does not increase in multiple sclerosis- and Alzheimer's disease-related animal models despite reported blood-brain barrier disruption. Drug Metabolism and Disposition, 38 (8), 1355–1361.

Choi, J.-W., Park, J.W., Na, Y., Jung, S.-J., Hwang, J.K., Choi, D., Lee, K.G., and Yun, C.-O., 2015. Using a magnetic field to redirect an oncolytic adenovirus complexed with iron oxide augments gene therapy efficacy. Biomaterials, 65, 163–174.

Cicha, I., Scheffler, L., Ebenau, A., Lyer, S., Alexiou, C., and Goppelt-Struebe, M., 2015. Mitoxantrone-loaded superparamagnetic iron oxide nanoparticles as drug carriers for cancer therapy: uptake and toxicity in primary human tubular epithelial cells. Nanotoxicology, 5390 (February 2016), 1–10.

Cobb, L., 2013. Cell based assays: the cell cycle, cell proliferation and cell death. Mater Methods, 2013 (3), 172.

Collins, A.R., 2015. The comet assay: a heavenly method!. Mutagenesis, 30 (1), 1–4.

Colognato, R., Park, M.V.D.Z., Wick, P., and De Jong, W.H., 2012. Interactions with the Human Body. In: Adverse Effects of Engineered Nanomaterials. Elsevier, 3–24.

Colombo, M., Carregal-Romero, S., Casula, M.F., Gutiérrez, L., Morales, M.P., Böhm, I.B., Heverhagen, J.T., Prosperi, D., and Parak, W.J., 2012. Biological applications of magnetic nanoparticles. Chemical Society Reviews, 41 (11), 4306–4334.

Cores, J., Caranasos, T., and Cheng, K., 2015. Magnetically targeted stem cell delivery for regenerative medicine. Journal of Functional Biomaterials, 6 (3), 526–546.

Costa, C., Brandão, F., Bessa, M.J., Costa, S., Valdiglesias, V., Kiliç, G., Fernández-Bertólez, N., Quaresma, P., Pereira, E., Pásaro, E., Laffon, B., and Teixeira, J.P., 2016. In vitro cytotoxicity of superparamagnetic iron oxide nanoparticles on neuronal and glial cells. Evaluation of nanoparticle interference with viability tests. Journal of Applied Toxicology, 36 (3), 361–372.

Couto, D., Sousa, R., Andrade, L., Leander, M., Lopez-Quintela, M.A., Rivas, J., Freitas, P., Lima, M., Porto, G., Porto, B., Carvalho, F., and Fernandes, E., 2015. Polyacrylic acid

coated and non-coated iron oxide nanoparticles are not genotoxic to human T lymphocytes. Toxicology Letters, 234 (2), 67–73.

Cromer Berman, S.M., Kshitiz, C.J., Wang, C.J., Orukari, I., Levchenko, A., Bulte, J.W.M., and Walczak, P., 2013. Cell motility of neural stem cells is reduced after SPIO-labeling, which is mitigated after exocytosis. Magnetic Resonance in Medicine, 69 (1), 255–262.

Crosby, M.E., 2007. Cell cycle: principles of control. The Yale journal of biology and medicine, 80 (3), 141–142.

Darzynkiewicz, Z., Traganos, F., and Melamed, M.R., 1980. New cell cycle compartments identified by multiparameter flow cytometry. Cytometry, 1 (2), 98–108.

Das, M., Saxena, N., and Dwivedi, P.D., 2009. Emerging trends of nanoparticles application in food technology: safety paradigms. Nanotoxicology, 3 (1), 10–18.

Davidovich, P., Kearney, C.J., and Martin, S.J., 2014. Inflammatory outcomes of apoptosis, necrosis and necroptosis. Biological Chemistry, 395 (10), 1163–1171.

Deng, M., Huang, Z., Zou, Y., Yin, G., Liu, J., and Gu, J., 2014. Fabrication and neuron cytocompatibility of iron oxide nanoparticles coated with silk-fibroin peptides. Colloids and Surfaces B: Biointerfaces, 116, 465–471.

Dickey, J.S., Redon, C.E., Nakamura, A.J., Baird, B.J., Sedelnikova, O.A., and Bonner, W.M., 2009. H2AX: functional roles and potential applications. Chromosoma, 118 (6), 683-692.

Dilnawaz, F. and Sahoo, S.K., 2015. Therapeutic approaches of magnetic nanoparticles for the central nervous system. Drug Discovery Today, 20 (10), 1256–1264.

Ding, J., Tao, K., Li, J., Song, S., and Sun, K., 2010. Cell-specific cytotoxicity of dextran-stabilized magnetite nanoparticles. Colloids and surfaces. B: Biointerfaces, 79 (1), 184–90.

Dissanayake, N.M., Current, K.M., and Obare, S.O., 2015. Mutagenic effects of iron oxide nanoparticles on biological cells. International journal of molecular sciences, 16 (10), 23482–23516.

Dorn, G.W., 2013. Molecular mechanisms that differentiate apoptosis from programmed necrosis. Toxicologic Pathology, 41 (2), 227–234.

Drasler, B., Vanhecke, D., Rodriguez-Lorenzo, L., Petri-Fink, A., and Rothen-Rutishauser, B., 2017. Quantifying nanoparticle cellular uptake: which method is best?. Nanomedicine, 12 (10), 1095–1099.

Du, S., Li, J., Du, C., Huang, Z., Chen, G., and Yan, W., 2017. Overendocytosis of superparamagnetic iron oxide particles increases apoptosis and triggers autophagic cell death in human osteosarcoma cell under a spinning magnetic field. Oncotarget, 8 (6), 9410–9424.

Duan, J., Dong, J., Zhang, T., Su, Z., Ding, J., Zhang, Y., and Mao, X., 2014. Polyethyleneimine-functionalized iron oxide nanoparticles for systemic siRNA delivery in experimental arthritis. Nanomedicine, 9 (6), 789–801.

Dwane, S., Durack, E., and Kiely, P.A., 2013. Optimising parameters for the differentiation of SH-SY5Y cells to study cell adhesion and cell migration. BMC Research Notes, 6 (1), 366.

Dwivedi, S., Siddiqui, M.A., Farshori, N.N., Ahamed, M., Musarrat, J., and Al-Khedhairy, A.A., 2014. Synthesis, characterization and toxicological evaluation of iron oxide nanoparticles in human lung alveolar epithelial cells. Colloids and Surfaces B: Biointerfaces, 122, 209–215.

Easo, S.L. and Mohanan, P. V., 2015. In vitro hematological and in vivo immunotoxicity assessment of dextran stabilized iron oxide nanoparticles. Colloids and Surfaces B: Biointerfaces, 134, 122–130.

Eichhorn, G.L. and Shin, Y.A., 1968. Interaction of metal ions with polynucleotides and related compounds. XII. The relative effect of various metal ions on DNA helicity. J. Am. Chem. Soc., 90 (26), 7323–7328.

Elmore, S., 2007. Apoptosis: a review of programmed cell death. Toxicologic Pathology, 35 (4), 495–516.

Elmore, S.A., Dixon, D., Hailey, J.R., Harada, T., Herbert, R.A., Maronpot, R.R., Nolte, T., Rehg, J.E., Rittinghausen, S., Rosol, T.J., Satoh, H., Vidal, J.D., Willard-Mack, C.L., and Creasy, D.M., 2016. Recommendations from the INHAND Apoptosis/Necrosis Working Group. Toxicologic Pathology, 44 (2), 173–188.

Elsaesser, A. and Howard, C.V., 2012. Toxicology of nanoparticles. Advanced Drug Delivery Reviews, 64 (2), 129–137.

Elzoghby, A.O., Hemasa, A.L., and Freag, M.S., 2016. Hybrid protein-inorganic nanoparticles: from tumor-targeted drug delivery to cancer imaging. Journal of Controlled Release, 243, 303–322.

Estelrich, J., Escribano, E., Queralt, J., and Busquets, M.A., 2015. Iron oxide nanoparticles for magnetically-guided and magnetically-responsive drug delivery. International Journal of Molecular Sciences, 16 (4), 8070–8101.

Estevanato, L., Cintra, D., Baldini, N., Portilho, F., Barbosa, L., Martins, O., Lacava, B., Miranda-Vilela, A.L., Tedesco, A.C., Báo, S., Morais, P.C., and Lacava, Z.G.M., 2011. Preliminary biocompatibility investigation of magnetic albumin nanosphere designed as a potential versatile drug delivery system. International journal of nanomedicine, 6, 1709–1717.

Al Faraj, A., Shaik, A.P., and Shaik, A.S., 2015. Effect of surface coating on the biocompatibility and in vivo MRI detection of iron oxide nanoparticles after intrapulmonary administration. Nanotoxicology, 9 (7), 825–834.

Favaloro, B., Allocati, N., Graziano, V., Di Ilio, C., and De Laurenzi, V., 2012. Role of apoptosis in disease. Aging, 4 (5), 330–349.

Fenech, M., 2000. The in vitro micronucleus technique. Mutation Research/Fundamental and Molecular Mechanisms of Mutagenesis, 455 (1–2), 81–95.

Fenech, M., 2008. The micronucleus assay determination of chromosomal level DNA damage. Methods in molecular biology (Clifton, N.J.), 410, 185–216.

Fenech, M., Kirsch-Volders, M., Natarajan, A.T., Surralles, J., Crott, J.W., Parry, J., Norppa, H., Eastmond, D.A., Tucker, J.D., and Thomas, P., 2011. Molecular mechanisms of micronucleus, nucleoplasmic bridge and nuclear bud formation in mammalian and human cells. Mutagenesis, 26 (1), 125–132.

Fernández-Bertólez, N., Costa, C., Brandão, F., Kiliç, G., Teixeira, J.P., Pásaro, E., Laffon, B., and Valdiglesias, V., 2018a. Neurotoxicity assessment of oleic acid-coated iron oxide nanoparticles in SH-SY5Y cells. Toxicology, 406–407 (May), 81–91.

Fernández-Bertólez, N., Costa, C., Brandão, F., Kiliç, G., Duarte, J.A., Teixeira, J.P., Pásaro, E., Valdiglesias, V., and Laffon, B., 2018b. Toxicological assessment of silica-coated iron oxide nanoparticles in human astrocytes. Food and Chemical Toxicology, 118, 13–23.

Figuerola, A., Di Corato, R., Manna, L., and Pellegrino, T., 2010. From iron oxide nanoparticles towards advanced iron-based inorganic materials designed for biomedical applications. Pharmacological Research, 62 (2), 126–143.

Finsterwald, C., Magistretti, P., and Lengacher, S., 2015. Astrocytes: new targets for the treatment of neurodegenerative diseases. Current Pharmaceutical Design, 21 (25), 3570–3581.

Forbe, T., García, M., and Gonzalez, E., 2011. Potencial risks of nanoparticles. Food Science and Technology (Campinas), 31 (4), 835–842.

Fraker, P. J., King, L. E., Lill-Elghanian, D., and Telford, W. G., 1995. Quantification of apoptotic events in pure and heterogeneous populations of cells using the flow cytometer. Methods Cell Biol., 46, 57–76.

Frankenberg-Schwager, M., 1989. Review of repair kinetics for DNA damage induced in eukaryotic cells in vitro by ionizing radiation. Radiotherapy and Oncology, 14 (4), 307–320.

Freitas, M.L.L., Silva, L.P., Azevedo, R.B., Garcia, V.A.P., Lacava, L.M., Grisólia, C.K., Lucci, C.M., Morais, P.C., Da Silva, M.F., Buske, N., Curi, R., and Lacava, Z.G.M., 2002. A double-coated magnetite-based magnetic fluid evaluation by cytometry and genetic tests. Journal of Magnetism and Magnetic Materials, 252 (1–3 SPEC. ISS.), 396–398.

Fröhlich, E., Meindl, C., Roblegg, E., Griesbacher, A., and Pieber, T.R., 2012. Cytotoxity of nanoparticles is influenced by size, proliferation and embryonic origin of the cells used for testing. Nanotoxicology, 6 (4), 424–439.

Galluzzi, L., Bravo-San Pedro, J.M., Vitale, I., Aaronson, S.A., Abrams, J.M., Adam, D., Alnemri, E.S., Altucci, L., Andrews, D., Annicchiarico-Petruzzelli, M., Baehrecke, E.H., Bazan, N.G., Bertrand, M.J., Bianchi, K., Blagosklonny, M. V, Blomgren, K., Borner, C., Bredesen, D.E., Brenner, C., Campanella, M., Candi, E., Cecconi, F., Chan, F.K., Chandel, N.S., Cheng, E.H., Chipuk, J.E., Cidlowski, J.A., Ciechanover, A., Dawson, T.M., Dawson, V.L., De Laurenzi, V., De Maria, R., Debatin, K.M., Di Daniele, N., Dixit, V.M., Dynlacht, B.D., El-Deiry, W.S., Fimia, G.M., Flavell, R.A., Fulda, S., Garrido, C., Gougeon, M.L., Green, D.R., Gronemeyer, H., Hajnoczky, G., Hardwick, J.M., Hengartner, M.O., Ichijo, H., Joseph, B., Jost, P.J., Kaufmann, T., Kepp, O., Klionsky, D.J., Knight, R.A., Kumar, S., Lemasters, J.J., Levine, B., Linkermann, A., Lipton, S.A., Lockshin, R.A., López-Otín, C., Lugli, E., Madeo, F., Malorni, W., Marine, J.C., Martin, S.J., Martinou, J.C., Medema, J.P., Meier, P., Melino, S., Mizushima, N., Moll, U., Muñoz-Pinedo, C., Nuñez, G., Oberst, A., Panaretakis, T., Penninger, J.M., Peter, M.E., Piacentini, M., Pinton, P., Prehn, J.H., Puthalakath, H., Rabinovich, G.A., Ravichandran, K.S., Rizzuto, R., Rodrigues, C.M., Rubinsztein, D.C., Rudel, T., Shi, Y., Simon, H.U., Stockwell, B.R., Szabadkai, G., Tait, S.W., Tang, H.L., Tavernarakis, N., Tsujimoto, Y., Vanden Berghe, T., Vandenabeele, P., Villunger, A., Wagner, E.F., Walczak, H., White, E., Wood, W.G., Yuan, J., Zakeri, Z., Zhivotovsky, B., Melino, G., and Kroemer, G., 2015. Essential versus accessory aspects of cell death: Recommendations of the NCCD 2015. Cell Death and Differentiation, 22 (1), 58-73.

Garcia-Canton, C., Anadón, A., and Meredith, C., 2012. γH2AX as a novel endpoint to detect DNA damage: applications for the assessment of the in vitro genotoxicity of cigarette smoke. Toxicology in Vitro, 26 (7), 1075-1086.

Geppert, M., Hohnholt, M., Gaetjen, L., Grunwald, I., Bäumer, M., and Dringen, R., 2009. Accumulation of iron oxide nanoparticles by cultured brain astrocytes. Journal of biomedical nanotechnology, 5 (3), 285–293.

Geppert, M., Hohnholt, M.C., Nürnberger, S., and Dringen, R., 2012. Ferritin up-regulation and transient ROS production in cultured brain astrocytes after loading with iron oxide nanoparticles. Acta Biomaterialia, 8 (10), 3832–3839.

Geppert, M., Hohnholt, M.C., Thiel, K., Nürnberger, S., Grunwald, I., Rezwan, K., and Dringen, R., 2011. Uptake of dimercaptosuccinate-coated magnetic iron oxide nanoparticles by cultured brain astrocytes. Nanotechnology, 22 (14), 145101.

Gkagkanasiou, M., Ploussi, A., Gazouli, M., and Efstathopoulos, E.P., 2016. USPIO-enhanced MRI neuroimaging: a review. Journal of Neuroimaging, 26 (2), 161–168.

Golbamaki, N., Rasulev, B., Cassano, A., Marchese Robinson, R.L., Benfenati, E., Leszczynski, J., and Cronin, M.T.D., 2015. Genotoxicity of metal oxide nanomaterials: review of recent data and discussion of possible mechanisms. Nanoscale, 7 (6), 2154–2198.

Gould, P., 2006. Nanomagnetism shows in vivo potential. Nano Today, 1 (4), 34-39.

Guichard, Y., Schmit, J., Darne, C., Gaté, L., Goutet, M., Rousset, D., Rastoix, O., Wrobel, R., Witschger, O., Martin, A., Fierro, V., and Binet, S., 2012. Cytotoxicity and genotoxicity

of nanosized and microsized titanium dioxide and iron oxide particles in syrian hamster embryo cells. Annals of Occupational Hygiene, 56 (5), 631–644.

Gupta, A.K. and Gupta, M., 2005. Synthesis and surface engineering of iron oxide nanoparticles for biomedical applications. Biomaterials, 26 (18), 3995–4021.

Hanot, C., Choi, Y., Anani, T., Soundarrajan, D., and David, A., 2015. Effects of iron-oxide nanoparticle surface chemistry on uptake kinetics and cytotoxicity in CHO-K1 cells. International Journal of Molecular Sciences, 17 (1), 54.

Harris, G., Palosaari, T., Magdolenova, Z., Mennecozzi, M., Gineste, J.M., Saavedra, L., Milcamps, A., Huk, A., Collins, A.R., Dusinska, M., and Whelan, M., 2015. Iron oxide nanoparticle toxicity testing using high-throughput analysis and high-content imaging. Nanotoxicology, 9 (S1), 87–94.

Henry, C.M., Hollville, E., and Martin, S.J., 2013. Measuring apoptosis by microscopy and flow cytometry. Methods, 61 (2), 90–97.

Hildebrand, H., Kühnel, D., Potthoff, A., Mackenzie, K., Springer, A., and Schirmer, K., 2010. Evaluating the cytotoxicity of palladium/magnetite nano-catalysts intended for wastewater treatment. Environmental Pollution, 158 (1), 65-73.

Hoeller, D. and Dikic, I., 2009. Targeting the ubiquitin system in cancer therapy. Nature, 458 (7237), 438–444.

Hoet, P.H.M., Brüske-Hohlfeld, I., and Salata, O. V., 2004. Nanoparticles - Known and unknown health risks. Journal of Nanobiotechnology, 2, 1–15.

Hohnholt, M.C., Geppert, M., and Dringen, R., 2010a. Effects of iron chelators, iron salts, and iron oxide nanoparticles on the proliferation and the iron content of oligodendroglial OLN-93 cells. Neurochemical Research, 35 (8), 1259–1268.

Hohnholt, M.C. and Dringen, R., 2013. Uptake and metabolism of iron and iron oxide nanoparticles in brain astrocytes. Biochemical Society Transactions, 41 (6), 1588–1592.

Hohnholt, M.C., Geppert, M., and Dringen, R., 2011. Treatment with iron oxide nanoparticles induces ferritin synthesis but not oxidative stress in oligodendroglial cells. Acta Biomaterialia, 7 (11), 3946–3954.

Hohnholt, M.C., Geppert, M., Luther, E.M., Petters, C., Bulcke, F., and Dringen, R., 2013. Handling of iron oxide and silver nanoparticles by astrocytes. Neurochemical Research, 38 (2), 227–239.

Hohnholt, M.C., Geppert, M., Nürnberger, S., von Byern, J., Grunwald, I., and Dringen, R., 2010b. Advanced biomaterials accumulation of citrate-coated magnetic iron oxide nanoparticles by cultured brain astrocytes. Advanced Engineering Materials, 12 (12), B690–B694.

Hong, S.C., Lee, J.H.J.J., Lee, J.H.J.J., Kim, H.Y., Park, J.Y., Cho, Lee, J.H.J.J., and Han, D.-W.W., 2011. Subtle cytotoxicity and genotoxicity differences in superparamagnetic iron

oxide nanoparticles coated with various functional groups. International Journal of Nanomedicine, 6, 3219.

Howarth, C., 2014. The contribution of astrocytes to the regulation of cerebral blood flow. Frontiers in Neuroscience, 8 (8 MAY), 1–9.

Huang, S., Li, C., Cheng, Z., Fan, Y., Yang, P., Zhang, C., Yang, K., and Lin, J., 2012. Magnetic Fe3O4@mesoporous silica composites for drug delivery and bioadsorption. Journal of Colloid and Interface Science, 376 (1), 312–321.

Huang, Y.-W., Cambre, M., and Lee, H.-J., 2017. The toxicity of nanoparticles depends on multiple molecular and physicochemical mechanisms. International Journal of Molecular Sciences, 18 (12), 2702.

Huber, D.L., 2005. Synthesis, properties, and applications of iron nanoparticles. Small, 1 (5), 482-501.

Ibuki, Y. and Toyooka, T., 2012. Nanoparticle uptake measured by flow cytometry. Methods in Molecular Biology, 926, 157-166.

Imam, S.Z., Lantz-McPeak, S.M., Cuevas, E., Rosas-Hernandez, H., Liachenko, S., Zhang, Y., Sarkar, S., Ramu, J., Robinson, B.L., Jones, Y., Gough, B., Paule, M.G., Ali, S.F., and Binienda, Z.K., 2015. Iron oxide nanoparticles induce dopaminergic damage: in vitro pathways and in vivo imaging reveals mechanism of neuronal damage. Molecular Neurobiology, 52 (2), 913–926.

Ittrich, H., Peldschus, K., Raabe, N., Kaul, M., and Adam, G., 2013. Superparamagnetic iron oxide nanoparticles in biomedicine: applications and developments in diagnostics and therapy. RöFo - Fortschritte auf dem Gebiet der Röntgenstrahlen und der bildgebenden Verfahren, 185 (12), 1149–1166.

Ivashkevich, A., Redon, C.E., Nakamura, A.J., Martin, R.F., and Martin, O.A., 2012. Use of the γ-H2AX assay to monitor DNA damage and repair in translational cancer research. Cancer Letters, 327 (1-2), 123-133.

Iyama, T. and Wilson, D.M., 2013. DNA repair mechanisms in dividing and non-dividing cells. DNA Repair, 12 (8), 620–636.

Jaruga, P. and Dizdaroglu, M., 1996. Repair of products of oxidative DNA base damage in human cells. Nucleic acids research, 24 (8), 1389–1394.

Jeng, H.A. and Swanson, J., 2006. Toxicity of metal oxide nanoparticles in mammalian cells. Journal of Environmental Science and Health Part A-Toxic/Hazardous Substances & Environmental Engineering, 41 (12), 2699–2711.

Jin, R., Lin, B., Li, D., and Ai, H., 2014. Superparamagnetic iron oxide nanoparticles for MR imaging and therapy: design considerations and clinical applications. Current Opinion in Pharmacology, 18, 18–27.

De Jong, W.H. and Borm, P.J. a, 2008. Drug delivery and nanoparticles: applications and hazards. International journal of nanomedicine, 3 (2), 133–149.

Jud, C., Clift, M.J.D., Petri-Fink, A., and Rothen-Rutishauser, B., 2013. Nanomaterials and the human lung: what is known and what must be deciphered to realise their potential advantages? Swiss Medical Weekly, 143 (February), 1–20.

Jurisic, V. and Bumbasirevic, V., 2008. In vitro assays for cell death determination. Archive of oncology, 16 (3–4), 49–54.

Kanwar, J.R., Sun, X., Punj, V., Sriramoju, B., Mohan, R.R., Zhou, S.-F., Chauhan, A., and Kanwar, R.K., 2012. Nanoparticles in the treatment and diagnosis of neurological disorders: untamed dragon with fire power to heal. Nanomedicine: Nanotechnology, Biology and Medicine, 8 (4), 399–414.

Karlsson, H.L., 2010. The comet assay in nanotoxicology research. Analytical and Bioanalytical Chemistry, 398 (2), 651–666.

Karlsson, H.L., Di Bucchianico, S., Collins, A.R., and Dusinska, M., 2015. Can the comet assay be used reliably to detect nanoparticle-induced genotoxicity? Environmental and Molecular Mutagenesis, 56 (2), 82–96.

Karlsson, H.L., Cronholm, P., Gustafsson, J., and Möller, L., 2008. Copper oxide nanoparticles are highly toxic: a comparison between metal oxide nanoparticles and carbon nanotubes. Chemical research in toxicology, 21 (9), 1726–32.

Karlsson, H.L., Gustafsson, J., Cronholm, P., and Möller, L., 2009. Size-dependent toxicity of metal oxide particles-A comparison between nano- and micrometer size. Toxicology Letters, 188 (2), 112-118.

Kenzaoui, B.H., Angeloni, S., Overstolz, T., Niedermann, P., Chapuis Bernasconi, C., Liley, M., and Juillerat-Jeanneret, L., 2013. Transfer of ultrasmall iron oxide nanoparticles from human brain-derived endothelial cells to human glioblastoma cells. ACS Applied Materials & Interfaces, 5 (9), 3581–3586.

Kenzaoui, B.H., Bernasconi, C.C., Guney-Ayra, S., and Juillerat-Jeanneret, L., 2012a. Induction of oxidative stress, lysosome activation and autophagy by nanoparticles in human brain-derived endothelial cells. Biochemical Journal, 441 (3), 813–821.

Kenzaoui, B.H., Bernasconi, C.C., Hofmann, H., and Juillerat-Jeanneret, L., 2012b. Evaluation of uptake and transport of ultrasmall superparamagnetic iron oxide nanoparticles by human brain-derived endothelial cells. Nanomedicine, 7 (1), 39–53.

Kermanizadeh, A., Chauché, C., Brown, D.M., Loft, S., and Møller, P., 2015. The role of intracellular redox imbalance in nanomaterial induced cellular damage and genotoxicity: A review. Environmental and Molecular Mutagenesis, 56 (2), 111-124.

Kettiger, H., Schipanski, A., Wick, P., and Huwyler, J., 2013. Engineered nanomaterial uptake and tissue distribution: from cell to organism. International Journal of Nanomedicine, 8, 3255–3269.

Khan, M.I., Mohammad, A., Patil, G., Naqvi, S.A.H., Chauhan, L.K.S., and Ahmad, I., 2012. Induction of ROS, mitochondrial damage and autophagy in lung epithelial cancer cells by iron oxide nanoparticles. Biomaterials, 33 (5), 1477–1488.

Kiliç, G., Costa, C., Fernández-Bertólez, N., Pásaro, E., Teixeira, J.P., Laffon, B., and Valdiglesias, V., 2015. In vitro toxicity evaluation of silica-coated iron oxide nanoparticles in human SHSY5Y neuronal cells. Toxicol. Res., 5 (1), 235–247.

Kim, J.-E.E., Shin, J.-Y.Y., and Cho, M.-H.H., 2012. Magnetic nanoparticles: an update of application for drug delivery and possible toxic effects. Archives of Toxicology, 86 (5), 685-700.

Kim, J.-H., Sanetuntikul, J., Shanmugam, S., and Kim, E., 2015. Necrotic cell death caused by exposure to graphitic carbon-coated magnetic nanoparticles. Journal of Biomedical Materials Research Part A, 103 (9), 2875–2887.

Kim, J.S., Yoon, T.-J., Yu, K.N., Kim, B.G., Park, S.J., Kim, H.W., Lee, K.H., Park, S.B., Lee, J.-K., and Cho, M.H., 2006. Toxicity and tissue distribution of magnetic nanoparticles in mice. Toxicological Sciences, 89 (1), 338–347.

Kim, Y., Kong, S.D., Chen, L.-H., Pisanic, T.R., Jin, S., and Shubayev, V.I., 2013. In vivo nanoneurotoxicity screening using oxidative stress and neuroinflammation paradigms. Nanomedicine: Nanotechnology, Biology and Medicine, 9 (7), 1057–1066.

Kimelberg, H.K. and Nedergaard, M., 2010. Functions of astrocytes and their potential as therapeutic targets. Neurotherapeutics, 7 (4), 338–353.

Klein, S., Sommer, A., Distel, L.V.R., Neuhuber, W., and Kryschi, C., 2012. Superparamagnetic iron oxide nanoparticles as radiosensitizer via enhanced reactive oxygen species formation. Biochemical and Biophysical Research Communications, 425 (2), 393–397.

Könczöl, M., Ebeling, S., Goldenberg, E., Treude, F., Gminski, R., Gieré, R., Grobéty, B., Rothen-Rutishauser, B., Merfort, I., and Mersch-Sundermann, V., 2011. Cytotoxicity and genotoxicity of size-fractionated iron oxide (magnetite) in A549 human lung epithelial cells: role of ROS, JNK, and NF-κB. Chemical research in toxicology, 24 (9), 1460–75.

Kovalevich, J. and Langford, D., 2013. Considerations for the use of SH-SY5Y neuroblastoma cells in neurobiology. Methods in Molecular Biology, 1078, 9–21.

Krais, A., Wortmann, L., Hermanns, L., Feliu, N., Vahter, M., Stucky, S., Mathur, S., and Fadeel, B., 2014. Targeted uptake of folic acid-functionalized iron oxide nanoparticles by ovarian cancer cells in the presence but not in the absence of serum. Nanomedicine: Nanotechnology, Biology, and Medicine, 10 (7), 1421–1431.

Krötz, F., de Wit, C., Sohn, H.Y., Zahler, S., Gloe, T., Pohl, U., and Plank, C., 2003. Magnetofection-A highly efficient tool for antisense oligonucleotide delivery in vitro and in vivo. Molecular Therapy: The Journal of the American Society of Gene Therapy, 7 (5), 700–710.

Kuhn, D.A., Vanhecke, D., Michen, B., Blank, F., Gehr, P., Petri-Fink, A., and Rothen-Rutishauser, B., 2014. Different endocytotic uptake mechanisms for nanoparticles in epithelial cells and macrophages. Beilstein Journal of Nanotechnology, 5 (1), 1625-1636.

Kumar, A. and Dhawan, A., 2013. Genotoxic and carcinogenic potential of engineered nanoparticles: an update. Archives of Toxicology, 87 (11), 1883–1900.

Kumar, M., Medarova, Z., Pantazopoulos, P., Dai, G., and Moore, A., 2010. Novel membrane-permeable contrast agent for brain tumor detection by MRI. Magnetic Resonance in Medicine, 63 (3), 617–624.

Kumar, M., Singh, G., Arora, V., Mewar, S., Sharma, U., Jagannathan, N. r, Sapra, S., Dinda, A.K., Kharbanda, S., and Singh, H., 2012. Cellular interaction of folic acid conjugated superparamagnetic iron oxide nanoparticles and its use as contrast agent for targeted magnetic imaging of tumor cells. International Journal of Nanomedicine, 7, 3503–3516.

Kumari, M., Rajak, S., Singh, S.P., Kumari, S.I., Kumar, P.U., Murty, U.S.N., Mahboob, M., Grover, P., and Rahman, M.F., 2012. Repeated oral dose toxicity of iron oxide nanoparticles: biochemical and histopathological alterations in different tissues of rats. Journal of Nanoscience and Nanotechnology, 12 (3), 2149–2159.

Kunzmann, A., Andersson, B., Vogt, C., Feliu, N., Ye, F., Gabrielsson, S., Toprak, M.S., Buerki-Thurnherr, T., Laurent, S., Vahter, M., Krug, H., Muhammed, M., Scheynius, A., and Fadeel, B., 2011. Efficient internalization of silica-coated iron oxide nanoparticles of different sizes by primary human macrophages and dendritic cells. Toxicology and Applied Pharmacology, 253 (2), 81–93.

Kwon, D., Nho, H.W., and Yoon, T.H., 2014. X-ray and electron microscopy studies on the biodistribution and biomodification of iron oxide nanoparticles in daphnia magna. Colloids and Surfaces B: Biointerfaces, 122, 384–389.

Laffon, B., Fernández-Bertólez, N., Costa, C., Pásaro, E., and Valdiglesias, V., 2017. Comparative study of human neuronal and glial cell sensitivity for in vitro neurogenotoxicity testing. Food and Chemical Toxicology, 102, 120–128.

Laffon, B., Valdiglesias, V., Pásaro, E., and Méndez, J., 2010. The organic selenium compound selenomethionine modulates bleomycin-induced DNA damage and repair in human leukocytes. Biological Trace Element Research, 133 (1), 12–19.

Lai, D.Y., 2015. Approach to using mechanism-based structure activity relationship (SAR) analysis to assess human health hazard potential of nanomaterials. Food and Chemical Toxicology, 85, 120–126.

Lai, X., Wei, Y., Zhao, H., Chen, S., Bu, X., Lu, F., Qu, D., Yao, L., Zheng, J., and Zhang, J., 2015. The effect of Fe2O3 and ZnO nanoparticles on cytotoxicity and glucose metabolism in lung epithelial cells. Journal of Applied Toxicology, 35 (6), 651–664.

Laingam, S., Froscio, S.M., and Humpage, A.R., 2008. Flow-cytometric analysis of in vitro micronucleus formation: comparative studies with WIL2-NS human lymphoblastoid and

L5178Y mouse lymphoma cell lines. Mutation Research - Genetic Toxicology and Environmental Mutagenesis, 656 (1–2), 19–26.

Landsiedel, R., Fabian, E., Ma-Hock, L., Wohlleben, W., Wiench, K., Oesch, F., and Van Ravenzwaay, B., 2012. Toxico-/biokinetics of nanomaterials. Archives of Toxicology, 86 (7), 1021-1060.

Laskar, A., Ghosh, M., Khattak, S.I., Li, W., and Yuan, X.-M., 2012. Degradation of superparamagnetic iron oxide nanoparticle-induced ferritin by lysosomal cathepsins and related immune response. Nanomedicine, 7 (5), 705–717.

Laurent, S., Dutz, S., Häfeli, U.O., and Mahmoudi, M., 2011. Magnetic fluid hyperthermia: focus on superparamagnetic iron oxide nanoparticles. Advances in Colloid and Interface Science, 166 (1-2), 8-23.

Laurent, S. and Mahmoudi, M., 2011. Superparamagnetic iron oxide nanoparticles: promises for diagnosis and treatment of cancer. International Journal of Molecular Epidemiology and Genetics, 2 (4), 367–390.

Lee, S.H., Lee, J.B., Bae, M.S., Balikov, D.A., Hwang, A., Boire, T.C., Kwon, I.K., Sung, H.-J., and Yang, J.W., 2015. Current progress in nanotechnology applications for diagnosis and treatment of kidney diseases. Advanced Healthcare Materials, 4 (13), 2037–2045.

Lesniak, A., Campbell, A., Monopoli, M.P., Lynch, I., Salvati, A., and Dawson, K.A., 2010. Serum heat inactivation affects protein corona composition and nanoparticle uptake. Biomaterials, 31 (36), 9511–9518.

Lévy, M., Lagarde, F., Maraloiu, V.-A., Blanchin, M.-G., Gendron, F., Wilhelm, C., and Gazeau, F., 2010. Degradability of superparamagnetic nanoparticles in a model of intracellular environment: follow-up of magnetic, structural and chemical properties. Nanotechnology, 21 (39), 395103.

Li, L., Jiang, W., Luo, K., Song, H., Lan, F., Wu, Y., and Gu, Z., 2013. Superparamagnetic iron oxide nanoparticles as MRI contrast agents for non-invasive stem cell labeling and tracking. Theranostics, 3 (8), 595-615.

Li, L., Mak, K.Y., Shi, J., Koon, H.K., Leung, C.H., Wong, C.M., Leung, C.W., Mak, C.S.K., Chan, N.M.M., Zhong, W., Lin, K.W., Wu, E.X., and Pong, P.W.T., 2012. Comparative in vitro cytotoxicity study on uncoated magnetic nanoparticles: effects on cell viability, cell morphology, and cellular uptake. Journal of Nanoscience and Nanotechnology, 12 (12), 9010–9017.

Li, Y., Liu, J., Zhong, Y., Zhang, J., Wang, Z., Wang, L., An, Y., Lin, M., Gao, Z., and Zhang, D., 2011. Biocompatibility of Fe_3O_4@Au composite magnetic nanoparticles in vitro and in vivo. International journal of nanomedicine, 6, 2805–2819.

Lin, Z., Monteiro-Riviere, N.A., and Riviere, J.E., 2015. Pharmacokinetics of metallic nanoparticles. Wiley Interdisciplinary Reviews: Nanomedicine and Nanobiotechnology, 7 (2), 189–217.

Liu, G., Gao, J., Ai, H., and Chen, X., 2013. Applications and potential toxicity of magnetic iron oxide nanoparticles. Small, 9 (9–10), 1533–1545.

Liu, Y., Xia, Q., Liu, Y., Zhang, S., Cheng, F., Zhong, Z., Wang, L., Li, H., and Xiao, K., 2014. Genotoxicity assessment of magnetic iron oxide nanoparticles with different particle sizes and surface coatings. Nanotechnology, 25 (42), 425101.

Lloyd, D.R. and Phillips, D.H., 1999. Oxidative DNA damage mediated by copper(II), iron(II) and nickel(II) Fenton reactions: evidence for site-specific mechanisms in the formation of double-strand breaks, 8-hydroxydeoxyguanosine and putative intrastrand cross-links. Mutation Research - Fundamental and Molecular Mechanisms of Mutagenesis, 424 (1–2), 23–36.

Loh, J.W., Saunders, M., and Lim, L.Y., 2012. Cytotoxicity of monodispersed chitosan nanoparticles against the Caco-2 cells. Toxicology and Applied Pharmacology, 262 (3), 273–282.

Long, N.V., Yang, Y., Teranishi, T., Thi, C.M., Cao, Y., and Nogami, M., 2015. Biomedical applications of advanced multifunctional magnetic nanoparticles. Journal of Nanoscience and Nanotechnology, 15 (12), 10091–10107.

Lorenz, C., Goetz, N. Von, Scheringer, M., Wormuth, M., and Hungerbühler, K., 2011. Potential exposure of German consumers to engineered nanoparticles in cosmetics and personal care products. Nanotoxicology, 5 (1), 12–29.

Lu, A.-H., Salabas, E.L., and Schüth, F., 2007a. Magnetic nanoparticles: synthesis, protection, functionalization, and application. Angewandte Chemie International Edition, 46 (8), 1222–1244.

Lu, M., Cohen, M.H., Rieves, D., and Pazdur, R., 2010. FDA report: ferumoxytol for intravenous iron therapy in adult patients with chronic kidney disease. American Journal of Hematology, 85 (5), 315–319.

Lu, C.-W., Hung, Y., Hsiao, J.-K., Yao, M., Chung, T.-H., Lin, Y.-S., Wu, S.-H., Hsu, S.-C., Liu, H.-M., Mou, C.-Y., Yang, C.-S., Huang, D.-M., and Chen, Y.-C., 2007b. Bifunctional magnetic silica nanoparticles for highly efficient human stem cell labeling. Nano Letters, 7 (1), 149–154.

Lukamowicz, M., Woodward, K., Kirsch-Volders, M., Suter, W., and Elhajouji, A., 2011. A flow cytometry based in vitro micronucleus assay in TK6 cells-validation using early stage pharmaceutical development compounds. Environmental and Molecular Mutagenesis, 52 (5), 363–372.

Luther, E.M., Petters, C., Bulcke, F., Kaltz, A., Thiel, K., Bickmeyer, U., and Dringen, R., 2013. Endocytotic uptake of iron oxide nanoparticles by cultured brain microglial cells. Acta Biomaterialia, 9 (9), 8454–8465.

Maes, M., Vanhaecke, T., Cogliati, B., Yanguas, S.C., Willebrords, J., Rogiers, V., and Vinken, M., 2015. Measurement of apoptotic and necrotic cell death in primary hepatocyte cultures. Methods in molecular biology (Clifton, N.J.), 1250, 349–361.

Magdolenova, Z., Collins, A., Kumar, A., Dhawan, A., Stone, V., and Dusinska, M., 2014. Mechanisms of genotoxicity. A review of in vitro and in vivo studies with engineered nanoparticles. Nanotoxicology, 8 (July), 233-278.

Magdolenova, Z., Drlickova, M., Henjum, K., Rundén-Pran, E., Tulinska, J., Bilanicova, D., Pojana, G., Kazimirova, A., Barancokova, M., Kuricova, M., Liskova, A., Staruchova, M., Ciampor, F., Vavra, I., Lorenzo, Y., Collins, A., Rinna, A., Fjellsbø, L., Volkovova, K., Marcomini, A., Amiry-Moghaddam, M., and Dusinska, M., 2013. Coating-dependent induction of cytotoxicity and genotoxicity of iron oxide nanoparticles. Nanotoxicology, 9 (sup1), 44–56.

Magdolenova, Z., Lorenzo, Y., Collins, A., and Dusinska, M., 2012. Can standard genotoxicity tests be applied to nanoparticles? Journal of Toxicology and Environmental Health, Part A, 75 (13–15), 800–806.

Mah, L.J., El-Osta, A., and Karagiannis, T.C., 2010. γH2AX: A sensitive molecular marker of DNA damage and repair. Leukemia, 24 (4), 679–686.

Mahdavi, M., Ahmad, M. Bin, Haron, M.J., Namvar, F., Nadi, B., Rahman, M.Z.A., and Amin, J., 2013. Synthesis, surface modification and characterisation of biocompatible magnetic iron oxide nanoparticles for biomedical applications. Molecules, 18 (7), 7533–7548.

Mahler, G.J., Esch, M.B., Tako, E., Southard, T.L., Archer, S.D., Glahn, R.P., and Shuler, M.L., 2012. Oral exposure to polystyrene nanoparticles affects iron absorption. Nature Nanotechnology, 7 (4), 264–271.

Mahmoudi, M., Laurent, S., Shokrgozar, M.A., and Hosseinkhani, M., 2011a. Toxicity evaluations of superparamagnetic iron oxide nanoparticles: cell 'vision' versus physicochemical properties of nanoparticles. ACS Nano, 5 (9), 7263–7276.

Mahmoudi, M., Lynch, I., Ejtehadi, M.R., Monopoli, M.P., Bombelli, F.B., and Laurent, S., 2011b. Protein−Nanoparticle interactions: opportunities and challenges. Chemical Reviews, 111 (9), 5610–5637.

Mahmoudi, M., Saeedi-Eslami, S.N., Shokrgozar, M.A., Azadmanesh, K., Hassanlou, M., Kalhor, H.R., Burtea, C., Rothen-Rutishauser, B., Laurent, S., Sheibani, S., and Vali, H., 2012. Cell "vision": complementary factor of protein corona in nanotoxicology. Nanoscale, 4 (17), 5461.

Mahmoudi, M., Sant, S., Wang, B., Laurent, S., and Sen, T., 2011c. Superparamagnetic iron oxide nanoparticles (SPIONs): Development, surface modification and applications in chemotherapy. Advanced Drug Delivery Reviews, 63 (1–2), 24–46.

Mahmoudi, M., Sheibani, S., Milani, A.S., Rezaee, F., Gauberti, M., Dinarvand, R., and Vali, H., 2015. Crucial role of the protein corona for the specific targeting of nanoparticles. Nanomedicine, 10 (2), 215–226.

Mahmoudi, M., Simchi, A., and Imani, M., 2009a. Cytotoxicity of uncoated and polyvinyl alcohol coated superparamagnetic iron oxide nanoparticles. The Journal of Physical Chemistry C, 113 (22), 9573–9580.

Mahmoudi, M., Simchi, A., Milani, A.S., and Stroeve, P., 2009b. Cell toxicity of superparamagnetic iron oxide nanoparticles. Journal of Colloid and Interface Science, 336 (2), 510–518.

Mahon, E., Hristov, D.R., and Dawson, K.A., 2012. Stabilising fluorescent silica nanoparticles against dissolution effects for biological studies. Chemical Communications, 48 (64), 7970–7972.

Maier-Hauff, K., Ulrich, F., Nestler, D., Niehoff, H., Wust, P., Thiesen, B., Orawa, H., Budach, V., and Jordan, A., 2011. Efficacy and safety of intratumoral thermotherapy using magnetic iron-oxide nanoparticles combined with external beam radiotherapy on patients with recurrent glioblastoma multiforme. Journal of Neuro-Oncology, 103 (2), 317–324.

Maity, D. and Agrawal, D.C., 2007. Synthesis of iron oxide nanoparticles under oxidizing environment and their stabilization in aqueous and non-aqueous media. Journal of Magnetism and Magnetic Materials, 308 (1), 46–55.

Malvindi, M.A., De Matteis, V., Galeone, A., Brunetti, V., Anyfantis, G.C., Athanassiou, A., Cingolani, R., and Pompa, P.P., 2014. Toxicity assessment of silica coated iron oxide nanoparticles and biocompatibility improvement by surface engineering. PLoS ONE, 9 (1), e85835.

Mao, H., Chen, H., Wang, L., Yu, Q., Qian, W., Tiwari, D., Yi, H., Wang, A., Huang, J., and Yang, L., 2013. Anti-HER2 antibody and ScFvEGFR-conjugated antifouling magnetic iron oxide nanoparticles for targeting and magnetic resonance imaging of breast cancer. International Journal of Nanomedicine, 8, 3781.

Marcus, M., Karni, M., Baranes, K., Levy, I., Alon, N., Margel, S., and Shefi, O., 2016. Iron oxide nanoparticles for neuronal cell applications: Uptake study and magnetic manipulations. Journal of Nanobiotechnology, 14 (1), 37.

Martin, S.J. and Henry, C.M., 2013. Distinguishing between apoptosis, necrosis, necroptosis and other cell death modalities. Methods, 61 (2), 87–89.

Martirosyan, A. and Schneider, Y.J., 2014. Engineered nanomaterials in food: implications for food safety and consumer health. International Journal of Environmental Research and Public Health, 11 (6), 5720–5750.

Masserini, M., 2013. Nanoparticles for brain drug delivery. ISRN Biochemistry, 2013, 1–18.

Matsuzaki, K., Harada, A., Takeiri, A., Tanaka, K., and Mishima, M., 2010. Whole cell-ELISA to measure the γH2AX response of six aneugens and eight DNA-damaging chemicals. Mutation Research - Genetic Toxicology and Environmental Mutagenesis, 700 (1–2), 71–79.

Maynard, A.D., Warheit, D.B., and Philbert, M.A., 2011. The new toxicology of sophisticated materials: nanotoxicology and beyond. Toxicological Sciences, 120 (Supplement 1), S109–S129.

Mc Carthy, D.J., Malhotra, M., O'Mahony, A.M., Cryan, J.F., and O'Driscoll, C.M., 2015. Nanoparticles and the blood-brain barrier: advancing from in-vitro models towards therapeutic significance. Pharmaceutical Research, 32 (4), 1161–1185.

McBain, S.C., Yiu, H.H.P., and Dobson, J., 2008. Magnetic nanoparticles for gene and drug delivery. International Journal of Nanomedicine, 3 (2), 169–180.

Migliore, L., Uboldi, C., Di Bucchianico, S., and Coppedè, F., 2015. Nanomaterials and neurodegeneration. Environmental and Molecular Mutagenesis, 56 (2), 149–170.

Mohapatra, M. and Anand, S., 2010. Synthesis and applications of nano-structured iron oxides / hydroxides – a review. International Journal of Engineering, Science and Technology, 2 (8), 127–146.

Monopoli, M.P., Åberg, C., Salvati, A., and Dawson, K.A., 2012. Biomolecular coronas provide the biological identity of nanosized materials. Nature Nanotechnology, 7 (12), 779–786.

Namvar, F., Rahman, H.S., Mohamad, R., Baharara, J., Mahdavi, M., Amini, E., Chartrand, M.S., and Yeap, S.K., 2014. Cytotoxic effect of magnetic iron oxide nanoparticles synthesized via seaweed aqueous extract. International Journal of Nanomedicine, 9 (1), 2479–2488.

Naqvi, S., Samim, M., Abdin, M.Z., Ahmed, F.J., Maitra, A.N., Prashant, C.K., and Dinda, A.K., 2010. Concentration-dependent toxicity of iron oxide nanoparticles mediated by increased oxidative stress. International Journal of Nanomedicine, 5 (1), 983–989.

Nel, A., 2006. Toxic potential of materials at the nanolevel. Science, 311 (5761), 622–627.

Nel, A.E., Mädler, L., Velegol, D., Xia, T., Hoek, E.M. V., Somasundaran, P., Klaessig, F., Castranova, V., and Thompson, M., 2009. Understanding biophysicochemical interactions at the nano–bio interface. Nature Materials, 8 (7), 543–557.

Nikolova, T., Dvorak, M., Jung, F., Adam, I., Krämer, E., Gerhold-Ay, A., and Kaina, B., 2014. The γH2AX assay for genotoxic and nongenotoxic agents: comparison of H2AX phosphorylation with cell death response. Toxicological Sciences, 140 (1), 103–117.

Nunez, R., 2001. DNA measurement and cell cycle analysis by flow cytometry. Current Issues in Molecular Biology, 3 (3), 67–70.

Nüsse, M., Beisker, W., Kramer, J., Miller, B.M., Schreiber, G.A., Viaggi, S., Weller, E.M., and Wessels, J.M., 1994. Chapter 9 Measurement of micronuclei by flow cytometry. Methods in Cell Biology, 42 (C), 149–158.

Nüsse, M. and Kramer, J., 1984. Flow cytometric analysis of micronuclei found in cells after irradiation. Cytometry, 5 (1), 20–25.

Oberdörster, G., 2010. Safety assessment for nanotechnology and nanomedicine: Concepts of nanotoxicology. Journal of Internal Medicine, 267 (1), 89–105.

Oberdörster, G., Elder, A., and Rinderknecht, A., 2009. Nanoparticles and the Brain: Cause for Concern? Journal of Nanoscience and Nanotechnology, 9 (8), 4996–5007.

Oberdörster, G., Oberdörster, E., and Oberdörster, J., 2005. Nanotoxicology: an emerging discipline evolving from studies of ultrafine particles. Environmental Health Perspectives, 113 (7), 823–839.

de Oliveira, G.M.T., Kist, L.W., Pereira, T.C.B., Bortolotto, J.W., Paquete, F.L., de Oliveira, E.M.N., Leite, C.E., Bonan, C.D., de Souza Basso, N.R., Papaleo, R.M., and Bogo, M.R., 2014. Transient modulation of acetylcholinesterase activity caused by exposure to dextran-coated iron oxide nanoparticles in brain of adult zebrafish. Comparative Biochemistry and Physiology Part C: Toxicology & Pharmacology, 162, 77–84.

Ostling, O. and Johanson, K.J., 1984. Microelectrophoretic study of radiation-induced DNA damages in individual mammalian cells. Biochemical and Biophysical Research Communications, 123 (1), 291–298.

Paolini, A., Guarch, C.P., Ramos-López, D., de Lapuente, J., Lascialfari, A., Guari, Y., Larionova, J., Long, J., and Nano, R., 2016. Rhamnose-coated superparamagnetic iron-oxide nanoparticles: an evaluation of their in vitro cytotoxicity, genotoxicity and carcinogenicity. Journal of Applied Toxicology, 36 (4), 510–520.

Park, E.-J., Choi, D.-H., Kim, Y., Lee, E.-W., Song, J., Cho, M.-H., Kim, J.-H., and Kim, S.-W., 2014. Magnetic iron oxide nanoparticles induce autophagy preceding apoptosis through mitochondrial damage and ER stress in RAW264.7 cells. Toxicology in Vitro, 28 (8), 1402–1412.

Patil, U.S., Adireddy, S., Jaiswal, A., Mandava, S., Lee, B.R., and Chrisey, D.B., 2015. In vitro/in vivo toxicity evaluation and quantification of iron oxide nanoparticles. International Journal of Molecular Sciences, 16 (10), 24417-24450.

Pedram, M.S.Z., Shamloo, A., GhafarZadeh, E., and Alasty, A., 2014. Modeling and simulation of crossing magnetic nanoparticles through blood brain barrier (BBB). In: 2014 36th Annual International Conference of the IEEE Engineering in Medicine and Biology Society. IEEE, 5280–5283.

Pekny, M. and Pekna, M., 2014. Astrocyte reactivity and reactive astrogliosis: costs and benefits. Physiological Reviews, 94 (4), 1077–1098.

Periasamy, V.S., Athinarayanan, J., Alhazmi, M., Alatiah, K.A., and Alshatwi, A.A., 2016. Fe3O4 nanoparticle redox system modulation via cell-cycle progression and gene expression in human mesenchymal stem cells. Environmental Toxicology, 31 (8), 901–912.

Petters, C., Bulcke, F., Thiel, K., Bickmeyer, U., and Dringen, R., 2014a. Uptake of fluorescent iron oxide nanoparticles by oligodendroglial OLN-93 cells. Neurochemical Research, 39 (2), 372–383.

Petters, C. and Dringen, R., 2015. Uptake, metabolism and toxicity of iron oxide nanoparticles in cultured microglia, astrocytes and neurons. SpringerPlus, 4 (Suppl 1), L32.

Petters, C., Irrsack, E., Koch, M., and Dringen, R., 2014b. Uptake and metabolism of iron oxide nanoparticles in brain cells. Neurochemical Research, 39 (9), 1648–1660.

Petters, C., Thiel, K., and Dringen, R., 2016. Lysosomal iron liberation is responsible for the vulnerability of brain microglial cells to iron oxide nanoparticles: comparison with neurons and astrocytes. Nanotoxicology, 10 (3), 332–342.

Pettitt, M.E. and Lead, J.R., 2013. Minimum physicochemical characterisation requirements for nanomaterial regulation. Environment International, 52, 41-50.

Phatnani, H. and Maniatis, T., 2015. Astrocytes in neurodegenerative disease. Cold Spring Harbor Perspectives in Biology, 7 (6), 1–18.

Pisanic, T.R., Blackwell, J.D., Shubayev, V.I., Fiñones, R.R., and Jin, S., 2007. Nanotoxicity of iron oxide nanoparticle internalization in growing neurons. Biomaterials, 28 (16), 2572–2581.

Podila, R. and Brown, J.M., 2013. Toxicity of engineered nanomaterials: a physicochemical perspective. Journal of Biochemical and Molecular Toxicology, 27 (1), 50-55.

Pongrac, I.M., Dobrivojevic, M., Ahmed, L.B., Babic, M., Slouf, M., Horák, D., and Gajovic, S., 2016. Improved biocompatibility and efficient labeling of neural stem cells with poly(L-lysine)-coated maghemite nanoparticles. Beilstein Journal of Nanotechnology, 7 (1), 926–936.

Pöttler, M., Staicu, A., Zaloga, J., Unterweger, H., Weigel, B., Schreiber, E., Hofmann, S., Wiest, I., Jeschke, U., Alexiou, C., and Janko, C., 2015. Genotoxicity of Superparamagnetic Iron Oxide Nanoparticles in Granulosa Cells. International journal of molecular sciences, 16 (11), 26280–90.

Powers, K.W., Brown, S.C., Krishna, V.B., Wasdo, S.C., Moudgil, B.M., and Roberts, S.M., 2006. Research strategies for safety evaluation of nanomaterials. Part VI. characterization of nanoscale particles for toxicological evaluation. Toxicological Sciences, 90 (2), 296–303.

Powers, K.W., Palazuelos, M., Moudgil, B.M., and Roberts, S.M., 2007. Characterization of the size, shape, and state of dispersion of nanoparticles for toxicological studies. Nanotoxicology, 1 (1), 42–51.

Qiang, L., Yang, Y., Ma, Y.-J., Chen, F.-H., Zhang, L.-B., Liu, W., Qi, Q., Lu, N., Tao, L., Wang, X.-T., You, Q.-D., and Guo, Q.-L., 2009. Isolation and characterization of cancer stem like cells in human glioblastoma cell lines. Cancer Letters, 279 (1), 13–21.

Rajiv, S., Jerobin, J., Saranya, V., Nainawat, M., Sharma, A., Makwana, P., Gayathri, C., Bharath, L., Singh, M., Kumar, M., Mukherjee, A., and Chandrasekaran, N., 2015. Comparative cytotoxicity and genotoxicity of cobalt (II, III) oxide, iron (III) oxide, silicon dioxide, and aluminum oxide nanoparticles on human lymphocytes in vitro. Human & Experimental Toxicology, 35 (2), 170–183.

Ramesh, V., Ravichandran, P., Copeland, C.L., Gopikrishnan, R., Biradar, S., Goornavar, V., Ramesh, G.T., and Hall, J.C., 2012. Magnetite induces oxidative stress and apoptosis in lung epithelial cells. Molecular and Cellular Biochemistry, 363 (1–2), 225–234.

Ratner, B.D., 1996. The engineering of biomaterials exhibiting recognition and specificity. Journal of Molecular Recognition, 9 (5–6), 617–625.

Reif, D.W., 1992. Ferritin as a source of iron for oxidative damage. Free Radical Biology and Medicine, 12 (5), 417–427.

Reimer, P. and Balzer, T., 2003. Ferucarbotran (Resovist): a new clinically approved RES-specific contrast agent for contrast-enhanced MRI of the liver: properties, clinical development, and applications. European Radiology, 13 (6), 1266–1276.

Revia, R.A. and Zhang, M., 2016. Magnetite nanoparticles for cancer diagnosis, treatment, and treatment monitoring: Recent advances. Materials Today, 19 (3), 157–168.

Rivet, C.J., Yuan, Y., Borca-Tasciuc, D.A., and Gilbert, R.J., 2012. Altering iron oxide nanoparticle surface properties induce cortical neuron cytotoxicity. Chemical Research in Toxicology, 25 (1), 153–161.

Rogakou, E.P., Pilch, D.R., Orr, A.H., Ivanova, V.S., and Bonner, W.M., 1998. DNA double-stranded breaks induce histone H2AX phosphorylation on serine 139. Journal of Biological Chemistry, 273 (10), 5858–5868.

Rogakou, E.P. and Sekeri-Pataryas, K.E., 1999. Histone variants of H2A and H3 families are regulated during in vitro aging in the same manner as during differentiation. Experimental Gerontology, 34 (6), 741–754.

Roman, D., Locher, F., Suter, W., Cordier, A., and Bobadilla, M., 1998. Evaluation of a new procedure for the flow cytometric analysis of in vitro, chemically induced micronuclei in V79 cells. Environmental and Molecular Mutagenesis, 32 (4), 387–396.

Rosenberg, J.T., Sachi-Kocher, A., Davidson, M.W., and Grant, S.C., 2012. Intracellular SPIO labeling of microglia: high field considerations and limitations for MR microscopy. Contrast Media and Molecular Imaging, 7 (2), 121–129.

Saallah, S. and Lenggoro, I.W., 2018. Nanoparticles carrying biological molecules: recent advances and applications. KONA Powder and Particle Journal, 2018 (35), 89–111.

Sadeghiani, N., Barbosa, L.S., Silva, L.P., Azevedo, R.B., Morais, P.C., and Lacava, Z.G.M., 2005. Genotoxicity and inflammatory investigation in mice treated with magnetite nanoparticles surface coated with polyaspartic acid. In: Journal of Magnetism and Magnetic Materials, 289, 466–468.

Saeed, Y., Xie, B., Xu, J., Rehman, A., Hong, M., Hong, Q., and Deng, Y., 2015. Glial U87 cells protect neuronal SH-SY5Y cells from indirect effect of radiation by reducing oxidative stress and apoptosis. Acta Biochimica et Biophysica Sinica, 47 (4), 250–257.

Sahay, G., Alakhova, D.Y., and Kabanov, A. V, 2010. Endocytosis of nanomedicine. Journal of Controlled Release, 145 (3), 182–195.

Sahoo, Y., Pizem, H., Fried, T., Golodnitsky, D., Burstein, L., Chaim N. Sukenik, A., Gil Markovich, Sahoo, Y., Pizem, H., Fried, T., Golodnitsky, D., Burstein, L., Sukenik, C.N.,

and Markovich, G., 2001. Alkyl phosphonate/phosphate coating on magnetite nanoparticles: a comparison with fatty acids. Langmuir: the ACS journal of surfaces and colloids, 17 (23), 7907–7911.

Sahu, S.C., 2009. Hepatotoxic Potential of Nanomaterials. In: Nanotoxicity: from in vivo and in vitro models to health risks. Chichester, UK: John Wiley & Sons, Ltd., 183–189.

Sakulkhu, U., Mahmoudi, M., Maurizi, L., Salaklang, J., and Hofmann, H., 2014. Protein corona composition of superparamagnetic iron oxide nanoparticles with various physico-Chemical properties and coatings. Scientific Reports, 4 (1), 1–9.

Salata, O., 2004. Applications of nanoparticles in biology and medicine. Journal of nanobiotechnology, 2 (1), 3.

Salvati, A., Pitek, A.S., Monopoli, M.P., Prapainop, K., Bombelli, F.B., Hristov, D.R., Kelly, P.M., Åberg, C., Mahon, E., and Dawson, K.A., 2013. Transferrin-functionalized nanoparticles lose their targeting capabilities when a biomolecule corona adsorbs on the surface. Nature Nanotechnology, 8 (2), 137–143.

Sánchez-Flores, M., Pásaro, E., Bonassi, S., Laffon, B., and Valdiglesias, V., 2015. γH2AX assay as DNA damage biomarker for human population studies: defining experimental conditions. Toxicological Sciences, 144 (2), 406–413.

Sanganeria, P., Sachar, S., Chandra, S., Bahadur, D., Ray, P., and Khanna, A., 2015. Cellular internalization and detailed toxicity analysis of protein-immobilized iron oxide nanoparticles. Journal of Biomedical Materials Research - Part B Applied Biomaterials, 103 (1), 125–134.

Santhosh, P.B. and Ulrih, N.P., 2013. Multifunctional superparamagnetic iron oxide nanoparticles: promising tools in cancer theranostics. Cancer Letters, 336 (1), 8-17.

Saptarshi, S.R., Duschl, A., and Lopata, A.L., 2013. Interaction of nanoparticles with proteins: relation to bio-reactivity of the nanoparticle. Journal of Nanobiotechnology, 11 (1), 26.

Sato, Y., Kurose, A., Ogawa, A., Ogasawara, K., Traganos, F., Darzynkiewicz, Z., and Sawai, T., 2009. Diversity of DNA damage response of astrocytes and glioblastoma cell lines with various p53 status to treatment with etoposide and temozolomide. Cancer Biology and Therapy, 8 (5), 452–457.

Scarpato, R., Castagna, S., Aliotta, R., Azzara, A., Ghetti, F., Filomeni, E., Giovannini, C., Pirillo, C., Testi, S., Lombardi, S., and Tomei, A., 2013. Kinetics of nuclear phosphorylation (γ-H2AX) in human lymphocytes treated in vitro with UVB, bleomycin and mitomycin C. Mutagenesis, 28 (4), 465–473.

Schmezer, P., Rajaee-Behbahani, N., Risch, a, Thiel, S., Rittgen, W., Drings, P., Dienemann, H., Kayser, K.W., Schulz, V., and Bartsch, H., 2001. Rapid screening assay for mutagen sensitivity and DNA repair capacity in human peripheral blood lymphocytes. Mutagenesis, 16 (1), 25–30.

Schütz, C.A., Staedler, D., Crosbie-Staunton, K., Movia, D., Bernasconi, C.C., Kenzaoui, B.H., Prina-Mello, A., and Juillerat-Jeanneret, L., 2014. Differential stress reaction of human colon cells to oleic-acid-stabilized and unstabilized ultrasmall iron oxide nanoparticles. International Journal of Nanomedicine, 9 (1), 3481–3498.

Seo, D.Y., Jin, M., Ryu, J.-C., and Kim, Y.-J., 2017. Investigation of the genetic toxicity by dextran-coated superparamagnetic iron oxide nanoparticles (SPION) in HepG2 cells using the comet assay and cytokinesis-block micronucleus assay. Toxicology and Environmental Health Sciences, 9 (1), 23–29.

Shah, V., Taratula, O., Garbuzenko, O.B., Patil, M.L., Savla, R., Zhang, M., and Minko, T., 2013. Genotoxicity of different nanocarriers: possible modifications for the delivery of nucleic acids. Current drug discovery technologies, 10 (1), 8–15.

Shander, A., Cappellini, M.D., and Goodnough, L.T., 2009. Iron overload and toxicity: the hidden risk of multiple blood transfusions. Vox Sanguinis, 97 (3), 185–197.

Shapiro, H.M., 1995. Practical Flow Cytometry. Cytometry, 19, 376.

Sharifi, S., Seyednejad, H., Laurent, S., Atyabi, F., Saei, A.A., and Mahmoudi, M., 2015. Superparamagnetic iron oxide nanoparticles for in vivo molecular and cellular imaging. Contrast Media & Molecular Imaging, 10 (5), 329–355.

Sharma, G., Kodali, V., Gaffrey, M., Wang, W., Minard, K.R., Karin, N.J., Teeguarden, J.G., and Thrall, B.D., 2014. Iron oxide nanoparticle agglomeration influences dose rates and modulates oxidative stress-mediated dose-response profiles in vitro. Nanotoxicology, 8 (6), 663–675.

Shi, M., Cheng, L., Zhang, Z., Liu, Z., and Mao, X., 2015. Ferroferric oxide nanoparticles induce prosurvival autophagy in human blood cells by modulating the Beclin 1/Bcl-2/VPS34 complex. International journal of nanomedicine, 10, 207–216.

Shim, K.H., Hulme, J., Maeng, E.H., Kim, M.-K., and An, S.S. a, 2014. Analysis of zinc oxide nanoparticles binding proteins in rat blood and brain homogenate. International journal of nanomedicine, 9 (Suppl. 2), 217–224.

Shin, S., Song, I., and Um, S., 2015. Role of physicochemical properties in nanoparticle toxicity. Nanomaterials, 5 (3), 1351–1365.

Shukla, S., Jadaun, A., Arora, V., Sinha, R.K., Biyani, N., and Jain, V.K., 2015. In vitro toxicity assessment of chitosan oligosaccharide coated iron oxide nanoparticles. Toxicology Reports, 2, 27–39.

Simonis, F. and Schilthuizen, S., 2006. Nanotechnology: innovation opportunities for tomorrow's defence. Science, 2006, 112.

Singh, N., Jenkins, G.J.S., Asadi, R., and Doak, S.H., 2010. Potential toxicity of superparamagnetic iron oxide nanoparticles (SPION). Nano Reviews, 1 (1), 5358.

Singh, N., Jenkins, G.J.S., Nelson, B.C., Marquis, B.J., Maffeis, T.G.G., Brown, A.P., Williams, P.M., Wright, C.J., and Doak, S.H., 2012. The role of iron redox state in the genotoxicity of ultrafine superparamagnetic iron oxide nanoparticles. Biomaterials, 33 (1), 163–170.

Singh, N.P., McCoy, M.T., Tice, R.R., and Schneider, E.L., 1988. A simple technique for quantitation of low levels of DNA damage in individual cells. Experimental Cell Research, 175 (1), 184–191.

Soares, P.I.P., Laia, C.A.T., Carvalho, A., Pereira, L.C.J., Coutinho, J.T., Ferreira, I.M.M., Novo, C.M.M., and Borges, J.P., 2016. Iron oxide nanoparticles stabilized with a bilayer of oleic acid for magnetic hyperthermia and MRI applications. Applied Surface Science, 383, 240–247.

Soenen, S.J. and De Cuyper, M., 2010. Assessing iron oxide nanoparticle toxicity in vitro: current status and future prospects. Nanomedicine, 5 (8), 1261–1275.

Soenen, S.J., De Cuyper, M., De Smedt, S.C., and Braeckmans, K., 2012. Investigating the toxic effects of iron oxide nanoparticles. Methods in Enzymology, 509, 195–224.

Soenen, S.J.H. and De Cuyper, M., 2009. Assessing cytotoxicity of (iron oxide-based) nanoparticles: an overview of different methods exemplified with cationic magnetoliposomes. Contrast media & molecular imaging, 4 (5), 207–19.

Sofroniew, M. V and Vinters, H. V, 2010. Astrocytes: biology and pathology. Acta Neuropathologica, 119 (1), 7-35.

Solier, S. and Pommier, Y., 2009. The apoptotic ring: A novel entity with phosphorylated histones H2AX and H2B and activated DNA damage response kinases. Cell Cycle, 8 (12), 1853-1859.

Stamatovic, M.S., Sladojevic, N., F., R., and V., A., 2011. Blood-brain barrier permeability: from bench to bedside. In: Management of Epilepsy - Research, Results and Treatment. InTech, 2, 113–140.

Stockmann-Juvala, H., Naarala, J., Loikkanen, J., Vähäkangas, K., and Savolainen, K., 2006. Fumonisin B1-induced apoptosis in neuroblastoma, glioblastoma and hypothalamic cell lines. Toxicology, 225 (2–3), 234–241.

Stone, V., Johnston, H., and Schins, R.P.F., 2009. Development of in vitro systems for nanotoxicology: methodological considerations. Critical reviews in toxicology, 39 (July 2015), 613–626.

Suh, W.H., Suslick, K.S., Stucky, G.D., and Suh, Y.-H., 2009. Nanotechnology, nanotoxicology, and neuroscience. Progress in Neurobiology, 87 (3), 133–170.

Sun, C., Lee, J.S.H., and Zhang, M., 2008. Magnetic nanoparticles in MR imaging and drug delivery. Advanced Drug Delivery Reviews, 60 (11), 1252-1265.

Sutariya, V.B., Pathak, V., Groshev, A., Mahavir, B., Naik, S., Patel, D., and Pathak, Y., 2016. Introduction—Biointeractions of Nanomaterials. Challenges and solutions. In: Biointeractions of Nanomaterials. Boca Raton: CRC Press, 1–48.

Suzuki, H., Toyooka, T., and Ibuki, Y., 2007. Simple and easy method to evaluate uptake potential of nanoparticles in mammalian cells using a flow cytometric light scatter analysis. Environmental Science and Technology, 41 (8), 3018–3024.

Szalay, B., Tátrai, E., Nyírő, G., Vezér, T., and Dura, G., 2012. Potential toxic effects of iron oxide nanoparticles in in vivo and in vitro experiments. Journal of Applied Toxicology, 32 (6), 446–453.

Tanaka, T., Halicka, D., Traganos, F., and Darzynkiewicz, Z., 2009. Cytometric Analysis of DNA Damage: Phosphorylation of Histone H2AX as a Marker of DNA Double-Strand Breaks (DSBs). In: Methods Mol Biol. 161–168.

Taton, T.A., 2002. Nanostructures as tailored biological probes. Trends in Biotechnology, 20 (7), 277-279.

Teske, S. and Detweiler, C., 2015. The biomechanisms of metal and metal-oxide nanoparticles' interactions with cells. International Journal of Environmental Research and Public Health, 12 (2), 1112–1134.

Thomsen, L.B., Linemann, T., Pondman, K.M., Lichota, J., Kim, K.S., Pieters, R.J., Visser, ‖ G M, Moos, T., Visser, G.M., and Moos, T., 2013. Uptake and transport of superparamagnetic iron oxide nanoparticles through human brain capillary endothelial cells. ACS Chemical Neuroscience, 4 (10), 1352–1360.

Thomsen, L.B., Thomsen, M.S., and Moos, T., 2015. Targeted drug delivery to the brain using magnetic nanoparticles. Therapeutic Delivery, 6 (10), 1145–1155.

Thorek, D.L.J. and Tsourkas, A., 2008. Size, charge and concentration dependent uptake of iron oxide particles by non-phagocytic cells. Biomaterials, 29 (26), 3583–3590.

Tice, R.R., Agurell, E., Anderson, D., Burlinson, B., Hartmann, A., Kobayashi, H., Miyamae, Y., Rojas, E., Ryu, J.-C.C., and Sasaki, Y.F., 2000. Single cell gel/comet assay: guidelines for in vitro and in vivo genetic toxicology testing. Environmental and molecular mutagenesis, 35 (3), 206–21.

Toduka, Y., Toyooka, T., and Ibuki, Y., 2012. Flow cytometric evaluation of nanoparticles using side-scattered light and reactive oxygen species-mediated fluorescence-correlation with genotoxicity. Environmental Science and Technology, 46 (14), 7629–7636.

Tong, L., Zhao, M., Zhu, S., and Chen, J., 2011. Synthesis and application of superparamagnetic iron oxide nanoparticles in targeted therapy and imaging of cancer. Frontiers of Medicine, 5 (4), 379–387.

Toyokuni, S. and Sagripanti, J.L., 1999. Iron chelators modulate the production of DNA strand breaks and 8-hydroxy-2'-deoxyguanosine. Free Radical Research, 31 (2), 123–128.

Turcheniuk, K., Tarasevych, A. V, Kukhar, V.P., Boukherroub, R., and Szunerits, S., 2013. Recent advances in surface chemistry strategies for the fabrication of functional iron oxide based magnetic nanoparticles. Nanoscale, 5 (22), 10729.

Valdiglesias, V., Costa, C., Kiliç, G., Costa, S., Pásaro, E., Laffon, B., Teixeira, J.P., and Paulo, J., 2013a. Neuronal cytotoxicity and genotoxicity induced by zinc oxide nanoparticles. Environment International, 55, 92–100.

Valdiglesias, V., Costa, C., Sharma, V., Kiliç, G., Pásaro, E., Teixeira, J.P., Dhawan, A., and Laffon, B., 2013b. Comparative study on effects of two different types of titanium dioxide nanoparticles on human neuronal cells. Food and Chemical Toxicology journal, 57 (July), 352–361.

Valdiglesias, V., Fernández-Bertólez, N., Kiliç, G., Costa, C., Costa, S., Fraga, S., Bessa, M.J., Pásaro, E., Teixeira, J.P., and Laffon, B., 2016. Are iron oxide nanoparticles safe? Current knowledge and future perspectives. Journal of Trace Elements in Medicine and Biology, 38, 53–63.

Valdiglesias, V., Kilic, G., Costa, C., Fernandez-Bertolez, N., Pasaro, E., Teixeira, J.P., and Laffon, B., 2014. Effects of iron oxide nanoparticles: cytotoxicity, genotoxicity, developmental toxicity, and neurotoxicity. Environmental and Molecular Mutagenesis, 56 (2), 125–148.

Valdiglesias, V., Laffon, B., Pásaro, E., and Méndez, J., 2011. Okadaic acid induces morphological changes, apoptosis and cell cycle alterations in different human cell types. Journal of environmental monitoring, 13 (6), 1831–40.

Valko, M., Leibfritz, D., Moncol, J., Cronin, M.T.D., Mazur, M., and Telser, J., 2007. Free radicals and antioxidants in normal physiological functions and human disease. The International Journal of Biochemistry & Cell Biology, 39 (1), 44–84.

Vance, M.E., Kuiken, T., Vejerano, E.P., McGinnis, S.P., Hochella, M.F., Rejeski, D., and Hull, M.S., 2015. Nanotechnology in the real world: redeveloping the nanomaterial consumer products inventory. Beilstein Journal of Nanotechnology, 6, 1769–1780.

Vasir, J.K. and Labhasetwar, V., 2008. Quantification of the force of nanoparticle-cell membrane interactions and its influence on intracellular trafficking of nanoparticles. Biomaterials, 29 (31), 4244–4252.

Veiseh, O., Gunn, J.W., and Zhang, M., 2010. Design and fabrication of magnetic nanoparticles for targeted drug delivery and imaging. Advanced Drug Delivery Reviews, 62 (3), 284–304.

Verkhratsky, A., Nedergaard, M., and Hertz, L., 2015. Why are astrocytes important? Neurochemical Research, 40 (2), 389–401.

Verma, A. and Stellacci, F., 2010. Effect of surface properties on nanoparticle-cell interactions. Small, 6 (1), 12–21.

Wang, J., Chen, Y., Chen, B., Ding, J., Xia, G., Gao, C., Cheng, J., Jin, N., Zhou, Y., Li, X., Tang, M., and Wang, X.M., 2010. Pharmacokinetic parameters and tissue distribution of magnetic Fe3O4 nanoparticles in mice. International Journal of Nanomedicine, 5, 861-866.

Wang, J., Sun, W., and Ali, S.F., 2009. Nanoparticles: is neurotoxicity a concern? In: Nanotoxicity: from in vivo and in vitro models to health risks. John Wiley & Sons, Ltd, 171–182.

Wang, Y., Ding, L., Yao, C., Li, C., Xing, X., Huang, Y., Gu, T., and Wu, M., 2017. Toxic effects of metal oxide nanoparticles and their underlying mechanisms. Science China Materials, 60 (2), 93–108.

Wang, Y., Wang, B., Zhu, M.-T.T., Li, M., Wang, H.-J.J., Wang, M., Ouyang, H., Chai, Z.-F.F., Feng, W.-Y.Y., and Zhao, Y.-L.L., 2011. Microglial activation, recruitment and phagocytosis as linked phenomena in ferric oxide nanoparticle exposure. Toxicology Letters, 205 (1), 26–37.

Wang, Y.X.J., Hussain, S.M., and Krestin, G.P., 2001. Superparamagnetic iron oxide contrast agents: physicochemical characteristics and applications in MR imaging. European Radiology, 11 (11), 2319–2331.

Watanabe, M., Yoneda, M., Morohashi, A., Hori, Y., Okamoto, D., Sato, A., Kurioka, D., Nittami, T., Hirokawa, Y., Shiraishi, T., Kawai, K., Kasai, H., and Totsuka, Y., 2013. Effects of Fe3O4 magnetic nanoparticles on A549 cells. International Journal of Molecular Sciences, 14 (8), 15546–15560.

Watters, G.P., Smart, D.J., Harvey, J.S., and Austin, C.A., 2009. H2AX phosphorylation as a genotoxicity endpoint. Mutation Research/Genetic Toxicology and Environmental Mutagenesis, 679 (1–2), 50–58.

Weissleder, R., Stark, D., Engelstad, B., Bacon, B., Compton, C., White, D., Jacobs, P., and Lewis, J., 1989. Superparamagnetic iron oxide: pharmacokinetics and toxicity. American Journal of Roentgenology, 152 (1), 167–173.

Wolff, J.E.A., Trilling, T., Mölenkamp, G., Egeler, R.M., and Jürgens, H., 1999. Chemosensitivity of glioma cells in vitro: a meta analysis. Journal of Cancer Research and Clinical Oncology, 125 (8–9), 481–486.

Wu, H.-Y., Chung, M.-C., Wang, C.-C., Huang, C.-H., Liang, H.-J., and Jan, T.-R., 2013a. Iron oxide nanoparticles suppress the production of IL-1beta via the secretory lysosomal pathway in murine microglial cells. Particle and Fibre Toxicology, 10 (1), 46.

Wu, J., Ding, T., and Sun, J., 2013b. Neurotoxic potential of iron oxide nanoparticles in the rat brain striatum and hippocampus. NeuroToxicology, 34 (1), 243–253.

Wu, J. and Sun, J., 2011. Investigation on mechanism of growth arrest induced by iron oxide nanoparticles in PC12 cells. Journal of Nanoscience and Nanotechnology, 11 (12), 11079–11083.

Wu, J., Wang, C., Sun, J., and Xue, Y., 2011. Neurotoxicity of silica nanoparticles: brain localization and dopaminergic neurons damage pathways. ACS Nano, 5 (6), 4476–4489.

Wu, W., Chen, B., Cheng, J., Wang, J., Xu, W., Liu, L., Xia, G., Wei, H., Wang, X., Yang, M., Yang, L., Zhang, Y., Xu, C., and Li, J., 2010. Biocompatibility of Fe3O4/DNR magnetic nanoparticles in the treatment of hematologic malignancies. International Journal of Nanomedicine, 5 (1), 1079–1084.

Wu, W., He, Q., and Jiang, C., 2008. Magnetic iron oxide nanoparticles: synthesis and surface functionalization strategies. Nanoscale Research Letters, 3 (11), 397–415.

Wu, W., Wu, Z., Yu, T., Jiang, C., and Kim, W.-S., 2015. Recent progress on magnetic iron oxide nanoparticles: synthesis, surface functional strategies and biomedical applications. Science and Technology of Advanced Materials, 16 (2), 023501.

Xia, J.G., Zhang, S., Zhang, Y., Ma, M., and Gu, N., 2009a. Maghemite nanoparticles and their protamine derivatives: cellular internalization and effects on cell-cycle progress. Journal of Nanoscience and Nanotechnology, 9 (2), 1025–1028.

Xia, T., Kovochich, M., Liong, M., Meng, H., Kabehie, S., George, S., Zink, J.I., and Nel, A.E., 2009b. Polyethyleneimine coating enhances the cellular uptake of mesoporous silica nanoparticles and allows safe delivery of siRNA and DNA constructs. ACS Nano, 3 (10), 3273–3286.

Xie, H.R., Hu, L.S., and Li, G.Y., 2010. SH-SY5Y human neuroblastoma cell line: in vitro cell model of dopaminergic neurons in Parkinson's disease. Chin Med J (Engl), 123 (8), 1086–1092.

Xu, P., Li, J., Chen, B., Wang, X., Cai, X., Jiang, H., Wang, C., and Zhang, H., 2012. The Real-Time Neurotoxicity Analysis of Fe_3O_4 nanoparticles combined with daunorubicin for rat brain *in vivo*. Journal of Biomedical Nanotechnology, 8 (3), 417–423.

Yang, C.Y., Hsiao, J.K., Tai, M.F., Chen, S.T., Cheng, H.Y., Wang, J.L., and Liu, H.M., 2011. Direct labeling of hMSC with SPIO: the long-term influence on toxicity, chondrogenic differentiation capacity, and intracellular distribution. Molecular Imaging and Biology, 13 (3), 443-451.

Yang, X., Ma, Luo, Chen, Gan, Du, Ding, and Xi, 2012. Intraperitoneal injection of magnetic Fe3O4-nanoparticle induces hepatic and renal tissue injury via oxidative stress in mice. International Journal of Nanomedicine, 7, 4809.

Yang, Z., Liu, Z.W., Allaker, R.P., Reip, P., Oxford, J., Ahmad, Z., and Ren, G., 2010. A review of nanoparticle functionality and toxicity on the central nervous system. Journal of The Royal Society Interface, 7 (Suppl. 4), S411–S422.

Yemisci, M., Caban, S., Gursoy-Ozdemir, Y., Lule, S., Novoa-Carballal, R., Riguera, R., Fernandez-Megia, E., Andrieux, K., Couvreur, P., Capan, Y., and Dalkara, T., 2015. Systemically administered brain-targeted nanoparticles transport peptides across the blood-brain barrier and provide neuroprotection. Journal of Cerebral Blood Flow and Metabolism, 35 (3), 469–475.

Yi, D.K., Lee, S.S., Papaefthymiou, G.C., and Ying, J.Y., 2006. Nanoparticle architectures templated by SiO2/Fe2O3 nanocomposites. Chemistry of Materials, 18 (3), 614–619.

Ying, E. and Hwang, H.-M., 2010. In vitro evaluation of the cytotoxicity of iron oxide nanoparticles with different coatings and different sizes in A3 human T lymphocytes. Science of The Total Environment, 408 (20), 4475–4481.

Yoshioka, Y., Higashisaka, K., Tsunoda, S., and Tsutsumi, Y., 2014. Engineered cell manipulation for biomedical application. Tokyo: Springer Japan, 259-271.

Young, S.P. and Garner, C., 1990. Delivery of iron to human cells by bovine transferrin. Biochem. J., 265, 587–591.

Yu, M., Huang, S., Yu, K.J., and Clyne, A.M., 2012. Dextran and polymer polyethylene glycol (PEG) coating reduce both 5 and 30 nm iron oxide nanoparticle cytotoxicity in 2D and 3D cell culture. International Journal of Molecular Sciences, 13 (5), 5554-5570.

Zanganeh, S., Spitler, R., Erfanzadeh, M., Alkilany, A.M., and Mahmoudi, M., 2016. Protein corona: opportunities and challenges. The International Journal of Biochemistry & Cell Biology, 75, 143–147.

Zeng, H. and Sanes, J.R., 2017. Neuronal cell-type classification: challenges, opportunities and the path forward. Nature Reviews Neuroscience, 18 (9), 530–546.

Zhang, T., Qian, L., Tang, M., Xue, Y., Kong, L., Zhang, S., and Pu, Y., 2012. Evaluation on cytotoxicity and genotoxicity of the L-glutamic acid coated iron oxide nanoparticles. Journal of Nanoscience and Nanotechnology, 12 (3), 2866–2873.

Zhu, X.-M., Wang, Y.-X.J., Cham-Fai Leung, K., Lee, S.-F., Zhao, F., Wang, D.-W., Lai, J.M., Wan, C., Cheng, C.H., and Ahuja, A.T., 2012. Enhanced cellular uptake of aminosilane-coated superparamagnetic iron oxide nanoparticles in mammalian cell lines. International Journal of Nanomedicine, 7, 953–964.